

Gerhard Olivier

Student Number: 4736095



# Fire Performance of Cross-Laminated Timber

Investigating adhesives, compartment configuration and design guidelines

---

# **FIRE PERFORMANCE OF CROSS- LAMINATED TIMBER**

---

*Investigating adhesives, compartment configuration and design  
guidelines*

---

MASTER'S THESIS REPORT

---

In partial fulfilment of the requirements for the degree of:

---

MASTER OF SCIENCE IN CIVIL ENGINEERING

---

BY  
GERHARD OLIVIER

---

Faculty of Civil Engineering and Geosciences  
Delft University of Technology  
July 2019

# Graduation Committee

Prof.dr.ir. J.W.G. van de Kuilen

Chairman Graduation Committee - Biobased Structures and Materials

T: (+31) (0)15 2782322

E: [J.W.G.vandeKuilen@tudelft.nl](mailto:J.W.G.vandeKuilen@tudelft.nl)

Dr.ir. G.J.P. Ravenshorst

Supervisor Delft University of Technology - Biobased Structures and Materials

T: (+31) (0)15 2785721

E: [G.J.P.Ravenshorst@tudelft.nl](mailto:G.J.P.Ravenshorst@tudelft.nl)

Ir. R. Crielaard

Supervisor Delft University of Technology – Building Engineering

T: (+31) (0) 642713767

E: [R.Crielaard@tudelft.nl](mailto:R.Crielaard@tudelft.nl)

Ir. P. Steenbakkers

Supervisor Arup – Fire Safety Engineering

T: (+31) (0) 20 3058500

E: [Pascal.Steenbakkers@arup.com](mailto:Pascal.Steenbakkers@arup.com)

Dr. L. van Gelderen

Supervisor Efectis – Fire Safety Engineering

T: (+31) (0) 88 3473 748

E [Laurens.vangelderen@EFFECTIS.COM](mailto:Laurens.vangelderen@EFFECTIS.COM)

## Graduate Student:

Gerhard Olivier

T: (+31) (0) 62 0375 131

E [g.olivier@student.tudelft.nl](mailto:g.olivier@student.tudelft.nl)

# Summary

Cross-Laminated timber (CLT), and other engineered timber products, are under high demand due to their prefabricated nature and environmental benefits. A key concern surrounding the application of CLT in buildings is its combustible nature and subsequent contribution to a compartment fire. Previous research has shown that exposed CLT, under certain circumstances, can achieve self-extinguishment. This research aims to further experimentally investigate the fire performance of small-scale compartments containing exposed CLT.

The focus of this study is threefold, namely to investigate: i) the influence of (commercially available) adhesives used in CLT panels on fire behaviour; ii) the influence of CLT panel configuration on fire behaviour and iii) the ability of design guidelines to predict experimentally obtained fire behaviour. By investigating these aspects, a detailed investigation into fire behaviour of compartments with exposed CLT is presented to characterise the influence of CLT on enclosure fire behaviour and assess the ability of CLT to reliably self-extinguish.

A series of small scale (0.5m x 0.5m x 0.5m internal dimensions) compartment tests was used to investigate compartment fire behaviour. All compartments were constructed of melamine-urea-formaldehyde (MUF) bonded CLT panels and non-combustible boards. An identical experimental methodology as implemented by Crielaard (2015) (who investigated poly-urethane (PU) -bonded CLT panels) was used in this investigation. By varying the adhesive type between investigations, practical adhesive comparisons were formulated.

Based on the experiments that sought to investigate the influence of adhesive type on fire behaviour, it was observed that in comparable compartment experiments with two exposed CLT side walls, panel burn-through behaviour (and the occurrence of a 2<sup>nd</sup> flashover) was observed in PU bonded panels as opposed to self-extinguishment in MUF bonded CLT panels. It was further observed in these two compartment experiments, that the tested MUF bonded CLT panels experience a process of local char fall off, as opposed to a process of delamination (of planks) in the investigated PU bonded CLT panels. In another comparable PU bonded CLT side wall compartment experiment, self-extinguishment was also recorded. When comparing the charring rates observed in CLT side wall compartments that self-extinguished, it was founded that 1<sup>st</sup> lamella charring rates were 14.1% to 19.4% higher in PU bonded panels as compared to MUF bonded CLT panels.

When considering the influence of CLT panel configuration on compartment fire behaviour, various conclusions were drawn. It was found that both compartment temperatures and the heat release rate (HRR) did not change with varying CLT panel orientation. Furthermore, compartments with only one exposed CLT panel as opposed to two CLT panels, displayed shorter decay phase durations (i.e.



achieved self-extinguishment faster). In addition, with one exposed CLT surface, the contribution to the total HRR by the CLT alone was half the contribution by the CLT in compartments with two exposed CLT surfaces (regardless of CLT panel orientation). Additionally, the most predictable fire behaviour (i.e. fast achievement of self-extinguishment) was achieved in compartments constructed with only an exposed ceiling: self-extinguishment was recorded between 21 and 27 minutes after the initial fire was stopped. It is hypothesised in this study that this accelerated decay phase is attributed to a lack of available oxygen to drive the combustion process, due to the accumulation of combustion gases at the ceiling. This hypothesis, however, requires further verification. It was further shown that relative CLT panel orientation in compartments containing two exposed CLT surfaces also proved influential. Facing CLT panels as opposed to adjacent CLT panels demonstrated a prolonged period of elevated compartment temperatures, which delayed the attainment of self-extinguishment. Two adjacent CLT panels were found to self-extinguish faster. It is hypothesised that this is due to direct mutual cross-radiation of heat between facing CLT panels.

In addition to the small-scale compartment experiments, a furnace test was performed which subjected four MUF bonded horizontal CLT panels to a 90 minute standard fire curve (SFC) exposure. An averaged panel charring rate of 0.59mm/min over 90 minutes was measured. Charring rates were recorded over multiple lamellas and in all instances were comparable to the 0.65 mm/min charring rate stipulated by EN1995-1-2 for solid softwood timber. Due to the similarities in charring rates and fire behaviour between the MUF bonded small-compartment tests and the SFC furnace test, it is deemed that the conclusions drawn from the compartment tests are also valid for longer initial fire durations (i.e. charring due to burning of the initial fuel load beyond the first lamella) as well as standard fire exposure conditions.

The investigation into the ability of a design guideline by Brandon (2018b) to predict fire behaviour, namely a Parametric Fire Curve (PFC) calculation method that includes the contribution of exposed CLT to the fuel load, provided mixed results. The investigated guideline was able to conservatively estimate the charring depth of the various CLT panels, but parameters such as the average compartment temperature during the heating phase of a fire, decay phase duration and amount of energy released by the combusting CLT were not predicted well. The discrepancy between predictions and experimental results were least in compartments with only an exposed CLT ceiling. These findings suggest that further research is required to first quantify the contribution of exposed CLT to the fuel load and then accurately include this contribution in design recommendations. The investigated design guideline may, however, be used to conservatively estimate charring depths, despite not accurately predicting small-compartment fire behaviour.

Based on the conclusions drawn in this study, it is recommended that both the **adhesive type** and **CLT panel configuration** should be selected with caution in order to achieve predictable and reliable fire

behaviour by means of self-extinguishment. This research, along with its recommendations and conclusions in Chapter 9, contribute to a better understanding of predictability and reliability of fire behaviour in compartments with exposed CLT elements. It is recommended that the findings of this research, which are based on small-scale compartment experiments, are further tested and validated for larger fire compartments.

# Acknowledgements

I would like to thank the following people for their invaluable contribution to this research:

- My supervisors for their continuous support and advice. Each of you has contributed to this research project. Geert Ravenshorst, thank you for guiding me in the initial phases of this project, for inspiring me to choose a thesis topic related to fire safety engineering, for putting me in contact with potential material suppliers and for your helpful suggestions throughout this project. Roy Crielaard, thank you for your extensive comments on my research scope, report and findings as well as sharing your experimental knowledge with me. Jan-Willem van de Kuilen, thank you for your inputs regarding my conclusions as well as help defining the scope of my research. Pascal Steenbakkens, thank you for your support in the project definition phase of this project, for your Fire Safety and Structural Engineering insights as well as for your continuous desire to make my research practically applicable. Laurens van Gelderen, thank you for sharing your wealth of fire safety knowledge with me which helped me understand fundamental concepts better and improved my experimental testing methodology, as well as for all your assistance at Efectis whilst performing the tests.
- Everyone at Efectis for their support prior to, during and after conducting my experiments.
- Mr Johan Borreman from Derix GmbH for sponsoring the CLT used in my experiments.
- Mr Frank van der Wal from Etex Building Performance for sponsoring the Promatect-H panels used in my experiments.
- Dr Daniel Brandon for all your help during the initial phases of this research project as well as your support with the modelling exercises.
- Prof Luke Bisby for your insight into current CLT research trends as well as for helping with establishing the most relevant research parameters.
- My family for their never ending support and patience with me.
- Jana Otzipka, for her unwavering positivity and willingness to proof read everything.
- My friends for all their help and discussions. Tal Ben-Gera, thank you for all your help with constructing the compartments and for your willingness to discuss ideas with you.

Without all of you this research would not exist.

I dedicate this report to my mother, Professor Lynette Olivier. May this be in your honour.

# Table of Contents

1) Introduction.....	1
2) Research Outline.....	4
2.1) Problem Description.....	4
2.2) Relevance of this research .....	5
2.3) Research Goals .....	6
2.4) Research Questions.....	6
2.5) Methodology.....	7
2.5.1) Literature Review .....	7
2.5.2) Experimental Characterisation.....	7
2.5.3) Additional experiment to assess the validity of conclusions .....	14
2.5.4) Assessing Design Guidelines.....	15
2.6) Research Scope Limitations .....	15
2.7) Sections of the report addressing the research questions.....	17
3) Literature Study .....	20
3.1) Enclosure Fire Dynamics.....	20
3.2) Combustion of Timber.....	23
3.3) Influence of Adhesives on CLT fire performance .....	27
3.4) Overview of CLT compartment fire behaviour.....	31
3.4.1) McGregor (2013): CLT Room Fires.....	33
3.4.2) Medina Hevia (2014): Partially Protected CLT Timber Rooms.....	35
3.4.3) Crielaard (2015): Self-extinguishment of CLT .....	36
3.4.4) Li <i>et al.</i> (2016): Real-Scale Fire Tests on Timber Constructions .....	39
3.4.5) Hadden <i>et al.</i> (2017): Effects of exposed CLT on compartment fire dynamics .....	39
3.4.6) Bateman <i>et al.</i> (2018): Effects of Fuel Load and Exposed CLT Surface Configuration in Reduced-Scale Compartments .....	41
3.4.7) Su <i>et al.</i> (2018): Cross Laminated Timber Compartment Fire Tests.....	42
3.4.8) Su, Leroux, <i>et al.</i> , (2018): Fire testing of rooms with exposed wood surfaces in encapsulated mass timber construction.....	45

3.5) A review of fire design recommendations.....	47
3.6) Chapter Conclusion .....	47
4) Selecting Experimental Parameters .....	50
4.1) Adhesive Type.....	50
4.2) Exposed CLT Panel Configuration.....	50
5) Experimental Methodology.....	52
5.1) Equipment.....	52
5.2) Prepared Samples .....	57
5.3) Experimental Procedure .....	59
6) Results.....	61
6.1) Configuration MUF-BW: CLT Back Wall.....	61
6.2) Results of Compartment Tests.....	66
6.3) Summary of Experimental Results .....	66
6.3.1) Temperatures .....	66
6.3.2) Heat Release Rates .....	68
6.4) Overview of Results .....	68
7) Analysis.....	70
7.1) Analysis of individual compartment experiments .....	70
7.1.1) Analysing HRR per compartment experiment.....	70
7.1.2) TER results .....	71
7.1.3) Charring Rates .....	74
7.1.3) Propagation of the charring front and time required to self-extinguish.....	75
7.2) Influence of adhesive type on compartment fire behaviour.....	77
7.2.1) Adhesive influence of compartments with a CLT back wall.....	82
7.2.2) Adhesive influence of compartments with CLT side walls .....	87
7.2.3) Answering Research Sub-Question 3 .....	92
7.3) Influence of panel configuration on compartment fire behaviour .....	93
7.3.1) Characterising the behaviour of compartments with one exposed CLT surface .....	94
7.3.2) Characterising the cross-radiation behaviour of facing CLT side walls.....	97



7.3.3) Characterising the addition of an exposed CLT Ceiling to a compartment with a CLT back wall.....	100
7.3.4) Characterising the behaviour of compartments with two exposed CLT surfaces.....	103
7.3.5) Answering Research Sub-Questions 4.....	106
7.4) Influence of char fall-off on compartment fire behaviour .....	107
7.5) Chapter Summary .....	108
8) Investigating Design Recommendations.....	113
8.1) Compartments with one exposed CLT panel.....	115
8.2) Compartments with two exposed CLT panels.....	118
8.3) Analysing the ability of the investigated design recommendation .....	120
8.3.1) Comparing the PFC to experimental results pertaining to one exposed CLT Surface .....	120
8.3.2) Comparing the PFC to experimental results pertaining to two exposed CLT Surfaces ...	121
8.4) Chapter Conclusion: Answering Research Sub-Question 5 .....	122
9) Conclusion and recommendations .....	124
9.1) Introduction .....	124
9.2) Conclusions .....	124
9.3) Recommendations .....	125
9.4) Limitations and Future Research.....	127
10) References.....	129
Appendix A.....	133
Compartment Configurations.....	133
Appendix B .....	135
B.1) CLT Fabrication.....	136
B.2) CLT Panel Data Sheet.....	139
B.3) GripPro Plus adhesive product information.....	140
Appendix C .....	150
C.1) A Review of Fire Design Recommendations.....	151
C.1.1) Fire Curves.....	151
C.1.2) Charring of Timber Design Equations according to EN 1995-1-2 .....	155

C.1.3) Recommendations proposed by Brandon (2018b) .....	159
C.1.4) Zone Modelling of Enclosure Fires .....	161
C.2) Worked example of determining a parametric time-temperature curve including the contribution of exposed CLT .....	164
Appendix D .....	168
CLT Emission Test .....	168
Appendix E .....	186
Results of Configuration MUF-2SW, MUF-SW-1, MUF-C-1 and MUF-BW+C-1 .....	186
E.1) Configuration MUF-2SW: Two CLT Side Walls .....	187
E.2) Configuration MUF-SW-1: One CLT Side Wall .....	193
E.3) Configuration MUF-C-1: CLT Ceiling .....	197
E.4) Configuration MUF-BW+C-1: CLT Back Wall and Ceiling .....	202
Appendix F .....	208
Results of the repetition experiments MUF-SW-2, MUF-C-2 and MUF-BW+C-2 .....	208
F.1) Configuration MUF-SW-2: One CLT Side Wall .....	209
F.2) Configuration MUF-C-2: CLT Ceiling .....	213
F.3) Configuration MUF-BW+C-2: CLT Back Wall and Ceiling .....	216
Appendix G .....	221
Configuration analysis based on results from the repetition experiments .....	221
G.1) Characterising the behaviour of compartments with one exposed CLT surface .....	222
G.2) Characterising the cross-radiation behaviour of facing CLT side walls .....	225
G.3) Characterising the addition of an exposed Ceiling CLT to a compartment with a CLT back wall .....	227
G.4) Characterising the behaviour of compartments with two exposed CLT surfaces .....	230
Appendix H .....	233
Charring Rates of the Compartment Experiments .....	233
Appendix I .....	236
Results of the 90 minute SFC Furnace Test on Ceiling CLT Panels .....	236

# 1) Introduction

Due to its prefabricated, aesthetic and sustainable nature, engineered timber has become a popular construction material (Bartlett *et al.*, 2016). Cross-Laminated Timber (CLT) is an example of engineered timber by which the inherent anisotropy of timber is effectively addressed to create structural sections. CLT consists of boards/planks that are arranged in panel configurations and then adhesively bonded on top of each other in a cross-wise manner (Johansson and Svenningsson, 2018). Since timber is inherently combustible, the full use of exposed CLT in construction, especially high-rise structures, has been limited until now (Bartlett, Hadden and Bisby, 2018).

In practice, timber buildings are commonly designed according to prescriptive regulations when considering fire safety due to the fire risk posed by the combustible nature of timber and subsequent uncertainties regarding its fire performance. As such, several European countries impose maximum height restrictions on timber buildings due to these uncertainties (Östman, Brandon and Frantzich, 2017). These prescriptive guidelines are generally inadequate to allow timber products to be utilised to their full potential and often require the use of fire rated gypsum boards to encapsulate timber elements. A new trend is emerging in fire safety design and research, where focus is placed on the characterisation of actual fire performance of timber products (especially CLT) in realistic fire scenarios and the investigation of its performance (Brandon, 2016). Furthermore, specifically when considering high-rise buildings, there is limited access available to the fire brigade during a fire. Additionally, high-rise buildings are to be designed in Europe in accordance with Consequence Class 3 (CC3) of EN1990 (2002). This leads to the heightened need for the reliability of building materials in fires, as CC3 is the highest level of reliability defined in EN1990 (2002) which requires the lowest probability of failure as specified in the standard. It is against the background of a rise in CLT demand and the need for research to characterise the fire behaviour of combustible CLT, that this Master's Thesis research project is conducted.

In essence, the research performed in this thesis is a continuation and extension of the research conducted by Crielaard (2015). In his Master's Thesis, Crielaard investigated the parameters and conditions leading to self-extinguishment of CLT. His research indicated that self-extinguishment is possible if the heat flux received by the CLT is below 5 to 6 kW/m<sup>2</sup>. In addition, he found that depending on its CLT panel configuration (depicted in Figure 1 below), small-scale compartment may undergo self-extinguishment or full CLT burn through. Furthermore, it was concluded that self-extinguishment is likely to occur below 6 kW/m<sup>2</sup> when additionally exposed to an airflow of 0.5m/s.

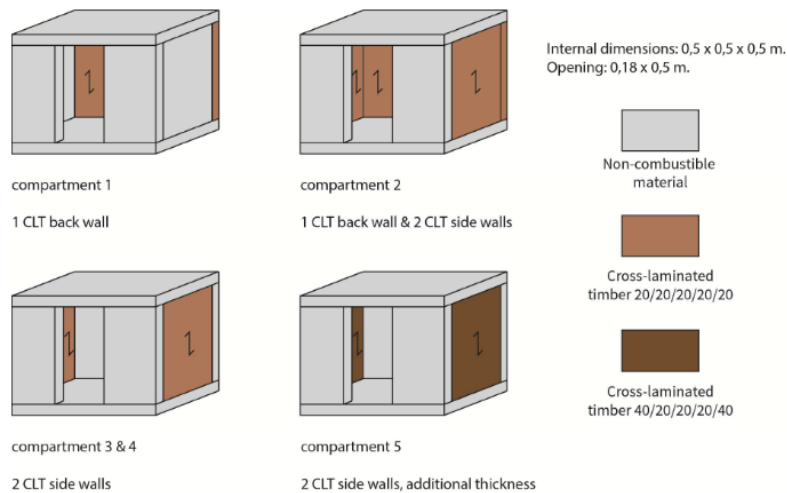


*Figure 1: Compartment configuration as implemented by Crielaard (2015)*

The aim of the research, as presented in this report, is to extend the available data of CLT fire performance to additionally characterise the influence of adhesive type and compartment configuration on fire behaviour. The influence of adhesive type on fire performance was practically investigated. Experiments were performed on CLT panels with an identical lay-up, lamella thickness, strength-grade and timber species as compared to CLT panels used by Crielaard (2015). The only difference was the type of adhesive used. These experiments were then compared to the experimental results of Crielaard (2015) to characterise the influence of adhesive type on fire behaviour.

Furthermore, the effect of exposed CLT panel configuration within a compartment on fire behaviour was investigated, by constructing small-scale compartments with various CLT panel configurations. In this manner, both the orientation of exposed CLT panels (for example a wall as compared to a ceiling), as well as the influence of increasing the number of exposed CLT panels (i.e. 1 or 2 CLT panels) were investigated. All fire tests conducted as part of this research project were performed on small-scale enclosures. These tests were not carried out on real compartment scales due to experimental and time limitations. The extrapolation of the results and conclusions listed in this document to larger enclosure scales is to be verified by future research.

Subsequent to this, the ability of parametric fire curve calculations to predict the contribution of CLT to the overall heat release rate (HRR) in the compartment was tested. By implementing the current design guidelines pertaining to exposed CLT in fire, the potential to adequately model CLT fire behaviour was assessed. Therefore, the applicability of design guidelines (such as those proposed by Brandon (2018b)), was investigated.

In general terms, experiments were carried out on CLT compartments to compare the conclusions drawn from compartment tests to conclusions drawn by Crielaard (2015) regarding adhesive

performance in fire conditions. Following this, the influence of CLT panel configuration was investigated, and the ability of current timber fire design recommendations was assessed to determine their ability to predict overall fire behaviour. These design guidelines, if improved upon further, may improve the confidence in designing exposed CLT constructions.

Furthermore, to assess the validity of conclusions drawn from these small-scale compartment experiments regarding charring rates and fire behaviour, an additional indicative test was performed. This test subjected a set of horizontal CLT panels to a standardised fire exposure for a period of 90 minutes to determine fire behaviour based on an extended fire exposure duration.

Especially considering the reliability considerations of Consequence Class 3 in High-Rise Buildings, the reliability of CLT as a building material is severely impacted by its fire performance. By investigating fire performance of CLT panels subjected to a fire exposure, the response of the building material is investigated which augments the body of knowledge pertaining to fire behaviour of this combustible material.



## 2) Research Outline

To quantify the scope of this research project, this section of the report presents a discussion of the research-problem, -relevance, -goals, -questions and methodology as well as limitations imposed on this study. Each will be described individually.

### 2.1) Problem Description

One of the main barriers to constructing enclosures with exposed CLT (and other timber products) is the uncertainty regarding the contribution of the construction material itself to the overall enclosure fire behaviour (Östman, Brandon and Frantzich, 2017). The contribution of combustible timber is required to be accurately and reliably predicted if CLT is to be used with confidence as a construction material. Various studies, as outlined in the literature study section of this report, have attempted to quantify the contribution of combustible CLT to enclosure fire behaviour. This Master's Thesis seeks to further address concerns regarding the use of combustible CLT as a building material. In particular, methods to promote the achievement of reliable self-extinguishment will be a focus of this research project.

Furthermore, guidelines such as those provided by Brandon (2018b) have been drafted to characterise the contribution of CLT panels to the overall heat release rate (HRR) within an enclosure. A key concern is to test the accuracy of such guidelines with respect to different compartment configurations.

The problem description, to be addressed by this research, is stated as follows:

*Due to the combustible nature of exposed timber, CLT panels contribute to the fuel load and fire behaviour of an exposed timber compartment. It is not clear what the influence of the type of adhesive used, as well as panel configuration is on fire behaviour. As such, uncertainties exist regarding the relationship between the adhesive used, panel configuration and the potential to achieve self-extinction. Additionally, the potential of current design guidelines to characterise the contribution of CLT to a fire is still an active field of research requiring further verification.*

In the interest of clarity, CLT self-extinguishment (also referred to in literature as auto-extinction) is defined as follows (based on the research of Crielaard (2015)):

*Self-extinction of CLT is obtained when a sample transitions from smouldering combustion to extinguishment after the initial fuel load has been depleted. Self-extinguishment is achieved by avoiding a second flashover as caused by the occurrence of delamination which exposes virgin timber.*

## 2.2) Relevance of this research

Östman, Brandon and Frantzich (2017) have highlighted the need to thoroughly investigate the potential of buildings constructed of timber products to undergo self-extinction. By obtaining a fundamental understanding of the process of self-extinction and the conditions required for its achievement, the confidence of designing structures with engineered timber products (such as CLT) may be improved. Furthermore, as will be illustrated in the literature study section of this report, compartment fire tests have predominantly been carried out on CLT panels bonded with polyurethane (PU) adhesives. A gap in the current research surrounding this topic is the influence of different kinds of adhesives on fire behaviour. The key scientific relevance of the research proposed in this document lies therefore in its aim to characterise the potential of melamine-based adhesively bonded CLT panels to undergo self-extinction. The influence of adhesives on fire behaviour has only, to the knowledge of the author, been studied on element level (and not compartment level) by Brandon & Dagenais (2018), where 1.5m x 0.5m x 0.175m CLT panels were tested in a horizontal configuration. From their study, it is evident that PU adhesively bonded CLT is prone to heat induced delamination. Furthermore, Frangi *et al.* (2009) illustrated in their study that CLT panels bonded with a Melamine-Urea-Formaldehyde (MUF) adhesive displayed improved fire performance as compared to PU adhesives, based on experimental tests results on horizontal panels exposed to a standard fire curve. The research presented in this report seeks to build on the work of previous researchers to both characterise the contribution of CLT to the fire load as well as the influence of adhesives on self-extinction on compartment level.

As will be discussed later in this report (see Section 3.4), various researchers have studied the impact of compartment configurations on fire behaviour. However, a full series of compartment configurations was to date not tested in a single study, highlighting the relevance of this study. The key aspects and compartment configurations tested by previous research are listed in the literature study of this report. The fire behaviour induced by an exposed CLT ceiling as compared to an exposed CLT wall, as well as the influence of combining a CLT ceiling with a CLT wall will be quantified as part of this research.

Finally, by verifying the ability of a design guideline to predict enclosure fire behaviour with exposed CLT panels, the confidence in designing structures containing exposed timber surfaces will be improved.

In summary, by testing a less investigated structural adhesive, performing tests on various exposed CLT configurations as well as quantify the ability of design guidelines to predict fire behaviour, the current body of knowledge pertaining to exposed CLT compartment fire behaviour will be expanded allowing for a more fundamental understanding of enclosure constructed of combustible materials. Due to experiments only being conducted on small-scale compartments, the results of this study

should be used as a basis to conduct further studies which investigate fire behaviour at real compartment scales.

## 2.3) Research Goals

To address the aforementioned research problem, the following overall research goal is formulated:

To contribute to the current body of knowledge related to compartments containing exposed CLT panels with the aim of increasing the confidence of designers and regulators alike, in building constructions with combustible materials

Due to the wide scope of the abovementioned overall goal, a specific research goal is formulated as follows:

*To experimentally investigate, by means of small-scale compartment fire tests, the differences in fire behaviour between two different types of adhesives (MUF and PU) and the influence of CLT panel configuration on compartment fire behaviour, as well as investigate the ability of design guidelines to predict experimentally measured compartment temperatures.*

## 2.4) Research Questions

When considering the specific research goal as stated above, one main research question can be formulated. In addition, 5 sub questions are formulated which seek to systematically answer the main research question. These questions are shown in Figure 2, along with the sections of this report (i.e. Parts 1 through 3) that address these questions.

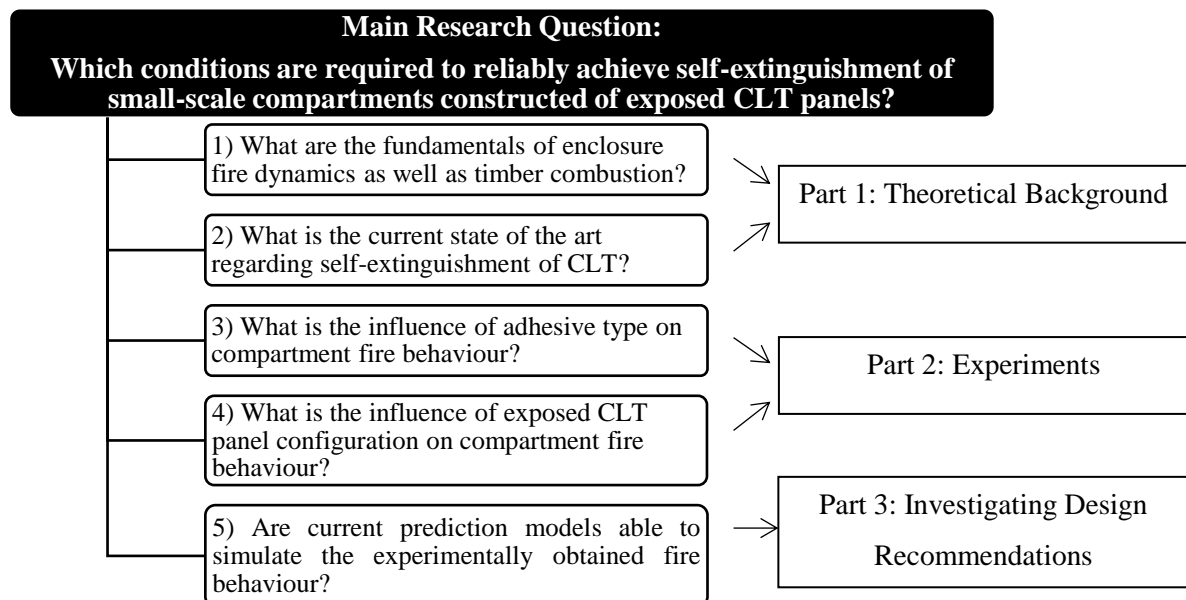


Figure 2: Main and sub research questions, as well as the report parts that address each sub-question

## 2.5) Methodology

To answer the research questions stated in the previous section of the report, a systematic research methodology is followed. This section is divided into three parts (according to Figure 2) and these will also be used to divide the entire research project into the same three parts, namely:

1. Literature review,
2. Experiments to characterise the influence of adhesive type and panel configuration
3. Testing the accuracy of design guidelines.

The research methodology relevant to each sub-section will now be discussed individually with reference to the sub-questions listed in Figure 2.

### 2.5.1) Literature Review

*Sub-Research Question 1: What are the fundamentals of enclosure fire dynamics as well as timber combustion?*

To answer this question, a literature review pertaining to fire dynamics as well as timber combustion is conducted. This will serve as the theoretical basis of this research, such that fire dynamics principles can be adequately observed and assessed during subsequent experiments.

*Sub-Research Question 2: What is the current state of the art regarding self-extinguishment of CLT?*

By performing a literature study of research work carried out on self-extinction of CLT compartments, knowledge gaps will be identified thereby effectively substantiating the scientific relevance of the research carried out in this Master's research project.

### 2.5.2) Experimental Characterisation

As seen in Figure 2, the main research questions requiring experimental verification are those concerning the effect of adhesive type and panel configuration on compartment fire behaviour. Before discussing the experimental set-up that was used to address the research questions, a discussion regarding the choice of adhesive will be presented.

After an introductory discussion with Dr Daniel Brandon from the Research institute of Sweden (RISE), it was established that the current stance towards CLT fire design (as well as scientific research) is to focus on utilising non-delaminating CLT in order to obtain more predictable behaviour. To address the inherent variability resulting from adhesive performance and heat induced delamination, it was, therefore, decided that an adhesive which displays improved fire performance compared to a PU adhesive, is to be used in this study. Delamination fundamentally alters burning

behaviour due to its exposure of virgin timber previously protected by the insulating char layer. Furthermore, due to its unpredictable nature and extent, delamination proves difficult to model using software as well as current design guidelines. Moreover, delamination leads to widely varying charring rates as well as the possible occurrence of a second flash-over which cause fire behaviour to significantly deviate from what would be expected with the charring of a solid piece of timber. By experimentally testing and verifying that a CLT sample manufactured using a certain adhesive type does not delaminate, stable fire performance can be demonstrated and modelling can be simplified.

A discussion of the various types of adhesives used in CLT manufacturing and their influence on fire behaviour is presented in Section 3.3 of this report. As previously stated, the overall research goal of this study is to increase the confidence of designers and regulators alike, in building constructions with combustible materials. Attention will, therefore, be focused on commercially available CLT products and to quantify the fire behaviour of these timber products. In Section 3.3, mention is also made of Phenol Resorcinol Formaldehyde (PRF) as well as Emulsion Polymer Isocyanate (EPI) adhesives. These adhesives were not considered to be used in this research project since they are not commonly used in Europe to adhesively bond timber lamellas in CLT panels. In contrast, based on the commercial availability of PU and MUF/MF adhesively bonded CLT panels in Europe, these adhesive types were considered as most valuable to characterise experimentally. When considering PU or MU/MUF adhesives, it has been substantiated that PU adhesives are prone to heat induced delamination resulting in sustained flaming or flaming re-ignition via a second flashover (Frangi *et al.*, 2009; McGregor, 2013; Medina Hevia, 2014; Crielgaard, 2015; Brandon, 2018a; Su, Lafrance, *et al.*, 2018). Delamination leads to unpredictable fire behaviour (Hopkin, Anastasov and Brandon, 2017), and if avoided will result in more predictable and reliable CLT fire behaviour. In contrast CLT panels bonded with a Melamine-Formaldehyde (MF) adhesive have displayed improved fire performance as compared to PU adhesives by means of delamination avoidance (Brandon (2018a). Furthermore, CLT panels bonded with a Melamine Urea-Formaldehyde (MUF) adhesive were also proven to not significantly delaminate and therefore display improved fire performance as compared to PU adhesively bonded CLT panels (Frangi *et al.*, 2009). Due to the (albeit limited) previous research on MUF/MF adhesives (Frangi *et al.*, 2009; Brandon and Dagenais, 2018), the use of this adhesive type proves to be a promising means by which to avoid delamination. In order to substantiate the selection of a MUF/MF adhesive, Table 1 displays the benefits and drawbacks associated with three CLT adhesives namely commercial PU, thermally resistant PU as well as MUF/MF.



Table 1: Summary of adhesive types and associated benefits and drawbacks

Commercial PU	MUF/MF	Thermally Resistant PU
Benefits:		
<ul style="list-style-type: none"> <li>• Widely Available (Crielaard, 2015)</li> <li>• Substantial scope of experimental work already conducted</li> <li>• Formaldehyde free</li> </ul>	<ul style="list-style-type: none"> <li>• Commercially available</li> <li>• Improved fire performance as compared to PU (Frangi <i>et al.</i>, 2009; Brandon, 2018)</li> </ul>	<ul style="list-style-type: none"> <li>• Same benefits as commercial PU</li> <li>• Less prone to delamination (Su, Leroux <i>et al.</i>, 2018)</li> </ul>
Drawbacks:		
<ul style="list-style-type: none"> <li>• Prone to heat induced delamination</li> </ul>	<ul style="list-style-type: none"> <li>• Contains formaldehyde</li> </ul>	<ul style="list-style-type: none"> <li>• Not commercially available in Europe</li> </ul>

The CLT panels used in this research are supplied by W. u. J. Derix GmbH & Co. (a German producer of CLT and Glue laminated Timber products). Their CLT panels are adhesively bonded using an MUF adhesive (this specific adhesive's product information document is listed in Appendix B.3) and are therefore believed to display improved fire performance as compared to PU bonded panels based on the results of previous research (Frangi *et al.*, 2009; Brandon, 2018). Therefore, subsequent to the aforementioned consideration regarding adhesive types as well as the sponsorship of MUF bonded CLT panels by Derix GmbH, MUF was selected as the adhesive to be experimentally investigated in this research project.

A key concern when considering MUF (and MF) adhesives is the formaldehyde component in these adhesives which is commonly associated with risk to human health and the environment (Frihart and Hunt, 2010). In response to this possible drawback, it has been established that there are emission regulations (in Europe) on structural products, which restrict the emission of volatiles such as formaldehyde. The results of a standardised emissions test on a timber sample adhesively bonded with the same adhesive type that is used during production of Derix's CLT products, is documented in Appendix D of this report. The emission tests results indicate that the emissions are within the allowable limits as stipulated by the "Principles for the Health Assessment of Construction Products", as published by the "German Institute for Structural Engineering" (Deutsches Institut für Bautechnik DIBt). Admittedly, the emission tests were carried out on Glue-laminated (Glulam) timber samples and not CLT samples, but it is reasoned based on the fact that the same adhesive is used to produce Glulam and CLT products by Derix GmbH, that these emission results are also applicable to CLT

samples. Therefore, the tested MUF bonded CLT panels are deemed safe for use due to compliance with emission restrictions.

Returning to the research questions concerning experimental characterisation, a discussion of the experiment to be carried in this research project is presented. Experiments were carried out to quantify the influence of adhesives type and panel configuration.

*Sub-Research Question 3: What is the influence of adhesive type on compartment fire behaviour?*

To answer this question, small scale compartment experiments (0.5x0.5x0.5m internal dimensions, with a single opening measuring 0.18, x 0.5m) were carried out to characterise the difference in obtained fire behaviour between the experiments conducted by Crielaard (2015) using a PU adhesive as compared to a MUF adhesive. These small scale experiments were conducted in an identical manner as compared to Crielaard (2015) to ensure comparability of results. Since the CLT panels tested by Crielaard are of the same species, lay-up and lamella thickness as compared to the CLT panels supplied by Derix GmbH, a practical comparison can be made between the adhesives (PU vs MUF). The producer-specified CLT panel densities are also comparable (namely 470kg/m<sup>3</sup> and 450kg/m<sup>3</sup> in the PU- and MUF bonded CLT panels, respectively).

All fire tests were performed at Efectis Nederland B.V. in Bleiswijk. The samples were placed under a gas extraction hood which was coupled to an exhaust gas analyser (which performs oxygen consumption calorimeter measurements to determine the overall HRR). By measuring the flow rate of propane gas supplied to the propane burners which delivered the input fire in the compartment, the initial fuel load was quantified and as such the contribution of CLT panels to the overall HRR was calculated. Additionally, thermocouples were installed at various depths within the CLT samples and locations within the compartments, to determine charring rates and enclosure gas temperatures, respectively. Figure 3 illustrates the test setup as implemented by Crielaard (2015), which was replicated in the experiments performed as part of this Master's Thesis. Note that a heat flux sensor in the opening of the compartment was not utilised in this study since it restricts the flow of oxygen into the compartment, thereby reducing available ventilation.

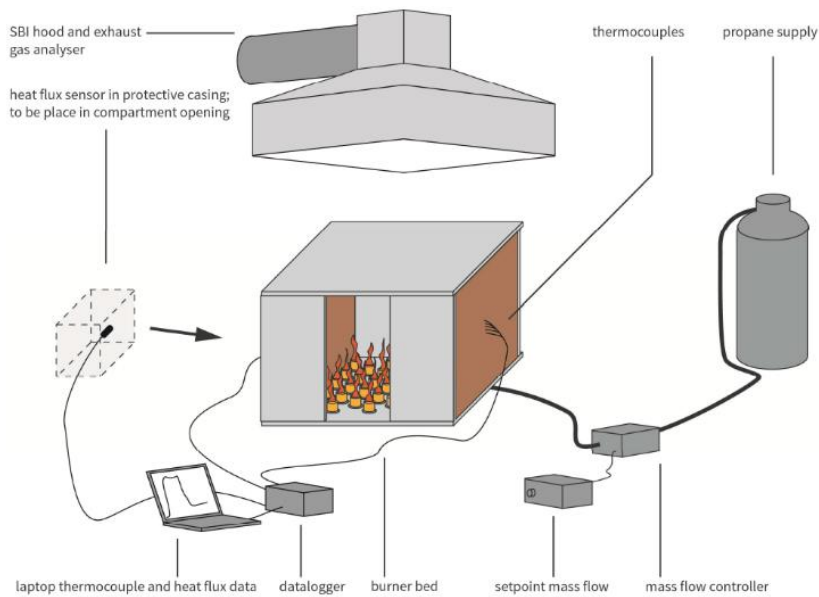


Figure 3: Experimental instrumentation as implemented by Crielaard (2015)

Based on the results of these experiments and subsequent comparison to the results of Crielaard (2015), the influence of adhesive type on fire performance was characterised.

*Sub-Research Question 4: What is the influence of exposed CLT panel configuration on compartment fire behaviour?*

When considering compartment configurations with exposed CLT (both on larger and small-scale) compartments with three exposed CLT panels have displayed burn-through behaviour and failed to self-extinguish in past compartment fire tests due to mutual cross-radiation between exposed CLT panels (McGregor, 2013; Crielaard, 2015; Hadden *et al.*, 2017; Su, Leroux, *et al.*, 2018). It is therefore expected that self-extinction is unlikely to occur with three exposed panels, even when employing a thermally superior adhesive, due to mutual cross radiation. Compartments with at most two exposed CLT walls were therefore investigated in various configurations, including replications based on experiments conducted by Crielaard (2015) involving compartments with an exposed CLT back wall or both CLT side walls. In the interest of clarity, Figure 4 depicts the panel naming convention that is used throughout this report.

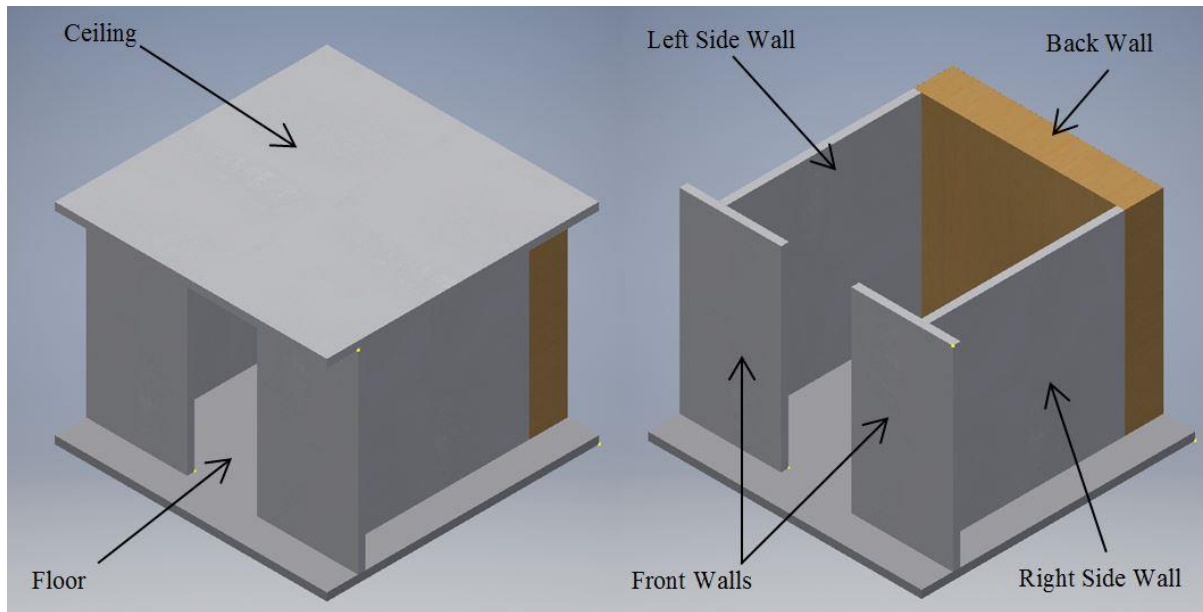


Figure 4: Panel naming convention

To answer sub-research question 4, a series of compartments with varying exposed CLT panel configurations were experimentally tested. In addition to the replication experiments performed to characterise adhesive performance, three more configurations were investigated. All compartment configurations, as investigated in this research project, are listed in Table 2, and the configuration naming convention depicted in this table will be used throughout this report. A visual representation of the various compartment configurations is presented in Appendix A.

Table 2: Compartment configurations

Panel	Configuration MUF-BW: Back Wall	Configuration MUF-2SW: Two Side Walls	Configuration MUF-SW-1: One Side Wall	Configuration MUF-SW-2: One Side Wall	Configuration MUF-C-1 and MUF-C-2: Ceiling	Configuration MUF-BW+C-1 and MUF-BW+C-2: Back Wall and Ceiling
<b>Back Wall</b>	<i>Exposed CLT</i>	Non-combustible	Non-combustible	Non-combustible	Non-combustible	<i>Exposed CLT</i>
<b>Left Side Wall</b>	Non-combustible	<i>Exposed CLT</i>	<i>Exposed CLT</i>	Non-combustible	Non-combustible	Non-combustible
<b>Right Side Wall</b>	Non-combustible	<i>Exposed CLT</i>	Non-combustible	<i>Exposed CLT</i>	Non-combustible	Non-combustible
<b>Ceiling</b>	Non-combustible	Non-combustible	Non-combustible	Non-combustible	<i>Exposed CLT</i>	<i>Exposed CLT</i>
<b>Floor</b>	Non-combustible	Non-combustible	Non-combustible	Non-combustible	Non-combustible	Non-combustible

In Table 2, experiments are labelled according to the following general convention: *Adhesive Type - Exposed CLT Panel(s) – Sample Number*. Note that Configurations MUF-BW and MUF-2SW were only performed once, and as such do not state a sample number. Furthermore, SW refers to a CLT side wall, C a CLT ceiling and BW a CLT back wall.

To facilitate the comparison of adhesive types, comparable experiments containing PU bonded CLT panels as investigated by Crielaard (2015) are assigned similar labels as compared to the MUF bonded CLT panels investigated in this research project. Crielaard tested a compartment that contained an exposed Back Wall, as well as three compartments that contained two exposed CLT side walls, and are labelled to as follows:

- PU-BW : Exposed CLT back wall
- PU-2SW-1: Two exposed CLT side walls (demonstrated burn- through behaviour)
- PU-2SW-2: Two exposed CLT side walls (demonstrated self-extinguishment)
- PU-2SW-40mm: Two exposed CLT side walls with thicker (40mm) outer lamellas (demonstrated self-extinguishment)

By testing these configurations, a detailed investigation into the influence of panel orientation was performed. To the knowledge of the author, no other research has focused, to this extent, on characterising the difference between an exposed CLT ceiling as compared to CLT wall. Table 7 (in the literature study section of this report) summarises the configurations tested by other researchers, as well as the configurations which will be investigated as part of this thesis which were not tested in the particular study

By systematically investigating configurations with ceilings and/or walls, the following hypothesis can be tested:

*An exposed CLT ceiling displays beneficial fire behaviour as compared to an exposed CLT wall.*

The background to this proposed hypothesis is found in the research conducted by Bateman, Bartlett, Rutkauskas, & Hadden (2018), in which it is hypothesised that an exposed ceiling, which would be engulfed by a hot smoke layer during a compartment fire, would effectively not contribute to the formation of an additional hot combustible surface (as would be the case with an exposed CLT wall). In compartments with exposed walls and no exposed ceiling, the hot smoke layer at the ceiling would form a hot surface in addition to the hot surfaces provided by CLT walls after being ignited. By using only an exposed CLT ceiling, a single hot surface is created. This was investigated by comparing the results of configurations containing only one exposed CLT surface.

Furthermore, Table 3 summarises additional comparisons that will be drawn from the fire tests and the relevance of each comparison.



Table 3: Comparisons to be drawn between configurations

Compared Configurations	Relevance
MUF-BW and MUF-2SW vs. PU-BW and PU-2SW	Characterising the influence of adhesive type (MUF vs. PU) regarding fire behaviour of compartments containing exposed CLT.
MUF-BW vs MUF-SW vs MUF-C	Influence of varying the position and orientation of a single exposed CLT panel (back wall vs side wall vs ceiling). The hypothesis of a second hot surface formed with only an exposed wall, compared to a single hot surface with an exposed ceiling, will also be investigated.
MUF-2SW vs MUF-SW	Influence of cross-radiation between two facing exposed walls as compared to only one exposed side wall
MUF-BW vs MUF-BW+C	Influence of adding an exposed CLT ceiling to an exposed back wall
MUF-2SW vs MUF-BW+C	Difference between two exposed side walls and an exposed ceiling and back wall

Table 4 lists the number of tests that were performed per compartment configuration. Configurations BW and 2SW were only tested once since they were directly compared to the results obtained by Crielaard (2015). Other configurations were tested twice. In total, 8 compartment experiments were conducted.

Table 4: Number of tests performed

Configuration	Number of tests to be performed
MUF-BW	1
MUF-2SW	1
MUF-SW	2
MUF-C	2
MUF-BW+C	2

### 2.5.3) Additional experiment to assess the validity of conclusions

Following the experimental methodology implemented by Crielaard (2015) in his compartment tests, the initial fire load (i.e. the propane burner) was extinguished once the first CLT lamella has been charred. Based on these compartment test results, conclusions were drawn. To assess if these conclusions are applicable to longer periods of fire duration (due to the initial fuel load), an additional

experiment was conducted to record charring rates and fire behaviour of CLT panels exposed to a SFC exposure for 90 minutes. This additional test, and the conclusions drawn from it, is documented in Appendix I of this report.

## 2.5.4) Assessing Design Guidelines

*Sub-Research Question 5: Are current prediction models able to simulate the experimentally obtained fire behaviour?*

Subsequent to the experimental tests, verification studies were performed to determine if the recommendations proposed by Brandon (2018b) (see Appendix C) are able to predict the experimentally obtained enclosure temperature development curve as well as HRR contribution by exposed CLT panels. In addition, the applicability of the charring rates as suggested in literature and norms will be compared to the experimentally obtained charring rates. As will be discussed later in this report, the parametric fire curve is unable to demonstrate delamination. Delamination should therefore be avoided and proved to not occur during experiments in order to perform meaningful verification calculations. An investigation into design recommendations concerning lamella fall-off (as suggested by methods such as equivalent gypsum board fall-off in Frangi *et al.* (2009)) will not be assessed due to the focus of this research which is to prevent heat induced delamination.

## 2.6) Research Scope Limitations

Due to the extensive scope associated with the overall research goal presented in Section 2.3 of this report, research limitations were imposed to ensure a clear research focus. The limitations are as follows:

- Focus was on post flashover fire conditions, as this phase is associated with high temperatures and subsequent structural degradation of timber members.
- Loading conditions were not considered in this research project. Unloaded compartments, in which only the configuration of exposed CLT is varied, were tested.
- The influence of active fire protection systems, such as sprinkler and smoke alarm systems was not investigated since the main research aim is to characterise the conditions required to achieve CLT self-extinction in a reliable manner, based on material and geometrical parameters only.
- Only CLT panels that are commercially available in the European timber construction market were considered to be experimentally tested. Novel adhesives such as heat resistant PU do show potential but are not currently being utilised commercially in Europe and were therefore not considered in this research project.
- The difference between timber species as well as strength grades and densities of the base timber and their associated effects on fire performance falls outside the scope of this research.

- A literature study on the different types of adhesives was performed to the extent that the main adhesives types are identified and characterised, as well their associated benefits and drawbacks are identified.
- The main parameters that were investigated experimentally in this research project are the configuration of CLT panels, adhesive used to bond the CLT panels, as well as the amount of exposed timber.
- The influence of structural connections on fire behaviour was not investigated in this research project. Connections in the compartments were designed such that they did not fail during fire conditions and therefore did influence fire behaviour.
- A literature study on fire dynamics, timber combustion and CLT compartment fires was carried out to the point at which it is deemed adequate to address the aforementioned research goals.
- The effect of experimental scale was not investigated. Due to this limitation of performing tests at small scale only, the results obtained from this experimental work are unable to directly predict compartment fire behaviour at real compartment scales. Effects such as cross-radiation between exposed CLT panels are expected to induce other phenomena at larger scales, especially when considering the change in distance between exposed timber surfaces across scales. Thus, the research conducted as part of this Thesis serves as an experimental basis on which to perform future research at larger experimental scales.
- Design recommendations were only compared against the results of small-scale experiments. Due to its simplified nature, the enhanced parametric fire curve verification investigation proposed as part of this research work was also not expected to accurately quantify all aspects of compartment fire behaviour. It is also unable to directly predict fire behaviour at larger scales since it does not account for radiation between exposed panels, nor does it account for panel orientation. Future research is to investigate more advanced models such as zone models or Finite Element models that account for cross-panel radiation and include heat transfer models, as recommended by Hopkin, Anastasov & Brandon (2017).

## 2.7) Sections of the report addressing the research questions

In the interest of clarity, Table 5 below presents as an overview of the sections of this report dedicated to answering the research question and sub-questions postulated in Figure 2.

*Table 5: Overview of sections addressing the research questions*

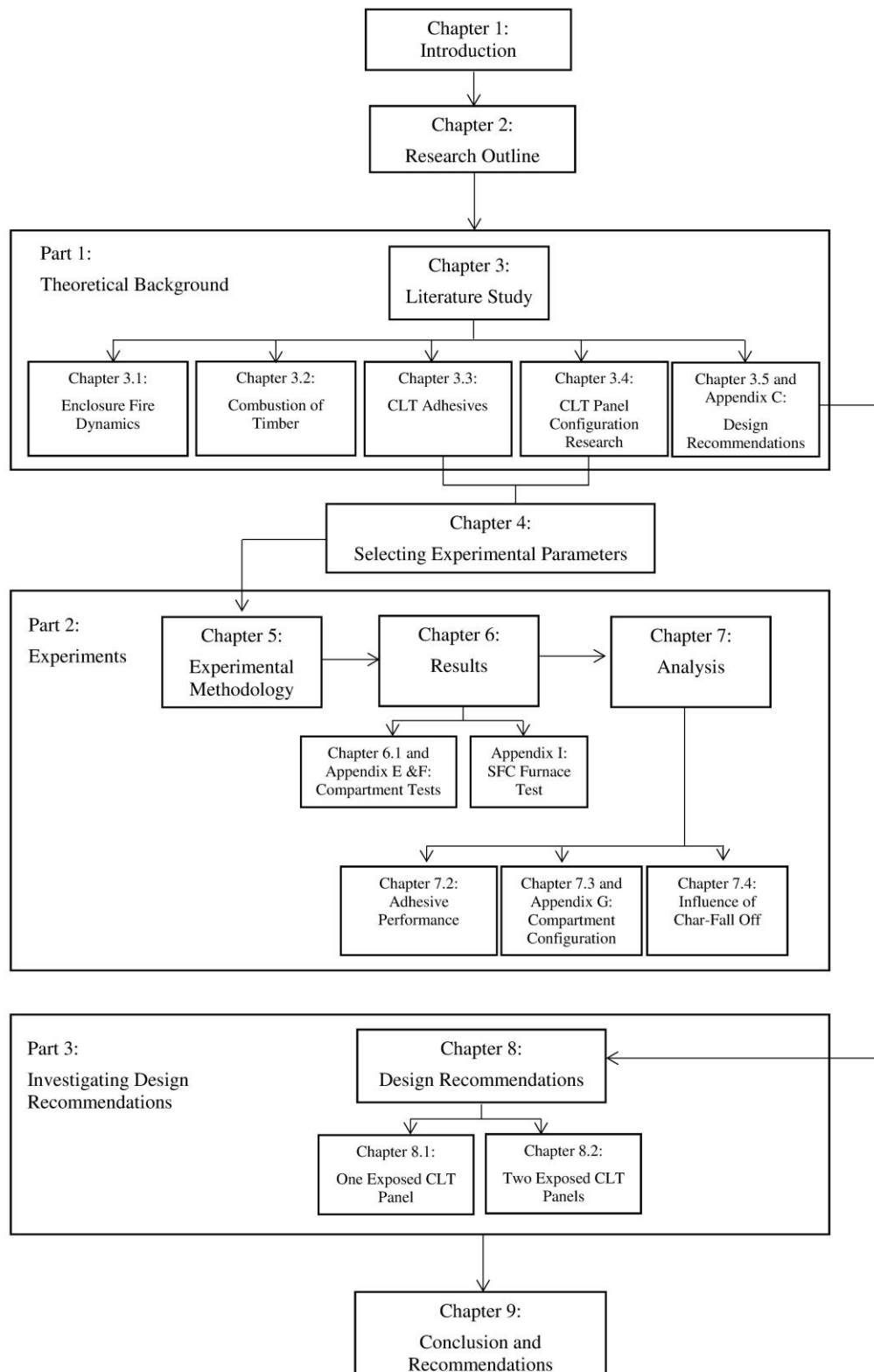
	Section	Reference
Sub-Question 1	Literature Study	§3.1 and §3.2
Sub-Question 2	Literature Study	§3.3 and §3.4
Sub-Question 3	Analysis	§7.2
Sub-Question 4	Analysis	§7.3 and Appendix G
Sub-Question 5	Investigating Design Recommendations	§8

As a general way-finder to this report, the flowchart presented on the next page will guide the reader through the various sections of the report. The same flowchart will be presented at the start of each of the 3 report parts.

The research sub-questions listed in the Table above are assigned to the 3 report parts as follows (as demonstrated in Figure 2):

- Research Sub-Questions 1 and 2 are addressed in Part 1 (Theoretical Background)
- Research Sub-Questions 3 and 4 are answered in Part 2 (Experiments).
- Research Sub-Questions 5 is addressed in Part 3 (Investigating Design Recommendations)

## **PART 1: THEORETICAL BACKGROUND**





### 3) Literature Study

In this section of the report, the fundamental theories behind enclosure fire dynamics, combustion of timber, the influence of adhesives on fire performance and finally the current fire design recommendations pertaining to CLT, are discussed. This serves as a background against which this research project is presented.

The literature summarised in this section of the report seeks to answer the first two sub-questions of this investigation as stated in Figure 2. These two questions are:

*Q1) What are the fundamentals of enclosure fire dynamics as well as timber combustion?*

This research sub-question will be addressed in Section 3.1 and Section 3.2.

*Q2) What is the current state of the art regarding self-extinguishment of CLT?*

This research sub-question will be addressed in Section 3.3 and Section 3.4.

#### 3.1) Enclosure Fire Dynamics

To introduce the fundamentals of fire dynamics, a description of the various stages present during an enclosure fire is presented below, followed by a discussion pertaining to various enclosure fire concepts. Unless referenced otherwise, technical data presented in this section is sourced from Karlsson & Quintiere (1999).

To sustain a fire, three fundamental components are required, namely fuel, oxygen and heat. The combustion process is interrupted only if one of these components is removed. Together these three components form a fire triangle, as depicted in the Figure 5, indicating the inter-related nature of all three components during a fire.



*Figure 5: The fire triangle (Elite Fire, n. d.)*

**Fuel** refers to the available combustible material present. The specific properties of the combustible material have a major influence on the fire behaviour that develops. Denser fuels (for example heavy wood) result in a more prolonged fire with a slower heat development rate, as compared to less dense flammable material (e.g. flammable liquids) that result in a more rapid fire development initially,

followed by a faster fire decay phase. **Heat** is required to bring the fuel to the conditions suitable for ignition (either by piloted- or self-ignition), and **oxygen** is required to sustain the combustion process.

Once all three elements of the fire triangle are present and conditions are suitable, the start of a fire commences. There are five phases during the development of an enclosure fire, namely: ignition, growth, flashover, fully developed phase and eventually decay (depicted in Figure 6, and discussed individually below).

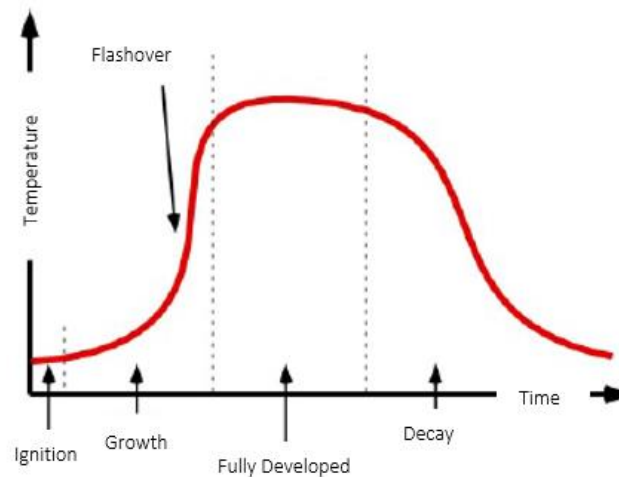


Figure 6: The five phases of a compartment fire (Hartin, 2005)

Prior to discussing each of the fire development phases, it is first noteworthy to mention the limiting factors restricting fire development, namely fuel and ventilation conditions. A fuel-controlled fire refers to combustion that is limited by the availability of fuel (generally during the growth phase). In contrast, a ventilation-controlled enclosure fire refers to combustion that is restricted by the amount of oxygen available (generally during the fully developed phase of the fire).

**Ignition:** this phase commences with the onset of the combustion process, and compartment temperatures start to increase above that of ambient. Ignition itself is facilitated in one of two ways: piloted ignition or spontaneous ignition. Piloted ignition occurs when fuel is physically ignited by another source (for an example a match or propane burner), whereas spontaneous ignition is facilitated if enough heat is available to result in ignition of the produced pyrolysis gases without a pilot flame. Energy is released during this stage, which heats additional combustible material which converts fuels into gases (Walls and Zweig, 2016).

**Growth:** the combustion of fuel occurs during this phase whereby combustion products are released in a gaseous form from fuel. These gases are referred to as *combustion gases* and they rise to the top of the compartment due to their lighter density in comparison to air, forming a layer of elevated temperature (referred to as a *hot layer*). As fuel is heated, pyrolysis gases are produced via a chemical



decomposition process (referred to as *pyrolysis*) during the combustion process. The combustion process is sustained as long there are sufficient amounts of each of the three components of the fire triangle present within the enclosure.

**Flashover:** this phase serves as a transition phase between the stages of fire growth and a fully developed fire. It is characterised by the transition from a few fuel sources combusting within an enclosure, to the rapid engulfment of an entire enclosure and subsequent combustion of all combustible material within it (Svensson, 2002). Flashover is attained as follows: the hot layer containing combustion gases accumulates during the growth stage. This hot layer grows and descends down the height of the enclosure due to the continuous combustion of fuel. Heat is transferred by means of *radiation* and *conduction* from the hot layer to the lower *cold layer*. This in turn results in the heating of more fuel, release of pyrolysis gases and subsequent ignition of other combustible materials within the enclosure. Once compartment temperatures in the cold layer are raised to that of the hot layer post flashover, a single hot layer is formed throughout the whole enclosure.

**Fully Developed Fire:** this phase follows after flashover, and is identified as the stage during which the total energy release rate and temperatures within the enclosure are at their highest. This stage is sustained as long as there is sufficient fuel and oxygen to drive the combustion process. Generally speaking, a typical enclosure fire may produce temperatures ranging from 700 to 1200 °C during this phase.

**Decay:** if an enclosure fire is left to combust without the introduction of new fuel, a point will be reached when the available fuel is depleted. Since the necessary components required to sustain the fully developed phase are no longer available, temperatures drop (Buchanan and Abu, 2017). Generally speaking, fire conditions transition from ventilation controlled to fuel controlled conditions during the fully developed stage and the decay phase, respectively.

To more clearly illustrate the various stages associated with an enclosure fire, Figure 7 is presented (from Svensson, 2002). Note that for a fire to be sustained, sufficient oxygen is required, which in enclosure fires is generally supplied via openings such as windows or doors. In Figure 7, flashover would only be attained if the oxygen supply to the enclosure is sufficient, which would not be the case in a fully enclosed compartment with a closed door such as in the Figure below.

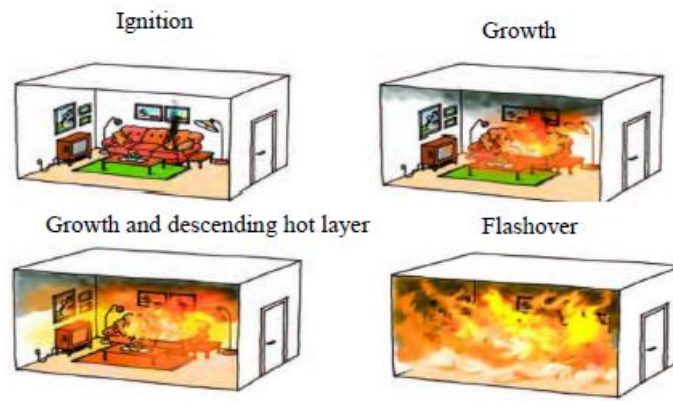


Figure 7: Fire development stages from Svensson (2002)

Various modes of heat transfer are present during the development of a fire. These modes are *radiation*, *convection* and *conduction*. *Radiation* refers to the process by which heat is transferred via electromagnetic waves (for example, heat is radiated from one fuel sources to another fuel source). Radiation is particularly important since it is the main mode by which heat is transferred from the hot layer to enclosure surfaces, from flames to adjacent fuels and from one burning enclosure to the next. In contrast, *convection* is the transfer of heat via the movement of a fluid (i.e. gases and liquids). Heat is either transferred to, or from, a material due to this motion, as for example during the upward transfer of hot gases via buoyancy within the fire plume. Finally, *conduction* refers to the transfer of heat between solids. Heat transfer in this mode is characterised by a heat flux where temperature moves from a region of high temperature to one of lower temperature. It is thus clear that all three of these modes are present in an enclosure fires, although radiation and convection generally govern enclosure fire behaviour (Drysdale, 2001; Buchanan and Abu, 2017).

*Oxygen starvation.* This occurs in enclosures where there are insufficient openings via which to replenish oxygen to sustain the combustion process. As the hot layer grows and descends down the enclosure, fuel becomes entrapped within the hot layer (which contains very little oxygen and high levels of toxic fumes and combustion gases). This entrapment results in fire decay due to starvation of oxygen.

### 3.2) Combustion of Timber

Fire dynamics within an enclosure is also affected by the nature of the combustible material within it. A discussion pertaining to the fundamentals of timber ignition and subsequent combustion will now be presented.

Timber does not burn directly under the influence of a heat source, but first undergoes pyrolysis, which, as mentioned in the previous section, refers to the process during which a fuel undergoes decomposition due to exposure to heat (Browne, 1958). When a timber element is heated, the natural

polymers of which the timber is composed, will be degraded and pyrolysis gases will form along with inorganic ash, liquid tars and a carbonaceous char layer with a low thermal conductivity and density (approximately only 20% the density of the unaffected timber) (Hadden *et al.*, 2017; Bartlett, Hadden and Bisby, 2018). The formation of char is generally assumed to commence at 300°C, and the pyrolysis of timber commencing approximately at 200°C (Bartlett *et al.*, 2015). Under appropriate conditions (refer to the aforementioned fire triangle), the pyrolysis products are ignited and result in flaming combustion of the timber. An important parameter is the critical heat flux to ignite timber. Under piloted ignition the critical heat flux is 12kW/m<sup>2</sup> and 28kW/m<sup>2</sup> for unpiloted ignition (Drysdale, 2001).

Before discussing the phases associated with its pyrolysis, the chemical structure of wood is presented. Generally, wood chemically consists of the following three polymers: *cellulose* (accounting for 50% of the chemical composition), *hemicellulose* (25%) and *lignin* (25%) (proportions vary between species) (Drysdale, 2001). Wood also contains absorbed water and its moisture content depends on the relative humidity and exposure conditions to which the material is subjected. Each of the three polymers will now be discussed individually.

*Cellulose* is a polymer compound which is built-up from glucose molecules. The molecules align themselves, due to their linear structure, into bundles (called microfibrils) which are primarily responsible for the strength and rigidity of the cell wall (and hence the wood). *Hemicellulose* possesses a similar structure to cellulose. *Lignin*, on the other hand is a far more complex chemical constituent. During the growth of the plant, hemicellulose and cellulose are joined by lignin via a process of lignification. Drysdale (2011) states that the pyrolysis temperature of the three constituents are as follows: 200-260°C for hemicellulose, 240-350°C for cellulose and 280-500°C for lignin.

As wood combusts a char layer is formed. The decomposition process generally leaves 15-25% of the original timber mass in the form of char, of which 10-12% originates from the lignin components. The yield from cellulose and hemicellulose is, however, more variable and influences the burning behaviour of wood (reinforcing the notion of natural variability associated with this material) (Drysdale, 2001).

During pyrolysis and subsequent combustion, timber undergoes three main combustion phases, namely (Browne, 1958):

1. Up to 200°C the timber undergoes dehydration during which free water within the timber evaporates as water vapour. The rate of pyrolysis is low if not zero, and small amounts, additional to the evaporated water, of carbon dioxide and carbon monoxide are released.
2. In the range of 200°C to 300°C the polymers of wood are pyrolysed, releasing pyrolysis gases.

3. 300°C to 500°C is the range in which active pyrolysis takes place, and the rate of pyrolysis greatly increases. Char is rapidly formed in this range and results in a higher degree of thermal insulation since the thermal conductivity of char is much lower than the unaffected wood. The wood below the char layer is insulated from high temperatures beyond the char layer. 300°C is considered the temperature at the base of the char layer (White, 2016). Above 300°C the physical structure of wood is broken down and cracks appear, as seen in Figure 8. Volatiles can escape through these cracks leading to an increase in the rate of pyrolysis. As the char layer depth increases, these cracks become more pronounced and result in the characteristic “crazed” crack pattern associated with combusted wood, also referred to as alligatoring/crocodiling (Drysdale, 2001).

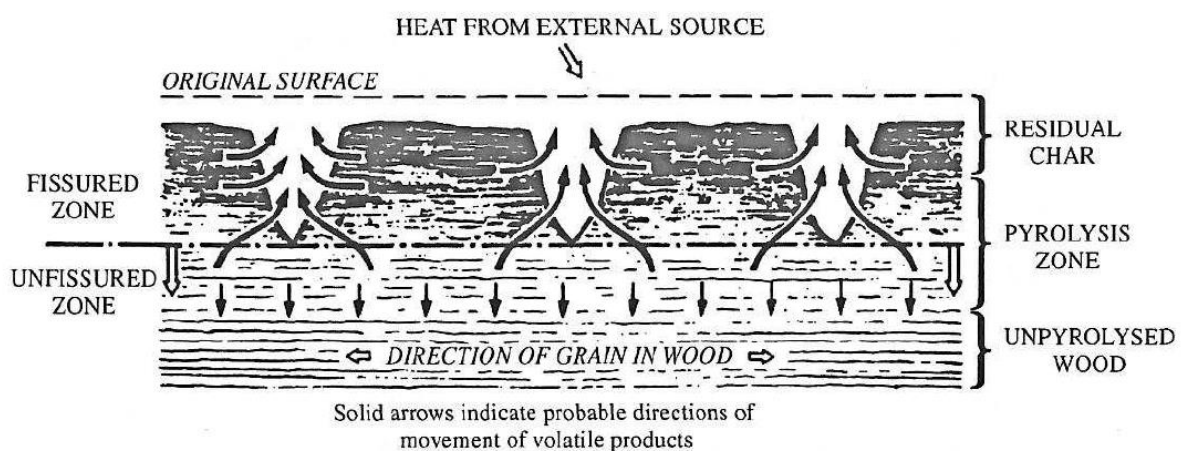


Figure 8: Graphical representation of the timber pyrolysis process, from Roberts (1971)

4. Above 500°C secondary oxidation of chars occurs whereby the thickness of the char layer is reduced and results in further pyrolysis and additional heating of the wood.

The various zones within a pyrolysing and combusting wood sample are illustrated in Figure 9: note the char layer, the char base pyrolysis zone as well as the unaffected wood. As mentioned before, the temperature at the base of the char layer is assumed to be 300°C. This will be used during experiments to calculate the depth of char and subsequently the charring rate. It should, however, be noted that a certain depth below the char layer is subjected to an elevated temperature (later referred to in EN1995-1-2 as the zero strength layer  $d_0$ ), and is labelled the pyrolysis zone in Figure 9.

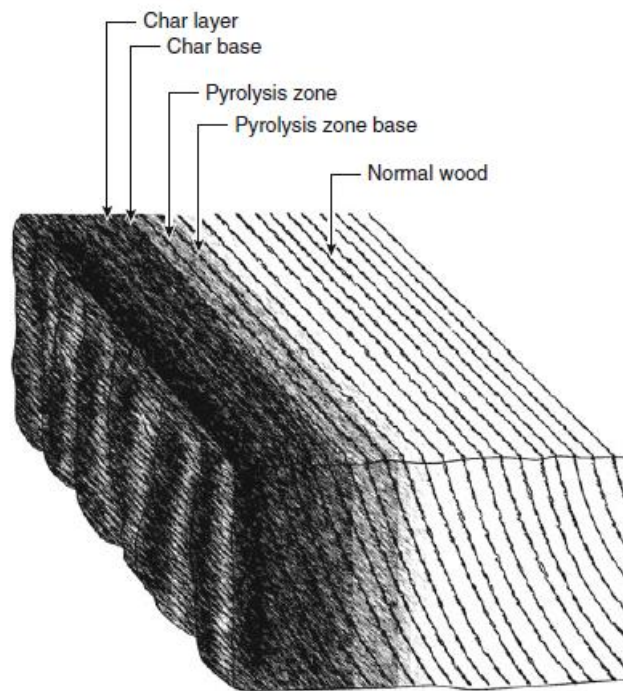


Figure 9: Zones within combusting timber (White, 2016)

The fire resistance capability of exposed timber is summarised in the following statement by the Society of Fire Protection Engineers: *“The fire-resistive characteristics of exposed wood members are due to the insulative characteristics of the char layer and the sharp temperature gradient beneath the base of the char layer.”* (White, 2016).

A distinction is also to be made when considering the cross-sectional size of structural timber elements when exposed to a fire. According to Gerard, Barber and Wolski (2013), most forms of timber products are generally divided into two categories, namely *light timber frame* and *heavy timber frame* members. Light timber frame members encompass structural members with cross-sections ranging from 50mm x 100mm to 50 x 300mm. In contrast, heavy timber frame members possess cross-sectional sizes of 150mm x 150mm and greater.

Light timber frame members are generally wall members consisting of timber studs and floor members composed of joist members. The general design philosophy pertaining to these timber members is to fully encase them with non-combustible boards (such as gypsum boards) to obtain satisfactory fire performance.

Heavy timber frame members include solid sawn sections as well as engineered timber products such as Glue-laminated (Glulam) wood, Laminated Veneer Lumber (LVL) as well as CLT. The satisfactory fire performance of these members may be achieved by encapsulation or by relying on

natural insulative nature of combusting timber via the formation of a char layer, as discussed earlier in this section of the report.

### 3.3) Influence of Adhesives on CLT fire performance

As a general background to this section of the report, an overview of the manufacturing process of CLT panels is presented in Appendix B.1 of this report. The type of adhesive used to bond panels within CLT elements during manufacturing has a significant influence on fire performance, and will be discussed in this section of the report.

The type of adhesive used in CLT has been proven to be an influential factor as it governs the occurrence of delamination (Frangi *et al.*, 2009). Delamination is defined in ASTM D907 (2015) as: “the separation of layers in a laminate because of failure of the adhesive, either in the adhesive itself or at the interface of the adhesive and the adherent”.

Before discussing the results of studies into the influence of adhesives on CLT fire performance, a discussion of the different adhesive types is first presented.

Currently, the most widely used adhesive during the production CLT (in Europe) is ***Poly-Urethane (PU)*** (Johansson and Svenningsson, 2018). PU adhesives are attractive due to their fast curing times at ambient temperatures. PU adhesives are generally single component adhesives which do, therefore, not require premixing before application. ***Melamine Formaldehyde (MF)*** is less frequently used to adhesively bond CLT boards, since the addition of melamine in MF adhesives is expensive. This has led to the addition of urea to create ***Melamine Urea Formaldehyde (MUF)*** to reduce production costs (Pizzi and Mittal, 2003). ***Emulsion Polymer Isocyanate (EPI)***, are two component adhesives that display favourable wood to wood bonding properties and do not require curing at high temperatures (Johansson and Svenningsson, 2018). EPI adhesives are generally not used to bond lamella layers in CLT products, but some producers such as Stora Enso employ EPI adhesives to edge bond individual planks within a panel (Crielaard, 2015). ***Phenol Resorcinol Formaldehyde (PRF)*** is a dark brown adhesive, which makes it less aesthetically pleasing than colourless adhesives. It is commonly used in North America during the production of Glulam beams. PRF shows good structural performance, long-term performance, strength at elevated temperatures as well as being a cheaper adhesive to manufacture (Johansson and Svenningsson, 2018).

The performance of different types of adhesives is discussed in the report by Brandon & Dagenais (2018). In their study several CLT samples, produced using various adhesive types, were tested in an intermediate scale furnace (1.0 x 1.0 x 1.0m). The CLT samples were tested in a horizontal configuration which represents the layout most prone to delamination. The CLT samples were all identical except for the adhesive used and measured 1.4m by 0.6m with 5 lamellas each 35mm thick, totalling to a thickness of 175mm. Four types of adhesives were tested including: PU; MF; EPI and

PRF. An additional modified (i.e. thermally resistant) PU adhesive type (labelled PU2) was also tested and compared against a commercially available PU bonded CLT elements (labelled PU1) to assess its effectiveness to avoid delamination.

The exact formulation of the adhesives tested in this study is not stipulated. As such it is advised that the results and conclusions drawn from this particular study are only valid for the specific adhesive specimens tested, and as such the results are not representative of all PU, MF, EPI and PRF adhesive types.

CLT samples were subjected to a *natural fire temperature-time curve* which included a growth, fully developed and decay phase. The target and experimental gas temperature-time curve (on which the investigation was based) is displayed in Figure 10. Test 1-4 in the legend of Figure 10 refers to the study by Su *et al.* (2018) on which this particular adhesive study was based. Test 1-4 by Su *et al.* (2018) consisted of an enclosure (9.1m x 4.6m x 2.7m (width x depth x height)) constructed of PU adhesively bonded CLT panels. All the walls as well as the floor of the enclosure were protected from fire by gypsum boards, whereas the CLT ceiling was left exposed. During the experiment, delamination and a subsequent second flashover were recorded and are clearly visible in Figure 10. In short, the fire exposure conditions stipulated in the adhesive comparison study by Brandon and Dagenais (2018) were based on the experimental compartment temperatures obtained by Su *et al.* (2018), although the experimental occurrence of a second flashover was neglected. Plate thermometers installed inside the furnace at 100mm and 150mm distances from the CLT specimens were used to calibrate the obtained fire exposure.

Note that a *natural fire temperature curve* seeks to address the shortcomings of the Standard Fire Curve (SFC), since the SFC does not include a decay phase and does not account for compartment geometry, ventilation opening sizes, fuel load nor the thermal properties of the compartment boundaries. Natural fire curves are generated by including the aforementioned factors in the establishment of a temperature vs. time fire curve (Karlsson and Quintiere, 1999).

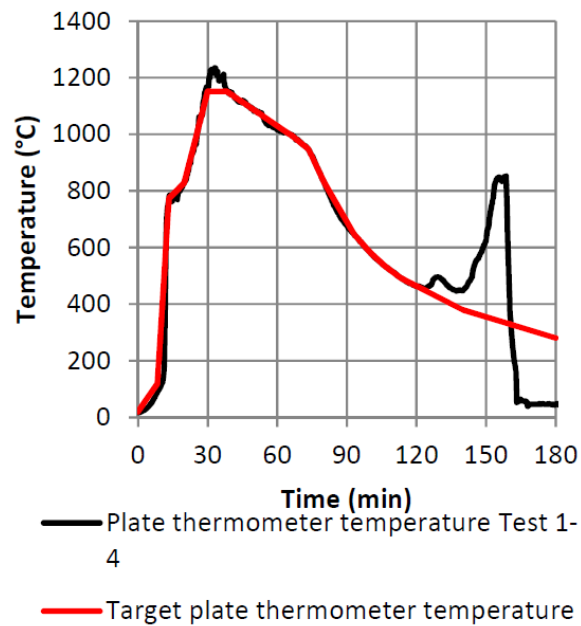


Figure 10: Target and (an) achieved temperature-time curve as reported in Brandon & Dagenais (2018)

In their study, Brandon and Dagenais (2018) assumed that the depth of the 300°C isotherm within the thickness of the specimen was the point at which the timber was transformed to char via the combustion processes. Figure 11 depicts the experimentally obtained (average) charring depth vs time curve for the 5 different adhesive types. It is important to note that a sudden increased rate in charring represents lamella delamination, as seen in Figure 12 (this was also recorded by Crielaard (2015) as well as Frangi *et al.*, (2009) in their experiments involving PU adhesively bonded CLT panels ). Due to the performed averaging of all the individual experiment results, distinct charring rate peaks are not as evident in Figure 11, but it is illustrated that a commercially available PU adhesive (PU1) performs poorly in comparison to MF, EPI and PU2.



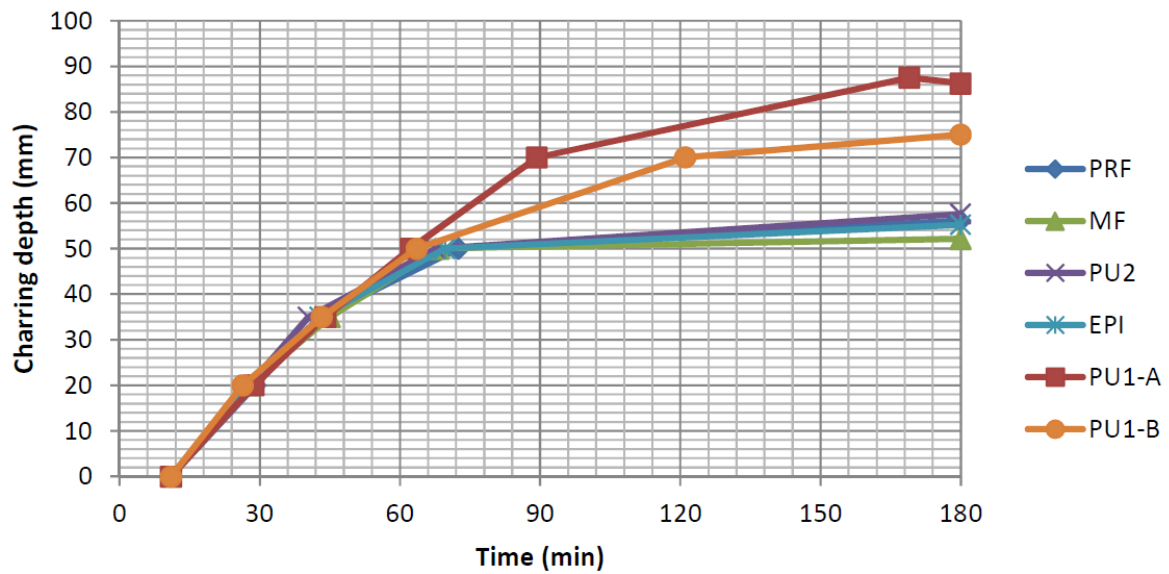


Figure 11: Charring depth vs time per adhesive type, as reported by Brandon & Dagenais (2018)

Johansson & Svenningsson (2018) also reported on the findings of the same investigation referred to previously. Delamination is more clearly illustrated in Figure 12, since individual experimental results depicting average charring rate vs. time, per specimen set are shown (two samples of each adhesive were tested).

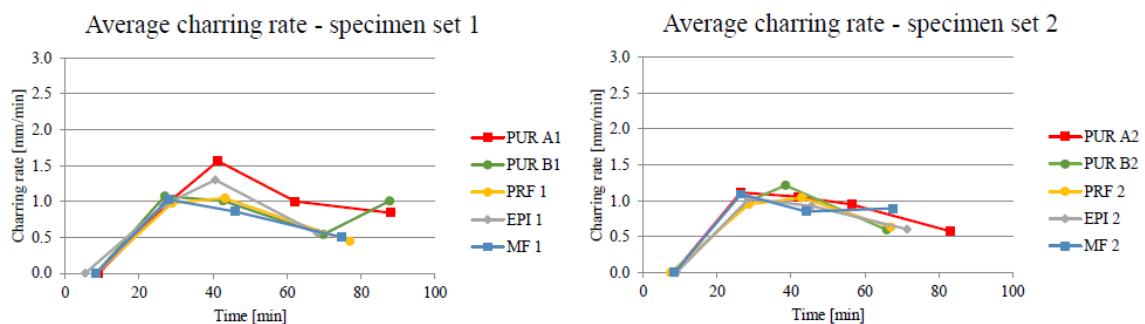


Figure 12: Average charring rate per sample set, as reported by Johansson & Svenningsson (2018)

Figure 12 indicates for specimen set 1 that PU Type 1 (the commercially produces PU bonded sample) displayed the highest charring rate. Note that the naming convention of PU1 and PU2, as reported in Brandon & Dagenais (2018), is changed to PUR A and PUR B, respectively in Johansson & Svenningsson (2018). In addition, it was reported following visual observations that the entire first lamella delaminated in both PU Type 1 samples, and the second lamella as well in the first sample of PU Type 1. A summary of the visual observations of delamination is shown below in Table 6. From this table it is clear that PU1 (commercially available PU) displayed a higher occurrence of delamination, whereas MF and PRF were resistant to delamination.

Table 6: Visual observation of delamination, as reported by Johansson & Svenningsson (2018).

Specimen	Observed Delamination?	Comments	Time until visually observed delamination [min]
PUR-A1	YES	Complete delamination of first and second lamella	52 min (first lamella) 2 h, 43 min (second lamella)
PUR-A2	YES	Complete delamination of first lamella, partial delamination of the second lamella	50 min (first lamella) 2h, 58 min (second lamella)
PUR-B1	NO	-	-
PUR-B2	NO	-	-
PRF-1	NO	-	-
PRF-2	NO	-	-
EPI-1	NO	-	-
EPI-2	Partial	Larger part fell off towards the end, no ignition of the underlying layer	1h, 24 min (parts of first lamella)
MF-1	NO	-	-
MF-2	NO	-	-

### 3.4) Overview of CLT compartment fire behaviour research

To substantiate the scientific relevance of the research presented in this report, an overview of the current state of the art pertaining to the fire behaviour of compartments constructed of exposed CLT is presented. Table 7 presents an overview of previous research conducted on this specific topic. Furthermore, Table 7 also lists the exposed CLT panel configuration tested by the various authors. To illustrate the relevance of the compartment configurations tested as part of this study, the configurations which are investigated in this thesis which were not tested in the particular study are also listed.

Table 7: Overview of research CLT compartment fire behaviour

Author(s) and date	Title	CLT adhesive type	Exposed surfaces	CLT	Compartment Size (width x depth x height)	Configuration not Addressed
McGregor (2013)	Contribution of Cross Laminated Timber Panels to Room Fires	PU	Fully unprotected	CLT compartment	3.5m x 4.5m x 2.5m	No partially exposed CLT compartments
Medina Hevia (2014)	Fire Resistance of Partially protected Cross-Laminated Timber Rooms	PU	Back Wall and one side wall  Both Side walls  One Side wall		3.5m x 4.5m x 2.5m	No exposed ceiling tests

Crielaard (2015)	Self-extinguishment of Cross-Laminated Timber	PU	Back Wall  Back and both side walls  Both side walls	0.5m x 0.5m x 0.5m	No exposed ceiling tests
Li <i>et al.</i> (2016)	Real-Scale Fire Tests on Timber Constructions	PU	Same as McGregor (2013) and Medina Hevia (2014)	3.5m x 4.5m x 2.5m	Same as McGregor (2013) and Medina Hevia (2014)
Hadden <i>et al.</i> (2017)	Effects of exposed cross laminated timber on compartment fire dynamics	PU	Back and one side wall  Back wall and ceiling  Back wall, one side wall and ceiling	2.72m x 2.72m x 2.77m	No direct comparison between an exposed wall and an exposed ceiling
Bateman <i>et al.</i> (2018)	Effects of Fuel Load and Exposed CLT Surface Configuration in Reduced-Scale Compartments	PU	Back and one side wall  Back wall and ceiling	0.64m x 0.66m x 0.64m  And 0.58m x 0.66m x 0.70m	No direct comparison between an exposed wall and an exposed ceiling.
Su <i>et al.</i> (2018)	Fire Safety Challenges of Tall Wood Buildings – Phase 2: Task 2 & 3 – Cross Laminated Timber Compartment Fire Tests	PU	One side wall  Ceiling  Ceiling and one side wall	9.1m x 4.6m x 2.7m	No comparison between two exposed side walls
Su, Leroux, <i>et al.</i> , (2018)	Fire testing of rooms with exposed wood surfaces in encapsulated mass timber construction	Thermal resistive PU (brand name HBX)	Back wall and 10% of ceiling  Ceiling  Both side walls and ceiling	4.5m x 2.4m x 2.7m	No comparison between two exposed side walls, and an exposed wall vs ceiling

A discussion of each of the research items listed in Table 7 will be individually presented in this section of the report.

### 3.4.1) McGregor (2013): CLT Room Fires

McGregor (2013) performed a series of 5 experiments that sought to determine the contribution of CLT to fire development, fire duration as well as fire intensity. The CLT panels used in the experiments were 105mm thick 3-ply panels and were used to construct either fully protected (by two layers of gypsum boards) or fully exposed compartments. The initial fire load was supplied via either a propane burner or furniture. The compartments all measured 3.5m x 4.5m x 2.5m (width x depth x height) and contained a single door measuring 1.07m x 2.0m (width x height), resulting in an opening factor of  $0.042 \text{ m}^{0.5}$ . An overview of the 5 experiments is presented in Table 8.

*Table 8: Tests performed by McGregor*

Test Number	1	2	3	4	5
Fully Protected (FP) / Unprotected (FU)	FP	FP	FU	FP	FU
Initial Fire Load Source	Propane Burner	Furniture	Propane Burner	Furniture	Furniture

HRR, enclosure temperatures and charring rates were recorded during each of the experiments. Table 9 displays the input heat release (in  $\text{MJ/m}^2$ ) for the 5 experiments as well as the observed heat release (also in  $\text{MJ/m}^2$ ). Tests 3 and 5, which involved unprotected CLT enclosures, demonstrated that the CLT panels increased the observed heat release during the experiments. In Test 3, the propane burners supplied an input heat of  $182 \text{ MJ/m}^2$  and the CLT panels contributed  $408 \text{ MJ/m}^2$ . In Test 5, the input furniture fire load was measured at  $366 \text{ MJ/m}^2$  and the CLT panels contributed  $612 \text{ MJ/m}^2$ . Test 5 was prematurely extinguished, suggesting that the actual total heat release during the experiment would be higher if allowed to burn further. In order to compare the propane and furniture input fuel sources, it was estimated that propane fires resulted in 68% of the fire load imposed during the furniture initial fuel load tests.

Table 9: Heat release values as recorded by McGregor (2013)

	Propane		Furniture		CLT	Total Heat Release (MJ/m <sup>2</sup> )
	Actual Heat released (MJ/m <sup>2</sup> )	Furniture equivalent (MJ/m <sup>2</sup> )	Measured Heat released (MJ/m <sup>2</sup> )	Estimated Fire Load (MJ/m <sup>2</sup> )	Calculated Heat Released (MJ/m <sup>2</sup> )	
Test 1	486	710	-	-	200	686
Test 2	-	-	379	533	-	379
Test 3	182	266	-	-	408	590
Test 4	-	-	364	553	-	364
Test 5	-	-	366	529	612	978

A key finding from this study was that when the charring front reached the adhesive layer, the PU adhesive debonded and resulted in delamination of whole CLT lamellas. Delamination led to an increase in the fire intensity after the depletion of the initial fire load and extended the fire duration. Additionally, when comparing the fully protected vs unprotected compartments, the exposed CLT result in an increased fire growth rate and the time to flashover was reduced. When comparing the HRR, the fully exposed CLT compartments resulted in approximately a doubled HRR as compared to the protected compartments. To illustrate the contribution of exposed CLT to total heat release, Figure 13 shows a comparison of the Total energy Released (TER) vs time curves for the 5 experiments. The fully unprotected compartments (Test 3 and 5) displayed approximately double the TER of their comparable protected compartment tests (Test 1 and 2 respectively). Test 3 resulted in an overall charring rate of 0.63 mm/min, whereas Test 5 yielded a charring rate of 0.85 mm/min. (due to the occurrence of delamination which exposed virgin lamellas in the CLT panels)

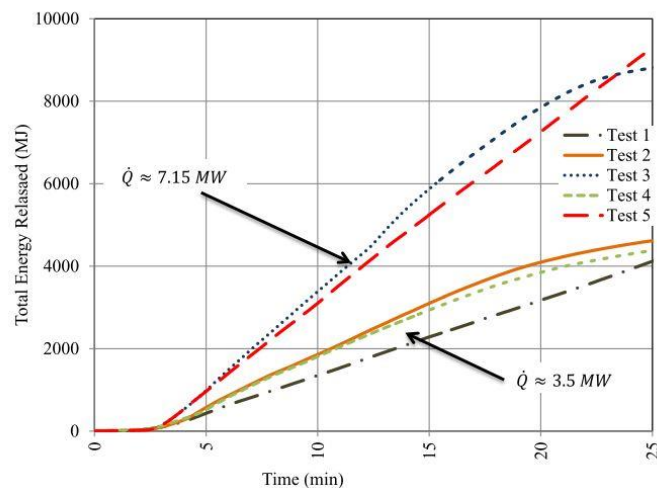


Figure 13: Total HRR as reported by McGregor (2013)

The main limitation of McGregor's research is that the experiments were not allowed to run till extinction since experiments were extinguished prematurely. A systematic study of the achievement of self-extinction was also not recorded. It was however concluded that the fully protected compartments achieved self-extinguishment after the depletion of the fire load, whereas self-extinguishment was not achieved in fully exposed CLT compartments due to delamination.

### 3.4.2) Medina Hevia (2014): Partially Protected CLT Timber Rooms

Medina Hevia (2014) continued the research of McGregor (2013) by investigating the effect of partially protected compartments on compartment fire behaviour. The overall aim of the research was to determine a suitable panel configuration that allows for the maximum exposed CLT area in the compartment whilst still resulting in similar fire behaviour to a fully protected CLT compartment. Three tests were conducted to characterise these effects, and are reported in Table 10.

*Table 10: Experiments carried out by Medina Hevia (2014)*

Test Number	1	2	3
Fire Load	Furniture and Clothes		
Unprotected Walls	Rear and one side wall	Both side walls	One side wall
Unprotected area as a percentage of the total interior surface area (excluding the door opening)	28.8 %	32.4%	16.2%

The partially protected CLT compartments measured 3.5m x 4.5m x 2.5m (width x depth x height) and were constructed (in Test 1 and 2) from 105mm thick 3-ply CLT panels (identical to the CLT panels used by McGregor). Test 3 made use of a different 3-ply CLT panel: each ply was also 35mm thick but the individual planks per ply were wider. Both types of CLT panels were manufactured using a PU adhesive. A single door, measuring 1.069m x 2.0m, was also placed on the shorter front wall, resulting in an opening factor of 0.042 m<sup>0.5</sup>. The fuel load was kept constant between the three experiments and was estimated to be 531.6 MJ/m<sup>2</sup>.

It was found that the HRR in tests involving 2 exposed CLT walls resulted in a much higher HRR as compared to the experiment containing only one exposed CLT wall, and also led to a slower temperature decrease rate. Furthermore, it was recorded that the HRR in Test 2 was higher than that of Test 1, suggesting that exposed panels that face one another experience greater cross-radiation than adjacently orientated exposed panels. During Experiment 1 and 2, delamination of whole lamellas was observed and caused spikes in the recorded HRR which prevented the occurrence of self-extinguishment. In contrast, Experiment 3 with only one exposed CLT wall did not undergo delamination and self-extinguishment was observed. It was concluded that a compartment with one

exposed wall displayed comparable fire behaviour to the fully protected compartment fire tests performed by McGregor (2013). Furthermore, the averaged charring rate of Tests 1, 2 and 3 were 0.69, 0.77 and 0.71 mm/min respectively.

### 3.4.3) Crielaard (2015): Self-extinguishment of CLT

Crielaard studied the conditions under which CLT may undergo self-extinguishment. Two sets of experiments were carried out to quantify the heat flux (and air flow conditions) resulting in smouldering extinction of CLT as well as the influence of compartment configurations on the achievability of self-extinction.

In his first experimental series, Crielaard tested small samples, measuring 100mm x 100mm x 500mm (width x breadth x height) in an ISO 5660-1 certified cone calorimeter and a separate cone heater. The cone calorimeter was used to subject the CLT sample to an initial heat flux of 75 kW/m<sup>2</sup> until a char layer of 20mm had formed. Subsequent to forming this char layer, the samples were transferred to a separate cone heater and exposed to a heat flux ranging between 0 and 10 kW/m<sup>2</sup>. Additional to the lower heat flux imposed in the second stage of the experiment, a fan supplied airflow over the sample surface to quantify the influence of airflow on the achievement of self-extinguishment. Based on these tests, Crielaard concluded that the threshold heat flux resulting in self-extinguishment of CLT is in the range of 5 to 6 kW/m<sup>2</sup>. Furthermore, it was found that an air flow speed of 1.0 m/s and a secondary heat flux of 6kW/m<sup>2</sup> resulted in burn-trough of the sample. It was subsequently postulated that an airflow speed of 0.5 m/s in combination with a heat flux lower than 6 kW/m<sup>2</sup> results in self-extinguishment.

In his experimental series, Crielaard additionally investigated small scale compartments (0.5m x 0.5m x 0.5m internal dimensions, with an opening of 0.18m by 0.5m, yielding an opening factor of 0.042m<sup>0.5</sup>) to further quantify the conditions required to achieve self-extinguishment of CLT. The compartments were constructed with 100mm thick 5-ply PU adhesively bonded CLT panels. The floor, ceiling and certain walls per configuration were constructed of non-combustible boards. In addition, a compartment constructed of CLT panels with thicker outer lamellas (40mm instead of 20mm) were tested to demonstrate the potential of a thicker outer lamella to prevent heat induced delamination. The 4 different tested compartment configurations are displayed in Figure 14.

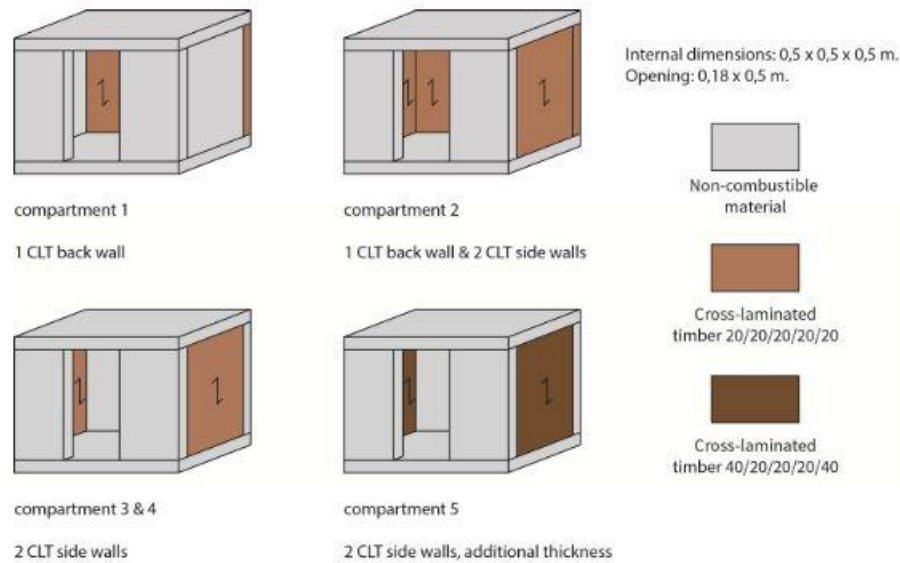


Figure 14: Compartment configurations as tested by Crielaard (2015)

A series of 5 compartment fire tests were carried out by Crielaard, and are summarised in Table 11. The table also lists the experimental names assigned to compartments that were investigated in the adhesive comparison analysis of Master's Thesis research project.

Table 11: Compartment experiments, reproduced from Crielaard (2015)

Experiment Number	CLT Panels	Remark	Experiment Name assigned in this report
1	Back wall	-	PU-BW
2	Back and both side walls	-	-
3	Both side walls	-	PU-2SW-1
4	Both side walls	Repetition of Experiment 3	PU-2SW-2
5	Both side walls	Thicker outer lamellas (40mm instead of 20mm)	PU-2SW-40mm

The input heat in the compartment tests was supplied by a bed of 7 rows each with 5 burners. The propane mass flow to the burners was adjusted in each experiment to obtain a HRR of 41kW. Note though that in the 1<sup>st</sup> experiment, the input propane HRR was 62kW but was adjusted after 12 minutes to 42 kW. The HRR supplied by the propane burners as well as the contribution of the CLT panels to the fuel load is illustrated in Table 12. The propane burners were switched off when a charring depth of 20mm was recorded.



Table 12: HRR as recorded by Crielaard (2015)

Experiment	Propane Input [kW]/(m <sup>2</sup> floor)	Average Total [kW]/(m <sup>2</sup> floor)	CLT contribution [kW]/(m <sup>2</sup> floor)	Increase
1	62 (248)	78(312)	16(64)	26-39%
1 after 12 minutes	41(164)	57(228)		
2	41(164)	110(440)	69(92)	168%
3	41(164)	102(408)	61(122)	149%
4	41(164)	95(380)	54(108)	132%
5	41(164)	79(316)	38(76)	93%

The total energy release rates (in MJ) were also measured, and are displayed in Table 13.

Table 13: Energy release measurements by Crielaard (2015)

Experiment	Propane [MJ]/(m <sup>2</sup> floor)	Total [MJ]/(m <sup>2</sup> floor)	CLT contribution [MJ]/(m <sup>2</sup> CLT)	Increase
1: Back Wall	112(448)	169(676)	57(228)	51%
2: Back Wall and Both Side Walls	77(308)	386(1544)	309(412)	401%
3: Two Side Walls	55(220)	240(960)	185(37)	336%
4: Two Side Walls	62(248)	183(732)	121(242)	195%
5: Two Side Walls *	63(252)	134(536)	71(142)	113%

\* Test 5 involved a thicker outermost lamella that was exposed to the fire (40mm instead of 20mm)

Crielaard recorded an averaged charring rate of 0.77mm/min in the compartments that burned-through. Compartment 1, 4 and 5 self-extinguished, whereas experiments 2 and 3 burned through via sustained flaming combustion and a second flashover respectively. It was also concluded that delamination had a severe influence on fire behaviour and resulted in a smouldering CLT panel being reignited and reverting back to flaming combustion, or in the continuation of flaming combustion. Additionally, exposed CLT panels increases the HRR and the total energy released during a fire as well as increasing the fire duration.

### 3.4.4) Li *et al.* (2016): Real-Scale Fire Tests on Timber Constructions

In this study, the results of McGregor (2013) and Medina Hevia (2014) are summarised and analysed. The following conclusions are drawn:

- Experiments with exposed CLT panels resulted in increased fire growth rates, reduction in the time to flashover, but did not increase the enclosure temperature in the top layer.
- The total energy released (TER) in the fully unprotected compartments was approximately double that of the fully protected compartments during the fully developed phase of the fire.
- Delamination occurred in the fully unprotected compartments as well as compartments with 2 unprotected CLT walls, but not in compartments with only one exposed wall. Delamination had a serious effect on the fire behaviour of the CLT compartments as it increased the measured energy release rates and extended the fire duration.
- Delamination and subsequent secondary flashover occurred earlier in the compartment test with two facing walls as compared to two adjacent walls due to direct cross-radiation between two facing CLT panels.
- In a compartment with only one exposed CLT wall (accounting for 29.7% of the total wall area) self-extinguishment was achieved and this compartment displayed comparable fire behaviour to the fully protected compartment test.
- It was recommended that further studies should investigate the behaviour of CLT panels manufactured from a more heat-resistant adhesive, especially adhesives with melting points higher than 300°C.

### 3.4.5) Hadden *et al.* (2017): Effects of exposed CLT on compartment fire dynamics

In this study, the influence of exposed CLT on compartment fire dynamics was investigated by means of experimental tests and analysis. Three compartment (labelled Alpha, Beta and Gamma) configurations were tested in compartments constructed of plasterboard and exposed CLT. The compartments' internal dimensions were 2.72m x 2.72m x 2.77m, and were constructed in three geometrical configurations, as displayed in Table 14. The opening factor of all the compartments was  $0.042 \text{ m}^{0.5}$ . The input fuel load was supplied by wooden cribs, measured at 56kg in all the experiments and yielding a fuel load of  $132 \text{ MJ/m}^2$ .

Table 14: Experimental configurations as tested by Hadden et al. (2017)

Experiment Name	Alpha	Beta	Gamma
Number of Repetitions	2	2	1
Exposed CLT surfaces	Back and side wall	Back wall and ceiling	Back wall, ceiling and side wall
Exposed Timber Area (m <sup>2</sup> )	15	14	22

Two main conclusions were formulated based on the experimental results. Firstly, delamination severely inhibits the potential of CLT compartment to achieve self-extinction since virgin timber becomes exposed to high heat flux leading to flaming combustion (as seen in experiment Beta, repetition 2). Compartments with two exposed CLT surfaces were able to self-extinguish unless delamination occurred. Secondly, compartments with three exposed CLT panels did not self-extinguish due to radiative heat exchange between the exposed timber surfaces, preventing heat flux in the compartment to drop below the threshold for self-extinguishment. It was observed in the first Alpha configuration experiment that localised char fall-off occurred in the ceiling panel, which resulted in partial delamination of the ceiling panel, as seen in the image below:

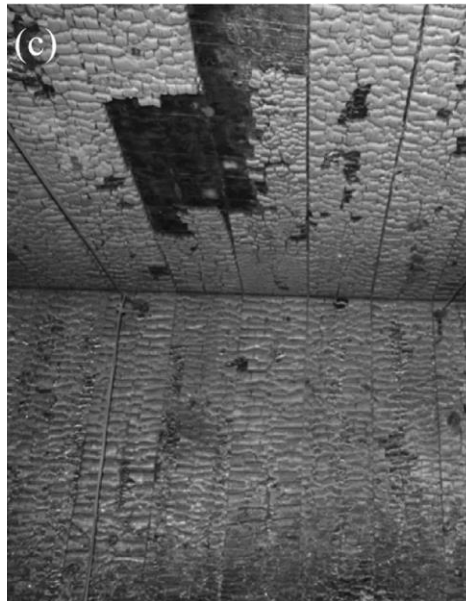


Figure 15: Localised char fall-off on the ceiling panel. From Hadden et al. (2017)

Other conclusions included:

- Char fall-off is likely to occur earlier in exposed panels that are horizontally orientated as compared to vertically due to the influence of gravity.

- Maximum compartment temperatures are not significantly different between compartments with exposed timber walls and compartments constructed of non-combustible materials.
- Ceiling CLT panels experienced lower char depths than back wall panels, possibly due to lower oxygen availability at the ceiling which lowers the pyrolysis rate.

It is also noteworthy to mention that plasterboard encapsulated walls in the Alpha-configuration experiments experienced extensive fall-off during the fire tests, whereas this was not observed in the Beta-configuration experiments.

### 3.4.6) Bateman *et al.* (2018): Effects of Fuel Load and Exposed CLT Surface Configuration in Reduced-Scale Compartments

In this study, Bateman *et al.* (2018) attempted to continue the work of Hadden *et al.* (2017) by further investigating the effect of varying the initial fuel load as well as the effect of varying compartment configurations. This was done by conducting experimental tests on two compartment configurations, labelled Alpha and Beta. The (small-scale) compartments with dimensional parameters as listed in Table 15.

Table 15: CLT compartment experiments conducted by Bateman *et al.* (2018)

Experiment	Width (mm)	Depth (mm)	Height (mm)	Exposed CLT Area (m <sup>2</sup> )	Exposed CLT Panels	Opening Factor (m <sup>0.5</sup> )
Alpha	637.5	660	637.5	0.83	Back and Right Side Walls	0.043
Beta	575	660	700	0.78	Back wall and Ceiling	0.042

Two fuel load sizes (namely low and medium) were investigated by placing two different wood crib sizes within the compartments. The Alpha-experiments were subjected to both a low and medium fuel loads, whereas compartment Beta was tested using both these fuel loads as well as an additional high fuel load. The low fuel load totalled  $47.26 \pm 9.42$  MJ/m<sup>2</sup>, the medium fuel load  $104.39 \pm 1.22$  MJ/m<sup>2</sup> and the high fuel load  $277.19 \pm 4.22$  MJ/m<sup>2</sup>. The general results of the 5 experiments are listed in Table 16.

Table 16: Visual Observations by Bateman *et al.* (2018)

Experiment	Time to Flashover [minutes:seconds]	Time to fuel burnout [min]	Time to Secondary Flashover	Auto-extinguished?
Alpha Low	5:00	16	43	No
Alpha Medium	5:30	30	90	No
Beta Low	5:00	20	-	Yes
Beta Medium	5:30	27	-	Yes
Beta High	5:30	70	-	No

In general, compartment configuration Beta, with one exposed back wall and ceiling, underwent self-extinguishment whereas in configuration Alpha (back and one side wall exposed) a second flashover that prevented the attainment of self-extinguishment due to sustained burning. Additionally, self-extinguishment was not achieved in the Beta configuration subjected to a high fuel load, especially since the fuel load occupied a significant volume of the compartment, required more time to burnout and led to the burn through of the CLT panels.

Bateman *et al.* (2018) hypothesises that configuration Alpha displayed worse fire behaviour as compared to configuration Beta due to the accumulation of smoke at the ceiling which acts as an additional hot surface. As smoke accumulates at the ceiling, any exposed CLT surface that does not coincide with the ceiling would experience heat exchange with the hot smoke layer. If the exposed CLT surface coincides with the ceiling, the formation of an additional “hot surface” is prevented. Furthermore, in the two Alpha-configuration experiments, lamella delamination was observed at the instance the charring depth reached the adhesive line. Delamination resulted in the exposure of uncharred timber and the fire behaviour reverting to flaming combustion. It was recorded, as was also done by Hadden *et al.* (2017), that ceiling panels displayed lower charring depths and as such were less prone to delamination.

### 3.4.7) Su *et al.* (2018): Cross Laminated Timber Compartment Fire Tests

In this study, CLT compartments measuring 9.1m x 4.6m x 2.7m (width x depth x height) were constructed from 175mm thick 5-ply CLT. Two ventilation opening sizes were tested by testing compartments with door sizes of either 1.8m x 2.0m or 3.6 x 2.0m, resulting in an opening factor of  $0.03\text{m}^{0.5}$  and  $0.06\text{m}^{0.5}$  respectively. Table 17 displays the details of the 6 compartment tests. The initial fuel load, in all 6 experiments, was supplied by furniture and was measured to vary between 548 and 556 MJ/m<sup>2</sup>. The performed experiments are listed in Table 17.

Table 17: Compartment tests as performed by Su et al. (2018)

Experiment	Exposed CLT surfaces	Opening Factor ( $\text{m}^{0.5}$ )
1	Fully protected	0.03
2	Fully protected	0.06
3	One side wall	0.06
4	Ceiling	0.03
5	One side wall	0.03
6	Ceiling and one side wall	0.03

Experiment 1 and 2 (fully protected compartments) served as baseline tests. The ventilation opening sizes were varied between the two experiments. With its smaller opening, Test 1 displayed a longer fully developed fire phase. The large opening in Test 2 facilitated faster burning of the fire load and resulted in a shorter fully developed fire. Test 2 also resulted in more external flaming suggesting that compartments with larger openings result in more severe external fire conditions but less severe conditions within the compartment. When comparing these two baseline tests with the partially exposed compartments, flashover occurred earlier in experiments 3 through 6 compared to experiments 1 and 2.

When comparing experiment 3 and 5, an increased ventilation opening resulted in an increased HRR and increased external heat flux. More heat was entrapped in the compartment with a smaller opening (experiment 5), and after the occurrence of delamination a second flashover was observed. Experiment 5 also yielded 3.6 times more volume of charred CLT as compared to experiment 3.

All compartments with exposed CLT surfaces, except experiment 3 with the increased ventilation opening, did not undergo self-extinction due to either sustained flaming conditions or a second flashover due to lamella delamination. This is displayed in Figure 16 which compares the HRR of the various experiments. Experiment 6, with an exposed ceiling and one side wall did not display a decay phase, whereas experiments 3, 4 and 5 experienced fire-regrowth during the decay phase due to delamination.

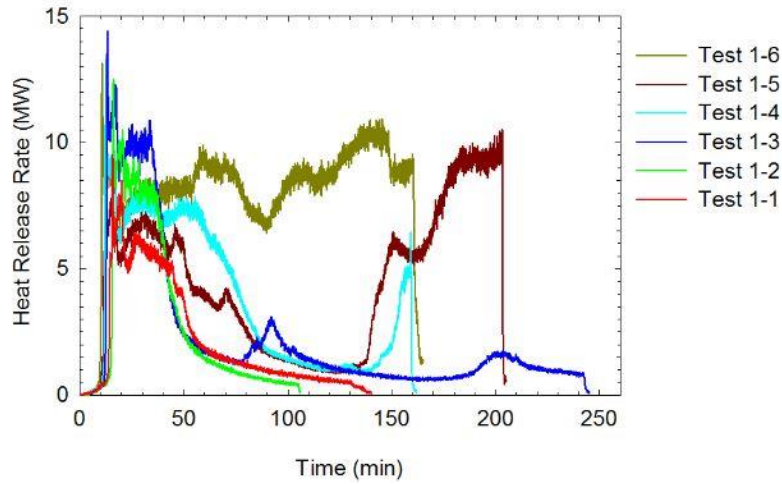


Figure 16: HRR of the 6 experiments as recorded by Su et al. (2018)

The contribution of CLT to the peak HRR was also quantified. A distinction was made in test 5 and 6, since unexposed surfaces became involved in the fire at specific times in the two tests (after 70 minutes in Test 5 and 75 minutes in Test 6). Two regression lines are reported for the two tested ventilation conditions, and are depicted in Figure 17.

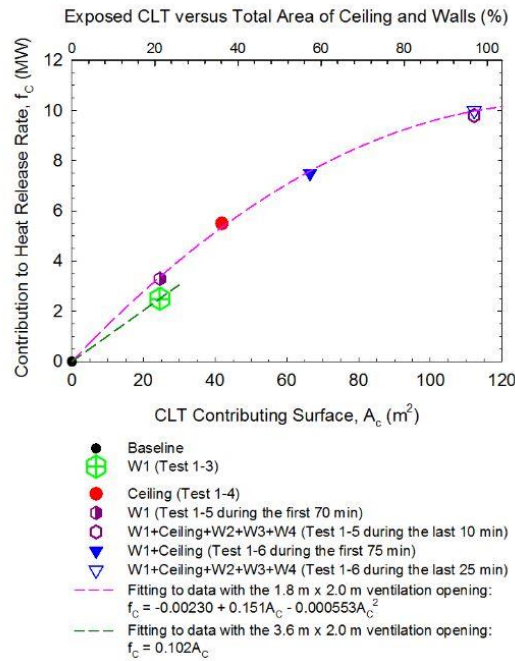


Figure 17: Estimation of the contribution of exposed CLT surfaces to the peak HRR, from Su et al. (2018)

Experiment 4 and 5 displayed severe second flashovers with the HRR rising sharply after the occurrence of delamination during the decay phase. In contrast, Experiment 3 (one exposed side wall with a larger ventilation opening) displayed less severe peaks in the HRR despite observed delamination.

### 3.4.8) Su, Leroux, *et al.*, (2018): Fire testing of rooms with exposed wood surfaces in encapsulated mass timber construction

This study demonstrated the potential of a novel thermally resistant PU adhesive to prevent the occurrence of heat induced delamination. CLT compartments, measuring 4.5m x 2.4m x 2.7m (width x depth x height) with a door of 0.76m x 2m (resulting in an opening factor of  $0.03\text{m}^{0.5}$ ), were constructed from 175mm thick 5-ply CLT panels bonded with a thermally resistant PU adhesive. 5 experiments with various exposed CLT panel configurations were carried out, and are displayed in Table 20. Partially exposed Glulam beams and columns were also installed in Experiments 3 and 4, but will not be discussed in this report. It is, however, important to note that Experiment 3 was conducted with protected CLT panels and partially exposed Glulam beams and columns. The initial fire load was supplied by wooden cribs with a calculated fire load density of  $550\text{MJ/m}^2$ . The composition of exposed panels per experiment is depicted in Table 18.

*Table 18: CLT Compartments as tested by Su, Leroux et al. (2018)*

Experiment	Exposed CLT panels	Exposed Glulam beams/columns
1	Fully Protected	N/A
2	Back wall and 10% of the ceiling	N/A
3	Fully Protected	11.5% / 24.5% of the perimeter
4	Ceiling	6.4% / 12.6% of the perimeter
5	Both side walls and the ceiling	N/A

All compartment tests with exposed CLT panels did not display significant delamination when the charring front passed through the glue line of the thermally resistant PU adhesive, and thereby greatly improved fire behaviour. Additionally, a general observation was made that the charring rate decreased as the charring depth increased. Initially, the char rate was in the order of 0.6-1.0mm/min and subsequently reduced. Self-extinction was recorded in Experiment 1 (the baseline fully protected compartment), 2 and 4. With both side walls and the ceiling exposed in Test 5, the two exposed side walls were reignited late in the decay phase and resulted in a sharp peak in the enclosure temperature. This study demonstrated the potential of a new PU to avoid the occurrence of heat induced delamination and the achievement of self-extinguishment in compartments with (approximately) only one exposed CLT surface (either a wall or a ceiling). These conclusions are enforced by the compartment temperature-time curves as shown in Figure 18. It was recorded that even with the occurrence of a second flashover in Experiment 5, that char remained intact on the CLT panels even after the charring front had passed through the adhesive line, demonstrating the ability of this adhesive to resist delamination.



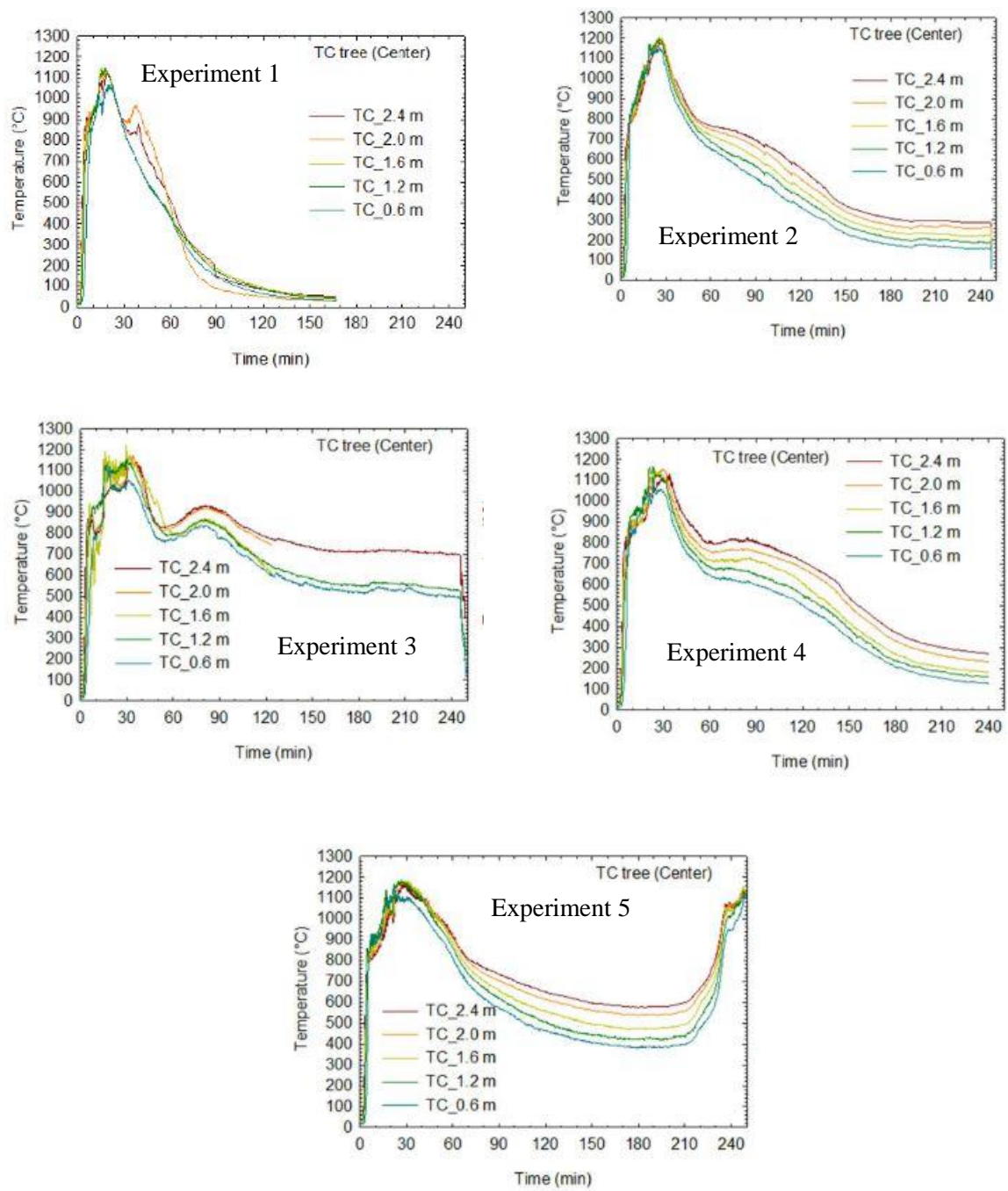


Figure 18: Temperature Time Curves as recorded by Su, Leroux et al. (2018)

### 3.5) A review of fire design recommendations

Now that the fundamentals of fire dynamics and timber combustion have been laid, a description of current design recommendations related to compartments containing exposed timber can be presented. In Appendix C of this report, a description of various types of fire curves is first presented, followed by the Eurocode codification of timber charring, a design recommendation that seeks to characterise the contribution of combustible CLT to the overall fuel load, and finally a brief description of zone modelling.

These design recommendations discussed in Appendix C will be investigated in Chapter 8 of this report.

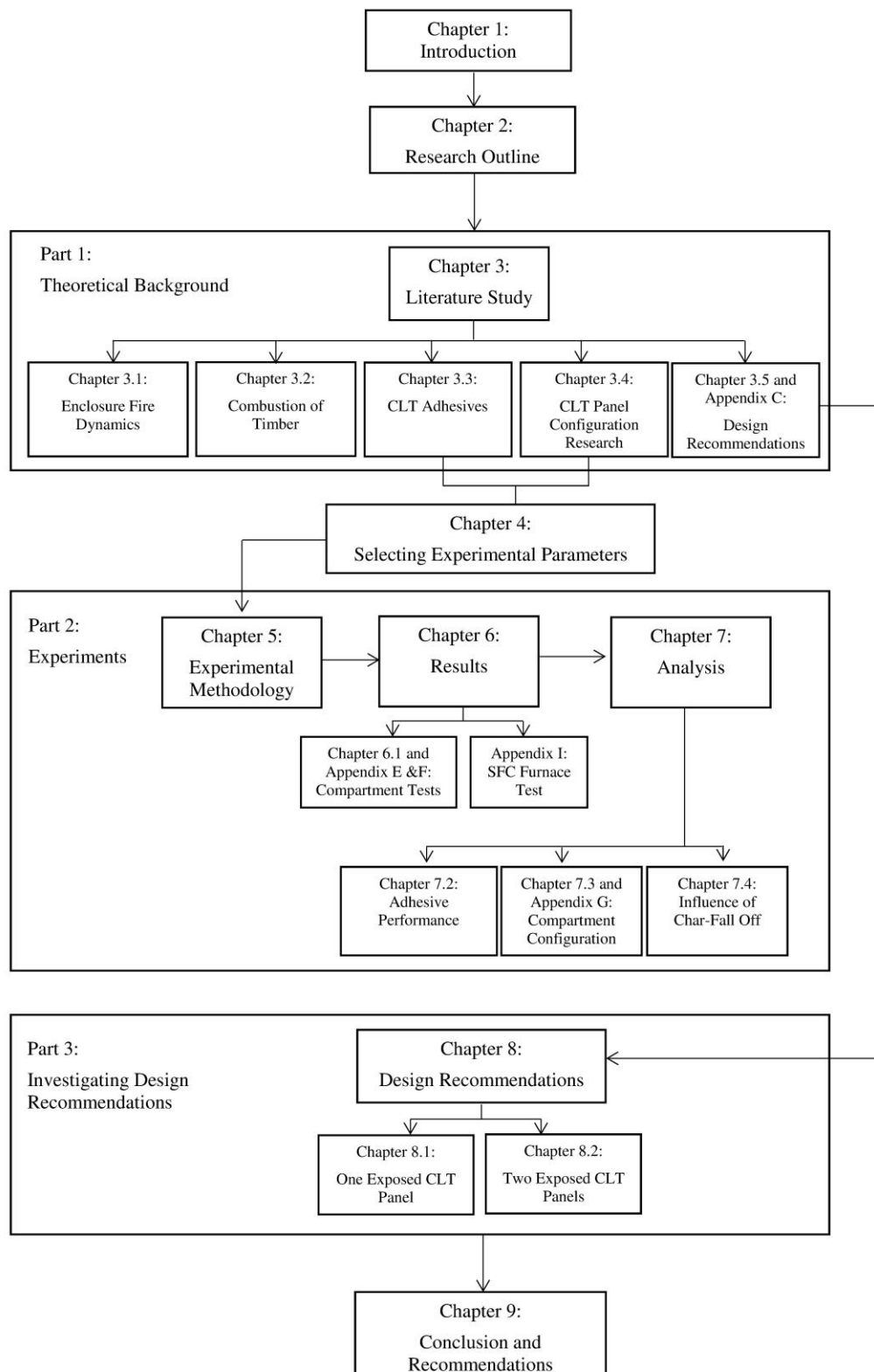
### 3.6) Chapter Conclusion

This chapter provided the theoretical basis on which the enclosure fire experiments of this research project were conceived and analysed. The fundamentals of enclosure fire dynamics, timber combustion, fire performance of CLT adhesives, as well as recent research on compartments containing exposed timber were presented. By discussing these theoretical topics, the first two sub-research questions of this study (as presented in Figure 2) were addressed.

In general terms, enclosure fire dynamics is a complex and inter-related system which depends on various parameters, one of which is the presence of combustible materials (such as exposed CLT). In turn, the fire performance of exposed CLT is influenced by the type of adhesive used to bond lamella with CLT panels, as well as the relative orientation of CLT panels within an enclosure. Research has been conducted into the aforementioned fire engineering topics, and the experiments conducted as part of this research project aim to further broaden the available body of knowledge pertaining to the performance of CLT in fire.

In addition, by systematically reviewing design recommendations related to the design of timber elements subjected to fire, the theoretical foundation is laid for the design recommendation investigation presented in Chapter 8 of this report.

## **PART 2: EXPERIMENTS**





## 4) Selecting Experimental Parameters

Based on the literature study presented in the previous chapter of this report, the rationale behind the selection of experimental parameters used in this investigation, are substantiated. The main parameters include the selection of CLT adhesive type to be investigated as well as the configuration of exposed CLT panels within compartments. And will be discussed individually.

### 4.1) Adhesive Type

Based on the information document in Section 3.3, it is clear that the adhesive type used to bond CLT lamella during production has a significant influence on the fire behaviour of CLT samples. It is therefore desired that a commercially available CLT product is to be tested as part of this investigation. Since melamine-based adhesively bonded CLT panels have been reported to demonstrate improved fire performance as compared to PU bonded CLT panels, it was decided to test MUF bonded CLT panels. Concerns regarding formaldehyde emissions of MUF bonded CLT panels are addressed in Section 2.5.2 as well as Appendix D.

### 4.2) Exposed CLT Panel Configuration

Based on the review of previous compartment fire tests, self-extinguishment is unlikely to occur in compartments with 3 or more exposed CLT surfaces. As such a restriction of a maximum of two exposed CLT surfaces is implemented in this study to investigate the influence of adhesive type and panel configuration on the attainability of self-extinguishment. To facilitate the comparison between two adhesive types (namely MUF and PU), the compartment configurations as tested by Crielaard (2015) with at most 2 exposed CLT panels are replicated in this investigation. As such, the following compartment configurations will be investigated:

- Compartment configuration with an exposed CLT back wall, as also investigated by Crielaard (2015)
- Compartment configuration with both side walls constructed of exposed CLT, as also investigated by Crielaard (2015)

Various researchers have investigated the influence of CLT panel configuration on enclosure fire behaviour, as documented in Section 3.4 of this report. Based on these tests, the following compartment configurations were selected as most pertinent to investigate further:

- Medina Hevia (2014) demonstrated that an enclosure with two exposed CLT side walls display longer fire durations as compared to an enclosure with only one side wall. To confirm this assessment, compartment configurations with only one CLT side wall (Configuration SW-1 and SW-2) and two CLT side walls (SW2) are investigated.

- Based on the research by Hadden *et al.*, (2017) and Bateman *et al.*, (2018), it is suggested that ceiling panels experience less charring than exposed walls (back or side walls). To investigate this observation further, compartment configurations with only an exposed CLT ceiling (Configuration C-1 and C-2) are tested in this investigation.
- To assess the influence of panel orientation in compartments containing two exposed CLT panels, an additional configuration containing an exposed CLT ceiling as well as CLT back wall was selected. Based on the work by Bateman *et al.*, (2018), it is suggested that a compartment configuration with an exposed back wall and ceiling, displays improved fire performance as compared to a compartment with an exposed back wall and one side wall. Based on this indication from previous compartment tests, it was decided to investigate a compartment configuration with a CLT back wall and CLT ceiling (Configuration BW+C-1 and BW+C-2) as an additional compartment configuration.

## 5) Experimental Methodology

In this section of the report, the experimental set-up of a series of fire tests is documented. As mentioned in Section 2 of this report, the methodology implemented by Crielaard (2015) was followed in this investigation. The general methodology is that small scale compartments constructed of combustible CLT and non-combustible panels in varying panel orientations, are subjected to an initial fire, allowed to transition to smouldering combustion and then assessed if self-extinguishment of the exposed CLT occurs.

According to the followed methodology, the compartments are subjected to a 41kW design fire. This amount of energy was experimentally determined by Crielaard (2015) such that the amount of external flaming occurring at the opening of the compartment was kept to a manageable level as to not damage any of the experimental equipment. All compartments are exposed to this design fire until a charring depth of 20mm is achieved at the centre of all exposed CLT panels. This level of charring reflects the formation of char layer in a CLT panel in a real fire. In a real fire, Crielaard hypothesised that after the formation of a 20mm char layer, the initial fire load present in a compartment would have been consumed. Upon the decay of the initial fire load, the exposed CLT panels are the only combustible material available to fuel the fire.

By performing experiments that follow the methodology of Crielaard (2015), as well as by using CLT and non-combustible panels comparable to those used by Crielaard, it is possible to draw a practical comparison between the results of Crielaard and this study. This facilitates the comparison of adhesive performance in CLT panels exposed to fire conditions. Furthermore, additional CLT and non-combustible panel configurations are tested in this study as compared to Crielaard (2015), which allows additional conclusion pertaining to the influence of compartment configuration to be drawn.

In this section of this chapter, a discussion of the equipment used, the specimens that were prepared as well as the experimental procedure that was followed is presented.

### 5.1) Equipment

The equipment used to capture data during the various experiments included a burner bed fuelled by a propane gas bottle, a gas extraction hood and associated exhaust gas analysis equipment to perform oxygen-consumption calorimetry, thermocouples to record CLT and compartment temperatures, a timber moisture content sensor as well as a video recorder.

#### *Burner Bed with propane gas supply*

To deliver the design fire of 41kW, a burner bed with 7 rows each containing 5 burners (each with a capacity of 26kW and head diameter of 40mm) was used. The burner bed encompasses a square area

of approximately 0.4m by 0.4m. The burner bed is elevated from the floor by placing it on top of concrete blocks. Additional concrete blocks were placed around the burner bed on which the various compartments were placed. The burner bed was allowed to protrude through the non-combustible floor panel of each compartment. This was done by drilling 50mm holes in the floor panel of each compartment in a pattern that corresponds to the burner bed. Figure 19.a) depicts the burner bed as well as the concrete blocks, whereas Figure 19.b) depicts the protrusion of the burner bed through the floor panel of a compartment. Moreover, to ensure that no additional ventilation openings are created by drilling holes in the floor panel that are larger than the burner head diameter, a layer of ceramic wool was placed on the floor on the inside of each compartment, as shown in Figure 19.b).

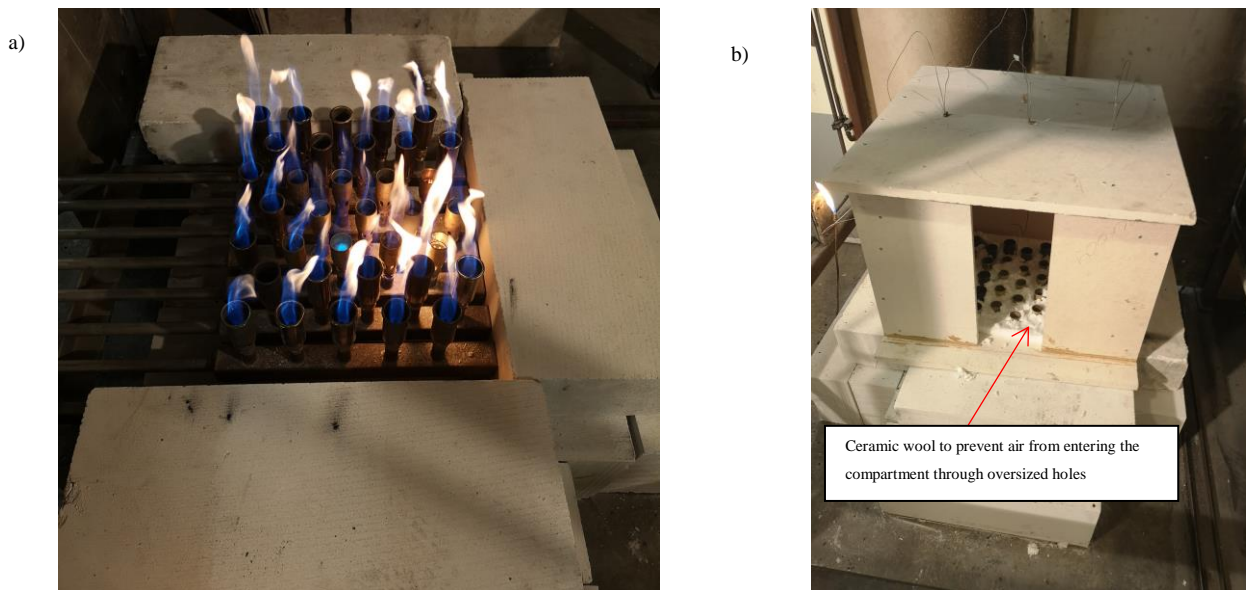


Figure 19: a) Burner bed and concrete blocks to facilitate placement of compartment. b) Burner bed protruding through the floor panel of a compartment

#### *Gas extraction hood and exhaust gas analyser*

A gas extraction hood and coupled exhaust gas analyser were used in these experiments to determine the total HRR as supplied by the design fire and the contribution of the combustible CLT to the fire. The gas analyser was used to perform oxygen calorimetry which is used to measure the total HRR during the experiments. Care was taken before each experiment to ensure that the gas analyser was calibrated to predefined concentrations of  $\text{CO}_2$  and  $\text{O}_2$ , such that reliable gas analysis was facilitated. As a background, oxygen calorimetry involves the calculation of total amount of heat being released per unit time (i.e. total HRR) based on the amount of oxygen being consumed. A relationship exists between oxygen consumption and HRR, and additional gas measurements (such as  $\text{CO}_2$ ) can be used to account for incomplete combustion (Drysdale, 2001). The compartments were placed on top of the aforementioned burner bed and positioned in such a way that the rising combustion gases were extracted into the hood during the various experiments.



### *Thermocouples*

Type K mantle thermocouples, 1mm in diameter, were placed inside the depth of CLT panels as well as inside a compartment in each tests. The data obtained from these thermocouples are used to assess the ability of the CLT to extinguish per configuration, as well as calculate the charring rate per CLT panel.

To record enclosure temperatures, thermocouples were placed in the middle of each compartment and suspended to a height of 0.2m and 0.4m from the floor of the compartment. This is illustrated in Figure 20. In Configuration 2SW, SW-1 and SW-2 additional thermocouples (also elevated to 0.2m and 0.4m from the floor panel and along the centre axis of the compartment) were installed in front of the left and right panels to be able to quantify the cross-radiation between exposed side CLT panels.

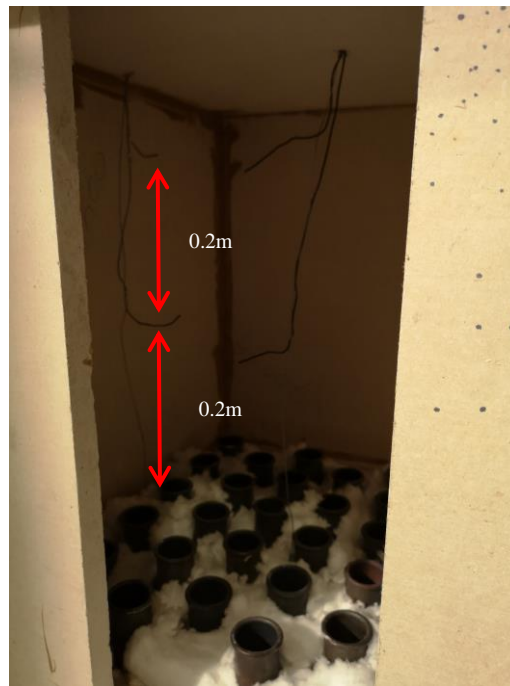


*Figure 20: Position of thermocouples to record enclosure temperatures*

To record the charring rate of an individual CLT panel, thermocouples were embedded at the centre of CLT panel. These thermocouples were installed at different depths as measured from the inside of the compartment (henceforth referred to as the fire side). Holes were drilled from the outside (cold side) using a 2mm drill bit to a depth of 20mm, 30mm, 40mm, 50mm and 60mm as measured from the fire side. These holes were spaced closed to one another to obtain the charring behaviour at the centre of a CLT panel. Figure 21.a) displays a thermocouple group installed in a side CLT wall as well as a thermocouple group installed in front of the CLT panel to quantify cross-radiation. Figure 21.b) depicts the typical configuration of a thermocouple group (where depths of thermocouples are quoted as the distance between the tip of the thermocouple and the fire exposed side of the panel). The thermocouples were installed in a circular pattern as indicated in the Figure (all dimensions in mm).

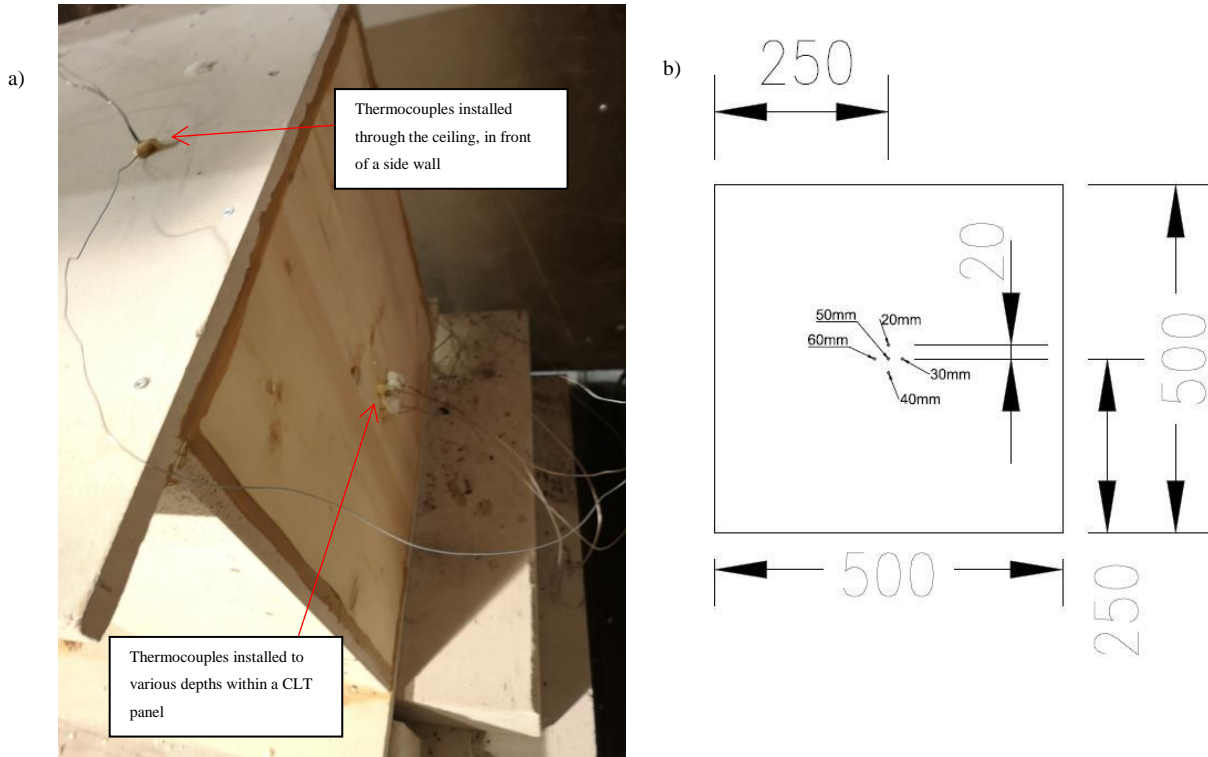


Figure 21: a) Installation of thermocouples inside the compartment as well as within the depth of a CLT panel. b) Thermocouple group configuration as installed at the centre of a panel

It is acknowledged by the author that temperature recording errors may be recorded since the thermocouples were installed perpendicular to the CLT lamella instead of parallel, as suggested by literature (Fahrni *et al.*, 2018). The CLT panels were prefabricated and sent to the testing location, which prevented the installation of thermocouples within the CLT panel parallel to the lamella during production. As such associated shortcomings of this thermocouple installation process are acknowledged, namely an underestimation of temperature within CLT samples (due to a cooling affect by which heat is transferred away from the tip) and possible underestimation of the charring rate by 10%.

#### Moisture content sensor

An electronic moisture content sensor was used to quantify the moisture content of CLT panels upon delivery as well as before testing. Care was taken to ensure that the electronic sensor was calibrated according to the ambient temperature at the time of measurement as well as the species of the wood that was measured (namely European Spruce). The two pins of the sensor were driven into a depth of 40mm from the surface of a specific panel to ensure that surface effects would not influence the results. Figure 22 displays the moisture content sensor as a measurement was taken.



Figure 22: Moisture content sensor being employed before testing a compartment

The moisture content of each exposed CLT panel was measured at panel delivery as well as directly prior to testing. The results of these measurements are summarised in Table 19. From the table it is recorded that prior to testing, the moisture content of the CLT panels were in a range of 12.2% to 13.9%.

Table 19: Moisture Content of each panel at delivery and before testing.

	Moisture Content at delivery (%)	Moisture Content prior to testing (%)
MUF-BW	11	12.3
MUF-2SW (Left Panel/ Right Panel)	10.2/11.8	13.9/12.7
MUF-SW-1	13.8	12.3
MUF-SW-2	10.5	12.4
MUF-C-1	13	12.2
MUF-C-2	12.8	13.4
MUF-BW+C-1 (Ceiling Panel/ Back Panel)	13.9/11	13.6/12.9
MUF-BW+C-2 (Ceiling Panel/ Back Panel)	9.3/10.5	13.3/13.5

In addition to all the data logging equipment attached to the aforementioned equipment, a video camera was employed to record the obtained fire behaviour of each compartment. The recordings were used to cross-correlate thermocouple and HRR results as well as verify visual observations.

## 5.2) Prepared Samples

As mentioned in Section 2.5.2 of this report, 5 compartment configurations are tested. Configuration MUF-BW and MUF-2SW are replication experiments to facilitate the comparison of adhesive performance between these experiments and those obtained by Crielaard (namely PU-BW and PU-2SW). Compartment configurations MUF-SW, MUF-C and MUF-BW+C are used to draw conclusions pertaining to the influence of panel configuration on fire behaviour. In the interest of clarity, Table 20 lists the configurations tested as part of this study, along with a description of the panel configuration per configuration as well as the number of samples prepared per configuration. In the description, mention is only made of the position of exposed CLT panel(s); all other panels are constructed of non-combustible boards. Furthermore, the compartment configurations are displayed graphically in Appendix A.

Table 20: Description of compartment configurations

Configuration Name	Description	Number of Samples	Notes
MUF-BW	Exposed CLT back wall	1	Replication Experiment to compare to Results of Crielaard (PU-BW).
MUF-2SW	Exposed CLT facing side walls	1	Replication Experiment to compare to Results of Crielaard (PU-2SW).
MUF-SW	Exposed single CLT side wall	2	Compartment MUF-SW -1 and MUF-SW-2 are tested once, each.
MUF-C	Exposed CLT ceiling	2	Compartment MUF-C -1 and MUF-C-2 are tested once, each.
MUF-BW+C	Exposed CLT back wall and ceiling	2	Compartment MUF-BW+C -1 and MUF-BW+C-2 are tested once, each.

All Compartment configurations possessed internal dimensions of 0.5mx0.5mx0.5m. Only the front panel contained a ventilation opening measuring 0.18m in width and 0.5m in height, yielding an

opening factor of  $0.042 \text{ m}^{1/2}$ . The CLT lay-up used in all compartment configurations was identical, namely 5 cross-wise stacked layers each 20mm in thickness (resulting in a total panel thickness of 100mm). Each layer is adhesively bonded to the next with an MUF adhesive (see Appendix B.2 and B.3 for a product data sheet of the implemented CLT panels and adhesive, respectively). Those panels that were not made of CLT consisted of non-combustible panels (namely 20mm thick PROMATECT-H panels produced from calcium silicates, cements and aggregates, with a density of approximately  $870 \text{ kg/m}^3$ ). CLT panels that were used as either a back wall or a side wall in a compartment, were installed in such a manner that the panels in the outer lamellas were orientated vertically.

In all configurations, the two front panels as well as the floor panel were constructed of non-combustible panels.

After constructing the compartments, all joints were sealed with fire-resistant (and non-combustible) adhesive to ensure that no flames were able to escape through gaps between the panels. Following this, holes for the burner bed to protrude through were drilled, as well as holes for the thermocouples within the depth of the CLT.

To ensure comparability between the various experiments, the compartments were all placed in a climate controlled room for a period of at least two weeks. The temperature and relative humidity was regulated in the climate controlled room at  $23^\circ\text{C}$  and 50%, respectively. This was also done by Crielaard (2015), further enabling comparison of results between this study (implementing a MUF adhesive) and Crielaard (implementing a PU adhesive).

As mentioned before, the moisture content of all the CLT panels was measured upon delivery as well as before testing. In addition, the weight of individual compartments was measured prior and after performing fire tests, and subsequently the mass loss percentage was subsequently calculated. In addition, the mass loss divided by the total surface area of exposed CLT is also listed. The results of these measurements are shown in Table 21. Note, that due to a measuring error, the mass of Configuration MUF-BW was not measured after testing. However, an estimation of the mass loss was made based on measuring only the CLT back wall of this configuration post testing and comparing it to the mass of an untested CLT back wall. Admittedly, this is not the same mass measurement procedure as the other configurations but it does give an indication of the mass loss percentage of this particular configuration.

Table 21: Mass of each compartment before and after testing.

	Mass prior to testing (kg)	Mass post testing (kg)	Mass Loss (%)	Mass Loss (kg/m <sup>2</sup> CLT)
MUF-BW	54.48	-	12.7*	-
MUF-2SW	53.84	39.41	26.8	28.8
MUF-SW-1	45.34	40.87	9.9	17.9
MUF-SW-2	45.64	39.16	12.3	21.9
MUF-C-1	59.55	54.46	8.6	20.4
MUF-C-2	59.28	54.69	7.8	18.4
MUF-BW+C-1	63.82	54.41	14.7	16.8
MUF-BW+C-2	67.34	57.00	15.4	20.7

\*Indirectly calculated by comparing the mass of the back wall panel post testing to an untested (but conditioned) CLT back wall.

### 5.3) Experimental Procedure

The procedure followed prior, during and after testing is listed in Table 22. This procedure was carried out during all tests in an identical manner. As mentioned before, the experimental methodology implemented in this study is a replication of the methodology implemented by Crielaard (2015). The definitions of self-extinguishment and burn-through were also obtained from Crielaard (2015)

Table 22: Experimental Procedure

Step	Description
1	Before placing the compartment on the burner bed, the propane gas supply was calibrated. This was done by performing a test run where the HRR obtained from the burner bed alone was verified to ensure that 41kW is supplied as input during each tests. The gas flow resulting in 41 kW was noted (approximately 0.88g/s) for verification during tests.
2	After allowing the burner heads to cool down, a compartment was placed on top of the burner bed, and the perforated ceramic wool sheet was placed such to prevent additional ventilation through the openings drilled in the floor panel.
3	Thermocouples are then installed in the depth of the CLT panel(s) as well as within the compartment itself. After installation, all holes were filled with the same aforementioned fire-resistant adhesive.
4	The data logging equipment connected to the Thermocouples and Oxygen Calorimetry system were activated and set to record data.
5	The premeasured gas flow (0.88g/s) was initiated and the burner bed was ignited, marking the start of a particular test.

6	Once a 20mm char layer had formed (as indicated by the position of the 300°C isotherm) in all the CLT panel(s) as measured at the centre of a panel, the gas flow to the burner bed was stopped. This marks the start of the decay phase of the fire.
7	<p>Two possible conditions were checked to execute termination of a test, namely <b>CLT Burn-Through</b> or <b>Self-extinguishment</b>. These conditions are defined as follows, according to Crielaard (2015).</p> <p><b>Self-extinguishment</b> is considered to be attained when the charring depth no longer propagates further into the CLT and all thermocouples register temperatures below 200°C (as shown in Section 3.2 this is the threshold temperature at which pyrolysis gases are released). Furthermore, the HRR recorded via oxygen calorimetry should be close to zero.</p> <p><b>CLT Burn-Through</b> is considered to have occurred once the charring depth has consumed 60% of a CLT panel. This is indicated by the progression of the 300°C to 60mm from the fire side of a panel.</p>
8	After terminating the test, the compartment is weighed and results are extracted from the data loggers connected to the calorimetry system and thermocouples. These results are then post-processed and care is taken to ensure that the time is zeroed from both data sets to the same moment.

## 6) Results

The results obtained from the experimental series are documented in this section of the report. In the interest of conciseness, only the results of one experimental configuration are presented. The results of other 1<sup>st</sup> series experiments (MUF-2SW; MUF-SW-1; MUF-C-1 and MUF-BW+C-1) are documented in Appendix E, and repeat tests (MUF-SW-2; MUF-C-2 and MUF-BW+C-2) are documented in Appendix F of this report.

During the presentation of compartment tests results, an important distinction is to be made between instances of char fall-off and delamination. During all compartment tests containing MUF bonded CLT panels, it was recorded that small pieces of char broke and fell-off from the CLT panels. Based on visual observations, it was recorded that at no instance did an entire plank (or multiple planks) within a lamella delaminate and fall-off (which would expose a large surface area of virgin timber). A distinction will also be made between char fall-off that occurred during the heating phase (i.e. before the charring front propagated through the first lamella and reach the adhesive line at 20mm from the fire side) and char fall-off that occurred after turning off the burner bed (i.e. after the charring front had passed the 1<sup>st</sup> adhesive line at 20mm).

### 6.1) Configuration MUF-BW: CLT Back Wall

This experiment investigates the influence of an exposed CLT back wall. All other panels were constructed from non-combustible boards. The visual observations recorded during the test are documented in this section of the report, as well as the recorded HRR and temperatures.

#### **Visual Observations**

After ignition of the burner bed (and as such supplying the 41kW initial HRR), it took approximately one and a half minutes for the CLT back wall to completely ignite and release pyrolysis gases, as seen in Figure 23. Due to a technical malfunction, the burner bed unexpectedly switched off at 3:30 minutes after ignition. This outage lasted a total of 5:30 minutes. As such, the burner bed was reignited at 9 minutes after the start of the test. Figure 24 and Figure 25 show the state of the CLT back wall at the moment of the burner outage and shortly before re-ignition of the burner, respectively. After the burner bed switched off for the 1<sup>st</sup> time, it took 1 minute for the CLT panel to cease flaming. After burner bed re-ignition, it took another 2 minutes for the CLT panel to enter flaming combustion as shown in Figure 26, and external flaming was observed as shown in Figure 27. After the thermocouple situated at 20mm from the fire side in the centre of the back panel registered 300°C after 47:30 minutes, the burner bed was switched off. During the period of time which the burner bed was switched on, small char pieces fell-off from the exposed back wall, as shown in Figure



28. This indicates that local char pieces broke off before the charring front had reached the adhesive line at 20mm from the fire exposed surface and as such did not indicate adhesive failure.

Subsequent to this, the back CLT only ceased to glow 10 minutes after switching off the burner bed. It took 174 minutes, measured from the start of the tests, for all thermocouples to register temperatures below 200°C indicating the achievement of self-extinguishment.

The charring behaviour was recorded after the tests and is shown in Figure 29. The first lamella had been charred and small char segments fell-off during the test during the heating phase of the fire, and to a far lesser extent during the decay phase of the fire. The outer 4 lamella (those furthest away from the exposed surface) were, however, unaffected. Due to handling of the compartment after the tests was stopped, various segments of char had broken off, and as such the extent of the exposure of the second lamella, as shown in Figure 29, is not solely due to the fire exposure. This statement is valid for all compartment test results presented in this report.

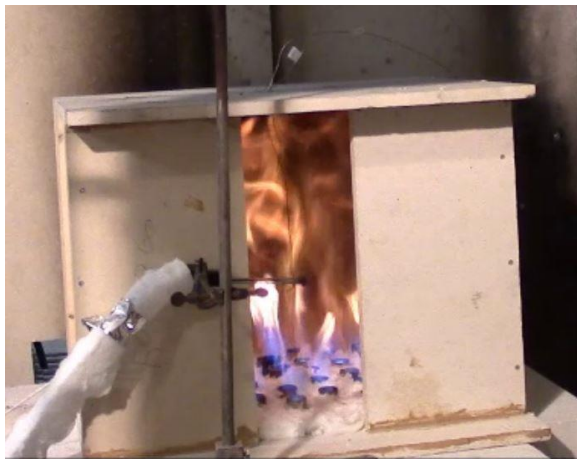


*Figure 23: CLT back wall in flaming combustion*



*Figure 24: CLT back wall at the moment of burner outage*



*Figure 25: CLT back wall before reignition of the burner bed*



*Figure 26: CLT again entering flaming combustion*

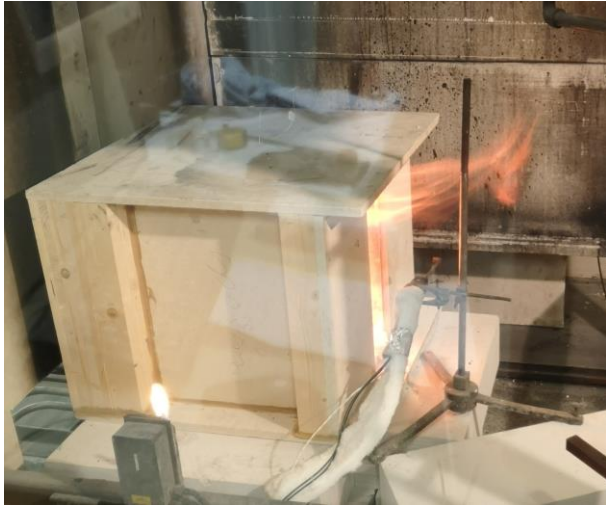


Figure 27: External Flaming occurring after burner bed reignition



Figure 28: Small char piece that fell off on the floor during the heating phase (as indicated by the white arrow)



Figure 29: Charring depths post testing with arrow indicating locations of visible char fall-off

## Heat Release Rates

Due to variations in the measured HRR, results were smoothed (whilst post-processing of results) during the heating phase. The heating phase is defined in this investigation as the period between flashover (where compartment temperatures were above  $600^{\circ}\text{C}$ ) and the moment when the burner bed was switched off. The smoothing process was performed by calculating a moving average at a certain time period using the HRR at one time step before, one after and the HRR itself at that time step. This was done for all HRR results in all experiments. Care was taken that no important peaks were averaged out. The HRR derived from the input propane fire is depicted in Figure 30 in blue, whereas the total HRR (including the propane input fire and contribution from the CLT) is displayed in orange.

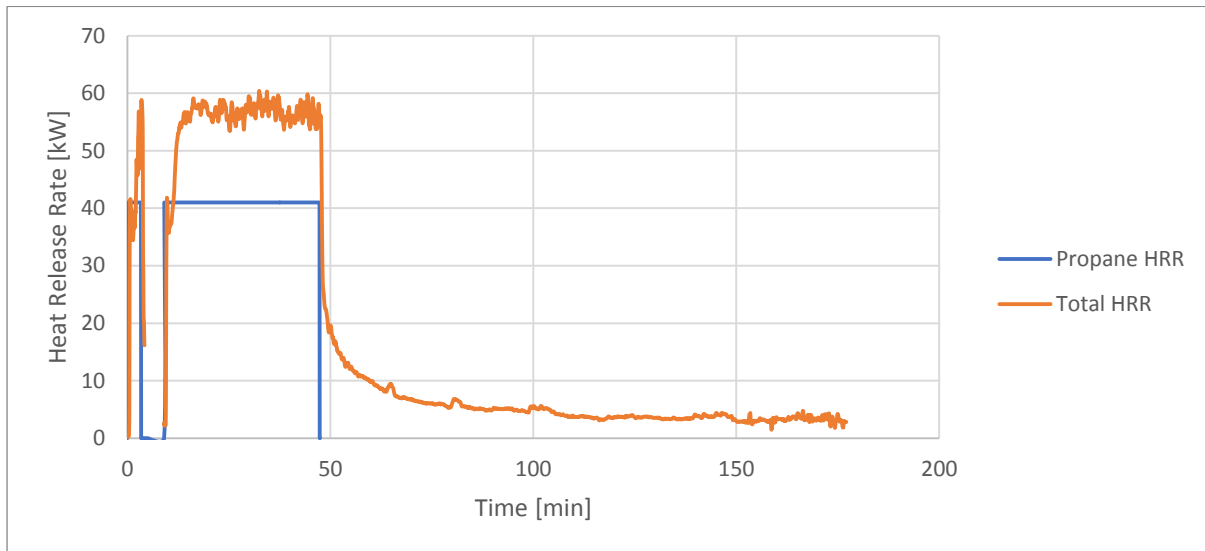


Figure 30: HRR of Configuration MUF-BW

As seen in Figure 30, the input propane fire delivered the specified HRR of 41 kW up until the burner outage occurred at 3:30 minutes, and supplied a 0kW HRR for a further 5:30 minutes. The burner bed was then reignited. The total HRR mimicked the input propane HRR curve in the sense that the total HRR rose rapidly to a maximum of 57kW, dropped immediately when the burner bed was switched off, and rose again to an average of 57kW following the burner outage. After switching off the burner bed at 47:30 minutes, the total HRR dropped rapidly during the period of few minutes and stabilised around 5kW. At the moment of ending the test, the HRR was below 3kW.

## Temperatures

Figure 31 depicts the measured temperature in the compartment during the test. As was the case with the HRR, compartment temperatures also dropped dramatically at 3:30 minutes when the burner bed was switched off. Temperatures rose to 810 °C at the top of the compartment (measured 0.1m from the ceiling) and 637°C at the bottom (measured 0.2m from the bottom). After the burner bed was reignited, temperatures at the top of the compartment rose to a maximum of 981°C and to 882°C at the bottom of the compartment. An average temperature of 774°C and 918°C was recorded at the bottom and top of the compartment, respectively. After switching off the burner, as was the case with the total HRR, temperatures reduced sharply at first and then more gradually to approximately 40°C.

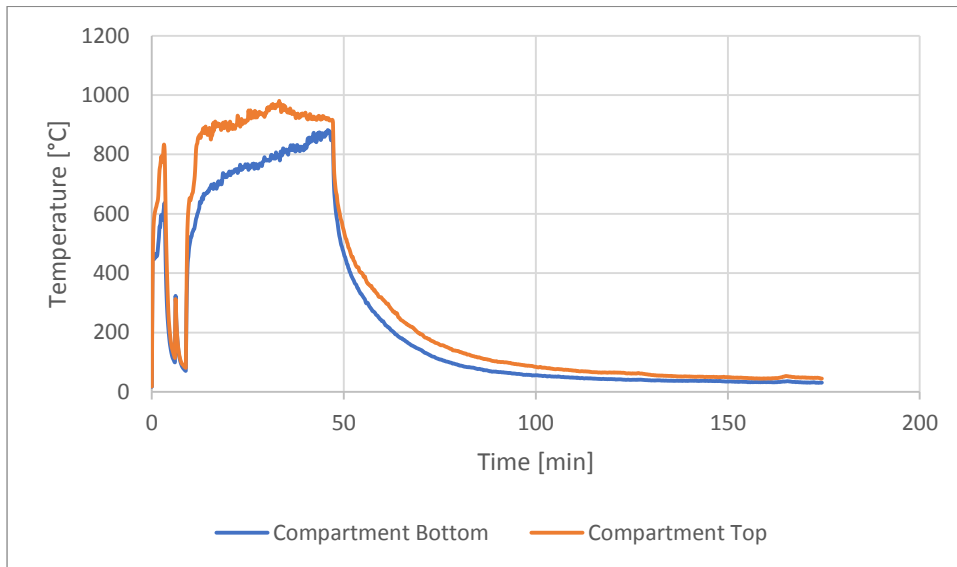


Figure 31: Configuration MUF-BW Compartment Temperatures

Figure 32 illustrated the temperatures recorded within the CLT back panel via the thermocouples installed at various depths at the centre of the back wall. In Figure 32, the **thermocouple depths** are stated and **are measured from the fire exposed surface** (therefore the surface of the CLT panel exposed within the compartment). The influence of the burner outage at 3:30 minutes is not evident in Figure 32, enforcing the notion that the outage did not have a significant influence on the experimental results, especially the temperatures recorded within the CLT back wall panel. Temperatures rose gradually in the CLT panel during the period in which the burner bed was switched on. All Thermocouples recorded an approximately constant temperature increase till 100°C and then a zero temperature increase period was recorded. This zero temperature increase period corresponds to the period of time required for moisture to evaporate from the CLT at a particular depth. Once the moisture had evaporated, temperatures rose sharply, especially at 20mm and 30mm depths. Once 300°C was registered at the 20mm thermocouple at 47:30 minutes, indicating that the first lamella had been charred, the propane burner was switched off. After switching off the burner, the 20mm thermocouple temperature still increased to 313°C for a few minutes, corresponding to the period during which the CLT panel remained in flaming combustion after switching off the burner bed. At approximately 90minutes, a gradual increase in temperature was recorded at the 20mm and 30mm thermocouples. This increase is substantiated by the visual observation that a small char piece in the vicinity of these thermocouples locally started to undergo flaming combustion (i.e. the whole panel did not re-enter flaming combustion, but only a small char piece attached to the 20mm and 30mm thermocouples). After 150 and 165minutes, the temperatures at 30mm and 20mm dropped sharply when the local char pieces ceased flaming and broke-off. After 174 minutes all thermocouples registered temperatures below 200°C and as such the test was stopped.

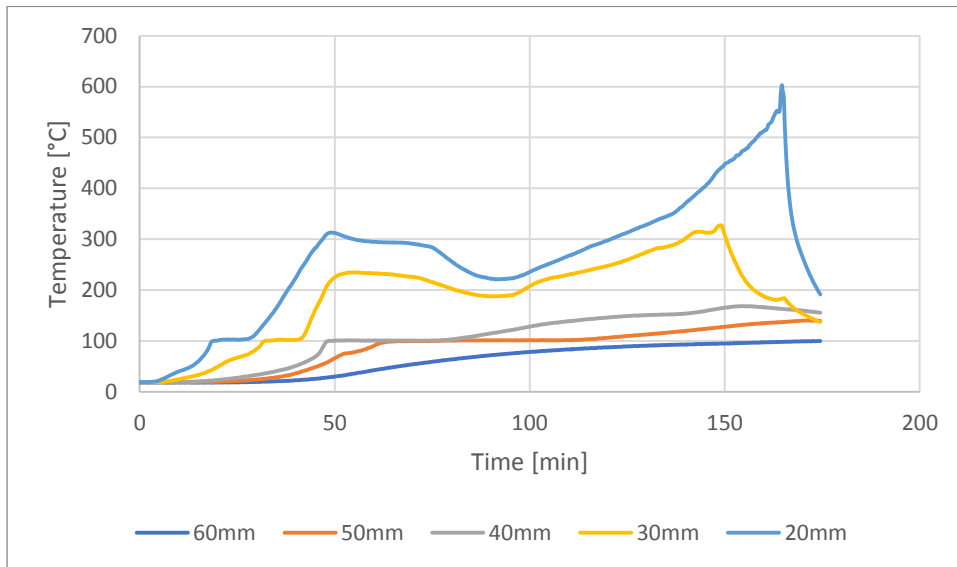


Figure 32: Back Wall Temperatures of Configuration MUF-BW

## 6.2) Results of Compartment Tests

The results of Configuration MUF-BW (containing only an exposed CLT back wall) are reported in the previous section of this report (Section 6.1). In the interest of conciseness, the results of the other compartment tests are recorded in the Appendices of this report. A distinction is made between the first configuration tested per configuration and its repeat experiment (for example between Configuration MUF-SW-1 and MUF-SW-2). The results of the first set of experiments (MUF-2SW; MUF-SW-1; MUF-C-1 and MUF-BW+C-1) are recorded in Appendix E of this report. The results of the repeat experiments (MUF-SW-2; MUF-C-2 and MUF-BW+C-2) are recorded in Appendix F.

## 6.3) Summary of Experimental Results

In this section, a summary of the recorded temperatures and HRRs is presented. These results serve as the basis on which subsequent analyses are performed. As a general observation, **self-extinguishment was recorded in all compartment tests.**

### 6.3.1) Temperatures

Table 23 depicts the temperature trends in the compartment during the *heating phase* of the compartment fire, which was defined as the period after flashover (compartment temperatures  $>600^{\circ}\text{C}$ ) to the moment when the gas flow to the burner was stopped. In addition, Table 23 shows the duration of the decay phase of each experiment. Self-extinguishment was recorded in all experiments and thus the *decay phase* duration refers to the time between terminating the gas flow to the burners and self-extinguishment (all temperatures  $<200^{\circ}\text{C}$ ).



Table 23: Average and Maximum Compartment Temperatures and Decay Phase Durations

	Average Temperature 0.2m [°C]	Maximum Temperature 0.2m [°C]	Average Temperature 0.4m [°C]	Maximum Temperature 0.4m [°C]	Decay Phase Duration [minutes:seconds]
MUF-BW	773.5	882.2	917.6	980.6	126:20
MUF-2SW	865.3	980.3	937.0	1037.9	251:50
MUF-SW-1	765.8	853.1	949.5	1007.6	38:50
MUF-SW-2	815.0	891.8	918.6	983.1	67:40
MUF-C-1	872.5	995.6	977.3	1055.7	21:00
MUF-C-2	1025.6	1107.7	927.3	1031.1	26:50
MUF-BW+C-1	924.1	1035.5	932.7	1026.6	91:20
MUF-BW+C-2	1011.0	1102.1	1003.6	1098.1	87:20

In addition to Table 23, Figure 33 below graphically depicts the enclosure compartment temperatures measured at the centre of each compartment at a height of 0.4m from the floor panel. Compartments containing only one exposed CLT panel are plotted as solid lines, whereas compartments containing two exposed CLT panels are depicted with dotted lines.

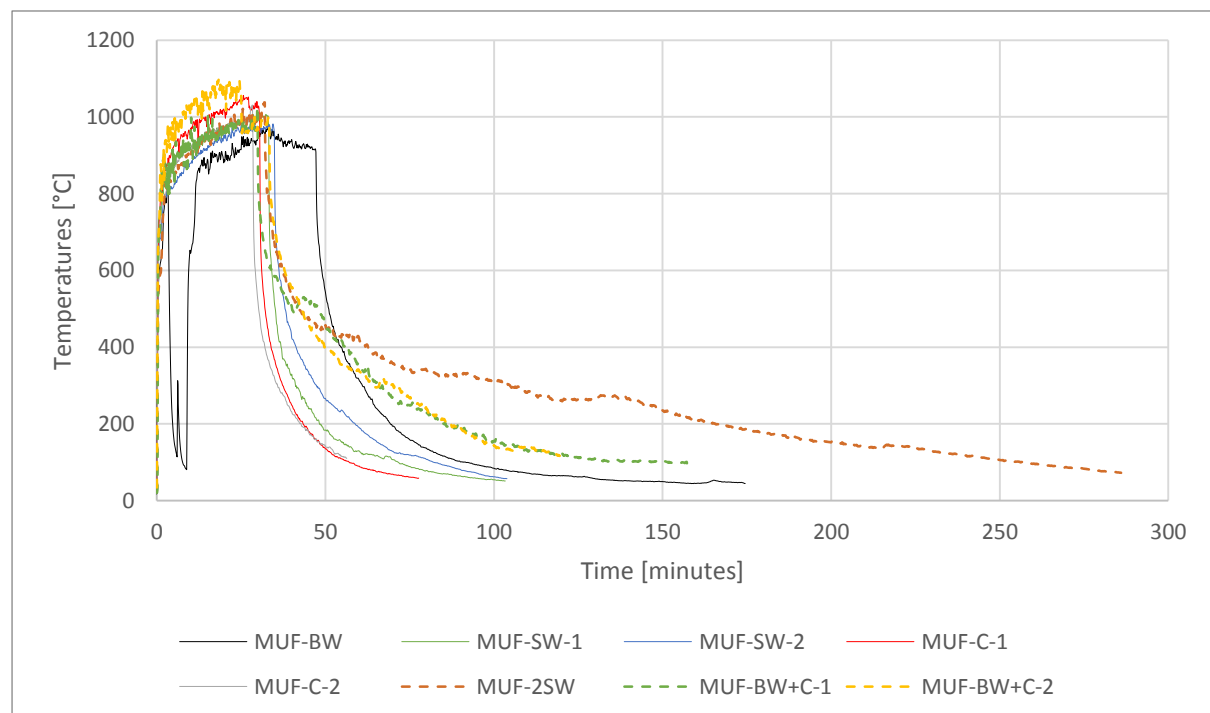


Figure 33: Compartment temperatures measured during all experiments

### 6.3.2) Heat Release Rates

The average as well as maximum HRRs during the heating phase of each experiment is shown in Table 24. The table also shows the average and maximum contribution of the CLT alone to the HRR (also stated in brackets per m<sup>2</sup> of exposed CLT area per compartment), as obtained by subtracting the 41kW input fire load from the obtained average and maximum HRRs.

Table 24: Summary of HRR results

	Average HRR during the heating phase [kW] (increase)	Maximum HRR during the heating phase [kW] (increase)	CLT only average HRR during the heating Phase [kW] (/m <sup>2</sup> CLT)	CLT only maximum HRR during the heating Phase [kW] (/m <sup>2</sup> CLT)
MUF-BW	56.6	60.4	15.6 (62.4)	19.4 (77.6)
MUF-2SW	73.4	79.5	32.4 (64.8)	38.5 (77.0)
MUF-SW-1	57.4	61.9	16.4 (65.6)	20.9 (83.6)
MUF-SW-2	56.9	63.1	15.9 (63.6)	22.1 (88.4)
MUF-C-1	59.1	63.9	18.1 (72.4)	22.9 (91.6)
MUF-C-2	55.0	62.6	14 (56.0)	21.6 (86.4)
MUF-BW+C-1	72.9	82.1	31.9 (63.8)	41.1 (82.2)
MUF-BW+C-2	72.3	84.7	31.3 (62.6)	43.7 (87.4)

### 6.4) Overview of Results

In the interest of clarity, Table 25 below presents as an overview of the performed experiments. Per configuration a description of the exposed CLT panels is stated as well as the number of experiments and the type of adhesive used in each test. Furthermore, reference is made to the section in this report where the results of each configuration are presented. Reference is also made to the relevant experiments performed by Crielaard (2015) (by means of the acronym PU), and are discussed in the Analysis Section of this report. Finally, the 90 minute SFC furnace experiment is presented and discussed in Appendix I of this report.

Table 25: Overview of experimental results

	Description	Number of experiments	Adhesive Type	Section Reference
Configuration MUF-BW	One exposed CLT Back Panel	1	MUF	§ 6.1
Configuration PU-BW	One exposed CLT Back Panel	1	PU	§ 7.2.1
Configuration MUF-2SW	Both CLT Side Walls exposed	1	MUF	§ E.1
Configuration PU-2SW-2	Crielaard: Both CLT Side Walls exposed	1*	PU	§ 7.2.2
Configuration MUF-SW-1 and MUF-SW-2	One exposed CLT Side Wall	2	MUF	§ E.2 and § F.1
Configuration MUF-C-1 and MUF-C-2	Exposed CLT Ceiling	2	MUF	§ E.3 and § F.2
Configuration MUF-BW+C-1 and MUF-BW+C-2	Exposed CLT back Wall and Ceiling	2	MUF	§ E.4 and § F.3
90 minute SFC Furnace Test	SFC charring experiment on 4 ceiling CLT panels	1	MUF	§ I

\*Note that only the compartment experiment conducted by Crielaard that displayed self-extinguishment with the same CLT build-up (namely experiment PU-2SW-2) will be compared to MUF-2SW in Section 7.2.2. A general comparison based on the results of PU-2SW-1 and PU-2SW-40mm is presented at the start of Section 7.2.



## 7) Analysis

This section of the report will serve to answer two of the research questions formulated as part of this study, namely:

*Q3) What is the influence of adhesive type on compartment fire behaviour?*

*Q4) What is the influence of exposed CLT panel configuration on compartment fire behaviour?*

Each of these questions will be addressed individually in separate sections. Preceding this, a summary of the experimentally measured HRRs, total energy released (TER) and charring rates is presented.

### 7.1) Analysis of individual compartment experiments

The results obtained from the post-processing performed on each experiment to analyse HRRs, obtain the TER (from the input fire as well as the contribution from the CLT) as well as the averaged charring rates per experiment across various depths, is documented.

Note, in the interest of clarity, the compartment naming convention is listed again (only exposed CLT panels listed per compartment): BW= Back Wall; 2SW= Two Side Walls; SW-1 and SW-2 = Tests with only one Side Wall; C-1 and C-2 = Tests with only one Ceiling; BW+C-1 and BW+C-2 = Tests with Back panel and Ceiling. All compartment tests as part of this research project were conducted on MUF bonded CLT panels. The abbreviation PU is used to refer to results obtained by Crielaard (2015), where his compartments were constructed of PU bonded CLT panels.

#### 7.1.1) Analysing HRR per compartment experiment

The average HRR measured during the heating phase (i.e. between flashover and extinguishing the propane burner), can be compared to the input HRR supplied by the propane burner bed (namely 41kW). The results of this post-processing analysis are presented in Table 26, and are stated as % increase in HRR from the input fire.

The average HRR recorded by Crielaard in his tests on compartments containing PU bonded CLT panels are also listed in Table 26. HRR were averaged in an identical manner in this study as compared to the study by Crielaard. In his CLT back wall configuration (PU-BW) test he obtained an average HRR of 57 kW. In his two Configuration 2SW experiments (PU-2SW-1 and PU-2SW-2), Crielaard obtained averaged HRR of 102 and 95 kW. Interestingly, in a Configuration 2SW test with a thicker innermost lamella (40mm instead of 20mm, namely PU-2SW-40mm), the averaged HRR during the post flashover heating phase was 79 kW.

Table 26: Summary of HRR Percentage increase as compared to the propane input HRR

	<b>Average heating phase HRR increase compared to the 41kW propane input</b>		<b>Average heating phase HRR increase compared to the 41kW propane input</b>
MUF-BW	38%	MUF-SW-1	40%
PU-BW	39%	MUF-SW-2	39%
MUF-2SW	80%	MUF-C-1	44%
PU-2SW-1	149%	MUF-C-2	34%
PU-2SW-2	132%	MUF-BW+C-1	78%
PU-2SW-40mm	93%	MUF-BW+C-2	76%

### 7.1.2) TER results

The HRRs recorded in Table 24 can also be represented graphically as TER during a particular test (quoted in MJ). TERs were calculated by incrementally adding the product of measured HRR and time across measurement intervals. These TER graphs (displaying the input TER by the propane burner and overall TER per tests), are shown in the graphs below. Figure 34 illustrates the TER curves as obtained from the 1<sup>st</sup> of experiments, whereas Figure 35 illustrates the results of the repeat experiments. In both graphs, a distinction is made between the TER obtained from the input (propane) fire as well as the total TER (including both the input fire and energy released by the CLT).

It is clear from the graphs that the TER is highest in the experiments that contained two exposed CLT surfaces, with the configuration containing two exposed side walls displaying the highest amount of total energy released (242MJ). The lowest TER (in both the 1<sup>st</sup> and repeat experiments) was obtained from experiments containing only an exposed CLT ceiling (namely 115 and 100 MJ in Test C1 and C2, respectively).

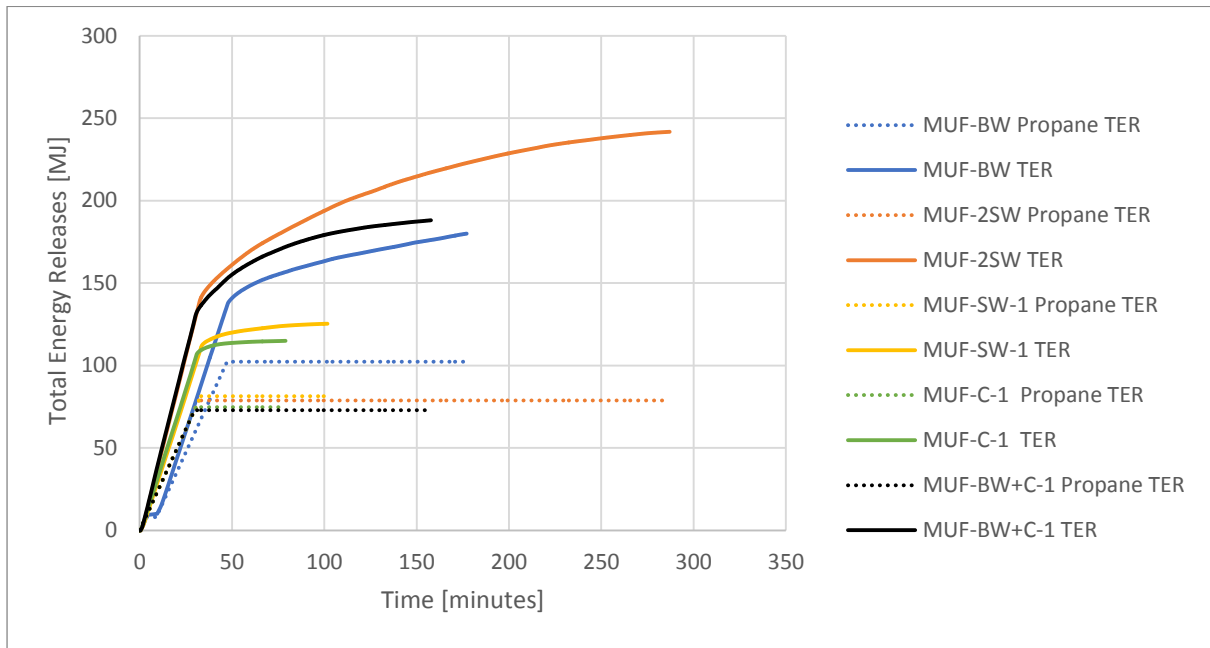


Figure 34: TER of the 1st set of experiments

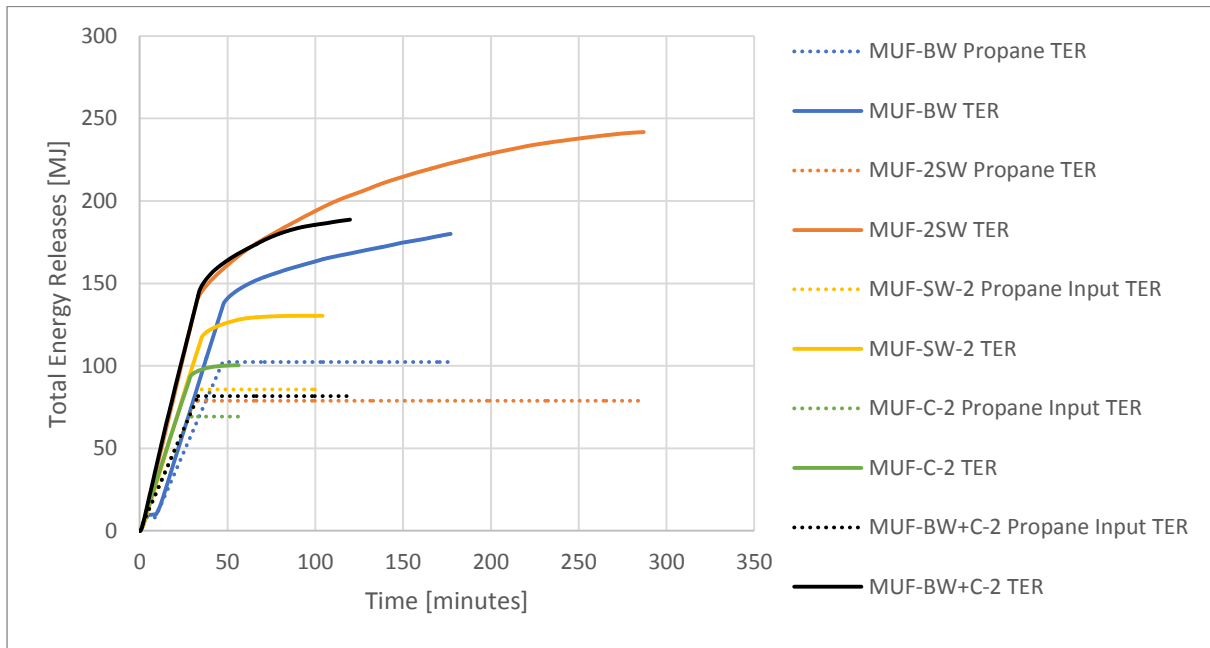


Figure 35: TER of the 2nd set of experiments

The maxima of the TER graphs are also recorded in Table 27 for comparative purposes, with the contribution of the CLT stated separately (in MJ as well as MJ/m<sup>2</sup> of exposed CLT). The percentage energy increase due to the CLT energy contribution is also stated.

Table 27: Maxima of TER curves

	MUF-BW	MUF-2SW	MUF-SW-1	MUF-SW-2	MUF-C-1	MUF-C-2	MUF-BW+C-1	MUF-BW+C-2
Propane Input TER [MJ] (/m <sup>2</sup> floor)	102 (409)	79 (315)	81 (326)	86 (343)	75 (299)	69 (277)	73 (292)	82 (327)
Total TER [MJ] (/m <sup>2</sup> floor)	180 (720)	242 (967)	125 (501)	130 (521)	115 (460)	100 (402)	188 (752)	189 (755)
CLT Contribution [MJ] (/m <sup>2</sup> CLT)	78 (311)	163 (326)	44 (176)	45 (178)	40 (161)	31 (125)	115 (230)	107 (214)
Increase from the propane input (%)	76	207	54	52	54	45	158	131

From Table 27, it is shown that the TER from the propane burner varied from 69MJ to 102 MJ. The input TER from propane burner delivered in the back wall experiment was an outlier. As discussed in the results section of this report, a technical error during testing lead to the burner bed being switched off for a period of 5:30 minutes in the back wall configuration experiment (MUF-BW). During that outage, it was noted that the CLT back wall had ceased flaming. As such, it took comparatively longer for this configuration to again be reheated (after an insulative char layer was formed) once the propane burner was reignited, resulting in a longer propane fire duration as would be the case if the technical error had not occurred, resulting in more energy being released in total. Excluding the back wall configuration, the input propane TER was measured between 69MJ and 86MJ.

From all experiments it can be seen that a lower increase in energy was recorded with one exposed CLT panel (ranging from 45% to 76%) than with two exposed CLT panels (131% to 207%), when comparing the contribution of the CLT and the propane input. The lowest CLT contribution was recorded during experiments containing only an exposed ceiling (average of 50% across the two experiments), followed by: one exposed side wall (53% increase on average between the two experiments); one back wall (76%); an exposed back wall and ceiling (averaging 145%) and finally two exposed side walls (207%). On average, with one exposed CLT panel the combusting timber contributed 47.6MJ, as compared to an averaged contribution of 128.3MJ in compartments containing two exposed panels (representing an increase in TER by the CLT alone by a factor of 2.7)

Crielaard also recorded the TER in his comparable PU bonded CLT compartment experiments. Table 28 lists the TER by the input propane burner, as well as the TER by the entire compartment (which includes both the energy released by the propane burner and combusting CLT). By subtracting the two aforementioned TERs from another, the contribution by the combusting CLT to the TER is calculated. The table below quotes the TERs in MJ as well as MJ per floor area (indicated in brackets). The contribution by the CLT to the TER is quoted in MJ and MJ per area of exposed CLT.

Finally, the table also lists the percentage increase in TER due to the combusting CLT, as compared to the TER of the propane input fire.

Table 28: TER maxima in PU bonded CLT compartments

	PU-BW	PU-2SW-1	PU-2SW-2	PU-2SW-40mm
Propane Input TER [MJ] (/m <sup>2</sup> floor)	112 (448)	55 (220)	62 (248)	63 (252)
Total TER [MJ] (/m <sup>2</sup> floor)	169 (676)	240 (960)	183 (732)	134 (536)
CLT Contribution [MJ] (/m <sup>2</sup> CLT)	57 (228)	185 (370)	121 (242)	71 (142)
Increase (%)	51	336	195	113

These PU bonded CLT TER results will be compared to the MUF bonded CLT results in Chapter 7.2.

### 7.1.3) Charring Rates

The position of the 300°C isotherm was used to determine the charring rate per CLT panel. Since the thermocouple positions were positioned at fixed intervals, these positions (i.e. depths) and the time for the 300°C isotherm to progress to this depth determined the charring rate. The depth to the first thermocouple in all tests was 20mm, and to subsequent thermocouples was 10mm deeper, up to a depth of 60mm from the fire side. Table 29 and Table 30 summarises the obtained charring rates per experiment and per thermocouple depth. Note that in Configuration BW, a burner bed outage of 5:30 minutes occurred. Charring rates for this experiment were calculated including the outage as well as excluding it (**with the latter indicated in round brackets**). Furthermore, 300°C was not recorded at any thermocouple situated at the connection between the ceiling and back panel of Compartments MUF-BW+C-1 and MUF-BW+C-1, and as such are not listed in the tables below. In the table below, **dashes are used** to indicate that the charring front did not propagate to that specific depth.

Table 29: Charring rates per configuration per thermocouple depth. LW= left wall; RW= right wall;

Charring Rate [mm/min]	MUF-BW	PU-BW	MUF-2SW LW	MUF-2SW RW	PU-2SW-1 / PU-2SW-2 LW	PU-2SW-1 / PU-2SW-2 RW	MUF-SW-1 LW
0-20mm	0.43 (0.48)	0.52	0.64	0.62	0.94/0.73	0.85/0.74	0.61
20-30mm	0.11 (0.11)	-	0.41	0.29	0.6/-	1.76/0.56	-
30-40mm	-	-	0.33	0.16	0.27/-	0.26/0.24	-
40-50mm	-	-	0.11	0.18	0.63/-	0.49/-	-
50-60mm	-	-	-	-	0.39/-	0.17/-	-
Average	0.27 (0.30)	0.52	0.37	0.31	0.57/0.73	0.71/0.51	0.61

Table 30: Charring rates per configuration per thermocouple depth. (Continued). C = ceiling; BW= back wall

Charring Rate [mm/min]	MUF-SW-2 RW	MUF-C-1	MUF-C-2	MUF- BW+C-1 C	MUF- BW+C-1 BW	MUF- BW+C-2 C	MUF- BW+C-2 BW
0-20mm	0.58	0.66	0.71	0.68	0.69	0.83	0.60
20-30mm	-	-	-	-	0.40	-	-
30-40mm	-	-	-	-	-	-	-
40-50mm	-	-	-	-	-	-	-
50-60mm	-	-	-	-	-	-	-
Average	0.58	0.66	0.71	0.68	0.55	0.83	0.60

Graphical representations of these charring rates are presented in Appendix H of this report, and are discussed there. In addition, Appendix I documents and discusses the charring rates obtained from the 90 minute SFC exposure Furnace Test. The results of this additional test will be used to assess the validity of the charring rates and charring behaviour recorded during the compartment tests for an extended initial fire exposure period.

### 7.1.3) Propagation of the charring front and time required to self-extinguish

As stated in Section 3.2, the position of the 300°C isotherm was used to determine the propagation of the charring front. Based on this, the depth of char, as measured experimentally at the centre of individual CLT panels, is recorded in Table 31:

Table 31: Charring depths based on the propagation of the 300°C isotherm

Compartment Test	300°C Charring Depth [mm]	Compartment Test	300°C Charring Depth [mm]
MUF-BW	30	MUF-C-1	20
MUF-2SW (Left Wall/ Right Wall)	50/ 50	MUF-C-2	20
MUF-SW-1	20	MUF-BW+C-1 (Back Wall/Ceiling)	30/ 20
MUF-SW-2	20	MUF-BW+C-2 (Back Wall/Ceiling)	20/ 20

It is important to note that the charring depths stated in the above table are only representative of charring that occurred at the centre of individual panels and are therefore not representative of charring depths that occurred over the entire panel. Additionally, the charring depths stated in the table above are not to be directly compared to the images in Section 6.1, Appendix E and Appendix F, which depict CLT panels post testing. As mentioned in the Literature Study Section of this report (namely Section 3.2), a pyrolysis zone is formed below the char base (i.e. position of the 300°C isotherm), in which the timber is subjected to elevated temperatures. Subsequently, the charring depths obtained from the position of the 300°C isotherm do not represent physical charring depths, but do facilitate comparisons to be drawn between the various compartment configurations.

Furthermore, the charring depths listed in Table 31 were based on the positions of the installed thermocouples alone. No interpolation was performed between thermocouple depths to determine the position of the 300°C isotherm.

Importantly, all MUF bonded CLT compartments demonstrated self-extinguishment, whereby in-depth CLT and compartment temperatures decreased to below 200°C, without the propagation of the charring front past 60% of any panel's thickness (i.e. 60mm of the total 100mm thickness). The time required to achieve self-extinguishment after removal of the initial fuel load in each MUF bonded CLT compartment tests is listed in Table 32:

Table 32: Time required to self-extinguish as measured from the moment the burner bed was turned off

Compartment Test	Time to self-extinguish [hours:minutes]	Compartment Test	Time to self-extinguish [hours:minutes]
MUF-BW	2:06	MUF-C-1	0:21
MUF-2SW	4:12	MUF-C-2	0:27
MUF-SW-1	0:39	MUF-BW+C-1	1:31
MUF-SW-2	1:08	MUF-BW+C-2	1:27

From Table 31 and Table 32, with only the exception of the Back Wall Configuration (MUF-BW), it is evident that compartments with one exposed CLT panel as compared to a two CLT panels experienced shallower charring depths and achieved self-extinguishment sooner. The MUF-BW is an outlier amongst single CLT-panel Compartments (a hypothesis pertaining to this observation is formulated in Section 7.3.1).

Based on the results recorded in Table 32, the following is observed: averaged across all compartment experiments, a decay phase duration of 56 minutes and 143 minutes was recorded in compartments with one and two exposed CLT panels, respectively. This indicates that on average the addition of a second exposed CLT surface to a compartment with one exposed CLT surface prolongs the decay phase duration by a factor of x2.6).

## 7.2) Influence of adhesive type on compartment fire behaviour

Before analysing the comparable compartment results, a general discussion regarding differences in fire behaviour is presented. It is acknowledged that the observation list in this Chapter cannot be generalised to all types of MUF and PU adhesives due to the limitation of only testing one type of MUF and PU adhesive. Furthermore, additional research is required to assess the validity of these observations, due to the difference in compartment openings between the PU bonded CLT experiments and the MUF bonded CLT experiments. Furthermore, the planks within a lamella of the PU bonded CLT samples were edge-glued, whereas planks were not edge glued in the MUF bonded CLT panels. Lastly, the CLT samples were not from the same producer and as such the base timber was not from the same source which could induce additional variation. As such, it is recommended that further experiments are to be conducted on identical CLT panels in which the only variable is the adhesive type used, to verify the adhesive performance observed in this section of this report.

As shown by Crielaard *et al.* (2019), it was recorded that the PU adhesive debonded from the timber lamella once the 300°C isotherm had progressed past the first lamella. This is illustrated in Figure 36 below, which shows the state of a small sample of PU bonded CLT after an exposure to 75kW/m<sup>2</sup> in a



cone calorimeter which transformed the first lamella to char. Once the first lamella has been charred (i.e. 300°C was recorded by the thermocouples installed at a depth of 20mm), the imposed heat flux was reduced to 0kW/m<sup>2</sup>. As visible in the Figure, the char contracted horizontally and was able to be removed by hand in one piece, indicating that it is likely to delaminate if placed in an unfavourable orientation (i.e. as a ceiling or wall panel). Delamination was also observed in the PU bonded CLT compartment experiments as tested by Crielaard (excluding the compartment that contained CLT panels with thicker outer lamellas, namely PU-2SW-40mm).



*Figure 36: Debonded PU bonded CLT sample, from Crielaard (2015)*

The experiment on sample-scale (100mmx100mm and 50mm thick) was not repeated for the MUF bonded CLT samples used in this research project, but comparisons can be drawn based on the visual observations recorded during the performed compartment experiments. A process of local char fall-off was recorded in all compartments constructed from MUF bonded CLT panels. At no instance did an whole planks break off from a CLT panel in a compartment test, but rather it was observed that small pieces of char broke off from the CLT panel both before and after the charring front had penetrated past the first adhesive line. Furthermore, these visual observations pertaining to a process of local char fall-off was also recorded in the additional SFC exposure test, as documented in Appendix I of this report.

The aforementioned observations regarding delamination/char fall-off are summarised visually in Figure 37. In the Figure, reference is made to three experiments containing both MUF and PU bonded CLT facing CLT side wall panels. The general fire behaviour of each experiment is discussed individually.

- **Solid Timber Behaviour** as shown in Compartment PU-2SW-40mm (tested by Crielaard). This compartment contained two facing CLT panels with thicker (40mm instead of 20mm) outer lamellas. In Figure 37, it is evident that the entire CLT surface is evenly charred. Furthermore, the CLT walls did not experience delamination (of planks) nor char fall-off. The behaviour recorded in this experiment is comparable to that of solid timber (i.e. no adhesive related fire behaviour such as delamination). Additionally, during the decay phase

compartment temperatures declined steadily until self-extinguishment was recorded 70 minutes after the start of the test, with no sharp increases in temperatures.

- **Local Char Fall-off Behaviour** as shown in Compartment MUF-2SW. As seen in in Figure 37, the surface of the CLT panel is uneven due to a process of local char fall-off. At no instance during the experiment was delamination of planks observed, but rather that local char pieces fell-off gradually. Compartment temperatures also declined gradually during the decay phase, although at a slower rate as compared to Compartment PU-2SW-40mm. Small peaks in compartment temperature ( $\pm 10^{\circ}\text{C}$ ) were recorded at 130 and 220 minutes, corresponding to occurrences of local char fall-off. Compartment temperatures declined gradually until self-extinguishment was recorded 284 minutes after the start of the test.
- **Burn-through Behaviour** as observed in Compartment PU-2SW-1 (tested by Crielaard). As seen in Figure 37, multiple CLT lamellas are visible due to delamination and falling-off of large char pieces (i.e. whole planks) during the experiment. During the decay phase of the compartment fire, temperatures decreased to  $350^{\circ}\text{C}$  after 140 minutes with a temporary spike to  $500^{\circ}\text{C}$  at 75 minutes. Subsequent to this, temperatures rose sharply to slightly more than  $800^{\circ}\text{C}$  which coincides with the visual observation of delamination. Subsequently, burn through behaviour (i.e. failure to self-extinguish) was recorded in this experiment.

The total amount of energy released (TER) released during each of the three aforementioned experiments is also compared. Table 33 below lists the total energy released by the propane burner as well as the contribution of the CLT to the TER during a particular experiment.

*Table 33: Comparing TER between experiments*

Compartment Fire Test	Behaviour	TER by the Propane Burner [MJ]	Contribution of the CLT to the TER [MJ]
PU-2SW-40mm	Solid Timber	63	71
MUF-2SW	Local Char Fall-Off	79	163
PU-2SW-1	Burn-through	55	185

In all compartment experiments, the input propane burner released an identical 41KW HRR and was ignited for a comparable period of time (24, 32 and 26 minutes in Compartments PU-2SW-40mm, MUF-2SW and PU-2SW-1, respectively), resulting in comparable total input energy amounts supplied by the burner bed.

From the Table above, it is clear that the lowest amount of energy was released in Compartment PU-2SW-40mm which demonstrated solid timber-like behaviour. In contrast to this behaviour,

Compartment PU-2SW-2 which showed burn through behaviour, released 114 MJ (i.e. 160%) more total energy as compared to compartment PU-2SW-40mm. Finally, Compartment MUF-2SW which showed local char fall-off behaviour released 92MJ (i.e. 130%) more energy than Compartment PU-2SW-40mm despite possessing a four-times longer fire duration (284 minutes as compared to 70 minutes in Compartments MUF-2SW and PU-2SW-40mm, respectively). Finally, when comparing Compartment MUF-2SW to PU-2SW-1, the PU bonded CLT compartment showed a 22MJ higher total amount of energy released (representing an increase of 13.5%).

In summary, it has been recorded that burn-through behaviour (i.e. failure to self-extinguish) occurred in a compartment containing exposed PU bonded CLT side panels, whereas self-extinguishment was recorded in a comparable compartment experiment containing exposed MUF bonded CLT side panels. It was further shown that PU bonded CLT side panels (with 20mm outer lamellas) released more energy (namely 13.5%) and displayed delamination (of planks) which resulted in a second flashover, in comparison to local char fall-off (which increased enclosure temperatures by  $\pm 10^{\circ}\text{C}$ ) in a comparable compartment experiment with MUF bonded CLT.

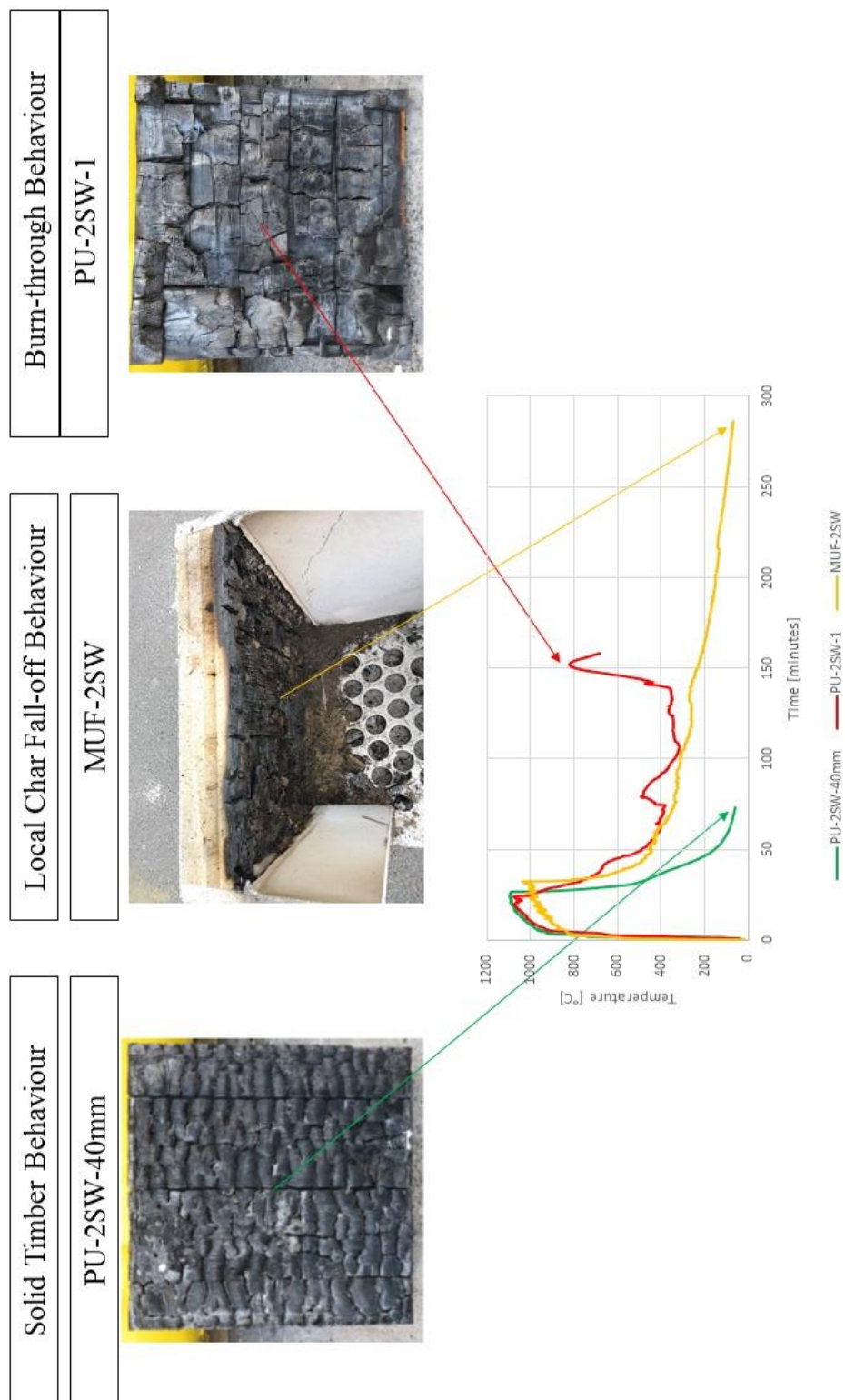


Figure 37: Solid Timber Behaviour as compared to delamination and local char fall-off behaviour

With the aforementioned fire behaviour discussion now presented, comparisons pertaining to the influence of adhesive type will be drawn per comparable configuration. The results from two compartment configurations, namely Configuration BW and 2SW are to be compared to the results obtained by Crielaard (2015) to further assess the influence of adhesive type on fire behaviour. The comparisons that will be drawn are depicted visually in Figure 38. It is important to note that Compartment PU-2SW-2 will be compared to the MUF-2SW experiment in the remainder of this section of the report due to the similarities in obtained fire behaviour (namely self-extinguishment). It is, however, important to keep in mind that Crielaard also recorded compartment burn through in a comparable experiment (PU-2SW-1).

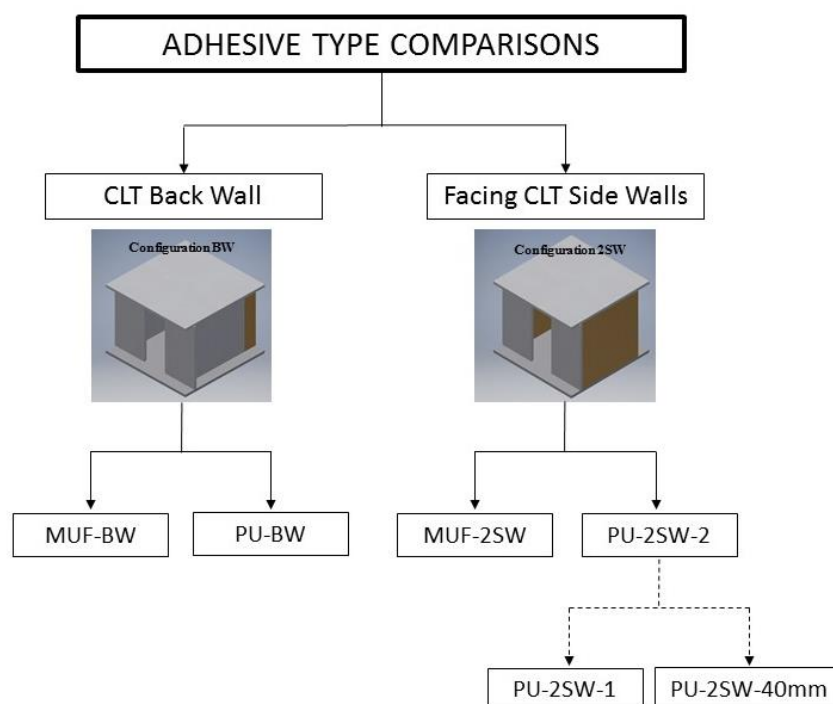


Figure 38: Compartment comparisons to characterise the influence of adhesive type on fire behaviour

### 7.2.1) Adhesive influence of compartments with a CLT back wall

A comparison between tests with only an exposed CLT back wall will be presented in this section. As mentioned before, a technical issue lead to the burner bed being switched off for a period of 5:30 minutes in Compartment MUF-BW. Additionally, a deviation from the experimental methodology was implemented by Crielaard in in Compartment PU-BW. During the first 12 minutes of his experiment, Crielaard implemented a propane input fire of 63kW instead of the prescribed 41kW. After this initial higher input HRR period, the propane gas flow was lowered to yield an input HRR of 42kW. As such, the comparisons drawn in this section will only consider the period during which the propane burner was ignited for a second time in the back wall compartment test of this study, and the

period post input HRR reduction to 42kW (therefore results after 12 minutes) for the comparable compartment test by Crielaard.

## Heat Release Rates

Figure 39 depicts the HRR measured during the comparable back wall compartment tests. A distinction is made between the input propane fire (depicted with dotted lines) as well as the total HRR (including the contribution from the burning CLT, depicted with solid lines).

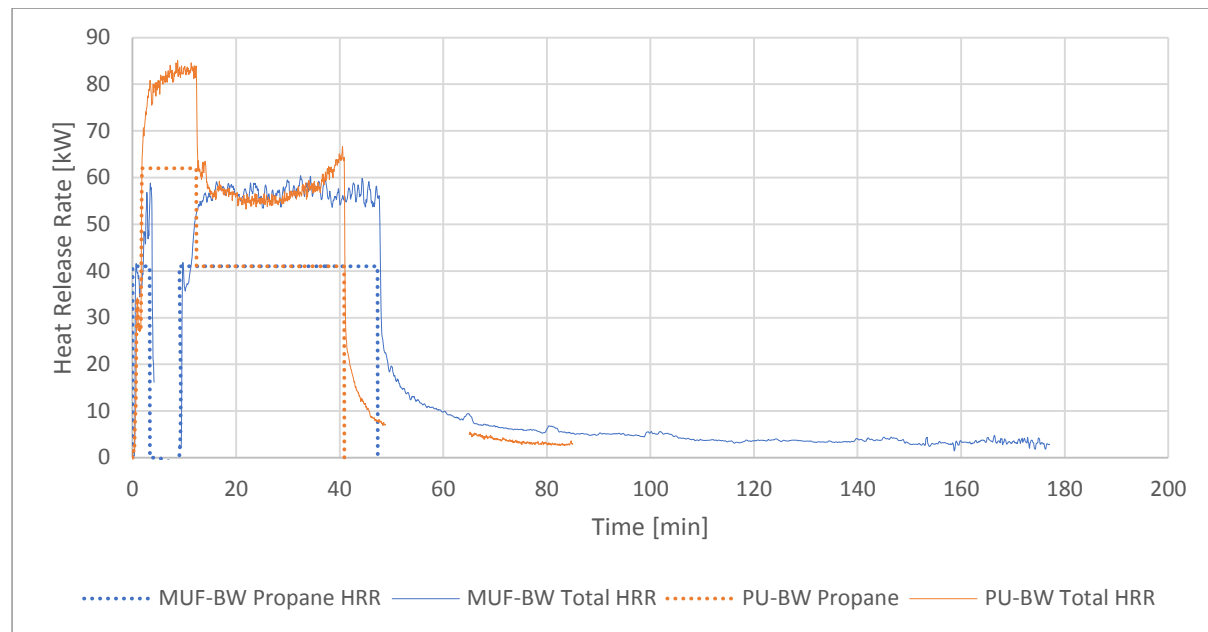


Figure 39: Comparing HRR from experiments with an exposed Back Wall

Crielaard measured an average total HRR of 57kW whilst the propane burner delivered a HRR of 42kW in his PU-BW compartment test. In comparison, the comparable MUF compartment experiment yielded an average total HRR 56.6kW which illustrates comparability between experimental set-ups.

## Temperatures

Figure 40 shows the enclosure temperature development as measured in the comparable back wall compartment experiments. Temperatures were recorded at identical locations in this study as compared to those by Crielaard, namely at the centre of the compartment at heights of 0.2m (referred to as bottom) and 0.4m (referred to as top) from the floor panel.

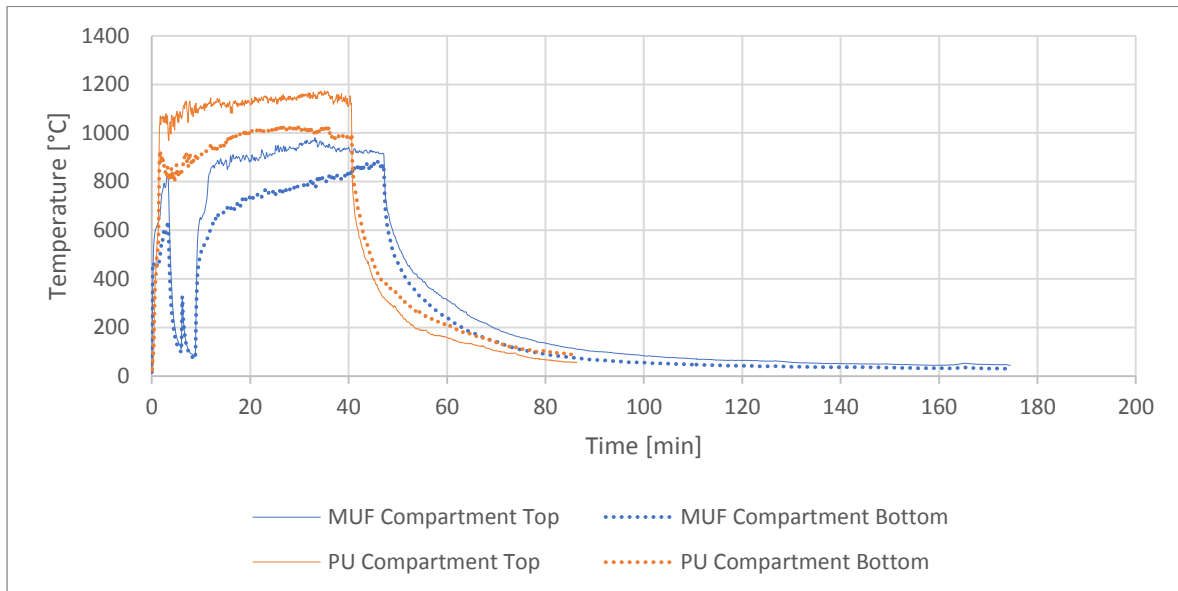


Figure 40: Comparing temperatures between experiments with an exposed Back Wall

It can be seen from Figure 40 that the compartment temperatures measured by Crielaard are higher during the period that the burner bed was ignited (i.e. the heating phase). It is postulated that these differences originate from a deviation in the experimental set-up implemented in this study as compared to Crielaard. In his experiments, Crielaard installed a heat flux gauge in the opening of the compartment which blocked-off a significant portion of the opening area. As such it is reasoned that there was a comparably larger opening implemented in the experimental series of this investigation, thereby allowing more heat to escape through the opening as compared to the experiments by Crielaard. Due to more heat escaping via the opening, the compartment temperatures measured in this study were lower, even during the period where the input energy supplied by the propane burner was comparable. It is subsequently noted that a direct comparison is not able to be drawn between these experiments, and general trends are therefore only documented in this report when comparing adhesive performance.

In addition to the differences in ventilation openings, the differences in HRR supplied by the propane burner bed amongst the compartment experiments also contributed to the higher enclosure temperatures in the PU bonded CLT experiments. From Figure 39 it is evident that during the first 12 minutes of the PU bonded CLT experiment that a significantly higher HRR (63KW) was applied by the propane burner as compared to the 41kW implemented in the MUF bonded CLT experiment (which also experienced a burner outage of 5:30 minutes during the same initial period). As such, the difference in compartment temperatures between the experiments is attributed to differences in ventilation as well as initial fire exposure.

Figure 41 illustrates the temperature development within the CLT back wall panel, as measured at identical depths and similar locations at the centre of the panel.

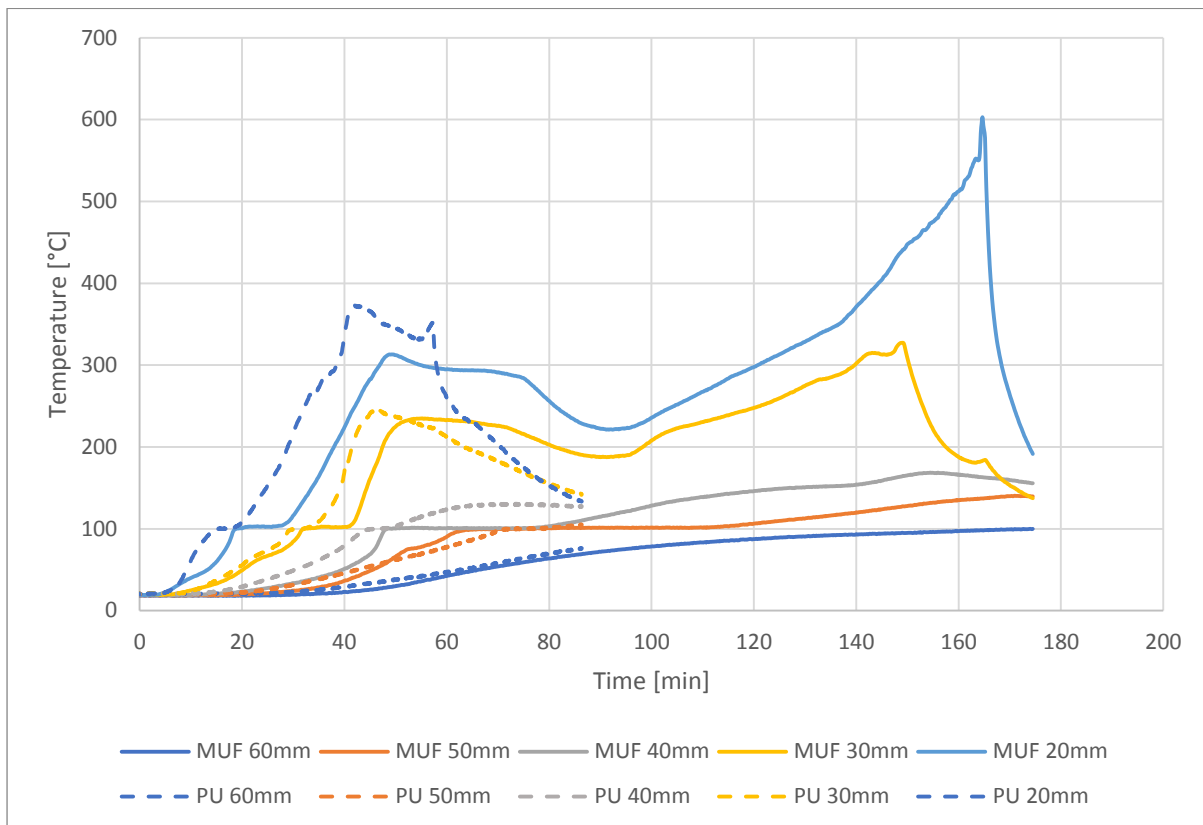


Figure 41: Comparing CLT back wall temperatures

From the CLT temperatures it is evident that the temperature within the first few layers of the CLT back panel rose at a faster rate in the test by Crielgaard (possibly due to the smaller ventilation opening trapping more heat within the compartment and the more severe initial fire exposure). It can also be seen that in-depth CLT temperatures remained elevated for a longer period of time in the MUF bonded back panel as compared to the PU bonded Back Wall Panel. It can be seen in the Figure above that after approximately 90 minutes temperatures measured at 20mm and 30mm from the fire exposed side of the MUF bonded back panel increased gradually due to local char flare up (as described in Section 6.1). This process of local char flare-up in the MUF bonded panel **did not increase compartment temperatures** (as seen in Figure 40) but did delay the achievement of self-extinguishment. Furthermore, the decay phase duration (as measured from the moment the burner bed was turned off until self-extinguishment was recorded) was extended by a factor of x2.9 in the MUF bonded CLT compartment as compared to the PU bonded CLT compartment (126 minutes as compared to 44 minutes, respectively), due to the occurrence of local char flare-up.

The charring front progression trends associated with the two experiments are also depicted graphically in Figure 42. The progression of the charring front depth (as identified by the position of the 300°C isotherm) is plotted against the time required to reach the specified temperature at those depths (as such the charring rate is the gradient of each curve). It should be noted that MUF-BW results were corrected by subtracting the burner outage time from the time required for the charring



front to progress to the specified depth. It is clear in the Figure, despite the charring rate being slightly lower (8.3%) in the MUF CLT panel across the first 20mm, that the duration during which the charring front propagated through the panel is longer in the MUF experiment. This is attributed to the extended duration of elevated temperatures measured in the MUF bonded CLT back panel as compared to the PU bonded CLT back panel.

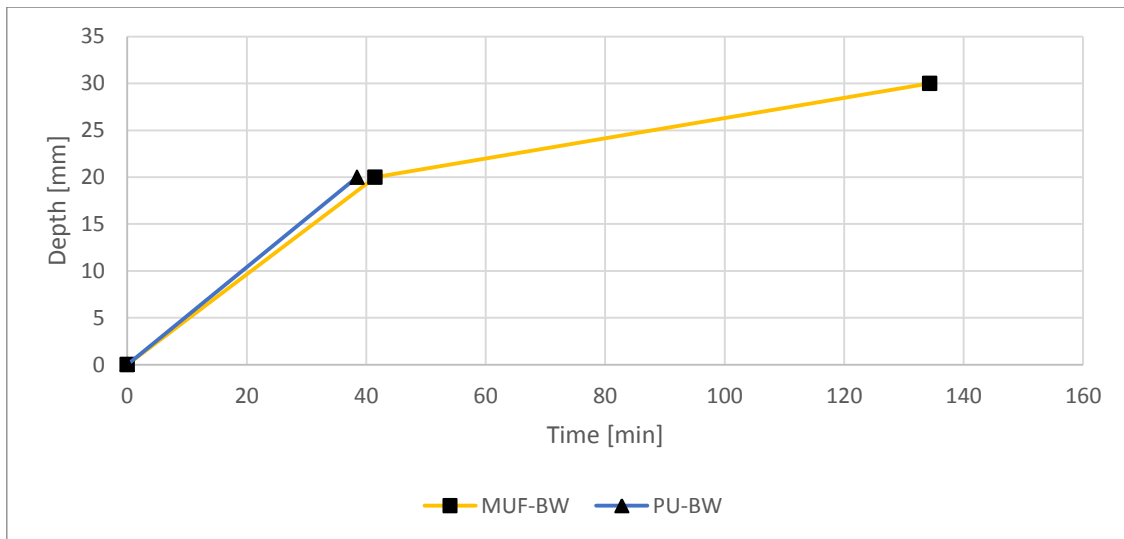


Figure 42: Comparing the progression of the charring front in Back Wall experiments

As mentioned, the difference in the abovementioned charring rates is believed to not only be dependent on the type of adhesive but also due to the input fire (heat) supplied by the propane burner amongst the experiments. These differences in input energy are further quantified in Figure 43 which depicts the TER by both the propane burner as well as the entire compartment (which includes the contributions of the propane burner bed and the combusting CLT):

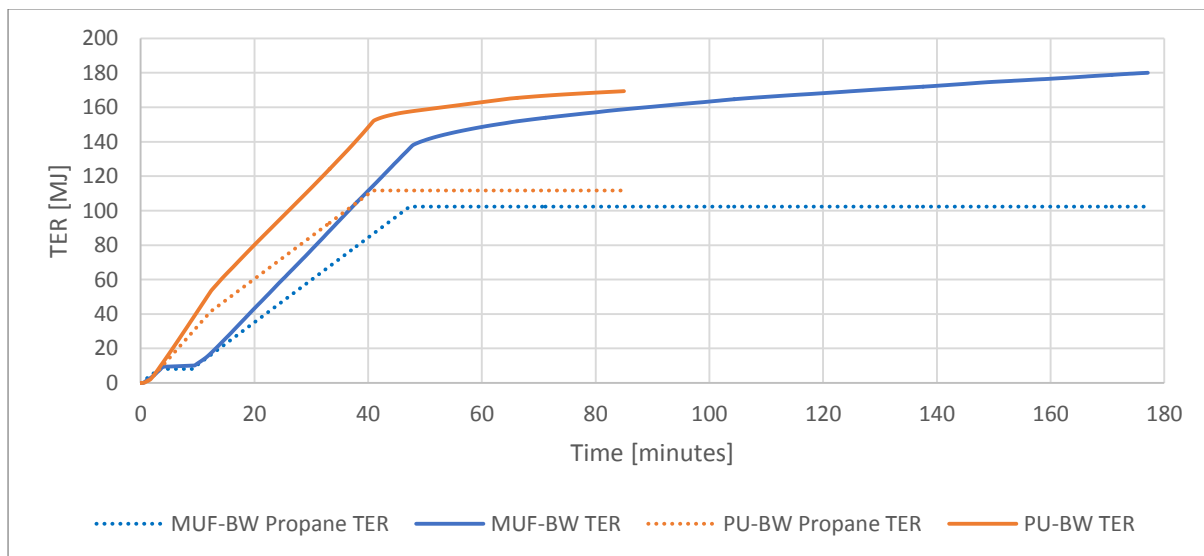


Figure 43: Compare TER amongst CLT Back Wall Compartments

From the figure above, it can be seen that the initial Propane HRR (gradient of the TER curve) was initially higher in the PU bonded CLT experiment, which is attributed to the higher input propane HRR of 63kW (as compared to 41kW) that was supplied during the first 12 minutes of the PU bonded CLT experiment. This more severe input fire exposure may have resulted in the higher first lamella charring rates, in addition to the smaller ventilation opening area available in the PU bonded CLT compartment.

The TER measured (including the CLT contribution) was measured at 180.0 MJ as compared to 169.3MJ in the MUF bonded and PU bonded CLT experiments, respectively. Additionally, the TER released by the propane burner was 102.3MJ and 111.7MJ in the MUF bonded and PU bonded CLT experiments, respectively.

### 7.2.2) Adhesive influence of compartments with CLT side walls

To facilitate a reasonable comparison related to fire behaviour, the experiment by Crielaard during which self-extinguishment of a compartment with two exposed CLT side walls was selected for comparison (namely PU-2SW-2). It is important to take cognisance of the fact that with an identical experimental set-up, Crielaard recorded that a compartment with two PU bonded CLT side panels (namely PU-2SW-1) underwent burn-through and as such did not extinguish (as discussed in Section 7.2).

#### **Heat Release Rates**

Figure 44 compares the input propane burner HRR as well as the total HRR between compartment tests MUF-2SW (this study) and PU-2SW-2 (study by Crielaard).

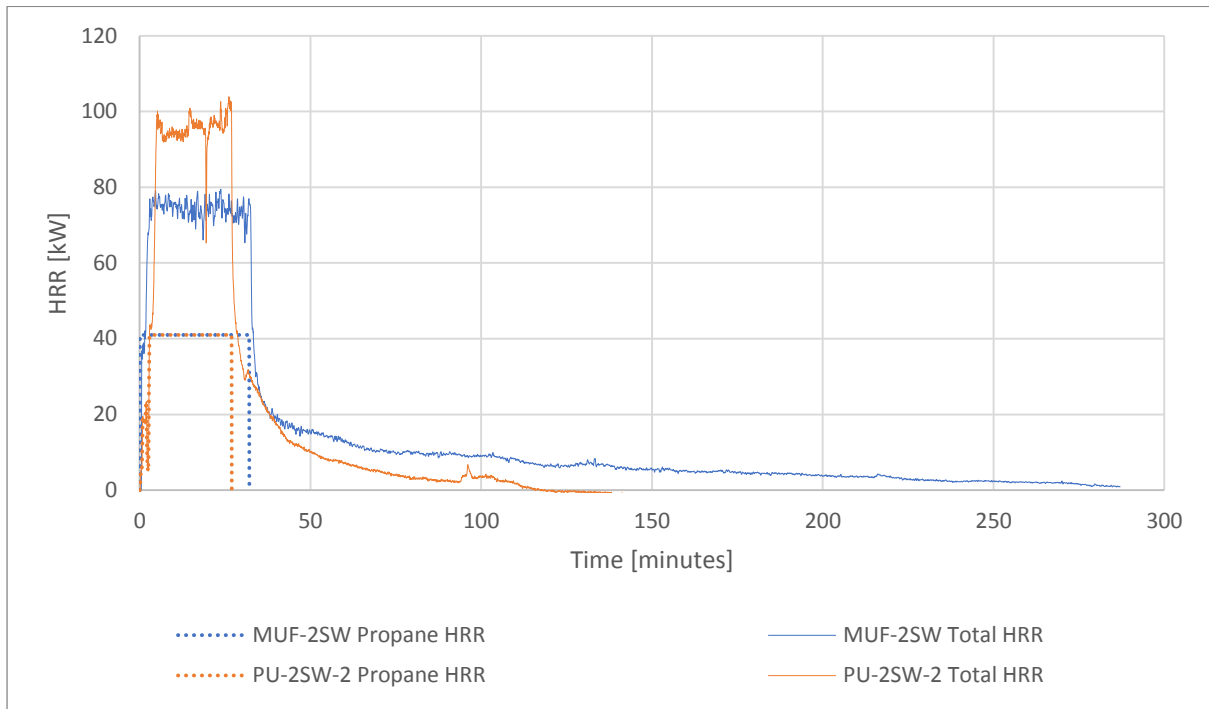


Figure 44: Comparing HRR of tests with CLT Side Panels

The average total HRR during the heating phase of Crielaard's compartment test containing PU bonded CLT panels was higher than that recorded during the experiment with MUF bonded CLT panels. In the MUF bonded CLT experiment, the two CLT side walls contributed on average 32.4kW in addition to the propane input fire, whereas in the PU bonded CLT experiment the CLT contribution during the heating phase was 54kW (i.e. 67% higher). Similarly to the back wall compartment tests, the duration of the decay phase was x2 longer in the MUF bonded CLT compartment test as compared to the PU bonded CLT compartment test (252 minutes as compared to 123 minutes).

## Temperatures

The compartment temperatures measured at identical positions are depicted in Figure 45. Once again, due to the larger available ventilation opening in the MUF bonded CLT experiment, compartment temperatures are higher in Crielaard's PU bonded CLT test during the heating phase. The temperature differences in the compartments may also have been due to the differences in HRR measured. A 67% higher HRR was measured in the PU bonded CLT compartment despite identical input propane HRRs delivered amongst the two experiments (i.e. 41kW).

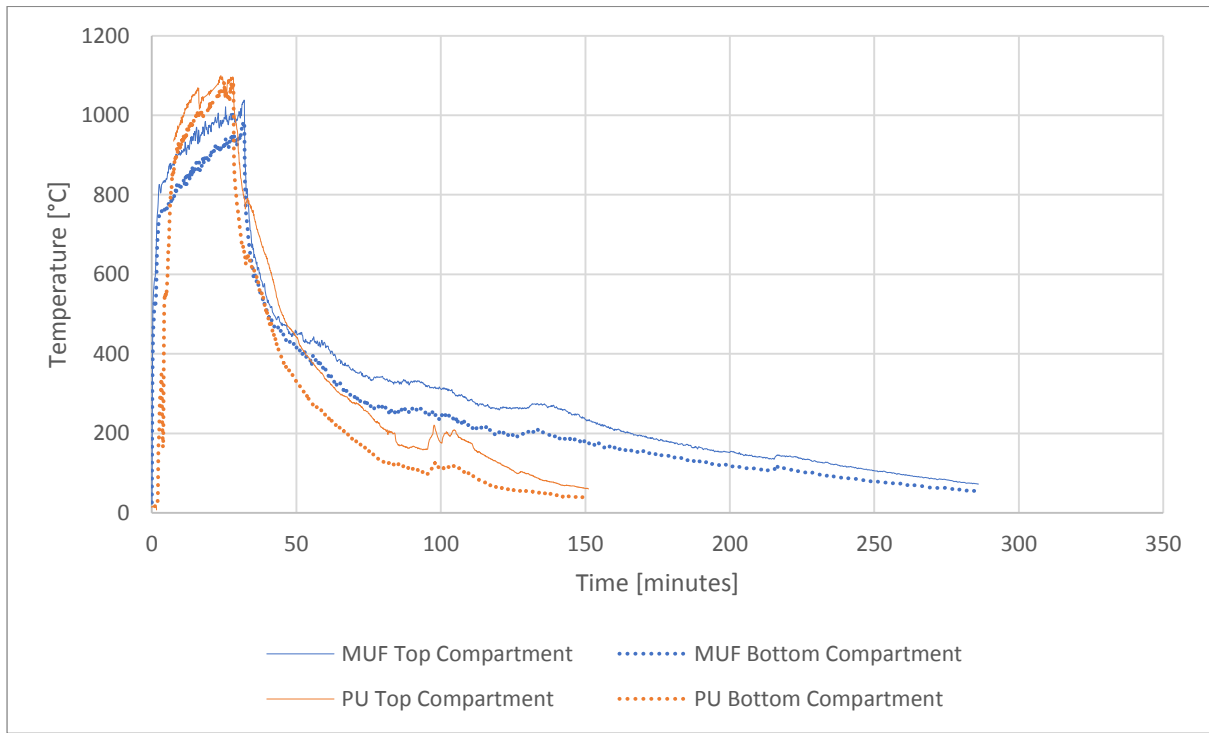


Figure 45: Comparing compartment temperatures in CLT Side wall experiments

The CLT panel temperatures in both the MUF and PU compartment tests, as measured in the right (R) and left (L) panel are depicted in Figure 46 and Figure 47, respectively.

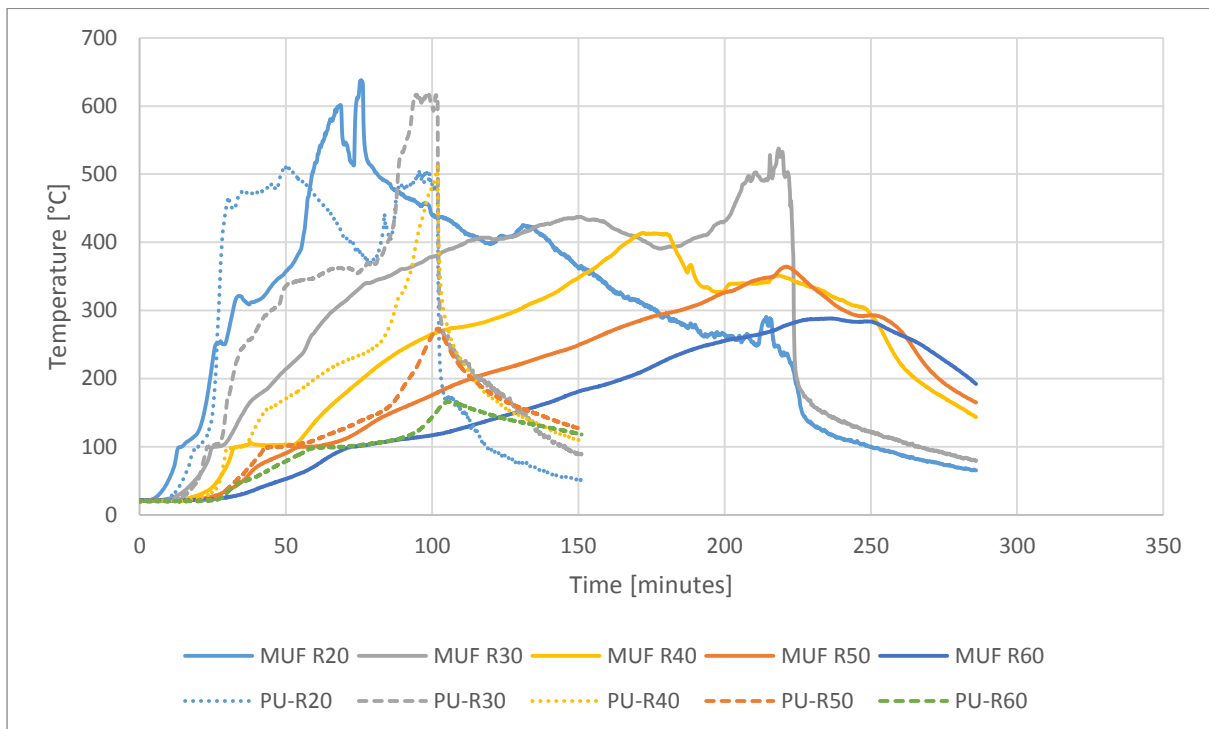


Figure 46: Comparing Right Panel Temperatures in experiments with two exposed side walls

From both Figure 46 and Figure 47 and it is clear to see that in-depth CLT temperatures remained elevated for a longer period in the MUF bonded panels as compared to the PU bonded CLT panels. This occurred despite the similarities in HRR delivered by the propane burner and the duration that the burner bed was ignited (namely 32 minutes and 27 minutes in the MUF bonded CLT and PU bonded CLT compartment tests, respectively).

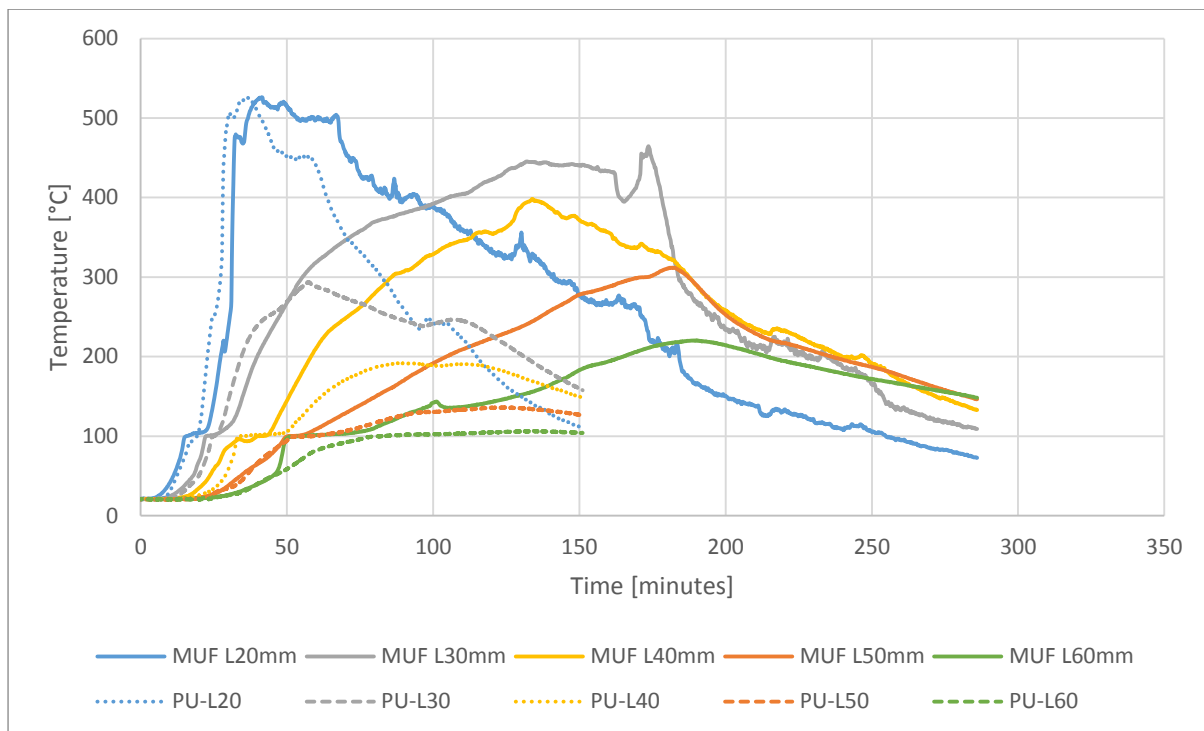


Figure 47: Comparing Left Panel Temperatures in experiments with two exposed side walls

The charring behaviour of these tests is more easily discernible when considering Figure 48 (by comparing the gradients of individual curves). It can be seen in the compartment test with PU bonded CLT side walls, that the charring rate during the heating phase of the fire was higher (14.1% and 19.4% in the left and right panel, respectively) compared to the MUF bonded CLT side walls. Despite this, the charring front did not propagate as far through the thickness of the panels within the PU bonded CLT side walls (20mm and 40mm) as compared in the MUF bonded CLT experiment (50mm in both panels).

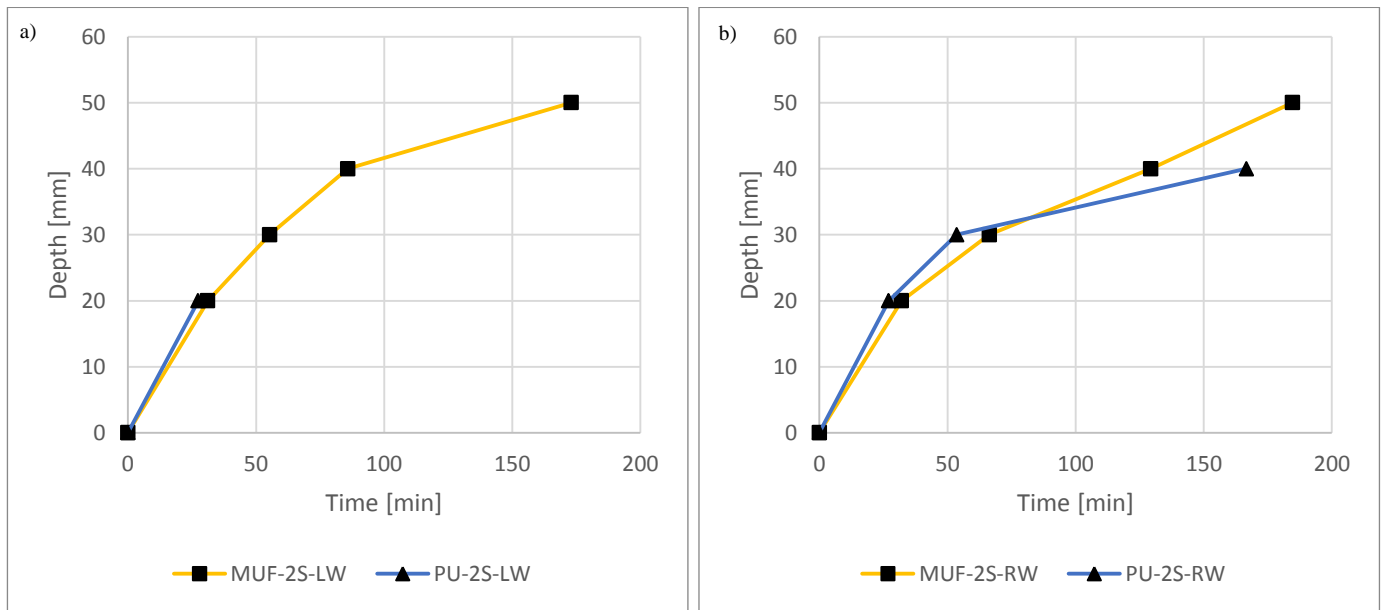


Figure 48: a) Left Wall (LW) Charring front progression in experiments with two exposed side Walls. b) Right Wall (RW) Charring front progression in experiments with two exposed side Walls

To assess the fire exposure conditions amongst these experiments, the TER by the propane fire as well as the entire compartment TER (which includes the heat energy released by the combusting CLT) are compared between the experiments, as shown in Figure 49:

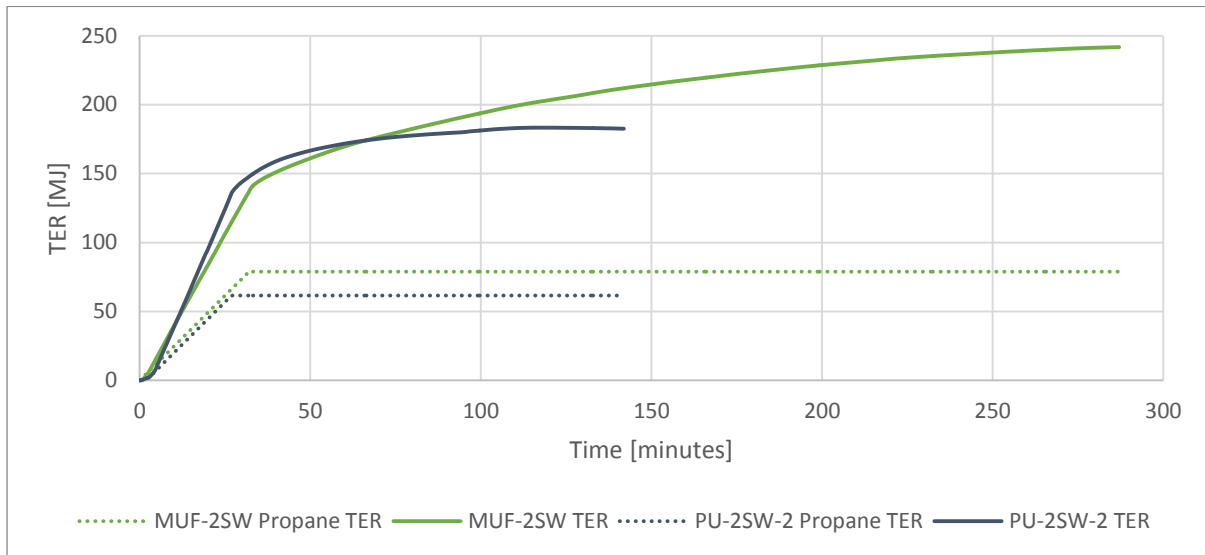


Figure 49: Compare TERs amongst CLT Back Wall Compartments

From the figure above, it can be seen that the initial Propane HRR (gradient of the TER curve) is comparable between the two experiments, indicating comparable initial fire exposures. Interestingly, the entire compartment HRR measured in experiment PU-2SW-2 was higher as compared to the MUF-2SW experiment. This difference is therefore not due to the differences in initial fire exposure.

The TER measured (including the CLT contribution) was measured at 241.8 MJ as compared to 183.3 MJ in the MUF bonded and PU bonded CLT experiments, respectively. Additionally, the TER released by the propane burner was 78.8 MJ and 61.5 MJ in the MUF bonded and PU bonded CLT experiments, respectively.

### 7.2.3) Answering Research Sub-Question 3

*Q3) What is the influence of adhesive type on compartment fire behaviour?*

Based on the comparable experiments performed on compartments containing MUF- and PU bonded CLT panels, general trends are identified. These trends are based on small-scale experiments, and would require further testing to assess their validity in larger-scale fire scenarios. The following general observations are recorded in order to answer the third sub-research question postulated in Figure 2.

- In compartments with two exposed CLT side walls, both CLT burn through and self-extinguishment was observed in compartments containing PU bonded CLT side panels. In contrast, with the same CLT build-up and fire exposure conditions, a compartment constructed of MUF bonded CLT side panels achieved self-extinguishment. In the MUF bonded CLT side panels, local char fall-off (which increased compartment temperatures by  $\pm 10^{\circ}\text{C}$ ) was observed as compared to delamination (of planks) in PU bonded CLT side panels

(which resulted in a second flashover). The total amount of released energy was 13.5% more in the PU bonded side panel experiment compared to the MUF bonded CLT side panel experiment.

- In compartment experiments containing **an exposed CLT back wall**, the duration of the decay phase was extended by a factor of 2.9 in the MUF bonded CLT back wall configuration. This extended duration was attributed to the occurrence of local chare flare-up which delayed the achievement of self-extinguishment but did not influence compartment temperatures. Charring rates are not to be compared amongst the aforementioned experiments due to difference in HRRs supplied by the propane burner. Lastly, the charring front progressed further into the MUF bonded CLT back wall (30mm) as compared to the PU bonded CLT back wall (20mm) due to the aforementioned prolonged decay phase duration.
- In compartment experiments containing **two exposed CLT side walls which self-extinguished**, the total HRR during the heating phase (including both the contribution of the propane burner and combusting CLT) was 67% higher in the PU bonded CLT compartment as compared to MUF bonded CLT compartment, despite identical HRRs being delivered by the propane burner in the two experiments. Additionally, during the heating phase, charring rates were 14.1% to 19.4% higher in the PU bonded CLT panels as compared to the MUF bonded CLT panels. Furthermore, in depth-temperatures remained elevated twice as long during the decay phase of the MUF bonded CLT compartments, due to elevated compartment temperatures. Lastly, the charring front progressed further into the MUF bonded CLT side wall panels (50mm) as compared to the PU bonded CLT side walls (20mm and 40mm).

### 7.3) Influence of panel configuration on compartment fire behaviour

Referring back to the Table 3, which lists the comparisons to be drawn between configurations, the following configurations will be compared to one another:

- i) MUF-BW vs MUF-SW-1 vs 1 MUF-C-1 to investigate the behaviour of compartments with only one exposed CLT surface. This comparison set will also be used to assess the hypothesis of a second hot surface being formed in tests with single exposed panels that are not a ceiling panel.
- ii) MUF-2SW vs MUF-SW-1 to characterise the cross-radiation between facing side-wall CLT panels
- iii) MUF-BW vs MUF-BW+C-1 to assess the influence of adding a CLT ceiling to a configuration with only a CLT back wall
- iv) MUF-2SW vs MUF-BW+C-1 to characterise the influence of panel orientation in compartments with two exposed CLT panels.



Each of these comparisons will be discussed individually in this section of the report. Only the first set of experiments per compartment configuration is discussed here. Panel configuration results pertaining to the repeat experiments (MUF-SW-2; MUF-C-2 and MUF-BW+C-2) are presented in Appendix G. As a general note, the adhesive type (i.e. MUF) will be omitted from the implemented experimental naming convention in this section of the report, since panel configuration comparisons are based on MUF bonded CLT panels only.

The 4 sets of compartment configurations are displayed visually in Figure 50:

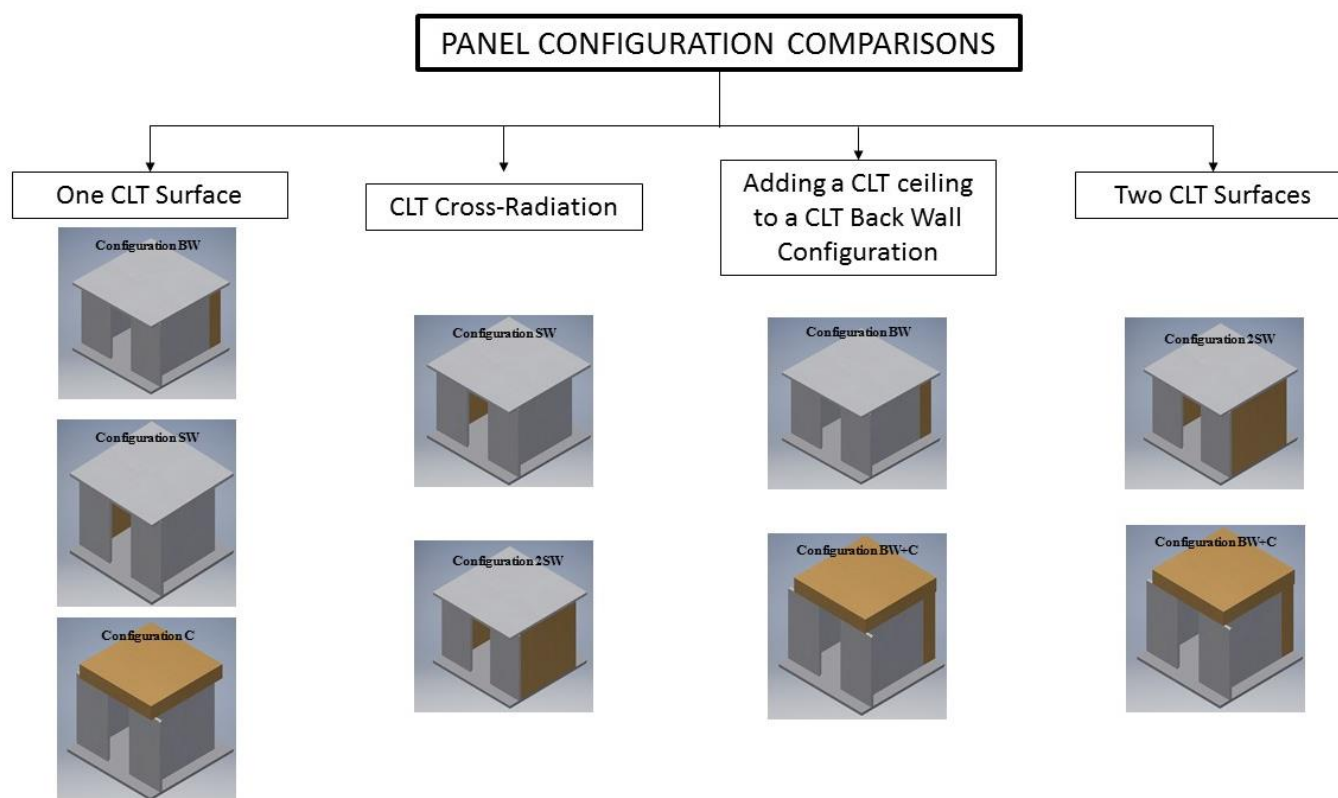


Figure 50: Visual illustration of CLT panel configuration comparisons investigated in this research project

### 7.3.1) Characterising the behaviour of compartments with one exposed CLT surface

A discussion of the influence of panel configuration in compartments containing a single exposed CLT wall is presented in this section. A discussion of the HRR and temperature development of compartments with a CLT back wall (BW), side wall (SW-1) or ceiling (C-1) is presented.

## Heat Release Rates

The Total HRR measured during each of the three experiments involving one exposed CLT surface is presented in Figure 51.

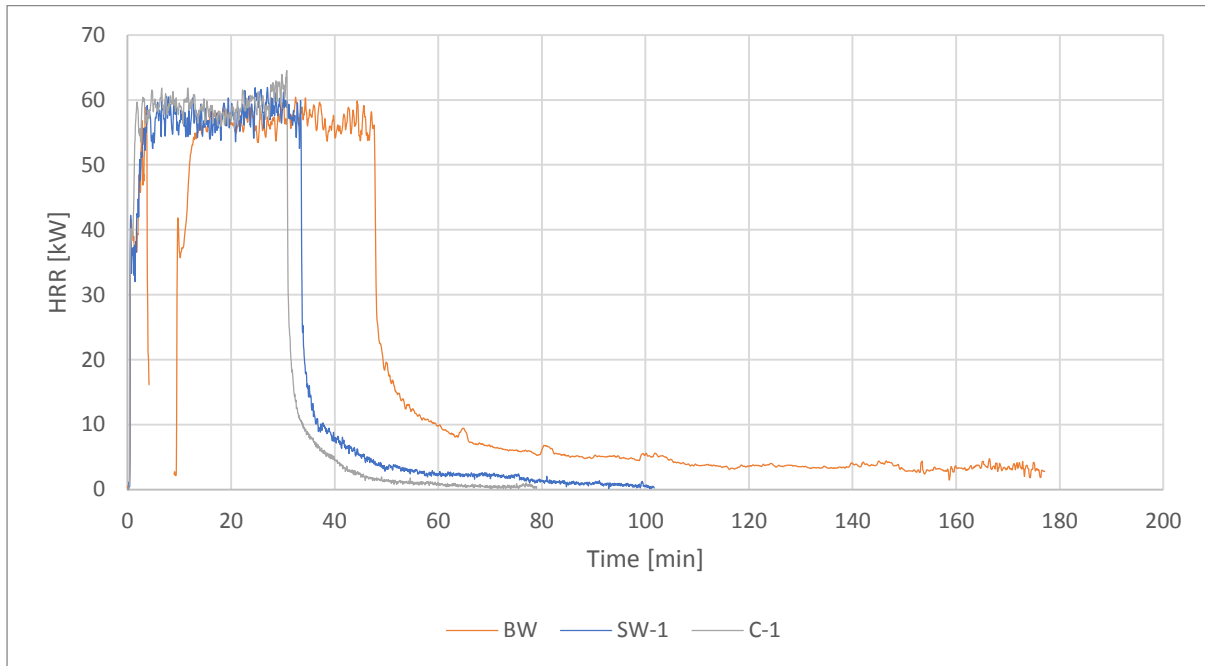


Figure 51: Comparing HRR amongst configurations with one exposed CLT surface

As depicted in Table 26, the average total HRR during the heating phase did not vary significantly between the three single CLT surface tests (namely 56.6kW, 57.4 and 59.1kW in tests BW, SW-1 and C-1 respectively). This tendency was also recorded in the repeat experiments, suggesting that the additional HRR due to the combustion of a single CLT surface is unaffected by panel orientation. One exposed CLT surface resulted in an increase in HRR of between 34% and 44% across all single exposed CLT surface tests (including repeat tests).

The duration of the decay phase, as documented in Table 23, is significantly longer in the Back Wall (BW) compartment tests as compared to a Side Wall (SW-1) and Ceiling (C-1) CLT surface tests (126:20 minutes as compared to 38:50 and 21:00 minutes, respectively). It is hypothesised that this extended decay phase duration is due to the increased distance of a back wall to the ventilation opening as compared to a side wall or ceiling configuration. This increased distance inhibits the escape of heat from within the compartment and subsequently sustains the smouldering combustion process. The shortest decay phase duration occurred in the Ceiling CLT configuration. It is hypothesised that this is as a result of the relatively lower amount of oxygen available at the ceiling as compared to other surfaces, due to the occurrence of combustion gases being emitted and rising to the ceiling (which reduces the oxygen concentration, thereby removing a component required to sustain combustion).

## Temperatures

Figure 52 also illustrates similar trends as identified when analysing the HRR results. The shortest decay phase duration was documented in the Ceiling CLT configuration, followed by the Side CLT wall configuration and finally the Back Wall configuration.

The average compartment temperature during the heating phase, as measured at the top of the compartment did not vary greatly between the 3 configurations, namely 918°C, 950°C and 977°C (Back, Side and Ceiling, respectively). The highest average compartment (Top) temperature was recorded during the exposed CLT ceiling test.

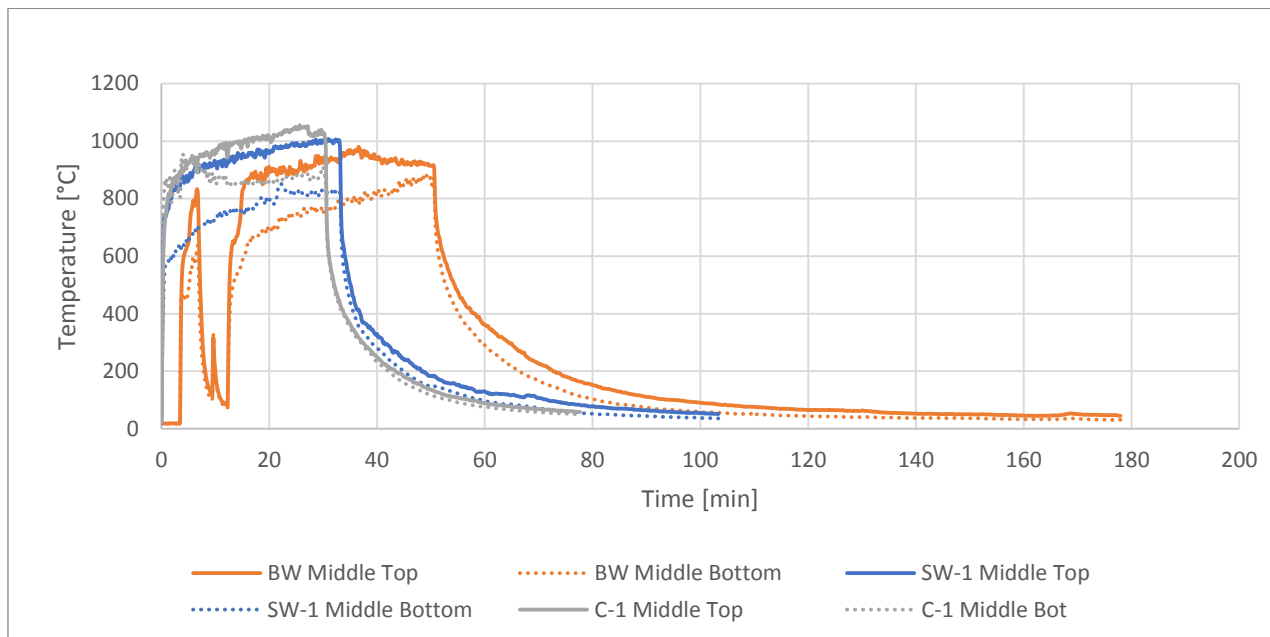


Figure 52: Comparing compartment temperatures amongst configurations with one exposed CLT surface

The charring behaviour recorded during the three tests is depicted in Figure 53. It is clear that temperatures within the CLT Back Wall remained elevated for a longer period of time as compared to the Side Wall and Ceiling tests. Temperature dropped faster within the ceiling panel as compared to the side panel and back wall, possibly due to the aforementioned hypothesis that the oxygen content at the ceiling is lower than in comparison to other surfaces due to the build-up of combustion gases.

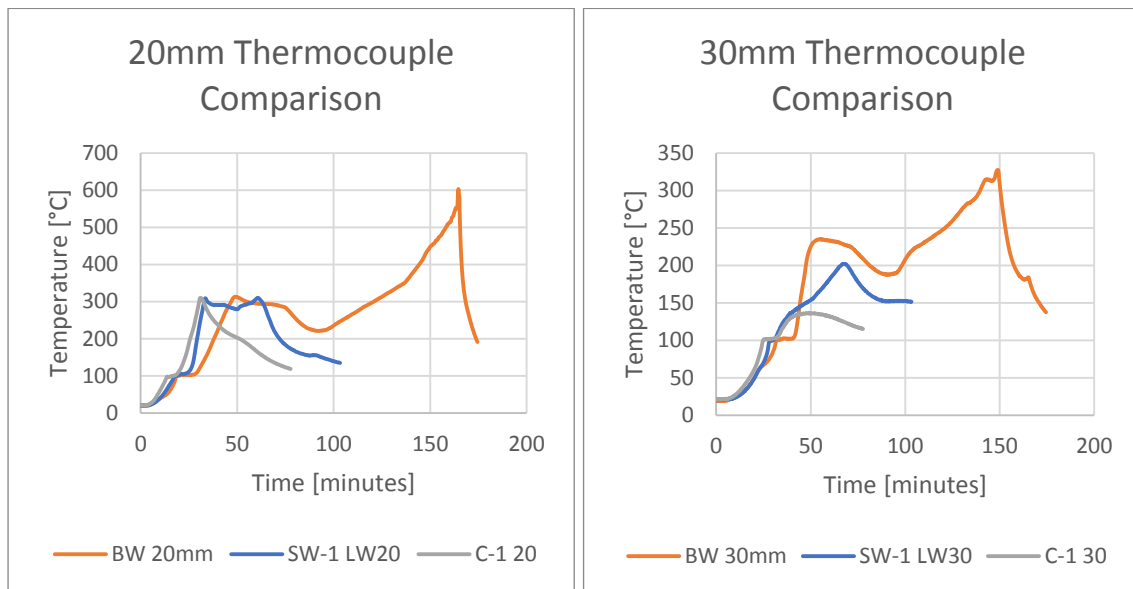


Figure 53: Comparing CLT panel temperature development amongst configurations with one exposed CLT surface

Table 3 of this report made mention of using these compartment configurations to assess the validity of a “Second Hot Surface”. The hypothesis states that an exposed CLT ceiling configurations demonstrates beneficial fire behaviour as compared to an exposed vertical CLT panel (side wall or back wall). This hypothesis is supported by the recorded temperature and HRR results. The notion that the formation of a second hot surface is prevented in an exposed CLT configuration requires further investigation in future research. Heat flux sensors are required to adequately measure the heat flux received by an exposed ceiling or vertical surface. The results recorded in this research suggest that ceiling temperatures are hotter in exposed ceiling configurations as compared to vertical CLT panel configurations. The suggested reasoning in this report concerning oxygen depletion at the ceiling level of a compartment with an exposed CLT ceiling is based on Fire Dynamics principles, but would also require further testing by means of oxygen level measurements across exposed CLT surfaces.

### 7.3.2) Characterising the cross-radiation behaviour of facing CLT side walls

To investigate the influence of cross-radiation between two exposed CLT side walls, the results of compartment tests with both exposed walls (2SW) are compared to those of compartments with only one side wall (SW-1). Based on these comparisons, trends are identified.

#### Heat Release Rates

Figure 54 illustrates the total HRR measured during the compartment experiment with two side CLT walls (2SW) and one CLT side wall (SW-1). On average, the total HRR during the heating phase was 73.4kW in the 2SW configuration, as compared to 57.4kW in the SW-1 configuration (representing an increase of 80% and 40% in addition to HRR delivered by the propane burner in both experiments).

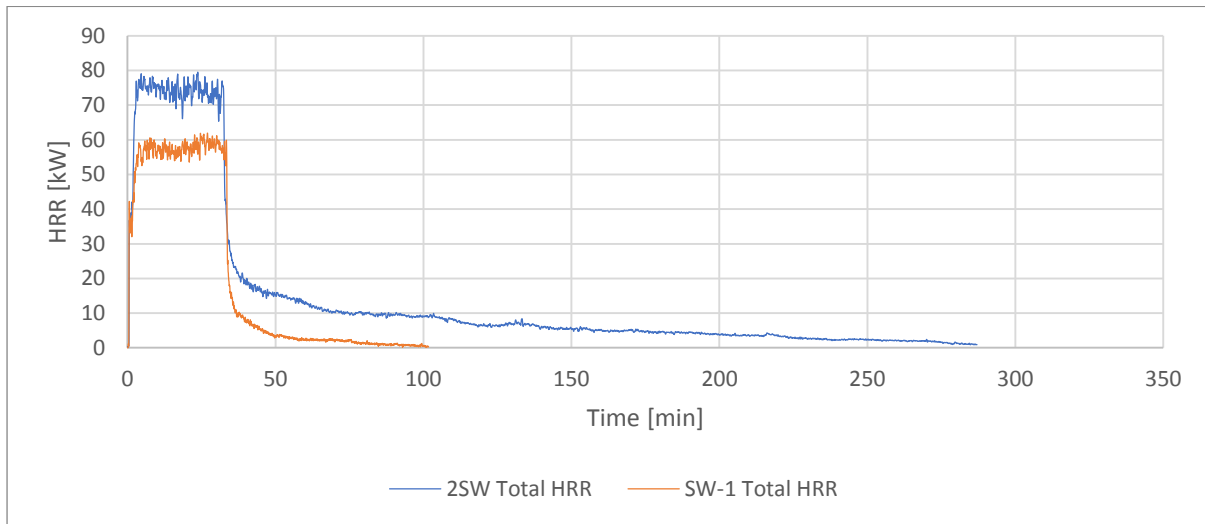


Figure 54: Comparing HRR amongst compartments with one or two exposed Side Walls

The decay phase was initiated at comparable moments in both compartment tests, but it is clear from the Figure that the duration of the decay phase was significantly prolonged in the 2SW Configuration experiment as compared to the SW-1 configuration (251:20 minutes as compared to 38:50 minutes, respectively). This 6.5 times longer decay phase in Test 2SW as compared to Test SW-1 indicates the influence of replacing a non-combustible side wall with a combustible CLT wall, in a compartment with only one exposed CLT side Wall.

## Temperatures

Figure 55 shows the compartment temperatures measured at the face of the exposed CLT side wall in both compartments 2SW and SW-1.

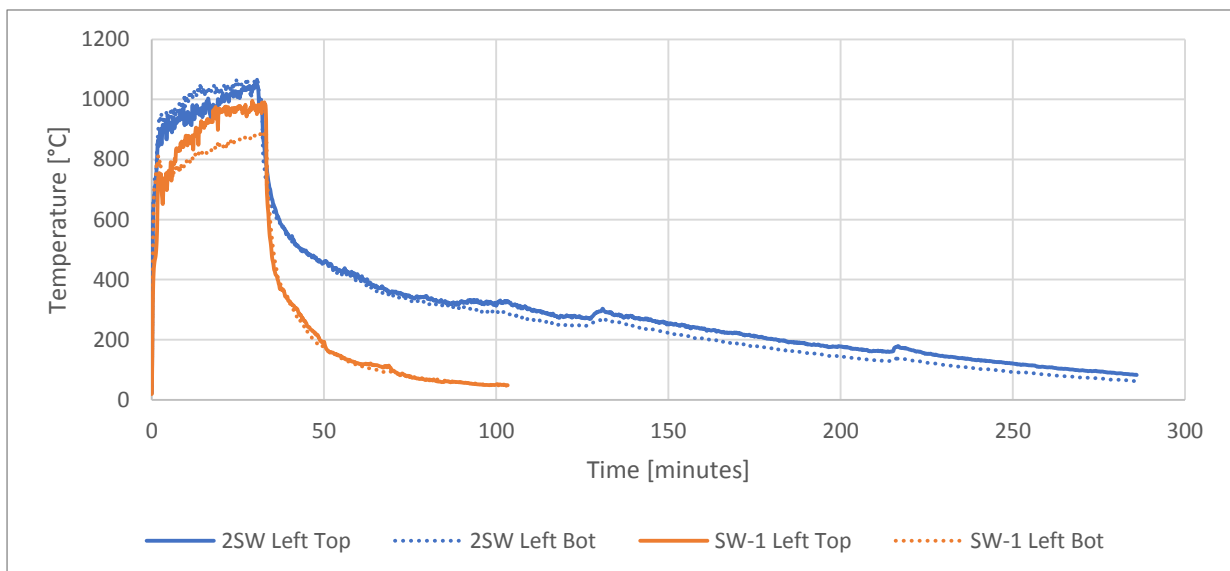


Figure 55: Comparing Compartment Temperatures at CLT surfaces in Configurations 2SW and SW-1

The temperature development during the heating phase is comparable between these two configurations, and the moment that the propane burner was switched off occurred at comparable instances. The temperature decay at the face of the CLT panel was however much more gradual in configuration 2SW as compared to configuration SW-1. Test SW-1 showed a sharp decline in compartment temperature and a decay phase duration of 38:50 minutes, as compared to the approximately 6.5 times longer decay phase recorded in Configuration 2SW.

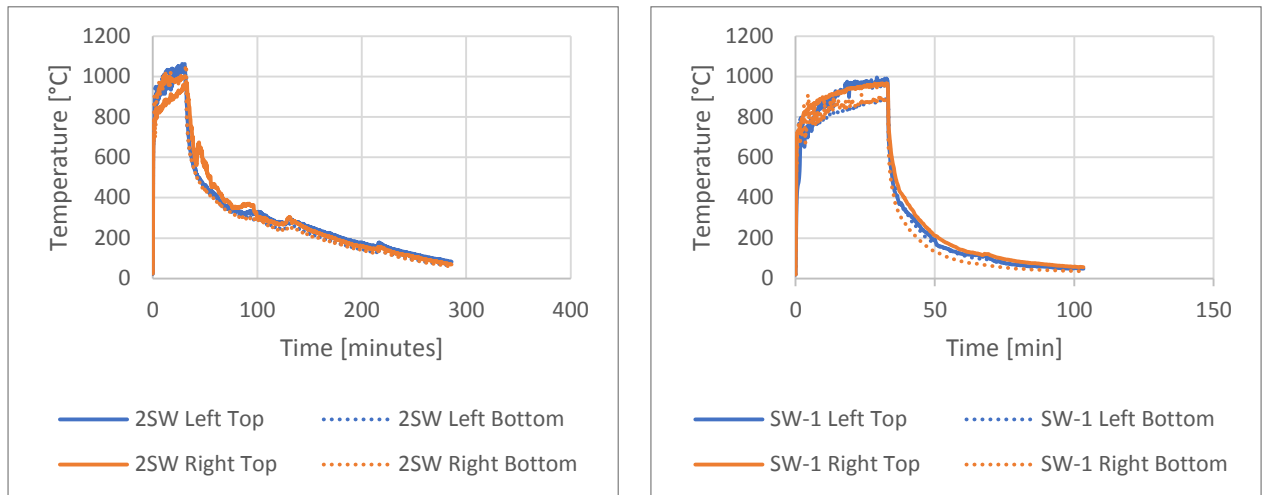


Figure 56: Wall Temperatures in Compartments 2SW and S-1

An important point to take note of is that the temperature in front of an exposed CLT side wall did not differ from that in front of a non-combustible board (as shown in Figure 56 above for Compartments 2SW, as well as SW-1 where the left wall was an exposed CLT wall and the right wall non-combustible).

Figure 57 illustrates that elevated temperatures within the CLT left side wall in Compartment 2SW were sustained for longer as compared to Compartment SW-1. Since the rate of temperature decrease inside the compartment with two exposed CLT side walls is slower than in Compartment SW-1, the CLT temperature decline is also slower, which prolongs the decay phase. In short, compartments with two exposed CLT walls leads to a sustained period of elevated temperatures within the compartment during the decay phase, leading to a deeper depth of charring within the CLT panels as well as a longer period required to achieve self-extinguishment. The charring rate of the first lamella was not increased significantly by the addition of another side wall when comparing Compartments SW-1 and 2SW (0.61 and 0.64 mm/min, respectively), but the charring front did propagate deeper into the Left CLT Panel of configuration 2SW as compared to the left panel in Compartment SW-1 (to a depth of 50mm as compared to 20 mm).

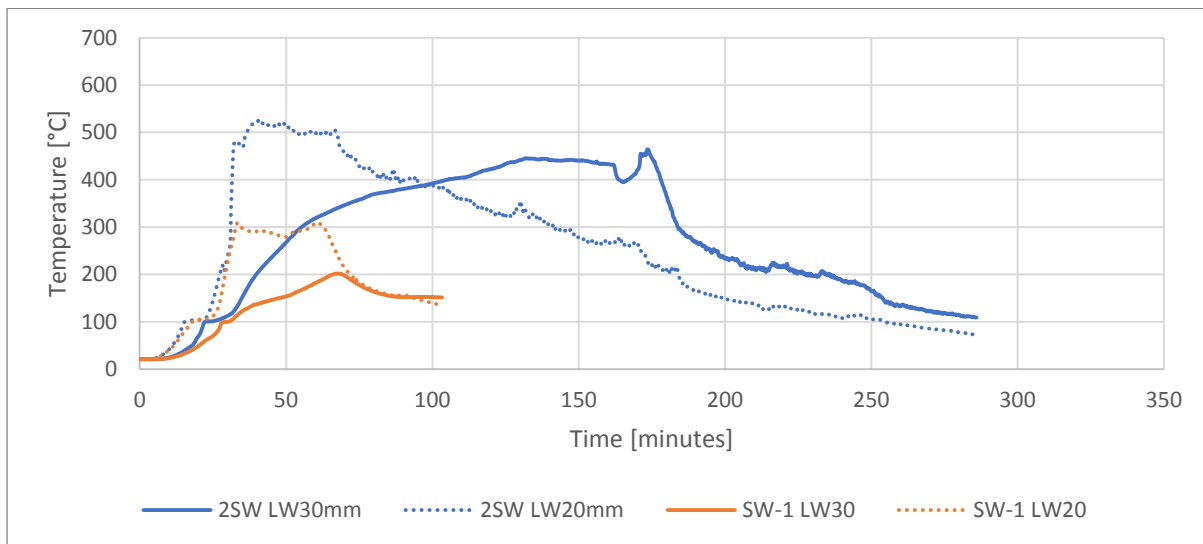


Figure 57: Charring behaviour of CLT panels in Compartments 2SW and SW-1

### 7.3.3) Characterising the addition of an exposed CLT Ceiling to a compartment with a CLT back wall

Due to the error that the propane burner bed turned off for a period of 5:30minutes, only general trends will be identified when comparing the BW Configuration to the BW+C-1 Configuration.

#### Heat Release Rates

Figure 58 compares the total HRR measured during the compartment test containing an exposed CLT back Wall (BW) and exposed Back Wall and Ceiling (BW+C-1). It can be seen that in both tests that the exposed CLT contributed to the total HRR in addition to the input 41kW fire as supplied by the propane burner. The CLT contributed on average 15.6kW and 31.9kW to the HRR during the heating phase during the BW Compartment Test and BW+C-1 compartment test, respectively. In the repeat test (BW+C-2) the CLT only HRR during the heating phase was measured as 31.3kW. The addition of a second exposed CLT surface to the BW configuration therefore approximately doubles the additional HRR released by the combusting CLT alone.

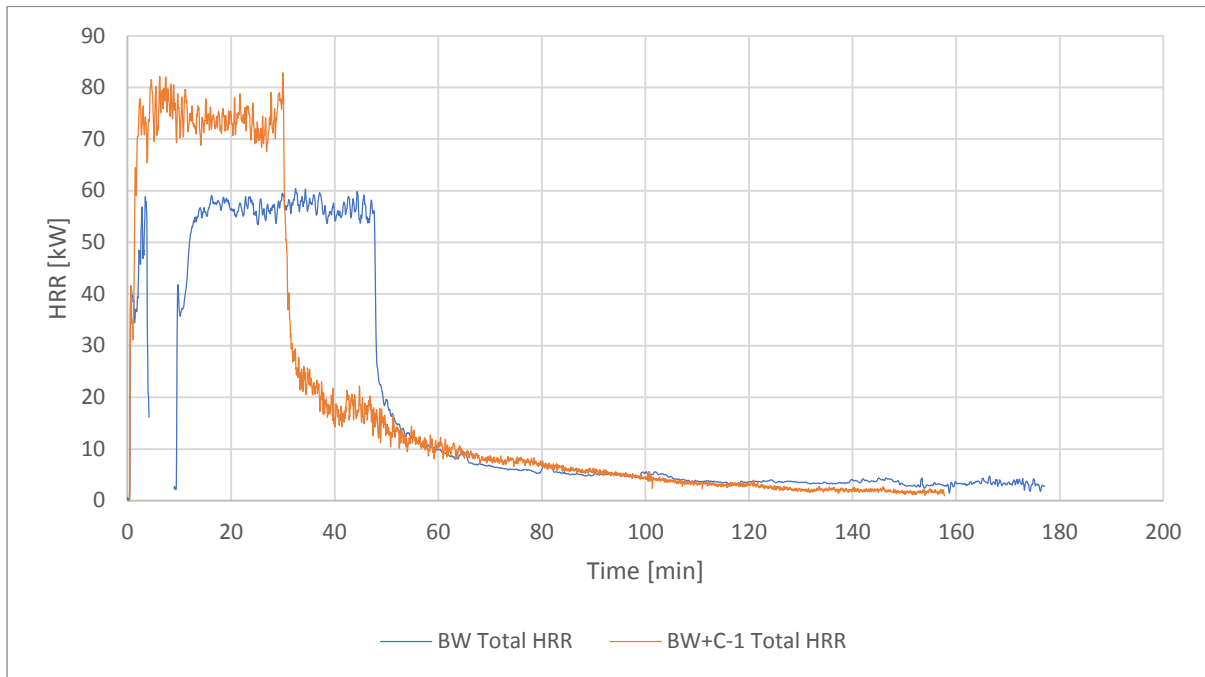


Figure 58: Comparing HRR between Configuration BW and BW+C-1

## Temperatures

Figure 59 plots the compartment temperatures measured during Compartment tests BW and BW+C-1. During the heating phase, the average temperature in the middle of the compartment, measured at a height of 0.4m from the floor panel, was comparable between the two experiments (917.6°C and 932.7°C Compartments BW and BW+C-1 respectively). This suggests that compartment temperatures are unaffected by the addition of a second exposed CLT surface. It is postulated that this is as a result of the under-ventilated nature of the fire, and this statement is backed up by the visual observation that relatively more external flaming occurred in test BW+C-1 as compared to test BW. In the under ventilated fire, the maximum compartment temperature is already attained and flames escape through the opening. With the addition of a second exposed surface, the compartment temperatures are not influenced, but the additional heat released by the second CLT panel increase the amount of external flaming and subsequently the total HRR. The duration of the decay phase, as documented in Table 23, was measured as 126:20minutes and 91:20 minutes in Compartments BW and BW+C-1, respectively. As mentioned previously, these durations should not be compared directly due to the occurrence of the burner bed outage in Compartment BW



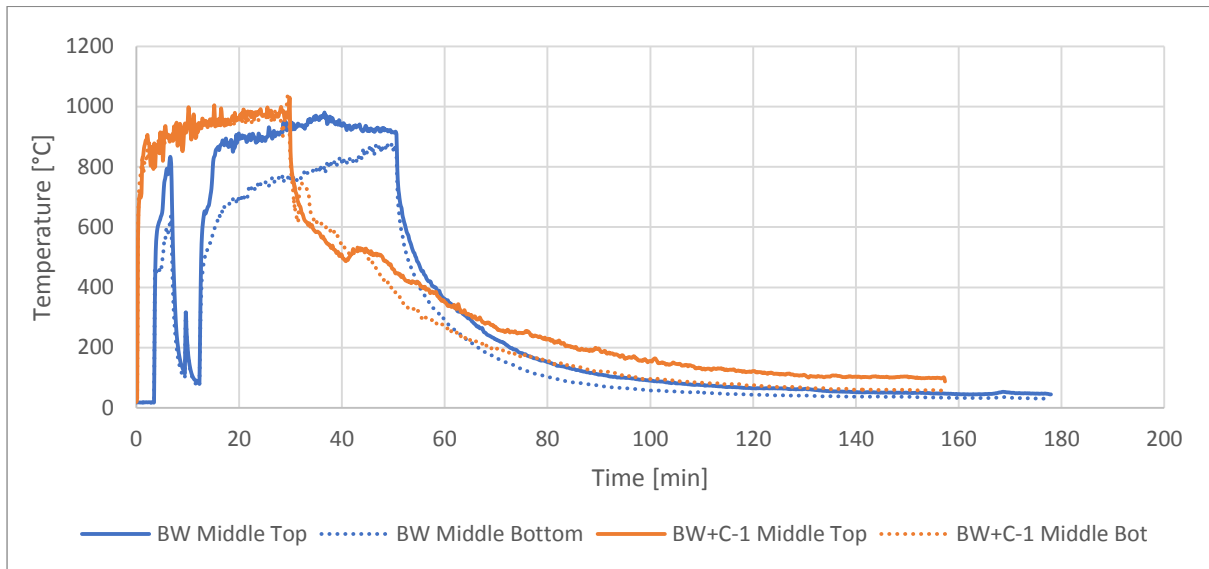


Figure 59: Comparing compartment temperatures between Configuration BW and BW+C-1

The charring behaviour of the BW and BW+C-1 configurations are illustrated in Figure 60.

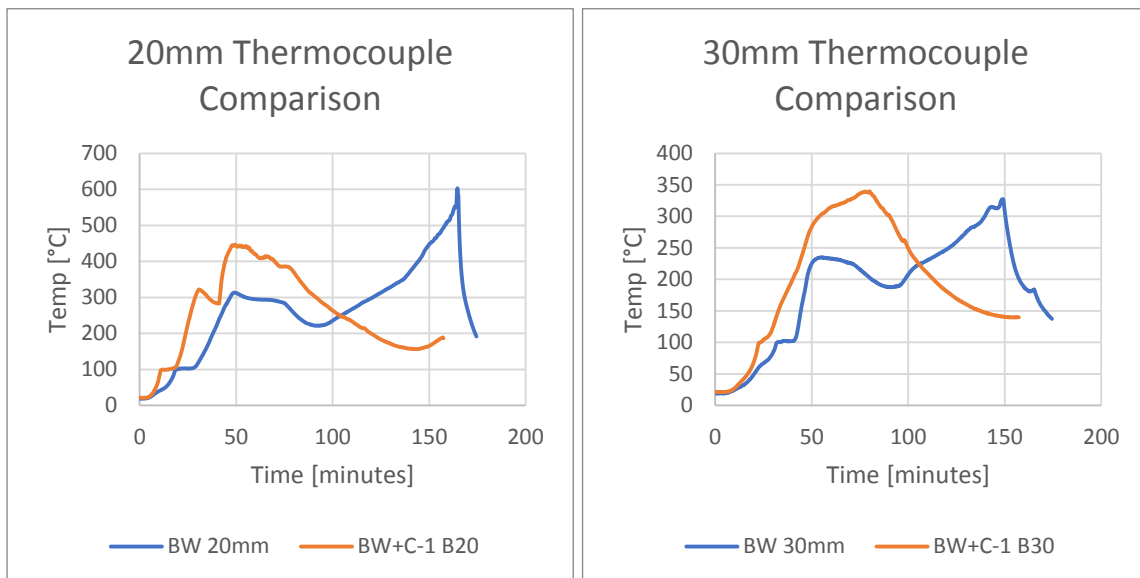


Figure 60: Charring behaviour of Compartments BW and BW+C-1

The charring rate of the back wall panel in Compartment BW+C-1 is 44% higher in the first lamella (20mm) as compared to Compartment BW (0.69mm/min compared to 0.48mm/min, respectively). In addition, as shown in Table 29, the charring depth penetrated to 30mm in the Back panel and only to 20mm in the ceiling pane, both in Compartment BW+C-1. This reinforces the argumentation presented in Section 7.3.1 concerning single exposed CLT panels. Since the back wall is positioned further away from the ventilation opening, the escape of heat is inhibited as compared to a ceiling panel which is positioned adjacent to the opening. Heat is trapped at the back wall and as such the combustion process is sustained longer at the back wall as compared to the ceiling panel.

### 7.3.4) Characterising the behaviour of compartments with two exposed CLT surfaces

This section of the Analysis Chapter is dedicated to comparing compartment configurations with two exposed CLT surfaces, namely Configuration 2SW and BW+C-1.

#### **Heat Release Rates**

Figure 61 illustrates the measured HRR during compartment Tests 2SW and BW+C-1. During the phase of the fire when the propane burner bed was ignited, the averaged total HRR did not vary significantly between the two compartment configurations (73.4kW and 72.9kW in Compartments 2SW and BW+C-1, respectively). This indicates that the additional HRR by two CLT panels is independent of the orientation of the CLT panels, and measures between 32.4kW and 31.9kW (approximately 75% additional HRR as supplied by only the propane burner bed). The duration of the decay phase was significantly longer (by a factor of x2.8) in the 2SW configuration as compared to the BW+C-1 Configuration (251:50 minutes and 91:20 minutes, respectively).

Despite the similarities in HRRs during the heating phase and time required to char the first CLT lamellas, the TER in both compartment experiments differed significantly. The TER released by the combusting CLT alone was measured at 163MJ and 115MJ in Compartments 2SW (facing panels) and BW+C-1 (adjacent panels), respectively. In the facing CLT configuration as compared to the adjacent CLT configuration, the contribution to the TER increased by a factor of x1.4 due to this configuration's x2.8 times longer decay duration.

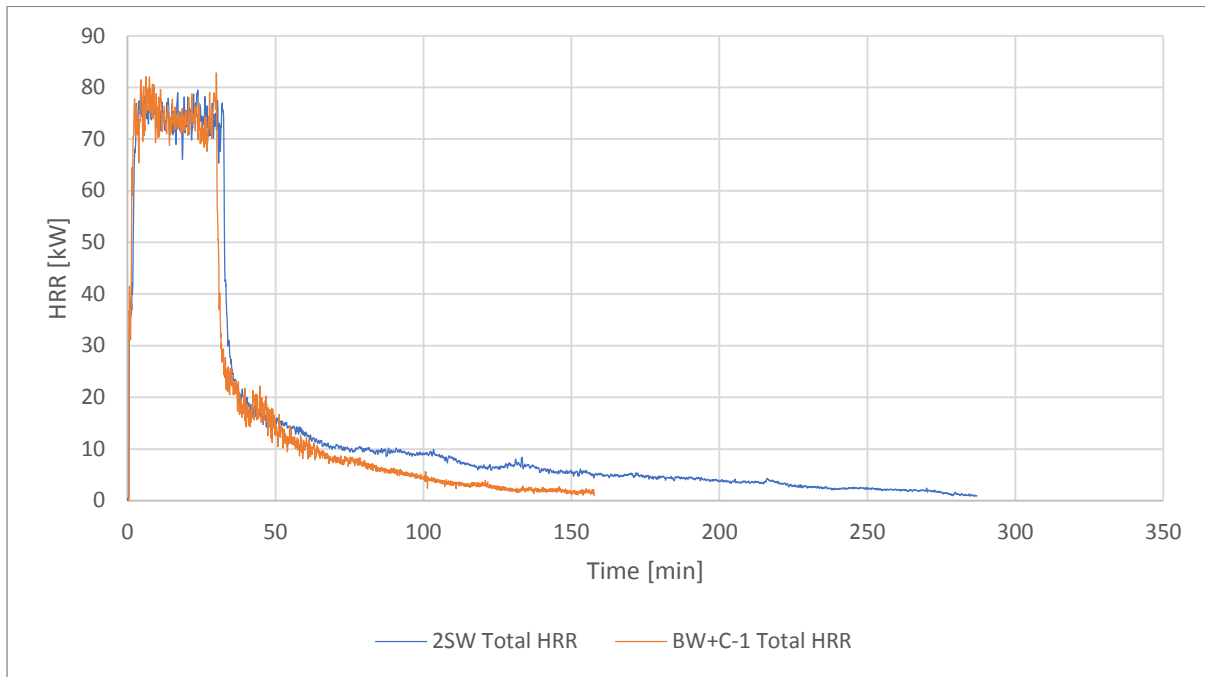


Figure 61: HRR of compartments with two exposed CLT surfaces

## Temperatures

Figure 62 shows that, during the heating phase of the fire, enclosure temperatures did not vary significantly at the top of compartments 2SW and BW+C-1 (averages of 937.0°C and 932.7°C). The decay phase did, however, differ significantly between the two compartments. The configuration with two side walls measured elevated enclosure temperatures for a longer period of time as compared to the BW+C-1 configuration. It is postulated that this is as a result of the relative orientation between the exposed CLT panels. In a configuration where the exposed surfaces face another, heat is emitted directly between the two CLT panels. As heat is released from one Side Wall, it is directly radiated onto the other opposing CLT side wall. In the BW+C configuration, this cross-radiation is less effective since the exposed CLT panels are positioned adjacent to one another (i.e. at right angles instead of parallel). This observation of an extended duration of increased temperatures in facing configurations was also observed by Medina Hevia (2014) in his tests involving compartments with two facing side walls and a compartment with adjacent CLT panels (a single side panel and back wall).

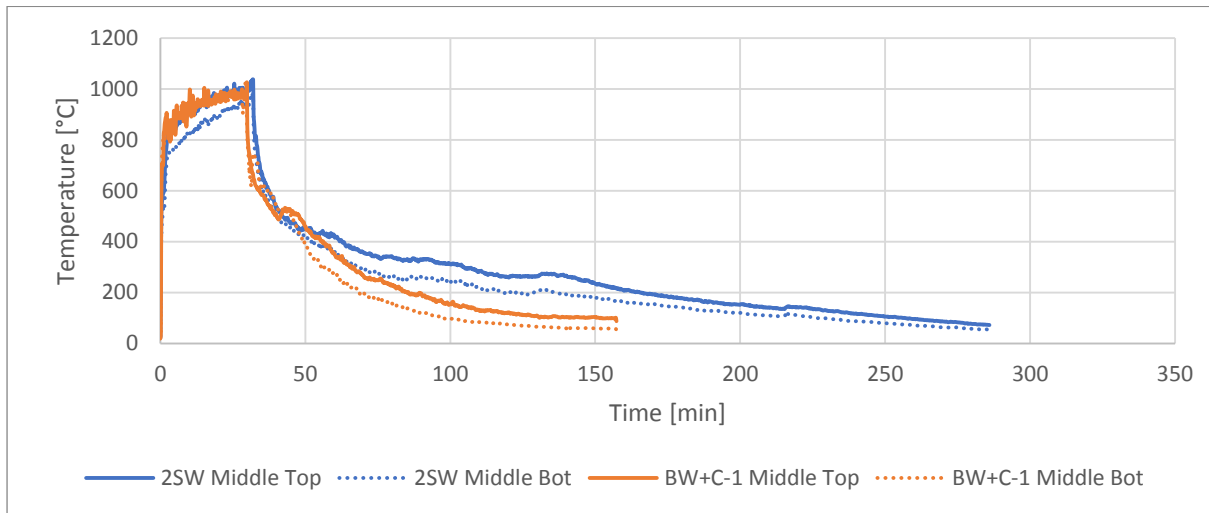


Figure 62: Enclosure temperatures in compartments with two exposed CLT surfaces

The charring behaviour of the exposed CLT panels in both Compartments 2SW and BW+C-1 are depicted in Figure 63 and the initial charring rates across the 1<sup>st</sup> lamella are shown to be comparable. CLT temperatures were elevated relatively longer in Compartment 2SW as compared to Compartment BW+C-1. This observation is also evident in the charring rates recorded in Table 29. The charring front penetrated to a depth of 50mm in Compartment 2SW and to a 30mm in Compartment BW+C-1. Charring rates across the 1<sup>st</sup> lamella in all panels, however, was similar and ranged between 0.62mm/min and 0.69mm/min.

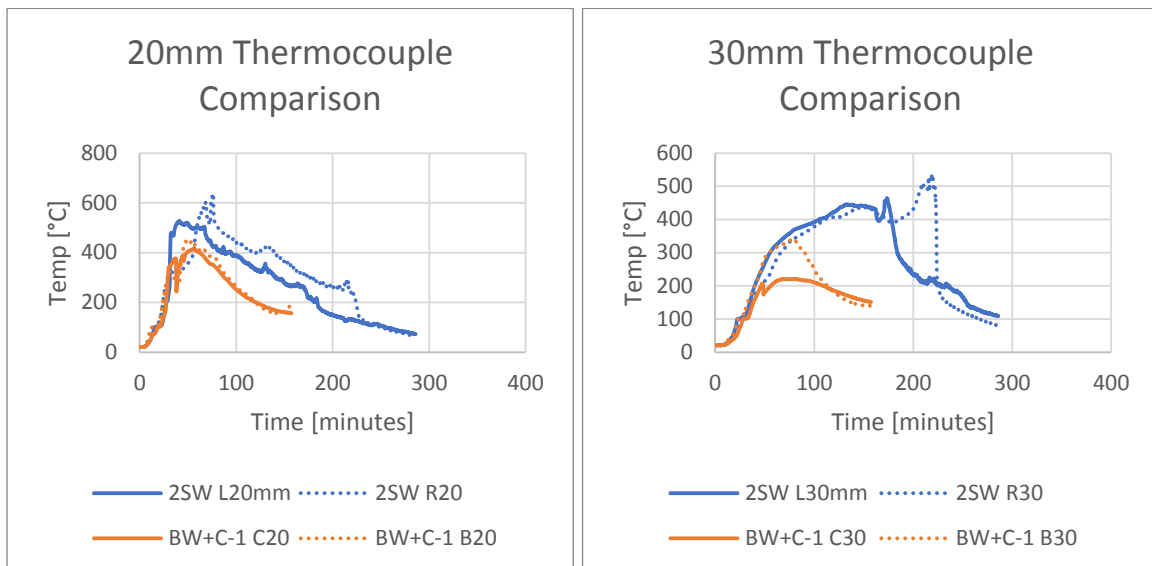


Figure 63: Comparing charring rates in compartments with two exposed CLT surfaces

### 7.3.5) Answering Research Sub-Questions 4

*Q4) What is the influence of exposed CLT panel configuration on compartment fire behaviour?*

The following general conclusions regarding the influence of panel configuration on compartment fire behaviour were identified in Section 7.3 (and confirmed in Appendix G):

- When comparing compartments with single exposed CLT surfaces, the total HRR and compartment temperature was comparable across all experiments. The duration of the decay phase was shorter in the experiment involving an exposed CLT ceiling as compared to an exposed CLT Back Wall or Side Wall. This demonstrates the beneficial fire behaviour associated with an exposed CLT ceiling configuration due to the observation of accelerated self-extinguishment.
- The addition of a another exposed CLT side wall to a compartment with only on exposed CLT side wall leads to a prolongation of the decay phase of the compartment fire (by a factor ranging from 3.7 to 6.5). Enclosure temperatures remain at an elevated level for a longer period during the decay phase, and as such the charring depth is deeper in a two side wall configuration as compared to a single side wall configuration (see Table 31), whilst the charring rates of the first lamella do not differ significantly between the configurations. Furthermore, the addition of another exposed CLT side panel to configuration SW leads to a doubling of the contribution to the total HRR due to the CLT only.
- By adding an exposed ceiling to a configuration with an exposed back wall, the HRR contributed by the CLT only is doubled. In contrast, average compartment temperatures are unaffected by the addition of another exposed CLT surface. Additionally, the charring rate of the Back Wall panel is increased by 25 to 44% due to the addition of an exposed ceiling.
- Total HRR is unaffected by the orientation of CLT panels in configurations with two exposed CLT walls. The duration of the decay phase is, however, significantly affected by panel orientation. Compartments that contain CLT surfaces that face one another experience a significantly longer (by a factor ranging between x2.8 and x2.9) decay phase duration as compared to compartments with 2 adjacent CLT surfaces. The charring front also propagates further into the CLT panels when the two CLT panels face another as compared to CLT panels orientated adjacent to one another. Compartment temperatures and first lamella charring rates were not influenced by panel orientation.

#### 7.4) Influence of char fall-off on compartment fire behaviour

As a final observation in this Analysis chapter, a short discussion will be presented pertaining to the influence of char fall-off on compartment fire behaviour.

From the observations recorded per experiment, it has become evident that char fall-off occurs both in the heating phase (i.e. whilst the propane burner was ignited) as well as the decay phase. The moment at which char fall-off occurs in relation to the stage of the fire (for example growth or decay), proved to be influential. A short discussion regarding to instances of char fall-off will now be discussed:

Char fall off that occurs whilst **compartment temperatures are elevated** exposes virgin timber to heat and leads to charring and sustained combustion of timber. This is clearly visible in the results of Compartment MUF-BW+C-1, where both the ceiling (see Figure 108) and the back wall (see Figure 110) panels experienced char fall off whilst compartment temperatures were elevated ( $\geq 500^{\circ}\text{C}$ ). Temperatures sharply rose behind the fallen-off char indicating exposure and renewed combustion of the previously insulated timber.

Char fall off that occurs **late in the decay phase** has the potential to remove the heat source that drives the combustion process, and as such accelerate self-extinguishment. This is visible in the temperature development of the back wall in Configuration BW (see Figure 32) as well as the right side wall of Configuration MUF-2SW (see Figure 86). In both compartment tests, local flaming of a small char piece led to the sustainment of elevated temperatures within CLT panels. At a certain instance, the small combusting char piece fell off and removed the heat source responsible for the continuation of the CLT panel combustion. These occurrences of char fall-off occurred late in the decay phase when compartment temperatures were low ( $< 200^{\circ}\text{C}$ ), and as such the virgin timber below the char was not reignited. These observations indicate that char fall-off may, under particular circumstances, actually contribute to the attainment of CLT self-extinguishment if the char fall-off occurs late in the decay phase of the fire (i.e. when compartment temperatures are sufficiently low).

The aforementioned scenarios are depicted graphically in Figure 64:

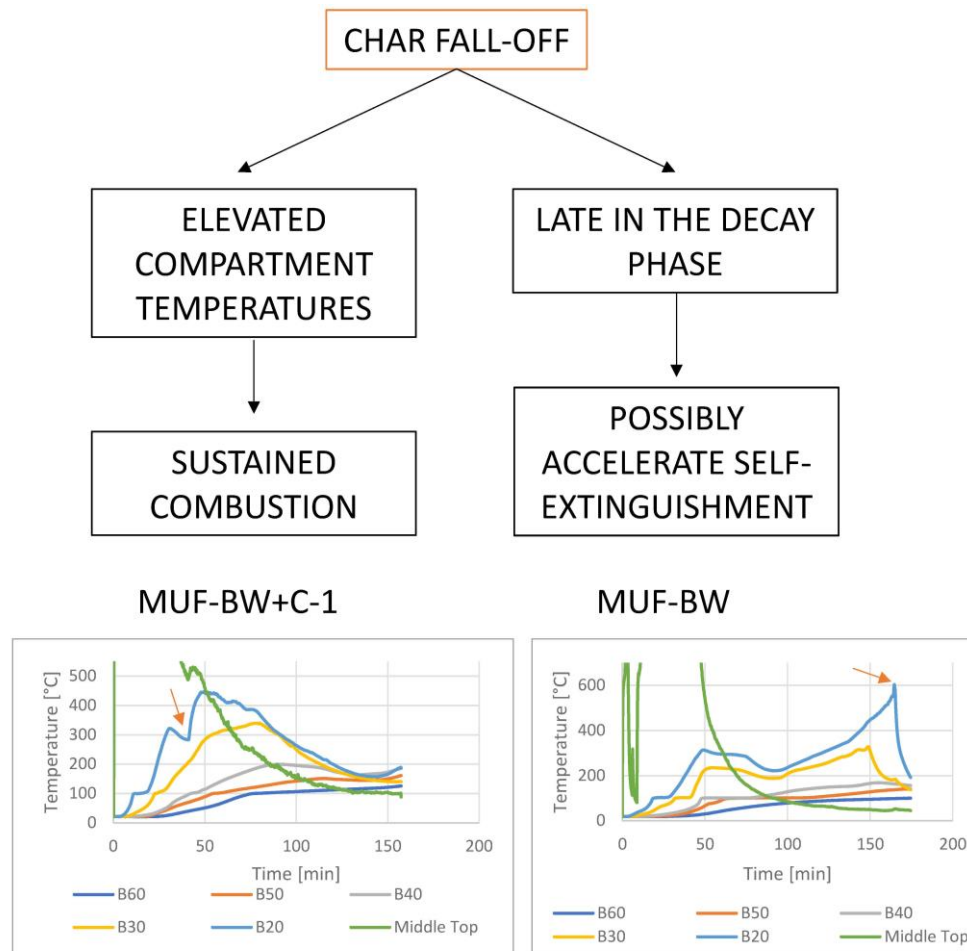


Figure 64: Comparing instances of Char Fall-Off

## 7.5) Chapter Summary

Chapter 7 investigated and analysed the experimental results obtained from small-scale compartment experiments containing exposed CLT panels in varying amounts and orientations. Chapters 7.2.3 and 7.3.5 sought to answer the 3<sup>rd</sup> and 4<sup>th</sup> research sub-questions formulated in Figure 2, respectively. As a summary of the answers to both questions (namely the influence of adhesive type and CLT panel configuration on small-compartment fire behaviour), the following was observed:

Regarding the influence of CLT adhesive type:

1. All compartment experiments on the tested MUF bonded CLT panels demonstrated self-extinguishment, whereas compartment burn-through was reported in a comparable compartment experiment containing PU bonded CLT side panels. In that particular CLT side wall compartment configuration, more total energy (i.e. 13.5%) was released in the PU

bonded CLT compartment that burned through as compared to the MUF bonded CLT compartment that self-extinguished. Local char fall-off was observed in the MUF-bonded CLT experiment (which resulted in enclosure temperature peaks of  $\pm 10^{\circ}\text{C}$ ), as compared to delamination of planks in the PU-bonded CLT experiment (which resulted in a second flashover).

2. The tested MUF bonded CLT panels display a lower charring rate (ranging between 14.1% and 19.4%) as compared to the investigated PU bonded CLT panels, in a compartment configuration with two exposed side walls that displayed self-extinguishment.
3. The fire duration was extended (by a factor ranging between x2 and x2.9) in the tested MUF bonded CLT panels as compared to the tested PU bonded CLT panels that self-extinguished, due to local char flare-up as well as a prolongation of elevated in-depth CLT temperatures.
4. In a two exposed CLT side wall configuration, PU bonded CLT panels demonstrated a 67% higher total HRR during the heating phase as compared to MUF bonded CLT panels, despite being subjected to an identical initial fire exposure (namely 41kW).

Regarding the influence of CLT panel configuration:

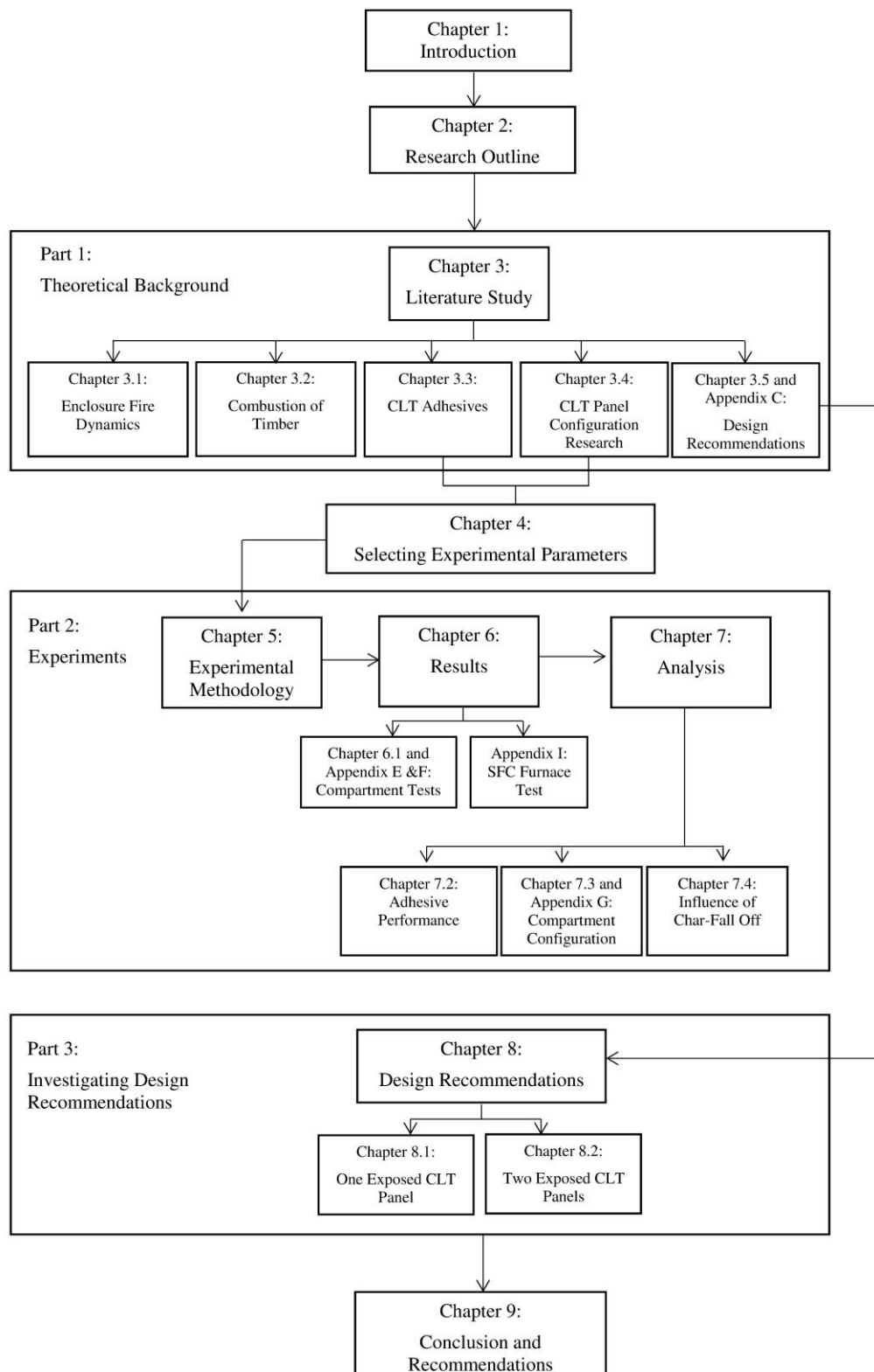
1. Small-scale compartments with a **single exposed MUF bonded panel** showed a charring front propagation ranging between 20mm and 30mm, and the time required to self-extinguish ranged between 0:21 hours and 2:06 hours (as measured from the moment the initial fire load was removed). The fastest achievement of self-extinguishment was recorded in a CLT ceiling configuration, followed by a CLT side wall configuration and finally a CLT back wall configuration. This demonstrates that configurations containing an exposed CLT ceiling demonstrate the most reliable self-extinguishment behaviour due to a shortened decay phase and lower amount of total released energy.
2. Small-scale compartments with a **two exposed MUF bonded panels** showed a charring front propagation ranging between 20mm and 50mm, and the time required to self-extinguish ranged between 1:27 hours and 4:12 hours (as measured from the moment the initial fire load was removed). Self-extinguishment was achieved sooner (by a factor ranging between x2.8 and x2.9) in a compartment configuration with adjacent CLT panels as opposed to facing CLT panels.
3. Subsequently, compartments with a single exposed CLT panel have shown shallower charring depths, on average released x2.7 times less total energy and self-extinguished x2.6 times faster as compared to compartments with two exposed CLT walls.
4. In general, a compartment containing two exposed CLT panels release double the amount of energy per unit time (based on only the contribution by the combusting CLT), regardless of panel orientation, as compared to a compartment with only one exposed CLT panel.



Compartment temperatures were also found to generally not vary with of the amount of exposed CLT as well as CLT panel orientation.

5. Configurations with two exposed surfaces which include facing CLT panels display extended decay phases (by a factor ranging between x2.8 and x2.9) due to promoted mutual cross-radiation as compared to non-facing (i.e. adjacent) CLT panels.
6. The addition of an exposed CLT ceiling to a configuration containing an exposed CLT back wall led to an increased back wall charring rate (in the range of 25 to 44%), but did not influence compartment temperatures.
7. The moment at which char fall-off occurs is highly influential on compartment fire behaviour, as demonstrated in Section 7.4 of this report. Char fall-off that occurs whilst compartment temperatures are elevated leads to sustained combustion via exposure of virgin timber. In contrast, char fall-off that occurs late in the decay phase (when compartment temperatures are low) has the potential to remove the heat source driving the combustion process, and as such contribute to the attainment of CLT self-extinguishment.

## **PART 3: INVESTIGATING DESIGN RECOMMENDATIONS**





## 8) Investigating Design Recommendations

This section of the report addresses the final research sub-question, namely:

*Q5) Are current prediction models able to simulate the experimentally obtained fire behaviour?*

As mentioned in Appendix C (which also supplies the theoretical background to this section of the report), design recommendations have been postulated that seek to include the contribution of exposed CLT to the fire load in a compartment. One such recommendation which iteratively calculates and includes the heat release by exposed CLT to the movable fuel load, has been suggested by Brandon (2018b).

The recommendation proposed by Brandon (2018b) does not take CLT panel orientation into account when considering the contribution of exposed CLT to the overall fuel load. As such, the modelling results obtained from this recommendation will be presented per surface area of exposed CLT in a compartment (namely  $0.25\text{m}^2$  and  $0.5\text{m}^2$  in compartments with one or two exposed CLT surface, respectively).

Based on the iterative calculation of Brandon (2018b), a final value of  $t_{\text{max}}$  (time to reach the maximum temperature and therefore the start of the PFC decay phase) is calculated as well the final charring depth and total energy released in the compartment (including the addition of burning CLT to the initial fuel load). The iterative calculation is stopped once the difference between charring depth between subsequent iterations is less than 0.1%. The process followed in the example documented in Appendix C was followed to obtain the results documented in this section of the report.

A few input parameters were required to calculate the PFC, namely the initial fuel load, charring rate of the CLT, thermal properties of the compartment linings as well as the fire growth rate according to EN 1991-1-2. These will be discussed individually in subsequent paragraphs.

In a Fire Safety Design, the **Initial Fuel Load** of a compartment is generally estimated based on the occupancy type according to Appendix E of EN 1991-1-2 (Table E.4). This was not done in this modelling exercise due to the nature of the input fuel load implemented in the experimental series of this research project. The propane burner bed was ignited for a duration equivalent to the time required to char the first lamella of each CLT panel per compartment. This was used as follows to estimate the initial fuel load to be used in all PFC modelling exercises:

The time to char through the first lamella (i.e.20mm) was calculated based on the one dimensional charring rate, which was assumed to be 0.65mm/min (as stated by the data sheet in Appendix B.2). This yielded 30:46 minutes and was multiplied by the HRR of the propane burner (41 kW) to

calculate the total amount of energy released during this 30:46 minute period. **The initial fuel load was subsequently estimated as 75.7MJ or 302.8MJ/m<sup>2</sup> (floor area).** This assumed initial fuel load can also compared to the TER by the burner bed alone, as documented in Table 27 as follows: disregarding the result of Compartment BW (due to the technical error experienced with the burner bed outage), the propane Input TER ranged between 69 and 86 MJ (with an average of 78MJ), indicating the suitability of the assumed initial fuel load.

The **charring rate** was calculated according to the recommendations of EN1995-1-2 Appendix A. The one dimensional charring rate of 0.65mm/min as specified for glue laminated softwood in Table 3.1 of EN1995-1-2 (and in the product data sheet in Appendix B.2) was used. The estimation of the parametric charring rate in turn requires the calculation of the heating rate factor ( $\Gamma$ ). Note that the parametric charring rate (equation 11 of this report) was used in this modelling exercise instead of the charring rate suggested by Brandon and Dagenais (2018) (equation 12 of this report). This was selected since the charring rate obtained from Equation 11 resulted in a lower (and thereby more comparable to the experiments) charring rate, as compared to Equation 12 (0.99mm/min as compared to 1.22mm/min, respectively in a compartment with one exposed CLT panel).

To calculate  $\Gamma$ , the thermal properties of the compartment linings are to be estimated. This was done by means of an area average between the properties of CLT and non-combustible (Promatec-H) boards. This requires the calculation of the absorptivity of the compartment linings ( $b = \sqrt{\rho \cdot c \cdot \lambda}$ ) per material (CLT and Promatect). The following was used, with CLT parameters obtained from the data sheet in Appendix B.2, and the values of the Promatect Panels from Crielaard (2015), Appendix K:

Table 34: Thermal properties of the compartment linings

	CLT	Promatect-H
Density ( $\rho$ ) [kg/m <sup>3</sup> ]	450	870
Specific heat (c) [J/kgK]	1610	1000
thermal conductivity ( $\lambda$ ) [W/mK]	0.13	0.175
Absorptivity (b) [J/m <sup>2</sup> s <sup>1/2</sup> K]	306.9	390.19

The results of the weighted area average are as follows, with a distinction made between compartments with one or two exposed CLT panels:

Table 35: Weighted Absorptivity per amount of exposed CLT

	Weighted absorptivity (b) [J/m <sup>2</sup> s <sup>1/2</sup> K]
One exposed CLT Surface	375.4
Two exposed CLT Surfaces	360.7

Due to the immediate delivery of a 41kW input HRR associated with the propane burner, a fast (0:15minutes) **fire growth rate** ( $t_{lim}$ ) was selected according to EN 1991-1-2.

With these input parameters defined, the recommendations of Brandon (2018b) were followed to estimate the additional energy released by the exposed CLT based on the iterative calculation of charring depths (as underpinned by Equation 18 in this report).

### 8.1) Compartments with one exposed CLT panel

Following the process stipulated in Appendix C.2, the following input parameters were implemented in correspondence with the experiments documented in this report:

Details:

- Internal compartment dimensions: 0.5m x 0.5m x 0.5m (width x depth x height)
- Single ventilation opening of 0.18m x 0.15m (width x height)
- One fully exposed CLT surface: 0.5m x 0.5m, all other surfaces are non-combustible Promatec-H boards (corresponding to Compartment BW, SW-1, SW-2, C-1 and C-2).

The Table (similar to Table 8 in Appendix C.2) below documents the steps required to calculate a PFC corresponding to a compartment in which the contribution to the fuel load by the burning CLT is not included.

Table 36: Steps to determine the intermediate parameters of a PFC that does not include the contribution of CLT to the fuel load

Step	Parameter	Equation and notes	Value
1	Opening Factor	$O = \frac{A_v}{A_t} \sqrt{h_{eq}}$	0.042 m <sup>1/2</sup>
2	Heating Factor	$\Gamma = \left( \frac{O}{\sqrt{\rho c \lambda}} \right)^2 / \left( \frac{0.04}{1160} \right)^2$	10.74
3	Start time of the decay phase (1st Iteration)	$t_{max}^1 = \max \left[ \frac{0.2E - 3.q_{t,d}}{O}; t_{lim} \right]$ Note: $q_{t,d} = 302.8 \text{ MJ/m}^2$ (floor)	15 minutes

4	Initial charring rate	$\beta_{par} = 1.5\beta_0 \cdot \frac{0.2\sqrt{\Gamma} - 0.04}{0.16\sqrt{\Gamma} + 0.08}$ $\beta_0 = 0.65 \text{ mm/min}$	0.99 mm/min
5	Time at which the charring rate reduces	$t_0 = \frac{0.009q_{t,d}}{O}$ <p>Note in this first iteration the additional fuel load from the CLT is not included. As such <math>q_{t,d} = 302.8 \text{ MJ/m}^2</math> (floor)</p>	10:42 minutes
6	Final charring depth (after the 1st iteration)	$d_{char}^1 = 2 \cdot \beta_{par} \cdot t_0$	21.3mm

With the parameters calculated in Table 36, the iterative calculation can be performed to include the contribution of the CLT to the fuel load ( $q_{t,d}$ ), based on the charring depth. The table below (similar to Table 9 in Appendix C.2) documents the steps to iteratively include the contribution of CLT to the fuel load:

Table 37: Steps to iteratively include the contribution of CLT to the fuel load

Step	Parameter	Equation
1	Total fuel load per total compartment surface area (iteratively calculated)	$q_{td}^{i+1} = q_{mfl} + \frac{A_{CLT} \cdot \alpha_1 \cdot (d_{char}^i - 0.7 \cdot \beta_{par} \cdot t_{max}^1)}{A_c}$ <p>Where <math>A_c</math> is the total compartment surface area and <math>t_{max}^1</math> does not change between iterations</p>
2	Start time of the decay phase (iteratively calculated)	$t_{max}^{i+1} = \max[\frac{0.2E - 3 \cdot q_{td}^{i+1}}{O}; t_{lim}]$
3	Time at which the charring rate reduces (iteratively calculated)	$t_0^{i+1} = \frac{0.009q_{td}^{i+1}}{O}$
4	Final charring depth (iteratively calculated)	$d_{char}^{i+1} = 2 \cdot \beta_{par} \cdot t_0^{i+1}$

Convergence of the charring rate was used to determine the number of iterations required (namely that the difference in  $d_{\text{char}}$  is less than 0.1%). The results from each iteration are recorded in Table 38:

Table 38: Iterative results

Iteration	$t_{\text{max}}$ [hours:minutes]	$d_{\text{char}}$ [mm]	% difference in charring depth between iterations
1	0:15	21.3	-
2	0:17	25.5	16.54
3	0:18	27.1	5.89
4	0:19	27.7	2.18
5	0:19	27.9	0.82
6	0:19	28.0	0.31
7	0:19	28.0	0.12
8	0:19	28.0	0.04

With the value of  $t_{\text{max}}$  now iteratively calculated, the PFC of EN1991-1-2 (Annex A) can be calculated (using Equation 2 of this report as well as 7 through 9). The (augmented) PFC, as calculated using the parameters described previously, is depicted in Figure 65. Additionally, the experimentally measured enclosure temperatures from compartments containing only a single exposed MUF bonded CLT panel are plotted.

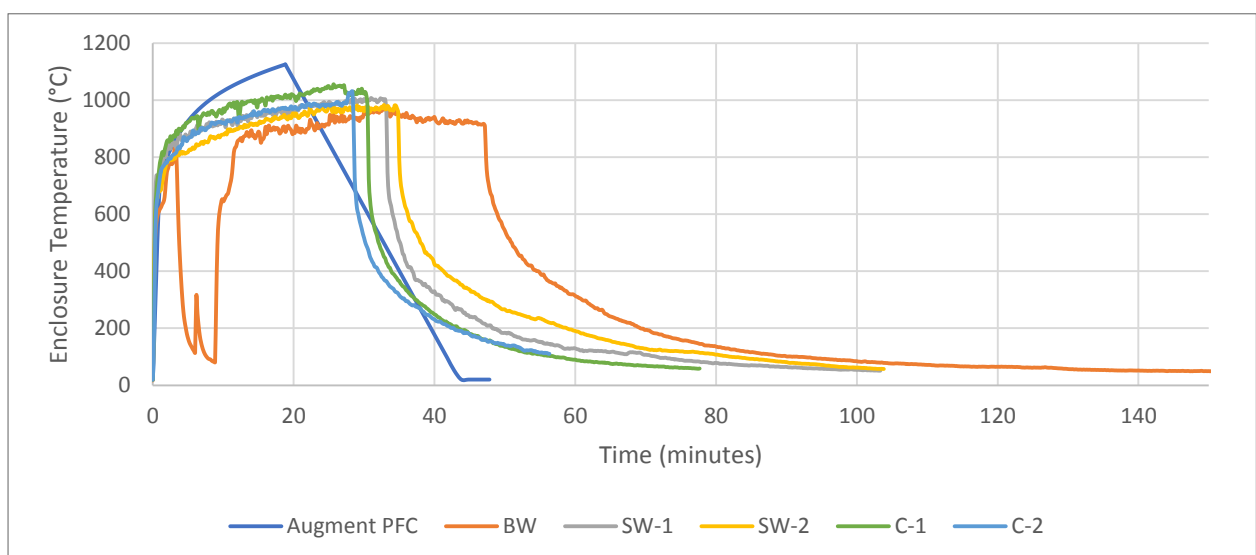


Figure 65: PFC of a compartment with one exposed CLT panel, plotted against corresponding experimental results



## 8.2) Compartments with two exposed CLT panels

The same calculation method as outlined in Section 8.1 was applied to a compartment with two exposed CLT surfaces. The following input parameters were used:

Details:

- Internal compartment dimensions: 0.5m x 0.5m x 0.5m (width x depth x height)
- Single ventilation opening of 0.18m x 0.15m (width x height)
- Two fully exposed CLT surfaces, each 0.5m x 0.5m, all other surfaces are non-combustible Promatec-H boards (corresponding to Compartment 2SW, BW+C-1 and BW+C-2).

The results from the 1<sup>st</sup> iteration (corresponding to a compartment which does not include the contribution of CLT to the fuel load) are listed in Table 39:

Table 39: Steps to determine the intermediate parameters of a PFC that does not include the contribution of CLT to the fuel load

Step	Parameter	Equation and notes	Value
1	Opening Factor	$O = \frac{A_v}{A_t} \sqrt{h_{eq}}$	0.042 m <sup>1/2</sup>
2	Heating Factor	$\Gamma = \left( \frac{O}{\sqrt{\rho c \lambda}} \right)^2 / \left( \frac{0.04}{1160} \right)^2$	11.64
3	Start time of the decay phase (1st Iteration)	$t_{max}^1 = \max\left[\frac{0.2E - 3 \cdot q_{t,d}}{O}; t_{lim}\right]$	15 minutes
4	Initial charring rate	$\beta_{par} = 1.5\beta_0 \cdot \frac{0.2\sqrt{\Gamma} - 0.04}{0.16\sqrt{\Gamma} + 0.08}$ $\beta_0 = 0.65 \text{ mm/min}$	1.00 mm/min
5	Time at which the charring rate reduces	$t_0 = \frac{0.009q_{t,d}}{O}$ Note in this first iteration the additional fuel load from the CLT is not included. As such $q_{t,d} = 302.8 \text{ MJ/m}^2$ (floor)	10:42 minutes
6	Final charring depth (after the 1st iteration)	$d_{char}^1 = 2 \cdot \beta_{par} \cdot t_0$	21.4mm

With these 1<sup>st</sup> iteration results, the iterative calculations listed in Table 37 are implemented to iteratively calculate  $t_{max}$  and  $d_{char}$ . The results per iteration are listed in Table 40:

Table 40: Iterative PFC results of a compartment with two exposed CLT surfaces

Iteration	t <sub>max</sub> [hours:minutes]	d <sub>char</sub> [mm]	% difference in charring depth between iterations	Iteration	t <sub>max</sub> [hours:minutes]	d <sub>char</sub> [mm]	% difference in charring depth between iterations
1	0:15	21.4	-	12	0:37	55.7	1.02
2	0:20	30.0	28.54	13	0:38	56.1	0.78
3	0:24	36.5	17.88	14	0:38	56.4	0.59
4	0:28	41.5	12.00	15	0:38	56.7	0.45
5	0:30	45.3	8.39	16	0:38	56.9	0.34
6	0:32	48.2	6.01	17	0:38	57.0	0.26
7	0:34	50.4	4.38	18	0:38	57.1	0.20
8	0:35	52.1	3.24	19	0:38	57.2	0.15
9	0:36	53.4	2.41	20	0:38	57.3	0.11
10	0:36	54.3	1.80	21	0:38	57.3	0.09
11	0:37	55.1	1.36				

Once again, with the value of t<sub>max</sub> now iteratively calculated, the PFC of EN1991-1-2 (Annex A) can be calculated (using Equation 2 of this report as well as 7 through 9). The (augmented) PFC, as calculated using the parameters described previously, is depicted in Figure 66. Additionally, the experimentally measured enclosure temperatures from compartments containing two exposed MUF bonded CLT panels are plotted.

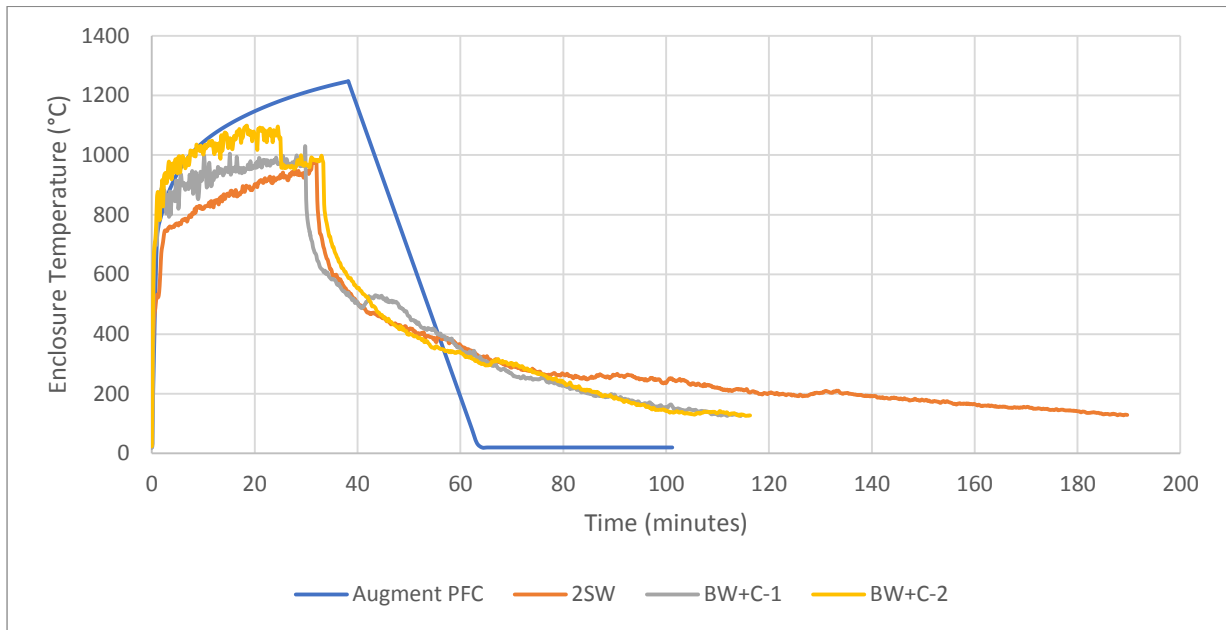


Figure 66: PFC of a compartment with two exposed CLT panels, plotted against corresponding experimental results

### 8.3) Analysing the ability of the investigated design recommendation

The applicability of the design recommendations postulated by Brandon (2018b) will be analysed based on the model's ability to predict fire behaviour, as compared against the results from the experiments documented in this report. The following parameters will be compared: charring depth ( $d_{char}$ ); time to start of the decay phase or attainment of the maximum compartment temperature in experiments and the prediction models respectively ( $t_{max}$ ); total fuel load ( $q_{td}$  including the contribution of CLT); decay phase duration ( $t_{decay}$ ) as well as the average enclosure temperatures during the heating phase ( $T_{avg}$ ).

Note that  $T_{avg}$  will be compared to the average enclosure temperature measured per experiment at the centre of the compartment (at 0.4m from the floor panel), as measured during the heating phase (i.e. between flashover and burner extinction). Additionally, the charring depth will be estimated based on the penetration of the 300°C isotherm (as recorded in Table 29 and Table 30).

Comparisons will again be presented per exposed area of CLT (namely 0.25m<sup>2</sup> and 0.50m<sup>2</sup> in compartments with one or two exposed surfaces, respectively).

#### 8.3.1) Comparing the PFC to experimental results pertaining to one exposed CLT Surface

The table below documents the results of the PFC prediction model of a compartment that contains a single exposed CLT panel, and also the results from corresponding experiments.

Table 41: Comparing the PFC prediction to experimental results with one exposed CLT surface

Prediction/ Experiment	$d_{\text{char}}$ [mm]	$t_{\text{max}}$ [hours:minutes]	$q_{td}$ [MJ] (/m <sup>2</sup> floor)	$t_{\text{decay}}$ [hours:minutes]	$T_{\text{avg}}$ [°C]
PFC Prediction	28.0	0:19	99.8 (399.2)	0:25	998.0
BW	30	0:42*	180 [720]	2:06	917.6
SW-1	20	0:33	125 [501]	0:39	949.5
SW-2	20	0:35	130 [521]	1:08	918.6
C-1	20	0:30	115 [460]	0:21	977.3
C-2	20	0:28	100 [402]	0:27	927.3

\* In compartment B, the 5:30 minute burner outage was subtracted to obtain  $t_{\text{max}}$

From Table 41 as well as Figure 65, the following comparisons are drawn:

- **Concerning the heating phase:** Compartment temperatures are overestimated by the PFC. Furthermore, the time to reach the maximum temperature ( $t_{\text{max}}$ ) was significantly under predicted by the PFC prediction due to the faster charring rate implemented in the prediction model ( $\beta_{\text{par}}$ ) as compared to the experimentally measured charring rates.
- In general, the charring depth is conservatively estimated by the PFC, except when compared the Compartment BW (although the discrepancy is minor: 2mm).
- The total fuel load (including the contribution by the exposed CLT) was underestimated by the PFC in all configurations, although the differences between the PFC and experimental results were least in compartments containing only an exposed ceiling.
- **Concerning the decay phase:** the duration of the decay phase was underestimated by the PFC in all cases except in the configuration containing an exposed ceiling. The decline of temperatures in the compartment as measured in the experiments did not follow a linear tendency as predicted by the PFC.

### 8.3.2) Comparing the PFC to experimental results pertaining to two exposed CLT Surfaces

The table below documents the results of the PFC prediction model of a compartment that contains two exposed CLT panels, and also the results from corresponding experiments.

Table 42: Comparing the PFC prediction to experimental results with two exposed CLT surfaces

Prediction/ Experiment	$d_{\text{char}}$ [mm]	$t_{\text{max}}$ [hours:minutes]	$q_{td}$ [MJ] (/m <sup>2</sup> floor)	$t_{\text{decay}}$ [hours:minutes]	$T_{\text{avg}}$ [°C]
PFC Prediction	57.3	0:38	202.6 [810.2]	0:25	1109.8
2SW	50	0:32	242[967]	4:12	937.0
BW+C-1	30	0:30	188 [752]	1:31	932.7
BW+C-2	20	0:33	189 [755]	1:27	1003.6

From Table 42 as well as Figure 66, the following comparisons are drawn:

- **Concerning the heating phase:** It can be seen that the compartment temperatures are overestimated by the PFC. Furthermore, the time to reach the maximum temperature ( $t_{\text{max}}$ ) was over-predicted by the PFC as compared to the experimental results.
- The charring depth is conservatively estimated by the PFC.
- The total fuel load was underestimated by the PFC in Configuration 2SW (Two Side Walls). In contrast, when considering Configuration BW+C (Back Wall and Ceiling), the PFC overestimated the total fuel load.
- **Concerning the decay phase:** the duration of the decay phase was underestimated by the PFC in all cases. In addition, the experimentally measured decay of temperatures post burner-bed extinguishment followed a non-linear path. This was predicted poorly by the linearly decreasing PFC prediction.

#### 8.4) Chapter Conclusion: Answering Research Sub-Question 5

Based on the aforementioned results, the following general conclusions are formulated pertaining to the veracity of the augment PFC design recommendation presented by Brandon (2018b):

- In all configurations (besides Configuration BW) the charring depth was conservatively predicted by the augmented PFC. The charring depth in Compartment BW was approximately 30mm as compared to the PFC prediction of 28.0mm, which is only a marginal difference.
- **Concerning the heating phase:** the PFC prediction underestimated the time to the start of the decay phase as compared to all experimental results related to compartments with one exposed CLT surface. The converse was true when considering the prediction model of a compartment with two exposed surfaces. As such, the PFC is unable to accurately estimate the start of the decay phase. Compartment temperatures were overestimated by the PFC in all cases.

- Compared to compartments with one exposed CLT surface, the PFC was able to predict the total fuel load obtained from a compartment with an exposed ceiling most closely. Concerning compartments with two exposed CLT surfaces, the PFC was most suited to predict the total fuel load obtained from a compartment with an exposed CLT back wall and ceiling (Configuration BW+C).
- **Concerning the decay phase:** the duration of the decay phase was significantly under predicted by the PFC when considering configurations with two exposed CLT surfaces. This is due to prediction model's inability to account for cross-radiation of heat between exposed CLT surfaces. Furthermore, generally the PFC was also not able to predict the duration of the decay phase of a compartment with one exposed panel, although decay phase durations were reasonable predicted by the PFC in Compartments with an exposed ceiling. Furthermore, the PFC does not account for the relative orientation of exposed CLT panels and subsequent influence on compartment fire behaviour. Finally, the PFC predicts a linear decay in compartment temperatures during the decay phase, as opposed to the logarithmic decay in temperatures recorded experimentally.

## 9) Conclusion and recommendations

### 9.1) Introduction

From the results presented, the specific research goal as stated in Section 2.3 of this report can be answered:

*To experimentally investigate, by means of small-scale compartment fire tests, the differences in fire behaviour between two different types of adhesives (MUF and PU) and the influence of CLT panel configuration on compartment fire behaviour, as well as investigate the ability of design guidelines to predict experimentally measured compartment temperatures.*

The following has been observed in relation to this specific research goal:

- In a set of comparable CLT side wall compartment experiments, MUF bonded CLT compartment self-extinguished and released less total energy as compared to a PU bonded CLT compartment which burnt-through and underwent a second flashover.
- Compartment configuration had a significant influence on fire behaviour. Compartments containing an exposed CLT ceiling only demonstrated the most beneficial fire behaviour by self-extinguishing sooner and releasing less total energy.
- The design guideline proposed by Brandon (2018b) may be used to estimate charring depths, but is unable to accurately predict general fire behaviour.

In addition to the specific research goal, a main research question was formulated:

*Which conditions are required to reliably achieve self-extinguishment of small-scale compartments constructed of exposed CLT panels?*

The recommendations listed in this section of the report seek to answer this main research question. In general, it was found that if a small-compartment fire test reveals the avoidance of burn-through behaviour (and a second flashover), due to the combined effect of CLT adhesive type and CLT panel configuration, then reliable self-extinguishment is promoted (but requires verification by a real-scale compartment fire test).

### 9.2) Conclusions

As a summary of the chapter conclusions which answered the sub-research questions of this research project (see Sections 7.5 and 8.4), the following conclusions are drawn based on the findings of this investigation:

1. In the tested CLT side-wall compartment configurations, MUF bonded CLT panels self-extinguished whereas a PU bonded CLT compartment showed burn-through behaviour and released 13.5% more total energy. When comparing CLT side-wall compartments that self-extinguished, PU bonded CLT side walls showed a 14.1% to 19.4 % higher charring rate during the heating phase as compared to MUF bonded CLT side walls.
2. Compartment configurations with a single exposed CLT panel displayed shallower charring depths, on average released x2.7 times less total energy and self-extinguished x2.6 times sooner as compared to configurations with two exposed CLT panels. Configurations with an exposed CLT ceiling self-extinguished the fastest and released the lowest total amount of energy, thereby demonstrating the most beneficial fire behaviour. It was additionally found that the energy per unit time (i.e. HRR) during the heating phase by CLT alone was doubled in compartments with two exposed CLT panels as compared to a single CLT panel, irrespective of panel orientation (measured at 32kW and 16kW, respectively).
3. In compartments with two exposed CLT surfaces, the relative orientation of the CLT panels greatly influenced the required time to self-extinguish. Due to mutual CLT cross-radiation, facing CLT panels demonstrated prolonged decay phases (by a factor ranging between x2.8 and x2.9) and released more total energy (by a factor ranging between x1.4 and x1.5) as compared to non-facing CLT configurations.
4. The design recommendation by Brandon (2018b) conservatively predicts CLT charring depths, but is unable to accurately predict small-scale compartment behaviour. The prediction errors were smallest compared to CLT ceiling compartment configurations.
5. The moment of char fall-off has a significant influence on the achievement of self-extinguishment. Fall-off that occurs whilst enclosure temperatures are elevated leads to prolonged fire durations due to ignition of virgin timber, as opposed to fall-off that occurs late in the decay phase which contributes to self-extinguishment.
6. CLT panel charring rates were measured at 0.59mm/min when subjected to a SFC exposure for 90 minutes, which is comparable to solid timber.

### 9.3) Recommendations

Based on the performed experiments and documented results, a set of recommendations are presented to answer the formulated main research question. A visual representation of the recommendations provided by this research is presented in Figure 67. In brief, both the type of **CLT adhesive** as well as the CLT **panel configuration** had an impact on compartment fire behaviour observed in (small-scale) enclosures and their ability to reliably self-extinguish.



Regarding the influence of adhesives on fire performance:

- If the charring front does propagate past the first adhesive line, a non-delaminating adhesive should be used. This research project does not give an overall recommendation as to which adhesive type inhibits delamination, but it has been observed that the tested MUF bonded panels consistently self-extinguished whereas burn-through and a second flashover was recorded in a comparably tested PU bonded CLT Compartment. Furthermore, to avoid the influence of adhesive performance on CLT fire behaviour, Crielaard (2015) demonstrated that delamination can be circumvented by using a sufficiently thick outermost CLT lamella.

Concerning the influence of CLT panel configuration on enclosure fire behaviour:

- Compartments containing only a single exposed CLT panel, as opposed to two exposed CLT panels, showed more reliable fire performance. CLT ceiling panel configurations in particular demonstrated the most beneficial fire behaviour (i.e. fastest self-extinguishment and lowest HRR) and are therefore recommended above exposed CLT side or back wall configurations. In compartments with two exposed CLT panels, more unreliable fire behaviour (i.e. delayed self-extinguishment and more total released energy) was recorded in compartments with facing CLT panels as opposed to adjacent CLT panels. As such it is recommended that facing CLT panels are to be avoided.

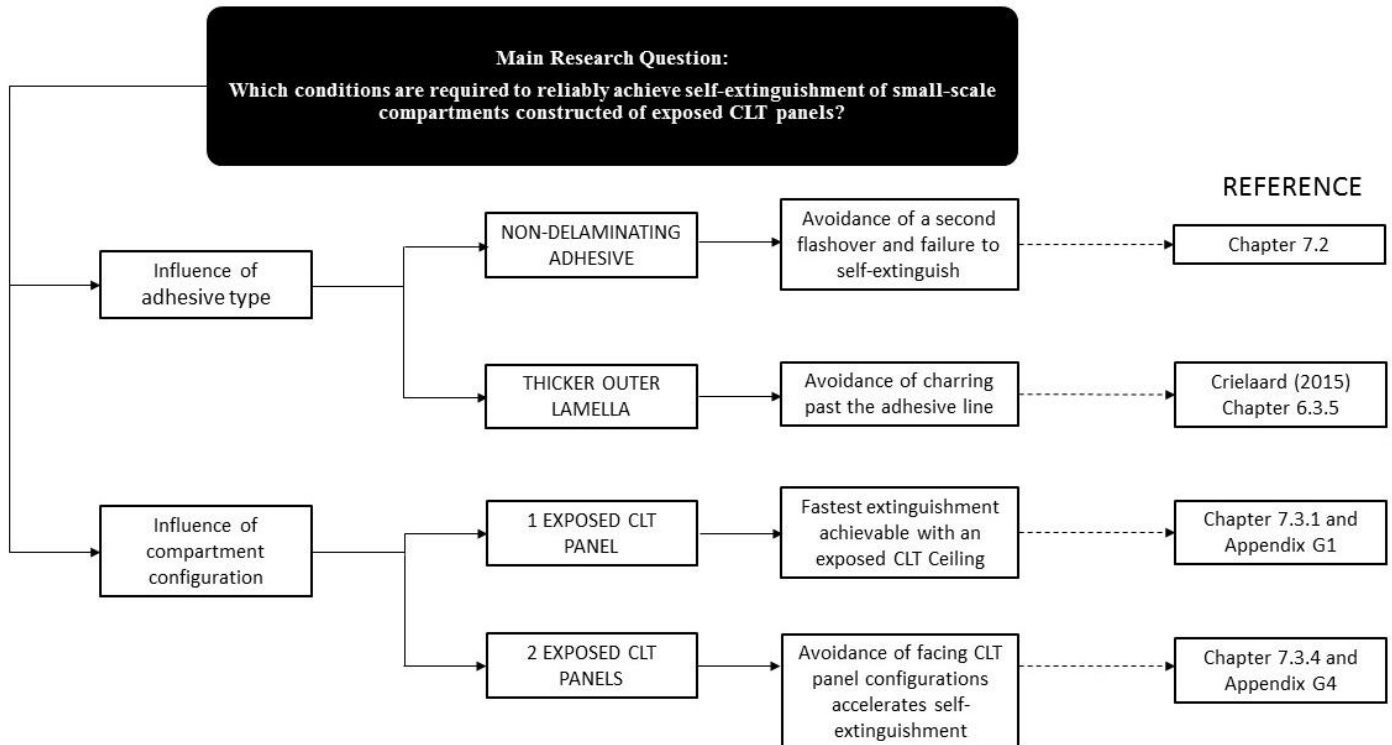


Figure 67: Recommendations derived from this research project

In addition to the aforementioned, the following is recommended:

1. Compartment configurations with an exposed CLT ceiling demonstrated the fastest attainment of self-extinguishment. As such, it is recommended that not only the amount (i.e. percentage exposed surface area) of CLT is to be restricted, but also the orientation of the CLT (i.e. rather an exposed ceiling as compared to an exposed CLT back wall).
2. The moment of char fall-off should be considered in fire safety engineering calculations. If char fall-off occurs late in the decay phase (i.e. once compartment temperatures are low), it could contribute to the attainment of CLT extinguishment. In contrast, if char fall-off occurs whilst compartment temperatures are elevated, the combustion process is sustained via the exposure of virgin timber. The time of char fall-off and subsequent fire behaviour should therefore be included in the fire design process of CLT elements.
3. The investigated design recommendation may be used to conservatively estimate the charring depth, but it is unable to accurately predict compartment fire behaviour. As such, the investigated design guideline is only recommended to conservatively estimate charring depths. Further refinement is required to improve the model's ability to predict compartment behaviour.

#### 9.4) Limitations and Future Research

The investigation performed in this project faced limitations. Subsequently, the following aspects to study further in future research are suggested:

1. The results, conclusions and recommendations contained in this report were obtained from experiments on compartment experiments with a specific CLT lamella build-up, adhesives, compartment scale, opening factor and base wood species. Further research is required to extrapolate these results to a range of CLT panel build-ups, different adhesive types (including different types of MUF and PU adhesives) as well as to real compartment scales.
2. An in-depth delamination comparison is required in future research to more quantifiably measure differences between MUF and PU bonded CLT panels. Conclusions in this study regarding delamination/ char-fall-off relied on visual observations. It is recommended that a testing method be developed that is able to quantify the extent of delamination in order to facilitate a verifiable adhesive performance comparison. Furthermore, a more substantial investigation into the differences in charring rates between PU and MUF-bonded CLT panels is required to directly compare adhesive performance. An example of such a study is that of Frangi et al. (2009).
3. It is recommended that future research is to include oxygen concentration and heat flux measurements within compartments to be able to assess the amount of oxygen available at, and heat flux received by, various panels within a compartment. For example, it was

postulated in this research project that exposed CLT ceilings were able to achieve self-extinguishment faster due to a hypothesised lack of oxygen available at the ceiling as compared to other vertical panels. This statement was based on fire engineering judgement and not on measured results. By measuring oxygen concentrations at exposed CLT surfaces, this hypothesis can be verified. Furthermore, by directly measuring the heat flux received on each panel, hypotheses regarding mutual cross-radiation in facing CLT panels can be further investigated.

4. Further studies are required to assess the validity of conclusions drawn regarding the moment of char fall-off, especially at larger compartment scales. Additional tests are required to assess the ability of char fall-off late in the decay phase to contribute to the attainment of CLT self-extinguishment. If established, this phenomenon could be included in fire safety engineering calculations.
5. Fire prediction models which include the contribution of CLT have been shown to be unable to predict fire behaviour accurately. Further research is required to refine these models, possibly by including parameters that account for CLT panel orientation as well as cross-radiation between two exposed CLT surfaces. Furthermore, the influence of fuel load type on the ability of design recommendations to predict fire behaviour should be investigated. By using more realistic fuel loads (for example wooden cribs) in compartment experiments, a comparison regarding the ability of design guidelines to predict behaviour may be further assessed. Finally, due to the restrictions of simplified design tools, such as parametric fire curves, intricate compartment fire behaviour was not predicted well. Further research should focus on the ability of more complex computer simulations (such as CFD modelling as well as Finite element Analysis models which heat transfer equations) to predict experimentally obtained fire behaviour.

## 10) References

- ASTM International (2015) 'ASTM D907-15, Standard Terminology of Adhesives'. PA, USA.
- Bartlett, A., Gajewski, K., Lineham, S., Thomson, D., Hadden, R. and Bisby, L. (2015) 'Overcoming the Fire Barrier to Tall Timber Construction', in *Infrastructure and Environment Scotland 3rd Postgraduate Conference*. Edinburgh.
- Bartlett, A., Hadden, R., Bisby, L. and Lane, B. (2016) 'Auto-Extinction of Engineered Timber as a Design Methodology', in *World Conference on Timber Engineering*.
- Bartlett, A. I., Hadden, R. M. and Bisby, L. A. (2018) 'A Review of Factors Affecting the Burning Behaviour of Wood for Application to Tall Timber Construction', *Fire Technology*. Springer US. doi: <https://doi.org/10.1007/s10694-018-0787-y>.
- Bateman, C. J., Bartlett, A. I., Rutkauskas, L. and Hadden, R. M. (2018) 'Effects of Fuel Load and Exposed CLT Surface Configuration in Reduced-Scale Compartments', in *2018 World Conference on Timber Engineering*.
- Brandon, D. (2016) 'Practical method to determine the contribution of structural timber to the rate of heat release and fire temperature of post-flashover compartment fires'.
- Brandon, D. (2018a) *Engineering methods for structural fire design of wood buildings— structural integrity during a full natural fire*.
- Brandon, D. (2018b) *Fire Safety Challenges of Tall Wood Buildings – Phase 2: Task 4 – Engineering Methods*. Borås, Sweden.
- Brandon, D. and Dagenais, C. (2018) *Fire Safety Challenges of Tall Wood Buildings – Phase 2: Task 5 – Experimental Study of Delamination of Cross Laminated (CLT) Timber in Fire*. Stockholm.
- Browne, F. L. (1958) *Theories of the combustion of wood and its control*.
- Buchanan, A. H. and Abu, A. K. (2017) *Structural Design for Fire Safety*. Second Ed. John Wiley & Sons, Ltd.
- Cadorin, J. F. and Franssen, J. M. (2003) 'A tool to design steel elements submitted to compartment fires — OZone V2 . Part 1 : pre- and post-flashover compartment fire model', *Fire Safety Journal*, 38(5), pp. 395–427.
- Crielaard, R. (2015) *Self-extinguishment of Cross-Laminated Timber*. Delft University of Technology.
- Crielaard, R., Kuilen, J. Van De, Terwel, K., Ravenshorst, G. and Steenbakkens, P. (2019) 'Self-

extinguishment of cross-laminated timber’, *Fire Safety Journal*. Elsevier B.V. doi: 10.1016/j.firesaf.2019.01.008.

Drysdale, D. (2001) *An Introduction to Fire Dynamics*. John Wiley & Sons, Ltd.

EN 1363-1 (1999) *Fire resistance tests - Part 1: General requirements*. Brussels.

EN 1991-1-2 (2002) *Eurocode 1: Actions on structures - Part 1-2: General actions - Actions on structures exposed to fire*. Brussels, Belgium.

EN 1995-1-2 (2004) *Eurocode 5: Design of timber structures - Part 1-2: General - Structural fire design*. Brussels.

EN1990 (2002) *Eurocode 0: Basis of structural design*. Brussels, Belgium.

Fahrni, R., Schmid, J., Klippel, M. and Frangi, A. (2018) ‘Correct temperature measurements in fire exposed wood’, in *2018 World Conference on Timber Engineering*. Seoul. Available at: [https://www.research-collection.ethz.ch/bitstream/handle/20.500.11850/289850/WCTE2018-Correcttemperaturemeasurementsinfireexposedwood\\_v8\\_submitted2.pdf?sequence=1&isAllowed=y](https://www.research-collection.ethz.ch/bitstream/handle/20.500.11850/289850/WCTE2018-Correcttemperaturemeasurementsinfireexposedwood_v8_submitted2.pdf?sequence=1&isAllowed=y).

FPIinnovations (2011) *CLT Handbook Canadian Edition*. Edited by S. Gagnon and C. Pirvu. Québec,.

Frangi, A., Fontana, M., Hugli, E. and Robert, J. (2009) ‘Experimental analysis of cross-laminated timber panels in fire’, *Fire Safety Journal*, 44, pp. 1078–1087. doi: 10.1016/j.firesaf.2009.07.007.

Frihart, C. R. and Hunt, C. G. (2010) *Wood Handbook, Chapter 10: Adhesives with Wood Materials- Bond Formation and Performance*. Madison, WI: U.S: Department of Agriculture, Forest Service, Forest Products Laboratory.

Gerard, R., Barber, D. and Wolski, A. (2013) *Fire Safety Challenges of Tall Wood Buildings*. San Francisco.

Hadden, R. M., Bartlett, A. I., Hidalgo, J. P., Santamaria, S., Wiesner, F., Bisby, L. A., Deeny, S. and Lane, B. (2017) ‘Effects of exposed cross laminated timber on compartment fire dynamics’, *Fire Safety Journal*. Elsevier Ltd, 91(March), pp. 480–489. doi: 10.1016/j.firesaf.2017.03.074.

Hadvig, S. (1981) *Charring of wood in building fires*. Lyngby: Laboratory of heating and air conditioning, Technical University of Denmark.

Hartin, E. (2005) *Fire Development and Fire Behavior Indicators*. Available at: <http://cfbt-us.com/pdfs/FBIandFireDevelopment.pdf>.

Hopkin, D., Anastasov, S. and Brandon, D. (2017) ‘Reviewing the veracity of a zone-model-based-

approach for the assessment Reviewing the veracity of a zone-model-based-approach for the assessment of enclosures formed of exposed CLT’, in *The International Conference of Applications of Structural Fire Engineering*. Manchester. doi: 10.1201/9781315107202-18.

Johansson, E. and Svenningsson, A. (2018) *Delamination of Cross-laminated timber and its impact on fire development*.

Jones, H. R. . (2000) *Radiation Heat Transfer*. Oxford: Oxford University Press.

Karlsson, B. and Quintiere, J. G. (1999) *Enclosure Fire Dynamics*. CRC Press LLC.

Li, X., McGregor, C., Medina, A., Sun, X., Barber, D. and Hadjisophocleous, G. (2016) ‘Real-Scale Fire Tests on Timber Constructions’, *Proceedings of the WCTE 2016 World Conference on Timber Engineering, Vienna / Austria*. doi: 10.1200/jco.2002.11.005.

McGregor, C. (2013) *Contribution of Cross Laminated Timber Panels To Room Fires*. Carleton University.

Medina Hevia, A. R. (2014) *Fire Resistance of Partially protected Cross-Laminated Timber Rooms*. Carleton University.

Östman, B., Brandon, D. and Frantzich, H. (2017) ‘Fire safety engineering in timber buildings’, *Fire Safety Journal*. Elsevier Ltd, 91(April), pp. 11–20. doi: 10.1016/j.firesaf.2017.05.002.

Pizzi, A. and Mittal, K. (2003) *Handbook of Adhesive Technology*. 2nd Editio. New York: CRC Press.

Roberts, A. F. (1971) ‘Problems associated with the theoretical analysis of the burning of wood’, in *Proceedings of the Combustion Institute*, pp. 893–903.

Su, J., Lafrance, P., Hoehler, M. and Bundy, M. (2018) *Fire Safety Challenges of Tall Wood Buildings – Phase 2: Task 2 & 3 – Cross Laminated Timber Compartment Fire Tests*.

Su, J., Leroux, P., Lafrance, P., Gratton, K., Gibbs, E. and Weinfurter, M. (2018) *Fire testing of rooms with exposed wood surfaces in encapsulated mass timber construction*. doi: <https://doi.org/10.4224/23004642>.

Svensson, S. (2002) *Fire Ventilation*. Edited by A.-L. Göransson. Swedish Rescue Services Agency.

Walls, R. and Zweig, P. (2016) ‘Sustainable Vital Technologies in Towards sustainable slums : understanding fire engineering in informal settlements’, *Sustainable Vital Technologies in Engineering & Informatics*, pp. 1–5. Available at: <http://cfbt-us.com/pdfs/FBIandFireDevelopment.pdf>.

Walton, W. D., Carpenter, D. J. and Wood, C. B. (2016) 'Zone Computer Fire Models for Enclosures', in Hurley, M. J. (ed.) *SFPE Handbook of Fire Protection Engineering*. Fifth Ed. New York: Springer Science+Business Media LLC, pp. 1024–1033.

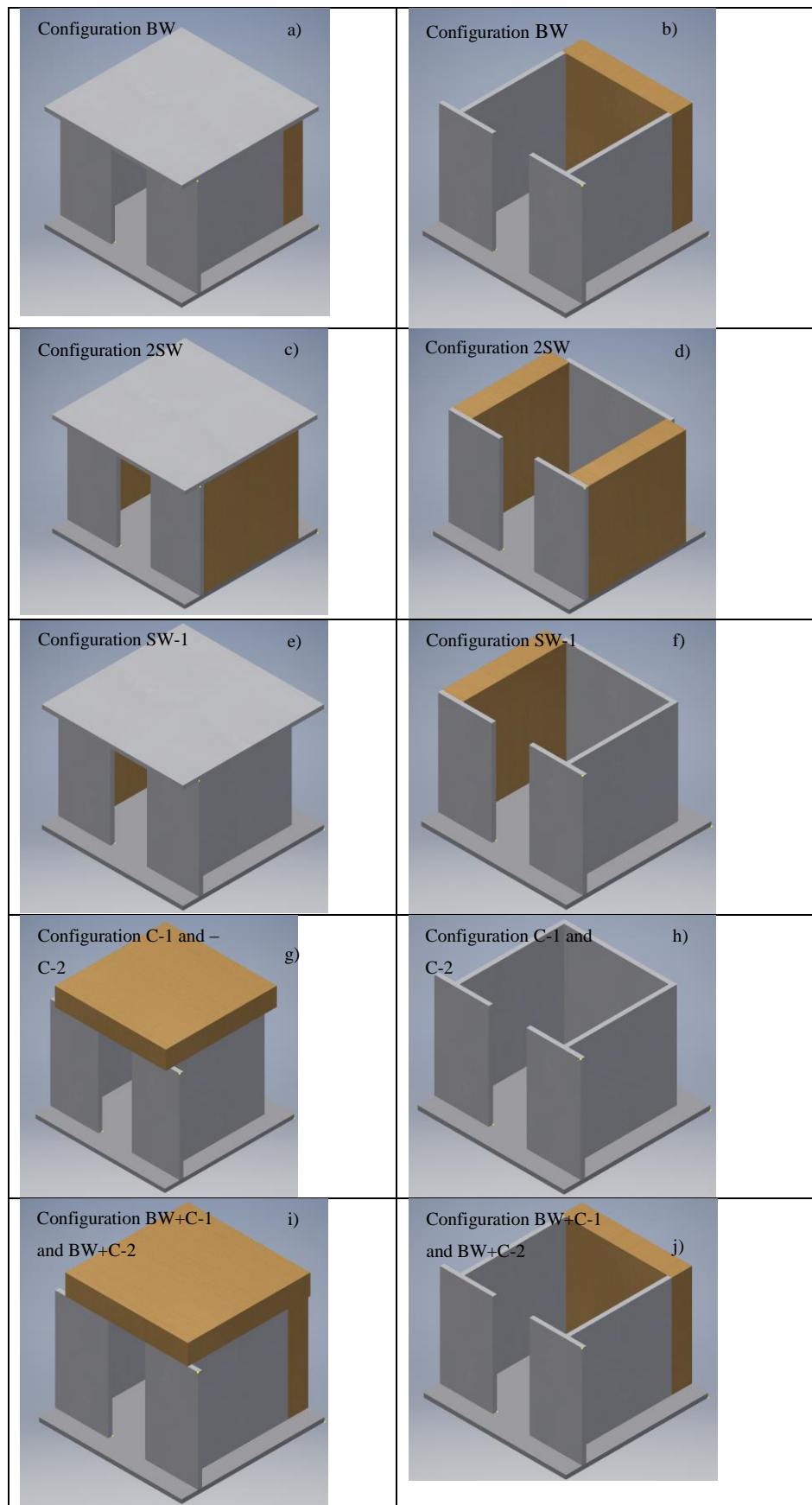
White, R. H. (2016) 'Analytical Methods for Determining Fire Resistance of Timber Members', in Hurley, M. J. (ed.) *SFPE Handbook of Fire Protection Engineering*. Fifth Ed. New York: Springer Science+Business Media LLC, pp. 1979–2011. doi: 10.1007/978-1-4939-2565-0\_55.

# Appendix A

## Compartment Configurations



Figure 68: a) Compartment BW including ceiling; b) Compartment BW excluding ceiling; c) Compartment 2SW including ceiling; d) Compartment 2SW excluding ceiling; e) Compartment SW-1 including ceiling; f) Compartment SW-1 excluding ceiling; g) Compartment C-1 and C-2 including ceiling; h) Compartment C-1 and C-2 excluding ceiling; i) Compartment BW+C-1 and BW+C-2 including ceiling; j) Compartment BW+C-1 and BW+C-2 excluding ceiling



## Appendix B

CLT Production, MUF bonded CLT panel product data sheet and GripPro Plus adhesive product information

Data Sheet Available online at:

[https://www.derix.de/data/DERIX\\_X\\_Lam\\_Brosch\\_EN\\_2019\\_03\\_\\_WEB.pdf](https://www.derix.de/data/DERIX_X_Lam_Brosch_EN_2019_03__WEB.pdf)

Note that CLT panels with 5 cross-wise stacked lamella (each 20mm) were used in this study. Planks within lamellas were not edge-glued to one another.

## B.1) CLT Fabrication

CLT is made up several layers of timber panels which are adhesively bonded in a cross-wise manner. Individual panels, in turn, consist of various timber planks. Individual planks can vary in thickness from 20 to 50mm, and their lengths are extended beyond single plank lengths by means of finger joining. A CLT element is typically made up of at least three panel layers.

In general terms, CLT elements are 0.6m, 1.2m, or 3m wide, 18m in length and are up to 400mm thick, although dimensions differ between manufacturers. The manufacturing process of CLT is divided into 9 steps including: 1) selecting the primary lumber; 2) grouping lumber; 3) lumber planing; 4) lumber/layer cutting to length; 5) applying adhesives; 6) panel lay-up; 7) assembly pressing; 8) quality control, optional surface sanding and cutting, and finally 9) product marking, packaging and shipping (FPInnovations, 2011). The various stages in CLT manufacturing are displayed in Figure 69, and will be briefly discussed in this section (as presented in FPInnovations (2011)).

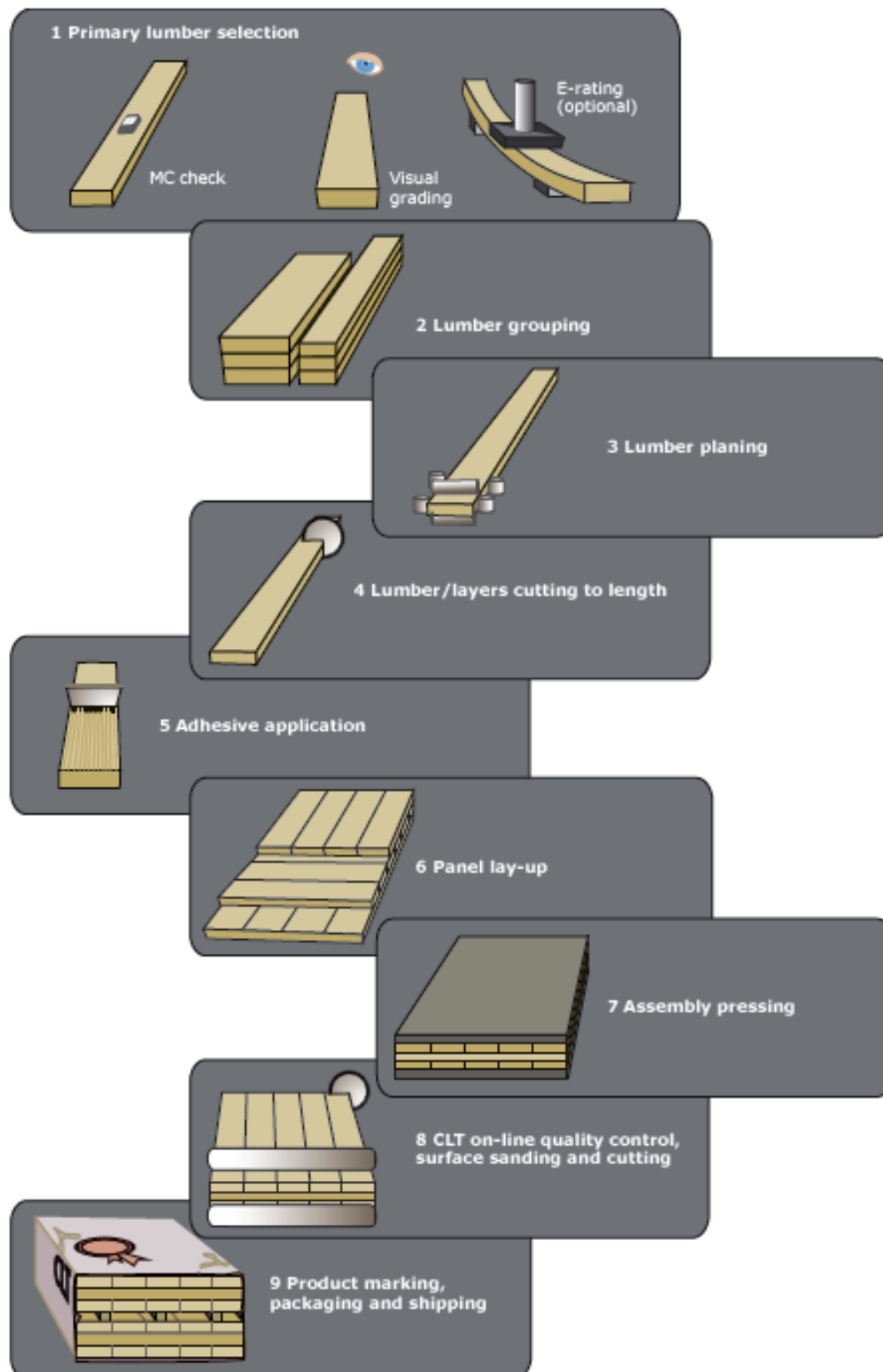


Figure 69: CLT Manufacturing

- 1) Selecting the primary lumber. This stage involves the selection of lumber, based on target moisture content (MC), visual grade (by visually observing the presence of knots in the lumber as well as grain angle deviations), and if required by performing mechanical tests to determine the Young's Modulus.
- 2) Grouping lumber: lumber with similar characteristics are placed in groups. A distinction is further made between the lumber that will be used in the major direction (main load carrying direction) as well as the minor direction (also referred to as the cross-ply direction).
- 3) Lumber planing is used to optimise the application of adhesives. This process activates the surface of the wood by removing a thin layer from its surface.
- 4) Lumber/layer cutting to length involves cutting the wood to the required size, as required by the final product size (which is restricted by the size of the press).
- 5) Applying adhesives is generally done by a through-feed process during which adhesive is extruded in parallel lines. Adhesive application should take place within 24 hours from planing to prevent undesired surface oxidation. It is important that the surface on which the adhesive is applied is to be free of oils or grease since these degrade bond quality. Edge bonding (within a board) is generally performed in a separate process.
- 6) Panel lay-up involves placing panels on top of each other in a predefined sequence and specified number of lamellas. Step 5 (adhesive application) is repeated between each lamella.
- 7) Assembly pressing is performed once the desired lay-up is assembled and is a crucial step in obtaining satisfactory inter-lamella bond strength. There are generally two methods by which pressing is performed, namely vacuum press and hydraulic press. Vacuum press is only capable of applying 0.1MPa pressure which is sometimes insufficient to overcome irregularities (such as warping). In contrast to this, hydraulic pressing can generate far higher pressures vertically as well as being able to apply side pressure. It is additionally recommended that pressing is to be performed at an ambient temperature of at least 15°C, since certain adhesives types require longer curing times at lower temperatures.
- 8) Quality control generally includes automated visual grading systems to detect irregularities. In addition, optional surface sanding and cutting may be used to obtain the required element thickness and tolerances.
- 9) Product marking finally ensures that the product is correctly labelled such that elements are used for their intended applications. Finally the CLT elements are packaged and prepared for transport.

# Roof, ceiling, wall – At a glance

At a glance

**Board dimensions:**

- Length: 6,00 – 17,80 m
- Width: up to 3,50 m
- Thickness: up to 400 mm

**Timber species/ Strength classes**

- Spruce: C24
- Moisture content: 10% ± 2%
- Moulded density: approx. 450 Kg/ m³ (other timber species and strength classes on request)

**Glueing - Adhesive based on melamine resin:**

- Adhesive type 1 to EN 301, approved for glueing load-bearing timber components for interiors and exterior, weather-resistant with transparent glue line (emulsion class E1)

**Cutting and Processing:**

- with 5-axis CNC portal machine, to customer specifications

**Computed burn rate:**

- 0,65 mm/ minute

Clear benefits

**Benefits for planners**

- European Technical Approval
- Individual design options
- Not limited to standard dimensions
- Large size
- High load-bearing capacity
- High level of fire protection
- Earthquake-resistant

**Benefits for building contractors**

- Pleasant room atmosphere
- Economical construction method
- High degree of prefabrication
- Short times for building and fitting
- Solid construction components
- Heat protection in summer
- Dimensionally stable

**Benefits for the environment**

- CO<sub>2</sub>-neutral
- Excellent eco-balance
- Airtight and windproof
- PEFC certified



**CHANGE OF SHAPE**

- II to the panel 0,01 % per % of timber moisture change
- I to the panel 0,20 % per % of timber moisture change

- Thermal conductivity λ: 0,13 W/(mK)
- Specific heat capacity c: 1 61 J/(kgK)
- Water vapour diffusion resistance μ: 20 - 50

**APPROVALS**

- ETA-11/0189
- EEC conformity declaration
- PEFC certificate (production sites Niederkirchen and Westerhappeln)



Construction components made of X-LAM are cut to size and are not constrained to have standard dimensions. This gives freedom for individual design. The data needed for planning is given in the European Technical Approval (ETA) and can be applied to projects rapidly with our draft design program. Buildings made with X-LAM are advantageous, including in earthquake zones, because of their low mass and high strength.



The natural building material wood is the preferred choice when there are high demands on a pleasant and comfortable atmosphere in the rooms. The high level of prefabrication results in fast building and assembly times, which makes the solid construction components very economical. Low thermal conductivity and high thermal protection in summer ensure comfortable living and save energy.



The raw material for making X-LAM is currently exclusively softwood. As a business certified by PEFC, we focus on sustainable, careful and responsible forestry. Compared to other solid construction methods, the manufacture and processing of X-LAM components requires only little energy and contributes to long-term CO<sub>2</sub> storage and so to minimising the greenhouse effect.

## B.3) GripPro Plus adhesive product information

AkzoNobel Wood Coatings  
Wood Finishes and Adhesives



### Product Information

#### Plus



AkzoNobel System GripPro™ Plus besteht aus Plus A011, einem flexiblen, flüssigen Melamin Leim und Plus H011, einem flüssigen Härter.

Es handelt sich um ein helles Leimsystem, welches in gemischtem oder getrenntem Auftrag von Leim und Härter für tragende Holzkonstruktionen, wie z. B. Brettschichtholz, Brettsperrholz oder Duo-/Trio-Balken eingesetzt werden kann.

Plus wird in der Holzverarbeitenden Industrie eingesetzt, wo Anforderungen an eine helle Leimfuge mit hoher Wasser- und Wetterfestigkeit gestellt werden.

Plus wurde gemäß den Anforderungen in EN 301:2013 als Klebstofftyp I durch die Materialprüfungsanstalt Universität Stuttgart – Otto-Graf-Institut - (MPA), Deutschland, für ein flexibles Mischungsverhältnis geprüft und anerkannt (siehe unten). Das Produkt ist für die Herstellung von Brettschichtholz gemäß EN14080:2013 geeignet.

Das Klebstoffsystem erfüllt die Anforderungen folgender Typen:

EN 301-I-90-GP-0,6-M  
EN 301-I-90-GP-0,3-S  
EN 301-I-90-FJ-0,1-M

Des Weiteren ist das Leimsystem durch die Materialprüfungsanstalt Universität Stuttgart – Otto-Graf-Institut - (MPA), Deutschland nach DIN 68141:2008, geprüft worden und erfüllt die Anforderungen an die Produktion von tragenden geklebten Holzbauteilen gemäß DIN 1052 für ein flexibles Mischungsverhältnis (siehe unten).

Bei getrenntem Auftrag von Leim und Härter wird der Einsatz der Gießanlage 6230 oder 7230 Ecoflex empfohlen.

#### Contact Information

Stockholm, Sweden +46 8 743 40 00  
High Point, USA +1 336 841 5111  
Singapore +65 6762 2088  
Medellin, Colombia +57 4 3618888  
[www.akzonobel.com/cascoadhesives](http://www.akzonobel.com/cascoadhesives)

Version: 4 (2015-06-15)

Reason for changes: update according to EN14080:2013

AkzoNobel approval code: AN\_200100\_210114

## Produktspezifikation

	Plus A011	Plus H011
<b>Produkt</b>	Melamin Klebstoff	Härter
<b>Lieferform</b>	Flüssig	Flüssig
<b>Farbe</b>	opak weiß	Weiß
<b>Viskosität</b> (zum Zeitpunkt der Produktion)	2000 - 9000 mPas (Brookfield LVT, sp.4, 12 rpm, 25°C)	1700 - 2700 mPas (Brookfield LVT, sp4, 60 rpm, 25°C)
<b>pH</b> (zum Zeitpunkt der Produktion)	8,5-9,3 (bei 25°C)	1,3 – 2,0
<b>Trockengehalt</b>	Ca. 65%	Entfällt
<b>Dichte</b>	ca. 1290 kg/m <sup>3</sup>	ca. 1070 kg/m <sup>3</sup>

## Lagerbedingungen und Lagerstabilität

Um die angegebene Lagerstabilität zu gewährleisten ist es äußerst wichtig, dass das Produkt unter den empfohlenen Lagerbedingungen bevorratet wird.

Die optimale Lagertemperatur für den Leim liegt zwischen 5°C und 20°C.

Nur kurzfristige Lagerung bei Temperaturen unter +5°C und über +30°C zulässig. Das Produkt darf gefrieren, muss dann jedoch aufgetaut, auf Raumtemperatur gebracht und vor Gebrauch homogenisiert werden.

Die optimale Lagertemperatur für den Härter liegt zwischen 15°C und 25°C.

Nur kurzfristige Lagerung bei Temperaturen unter +10°C und über +30°C zulässig. Gefrorenes Produkt kann, aufgrund irreversibler Veränderungen, nicht wieder aufgetaut und verarbeitet werden.

Die Lagerstabilität eines Produktes wird durch Parameter wie z. B. Reaktivität, Viskosität oder Rheologie bestimmt. Die Lagerfähigkeit endet, sobald sich die Reaktivität, Viskosität oder Rheologie von einem stabilen Wert in einen Wert, der die Verleimqualität beeinträchtigt, umwandelt.

Wenn das Gebinde über einen längeren Zeitraum unverschlossen ist, ist der Leim anfällig für Hautbildung an der Oberfläche. Zur Vermeidung halten Sie die Verpackung stets geschlossen, wenn sie nicht in Gebrauch ist.

Die Lagerzeit der Komponenten finden Sie bitte nachfolgend:

Lagerfähigkeit (Monate)	15°C	20°C	25°C	30°C
Plus A011	4	3	1,5	1
Plus H011	4	4	3	2,5

## Contact Information

Stockholm, Sweden +46 8 743 40 00  
 High Point, USA +1 336 841 5111  
 Singapore +65 6762 2088  
 Medellín, Colombia +57 4 3618888  
[www.akzonobel.com/cascoadhesives](http://www.akzonobel.com/cascoadhesives)

Version: 4 (2015-06-15)

Reason for changes: update according to EN14080:2013



## Verarbeitungshinweise

Plus wurde für die Verwendung in der Holzverarbeitenden Industrie in Anwendungsbereichen wie der BSH-Produktion gemäß EN14080:2013, CLT, Duo- und Trio-Balken sowie I-Träger entwickelt.

### Mischungsverhältnis

Plus ist gemäß EN301:2013 für nachfolgendes Mischungsverhältnis zugelassen:

<b>Fichte, Kiefer, Tanne</b> (nach Gewichtsteilen)	gemischt bei Keilzinkenverklebung	100 : 10-100 (Leim : Härter)
	gemischt und getrennt bei Flächenverklebung	100 : 30-100 (Leim : Härter)
<b>Europäische Lärche</b> (nach Gewichtsteilen)	gemischt bei Keilzinkenverklebung	100 : 30-60 (Leim : Härter)
	gemischt und getrennt bei Flächenverklebung	100 : 30-60 (Leim : Härter)
<b>Sibirische Lärche</b> (nach Gewichtsteilen)	gemischt bei Keilzinkenverklebung	Prüfung läuft
	gemischt und getrennt bei Flächenverklebung	Prüfung läuft

Leim und Härter müssen entsprechend dem oben genannten Mischungsverhältnis verwendet werden. Bei abweichendem Mischungsverhältnis werden unterschiedliche Faktoren, wie z. B. Presszeit, Topfzeit, Wartezeiten sowie die Leimfugenqualität beeinflusst.

Die maximal zulässige Abweichung der Härtermenge beträgt bei der Produktion von tragenden Holzbauteilen  $\pm 2$  Gewichtsteile.

Vor der Verwendung der Leimmischung im Untermischverfahren muss auf eine sorgfältige Vermischung von Leim und Härter geachtet werden. Bei manueller Vermischung von Leim und Härter immer den Härter dem Leim zuführen.

### Getrennter Auftrag von Leim und Härter

Plus ist für den getrennten Auftrag von Leim und Härter zur Flächenverleimung optimal geeignet, vorzugsweise mit der getrennten Gießanlage 6230 oder 7230 Ecoflex. Diese Anlagen gewährleisten eine exakte Dosierung beim Leim- und Härterauftrag. Die maximalen Wartezeiten werden bei gleichzeitiger Beibehaltung der kurzen Presszeiten verlängert.

Der Einsatz anderer getrennter Auftragsgeräte ist nur zulässig, wenn die Eignung der entsprechenden Anlage für die beabsichtigte Anwendung überprüft wurde.

Bei der Verwendung von Leim und Härter im getrennten Verfahren werden keine Probleme mit der Topfzeit auftreten, da die Komponenten erst beim Auftragen auf die Füge teil-Oberfläche vermischt werden.

Die maximal zulässige Klebfugendicke bei getrennter Anwendung von Leim und Härter bei der Flächenverleimung beträgt 0,3 mm.

### Untermischanwendung von Leim und Härter

Plus kann auch als Untermischsystem für Keilzinkenverklebungen verwendet werden, vorzugsweise mit automatischen Mischvorrichtungen. Hierbei ist die Einhaltung der Topfzeit zu beachten, da diese die Verarbeitungsdauer für das Leimsystem einschränkt.

Unter Topfzeit versteht man die Zeit, während der die Leim-/Härtermischung verarbeitet werden kann. Die Topfzeiten werden anhand genormter Analysemethoden gemessen, so dass die Topfzeiten unterschiedlicher Systeme verglichen werden können.

### Contact Information

Stockholm, Sweden +46 8 743 40 00  
High Point, USA +1 336 841 5111  
Singapore +65 6762 2088  
Medellin, Colombia +57 4 3618888  
www.akzonobel.com/cascoadhesives

Version: 4 (2015-06-15)

Reason for changes: update according to EN14080:2013

Nachfolgende Topfzeit wurde gemäß EN302-7 bestimmt:

	Mischungsverhältnis	15°C	20°C	30°C
<b>Topfzeit</b>	100:10	4 h 20 min	1 h 50 min	
	100:30	---	50 min	
	100:100	---	12 min	7,5 min

#### Wartezeit

Die Wartezeit ist die Zeit vom Moment des Leimauftrages bis zum Aufbringen des Pressdruckes auf die Fügeteile.

Die gesamte Wartezeit setzt sich aus offener (OAT) und geschlossener (CAT) Wartezeit zusammen. OAT ist die Zeit vom Aufbringen des Leims bis zum Zusammenlegen der Fügeteile. CAT ist die Zeit vom Zusammenlegen der Fügeteile bis zum Aufbringen des Pressdruckes.

OAT und CAT werden durch die Leimauftragsmenge, den Feuchtigkeitsgehalt des Holzes und die Raumtemperatur sowie Luftfeuchte beeinflusst. Höherer Leimauftrag, niedrigere Temperatur sowie höherer Feuchtigkeitsgehalt im Holz und in der Luft verlängern die OAT und CAT.

Der Pressdruck muss aufgebracht werden, solange der Leim klebfähig ist.

OAT und CAT -Werte sollten getrennt voneinander betrachtet werden. Die gesamte Wartezeit (OAT + CAT) muss für jeden speziellen Fall bewertet werden. Die offene Wartezeit sollte so kurz als möglich gehalten werden.

Nachfolgende Wartezeiten werden für Plus empfohlen:

	Verhältnis	Leimparameter	Maximale Wartezeit
<b>Wartezeiten, getrenntes Verfahren</b>	100:30	20°C/250 g/m <sup>2</sup>	1 h
		20°C/400 g/m <sup>2</sup>	2 h
	100:100	20°C/250 g/m <sup>2</sup>	35 min
		20°C/400 g/m <sup>2</sup>	50 min
	Verhältnis	Leimparameter	Maximale Wartezeit
<b>Wartezeiten, Untermisch Verfahren</b>	100:30	20°C/250 g/m <sup>2</sup>	1 h
		20°C/400 g/m <sup>2</sup>	1 h 20 min
	100:100	20°C/250 g/m <sup>2</sup>	25 min
		20°C/400 g/m <sup>2</sup>	25 min

#### Contact Information

Stockholm, Sweden +46 8 743 40 00  
 High Point, USA +1 336 841 5111  
 Singapore +65 6762 2088  
 Medellín, Colombia +57 4 3618888  
[www.akzonobel.com/cascoadhesives](http://www.akzonobel.com/cascoadhesives)

Version: 4 (2015-06-15)

Reason for changes: update according to EN14080:2013

Abhängig von der Umgebungstemperatur, der Lamellentemperatur und der Lamellenqualität kann die Leimmenge für spezielle Produktionen optimiert werden. Dieses darf nur in Absprache mit der Anwendungstechnik von AkzoNobel erfolgen.

#### Presszeit

Unter Presszeit versteht man das Zeitintervall, während dessen die Leimfuge unter Pressdruck steht, bevor das Material weiterverarbeitet wird. Die Presszeit wird mittels genormter Analyseverfahren gemessen, so dass Presszeiten verschiedener Systeme miteinander verglichen werden können.

Zahlreiche Parameter beeinflussen die Leistungsfähigkeit eines Leimsystems, z. B. Zustand der Presse, Feuchtigkeitsgehalt der Fügeteile, Art des Bauteils und die Holzart.

Die vorgegebenen Presszeiten beziehen sich auf eine Materialtemperatur von 20°C. Wenn die Temperatur des Materials niedriger ist, muss die Presszeit verlängert werden.

Materialtemperaturen < +18°C sind bei der Produktion von tragenden geklebten Holzbauteilen nach DIN 1052 nicht zulässig. Die in den Tabellen 1 + 2 angegebenen Werte dienen als Richtlinie.

Die Presszeiten werden nach DIN EN 302-6 bestimmt. Zur Brettschichtholz-Herstellung gemäß DIN 1052 werden normalerweise diese Presszeiten gewählt (s. Tabelle 2 unten).

Wenn durchgängig eine dünne Klebstofffuge (ca. 0,1 mm) gewährleistet ist, kann die Mindest-Presszeit niedriger sein als nach EN 302-6 festgelegt. Die Werte sind in Tabelle 1 aufgeführt (s. unten). In diesen Fällen muss die maximale Dicke der Leimfuge regelmäßig durch die firmeninterne Produktionskontrolle geprüft und die ordnungsgemäße Qualität der Leimfugen durch regelmäßige Delaminationsprüfungen nachgewiesen werden.

**Tabelle 1: Presszeiten bei garantierter dünner Leimfuge (ca. 0,1mm)**

Presszeiten bei garantierter dünner Leimfuge	Leimfugentemperatur	Verhältnis 100:30	Verhältnis 100:100
(250 g/m <sup>2</sup> , ca. 0.1 mm)	20°C	3 h	1 h 30 min

Neben anderen Faktoren kann die Presszeit durch die Klebstofffugendicke beeinflusst werden. In Fällen, bei denen eine Klebstofffugendicke von ca. 0,1mm nicht garantiert werden kann, müssen die Presszeiten gemäß EN 302-6 eingehalten werden. Diese Mindest-Presszeit ist nachfolgend aufgelistet.

**Tabelle 2: Presszeit gemäß EN 302-6**

Presszeit gemäß EN302-6	Leimfugentemperatur	Verhältnis 100:30	Verhältnis 100:100
(ca. 0.3 mm)	20°C	6 h 30 min	2 h 30 min

Die vorgegebenen Presszeiten beziehen sich auf die Produktion von geraden Bauteilen mit einer Holzfeuchte von ca. 12%. Bei Verleimung von gekrümmten Bauteilen oder Holz mit einem höheren Feuchtigkeitsgehalt muss die Presszeit verlängert werden.

Wenn die Brettschichtholz-Produktion bei erhöhten Temperaturen durchgeführt wird, entweder in einer Heipresse oder bei Hochfrequenz-Aushärtung, kann die Presszeit verkürzt werden. In diesen speziellen

#### Contact Information

Stockholm, Sweden +46 8 743 40 00  
 High Point, USA +1 336 841 5111  
 Singapore +65 6762 2088  
 Medellin, Colombia +57 4 3618888  
[www.akzonobel.com/cascoadhesives](http://www.akzonobel.com/cascoadhesives)

Version: 4 (2015-06-15)

Reason for changes: update according to EN14080:2013



Fällen muss stets ein AkzoNobel Anwendungstechniker hinzugezogen werden. Bevor Verleimungsbedingungen für eine spezielle Produktion festgelegt werden, müssen Delaminierungsprüfungen nach EN 14080:2013 Anhang C.4.3 oder C.4.4 durchgeführt und hierbei die Anforderungen gemäß EN14080:2013 Tabelle 9 erfüllt werden.

### Pressdruck

Bei der Produktion von Brettschichtholz hängt der benötigte Pressdruck u. a. von der Stärke der Lamellen sowie der Holzart ab.

Lamellen mit einer Stärke unterhalb 35 mm erfordern einen Pressdruck zwischen 0.6 – 0.8 MPa. Lamellen mit einer Stärke zwischen 35 – 45 mm benötigen einen Pressdruck von 0.8 MPa (genutete Lamellen) oder 1.0 MPa (nicht genutete Lamellen). Für Lamellen mit einer Stärke zwischen 45 – 80 mm sollte der Pressdruck bei 0.8 – 1.0 MPa liegen. Beachten Sie, dass Lamellen mit einer Stärke von mehr als 45 mm nicht zur Brettschichtholz-Produktion zugelassen sind. Bei getrenntem Auftrag von Leim und Härter kann derselbe Pressdruck für die Flächenverleimung verwendet werden.

Ein zu hoher Pressdruck verursacht einen zu hohen Leimaustritt, was zu einer schlechten Verklebung führt. Ein zu niedriger Pressdruck führt zu einem zu geringen Kontakt zwischen den zwei Oberflächen, wodurch die Qualität der Leimfuge beeinträchtigt wird.

### Leimauftrag

Die Leimauftragsmenge kann, abhängig von Holzart, Holzfeuchte, relativer Luftfeuchtigkeit, Raumtemperatur, Press-Typ, Wartezeit und Hobelqualität, variieren. Die Leimauftragsuntergrenze sollte jedoch nicht niedriger sein als die Werte in nachfolgender Tabelle:

**Die Leimauftragsmenge sollte bei Aushärtung bei Raumtemperatur nicht unter 220 g/m<sup>2</sup> liegen.**

**Die Leimauftragsmenge sollte bei Aushärtung mit Hochfrequenz nicht unter 180 g/m<sup>2</sup> liegen.**

Bei der Herstellung von tragenden Bauteilen darf eine Reduzierung der Leimauftragsmenge, z.B. bei sehr kurzen Wartezeiten, nur unter Zustimmung der Anwendungstechnik unter Berücksichtigung der Produktionsparameter bei der jeweiligen Produktionslinie erfolgen. Diese Optimierung setzt voraus, dass die vorgegebenen Parameter eingehalten und kontinuierliche Kontrollen in Form von Delaminationsprüfungen durchgeführt werden. Eine schriftliche und signierte Bestätigung von AkzoNobel und der Klebstoffprüfstelle ist dafür zwingend erforderlich.

Ein geringes Herauspressen von Leim entlang der Leimfuge bei Anbringen des Pressdruckes weist sowohl auf einen angemessenen Leimauftrag als auch auf die Einhaltung der Wartezeit hin.

Starker Leimaustritt deutet auf einen zu hohen Leimauftrag, sehr hohen Pressdruck oder eine Kombination aus Beidem hin.

Wird eine längere Wartezeit erforderlich, kann ein höherer Leimauftrag gewählt werden.

Ein gleichmäßiger Leimauftrag ist sehr wichtig.

### Holzfeuchte

Der Feuchtigkeitsgehalt des Holzes hat Auswirkungen auf das Verleimresultat. Eine hohe Holzfeuchte kann das System verlangsamen. Bei bestimmten Leimsystemen kann ein übermäßig hoher Feuchtigkeitsgehalt negative Auswirkungen auf die Leimfugenqualität haben.

In bestimmten Fällen kann eine viel zu geringe Holzfeuchte den Verklebungsprozess beschleunigen.

Der Feuchtigkeitsgehalt des Holzes hat auch eine Auswirkung auf die Gesamtqualität des Endproduktes. Eine ungleichmäßig, wesentlich zu hohe/niedrige Holzfeuchte kann zu Verzug, Schüsselung und

### Contact Information

Stockholm, Sweden +46 8 743 40 00  
High Point, USA +1 336 841 5111  
Singapore +65 6762 2088  
Medellin, Colombia +57 4 3618888  
www.akzonobel.com/cascodhesives

Version: 4 (2015-06-15)

Reason for changes: update according to EN14080:2013

Unebenheiten des Endproduktes führen.

Für die Brettschichtholz-Produktion sollte der Feuchtigkeitsgehalt vorzugsweise bei 10-12%, mindestens jedoch zwischen 8-15% liegen.

#### Vorbereitung des Holzes

Für beste Ergebnisse muss das Holz sauber gehobelt sein. Optimale Festigkeit wird erreicht, wenn die Verleimung spätestens 24 Stunden nach der Hobelung erfolgt.

Die Oberfläche muss frei von Staub, Fett, Öl und anderen Verunreinigungen sein.

Die Fügeile müssen sorgfältig ausgewählt werden, um eine optimale Leimfugenqualität erzeugen zu können. Um die Presszeiten in der oben stehenden Tabelle einhalten zu können, muss die Lamellentemperatur mindestens 20°C betragen. Materialtemperaturen unterhalb +18°C sind zur Produktion von tragenden Bauteilen gemäß DIN1052 nicht zugelassen.

Das Klebstoffsystem ist für folgende Holzarten zugelassen: Fichte, Kiefer, Tanne, Europäische Lärche

#### Nachhärtung

Nach erfolgter Presszeit verfügt die Leimfuge der Konstruktion über genügend Festigkeit, um weiterverarbeitet zu werden. Die Endfestigkeit wird nach einer Zeit, die abhängig von der Presszeit/-temperatur sowie der Lagertemperatur ist, erreicht.

Unter Nachhärtezeit versteht man die Zeit die benötigt wird, damit die Leimfuge die vollständige Festigkeit und Wasserbeständigkeit erhält.

Die Nachhärtezeit hängt von der Presszeit, Presstemperatur, Lamellentemperatur sowie der Nachhärtezeit ab. Aushärtung bei anderen Temperaturen als 20°C verändert die benötigte Nachhärtezeit. Die erforderliche Nachhärtezeit muss von der Anwendungstechnik bestimmt werden.

Bei 20°C beträgt die Nachhärtezeit 40 Stunden bei 100:30 und 12 Stunden bei 100:100.

#### Zusätzliche Informationen zum Keilzinken

Für die Produktion von Keilzinkverbindungen müssen die Anforderungen wie in DIN 1052 und EN14080:2013 beschrieben, befolgt werden. Die Applikation muss im Untermischverfahren stattfinden. Die unten angeführte Tabelle beinhaltet wichtige Verarbeitungsparameter:

<b>Nominales Mischungsverhältnis</b>	Untermischverfahren (Fichte, Tanne, Kiefer): 100:10-100 Untermischverfahren (Europäische Lärche): 100:30-60						
<b>Empfohlene Leimauftragsmenge</b>	zwischen 250 -350 g/m <sup>2</sup>						
<b>Maximale Wartezeit</b>	5 min						
<b>Aushärtezeit</b>	<table> <tr> <td>100:10</td><td>8 h 15 min</td></tr> <tr> <td>100:30</td><td>3 h</td></tr> <tr> <td>100:100</td><td>1 h 30 min</td></tr> </table>	100:10	8 h 15 min	100:30	3 h	100:100	1 h 30 min
100:10	8 h 15 min						
100:30	3 h						
100:100	1 h 30 min						

#### Contact Information

Stockholm, Sweden +46 8 743 40 00  
High Point, USA +1 336 841 5111  
Singapore +65 6762 2088  
Medellin, Colombia +57 4 3618888  
www.akzonobel.com/cascoadhesives

Version: 4 (2015-06-15)

Reason for changes: update according to EN14080:2013

<b>Pressdruck</b>	Gemäß EN 14080:2013
-------------------	---------------------

#### **Gemischte Applikation bei Keilzinken**

Im Untermischverfahren werden profilierte Auftragswalzen oder gleichwertige Applikationsgeräte empfohlen. Das Mischungsverhältnis beträgt von 100:10 (Leim:Härter) bis maximal 100:100 Gewichtsteile. Die Abweichung zwischen Leim und Härter darf maximal  $\pm 3$  GWT betragen. Die Benetzung der Zinkenflanken mit dem Leim- Härtergemisch muss mindestens 75% betragen. Die Topfzeit legt die mögliche Verarbeitungsdauer des Leimgemischs fest und muss deshalb gut überwacht werden. Die Tabelle unter „Topfzeit“ beinhaltet Angaben der Verarbeitungsdauer für verschiedene Mischungsverhältnisse. Ein gekühltes Gemisch verlängert die Topfzeit, höhere Temperaturen verkürzen sie.

#### **Aushärtung von Keilzinkverbindungen**

Gemäß EN 14080:2013 beträgt die Mindestaushärtetemperatur  $+20^{\circ}\text{C}$ . Bei Hochfrequenzaushärtung muss die Fugentemperatur mindestens  $65^{\circ}\text{C}$  betragen.

#### **Weiterverarbeitung von keilgezinkten Lamellen**

Eine direkte Weiterverarbeitung der Lamellen darf nur erfolgen, wenn Transport und Hobelung keinen mechanischen Einfluss auf die Keilzinkenverbindung ausüben. Andernfalls muss die in obiger Tabelle angegebene Aushärtezeit befolgt werden.

#### **Endfestigkeit von Keilzinkverbindungen**

Das Erreichen der Endfestigkeit ist von den Aushärtebedingungen und vom Klebstoffsystem abhängig. Wird Plus mit einem Mischungsverhältnis von 100:10 verarbeitet, so wird die volle Wasserfestigkeit bei 100:10 in 72 Stunden, bei 100:30 in 40 Stunden und bei 100:100 in 12 Stunden erreicht.

#### **Qualitätskontrolle von Keilzinkverbindungen**

Die Qualitätskontrolle muss gemäß der verwendeten Produktnorm erfolgen.

### **Handhabung und Umweltinformation**

#### **Reinigung**

Maschine stets vor Aushärtung des Leimes mit lauwarmem Wasser reinigen! Ausgehärteter Leim muss manuell entfernt werden. Die Verwendung von Leimwaschmittel 4450 oder Reinigungsmittel 2704 erleichtert die Reinigung der Leimauftragsgeräte.

#### **Reinigungsmittel 2704;**

Zur Reinigung von Gießanlagen fügen Sie 50/50 (Gewichtsteile) der Mixtur aus Wasser und Reinigungsmittel 2704 in die Anlage. Pumpen Sie die Lösung ca. 4 Minuten im Kreislauf der Gießanlage und spülen Sie danach mit warmem Wasser.

#### **Leimwaschmittel 4450;**

Fügen Sie 1% Leimwaschmittel 4450 (in Relation zum Restleim in der Gießanlage) der Anlage zu. Lassen

#### **Contact Information**

Stockholm, Sweden +46 8 743 40 00  
High Point, USA +1 336 841 5111  
Singapore +65 6762 2088  
Medellin, Colombia +57 4 3618888  
[www.akzonobel.com/cascoadhesives](http://www.akzonobel.com/cascoadhesives)

**Version:** 4 (2015-06-15)

**Reason for changes:** update according to EN14080:2013



Sie die Gießanlage ca. 5 Minuten weiterlaufen, damit die Mixtur ausreichend vermischt wird. Danach kann die Anlage mit lauwarmem Wasser gewaschen werden.

#### **Handhabung**

Vermeiden Sie den direkten Kontakt mit Leim und Härter. Tragen Sie stets Handschuhe und Schutzbrille. Bei Hautkontakt reinigen Sie die betroffene Hautstelle umgehend mit Seife und lauwarmem Wasser. Aufgrund seines niedrigen pH-Wertes reagiert der Härter korrosiv auf Kupfer und kupferhaltige Legierungen. Es wird daher Stahl oder Plastik für den Einsatz im direkten Gebrauch mit dem Produkt empfohlen. Das Sicherheitsdatenblatt informiert Sie hinsichtlich Gesundheit und Sicherheit. Lesen Sie diese Informationen sorgfältig durch.

#### **Mischbarkeit**

Ob ein Produkt mit einem anderen Produkt mischbar ist (z. B. beim Wechsel von Leim oder Härter auf ein anderes Produkt) muss in jedem speziellen Fall ermittelt werden. Bitte sprechen Sie mit Ihrer Kontaktperson von AkzoNobel zwecks weiterer Informationen.

#### **Abfallbehandlung**

**Leim** – das Produkt Plus A011 ist nicht kennzeichnungspflichtig.

**Härter** - Abhängig von der Klassifizierung des Härters muss er als Sondermüll angesehen werden (siehe Sicherheitsdatenblatt, Abschnitt 13)

**Leim-/Härtergemisch** – Das ausgehärtete System gilt im Normalfall nicht als Sondermüll.

**Achtung!** Es können nationale und/oder regionale Unterschiede bei den Vorschriften vorherrschen. Bitte nehmen Sie Kontakt mit den für Sie zuständigen Behörden auf.

#### **Waschwasser-Behandlung**

**Chemische Ausfällung** → kommunale Kläranlage mit biologischer Behandlung.

Die Zusätze 4410, 4411, 4412 und 4413 dienen der Verringerung von Leimrückständen im Leimwaschwasser. Diese Produkte agieren als Flockungsmittel, die die Leimpartikel konzentrieren und sedimentieren. Nach der Behandlung hat das Waschwasser einen geringeren Trockengehalt, wodurch einem Verstopfen von Rohren und Abflüssen vorgebeugt wird. Das entstandene Sediment kann, nachdem es ausgehärtet ist, als ungefährlicher Industrie-Müll entsorgt werden.

#### Auffangen von Leimwaschwasser

Leimwaschwasser kann auf einfache Art in leeren Leimfässern gesammelt werden. Abhängig von der Menge des anfallenden Leimwaschwassers sowie der Zeit, die für die Sedimentation nach der Ausfällung benötigt wird, sollten 2 oder mehr Leimfässer bereitgestellt werden.

#### Entsorgung von aufbereitetem Leimwaschwasser

Das aufbereitete Leimwaschwasser darf nicht ohne Zustimmung der lokalen Behörden in das Abwassernetz eingeleitet werden.

#### Entsorgung von Sediment

Wenn ein Fass mit Sediment gefüllt ist, lassen Sie es - möglichst bei hohen Temperaturen um die 50°C - stehen, bis die Ablagerungen ausgehärtet sind. Die Fässer mit den ausgehärteten Rückständen können später als ungefährlicher Industriemüll entsorgt werden. Bitte nehmen Sie Kontakt mit den für Sie zuständigen Behörden hinsichtlich einer fachgerechten Entsorgung auf.

#### **Contact Information**

Stockholm, Sweden +46 8 743 40 00  
High Point, USA +1 336 841 5111  
Singapore +65 6762 2088  
Medellin, Colombia +57 4 3618888  
www.akzonobel.com/cascoadhesives

**Version:** 4 (2015-06-15)

**Reason for changes:** update according to EN14080:2013

Weitere Informationen finden Sie in den Produktinformationen für 4410/4411/4412/4413.

**Mechanische Ausfällung → kommunale Kläranlage mit biologischer Behandlung** Mechanische Ausfällung (Sedimentation) wird zur Reduzierung des Trockengehaltes in Waschwasser angewandt, um die Gefahr einer Verstopfung von Leitungen zu minimieren. Zur Ausfällung geeignete Behälter sind leere Fässer oder IBC, abhängig von der anfallenden Menge an Waschwasser. Der sich im Behälter befindliche Schlamm sollte getrocknet werden (vorzugsweise bei  $> 50^{\circ}\text{C}$ ) und kann später als ungefährlicher Industriemüll entsorgt werden. Der restliche Wasseranteil sollte nicht ohne ausdrückliche Genehmigung durch die regionalen Behörden in das Abwassernetz eingeleitet werden.

**Achtung!** Es können nationale und/oder regionale Unterschiede bei den behördlichen Bestimmungen vorherrschen. Bitte nehmen Sie Kontakt mit den für Sie zuständigen Behörden auf. Zu weiteren Fragen steht Ihnen der Sachverständige in Umweltfragen von AkzoNobel zur Verfügung.

#### **Gesundheit und Sicherheit**

Bitte beachten Sie das entsprechende Sicherheitsdatenblatt

#### **Rechtliche Klausel:**

Diese Information basiert auf Laborversuchen und praktischen Erfahrungen. Sie dient als Einführung vor dem Hintergrund, die für den Anwender bestmögliche Verarbeitungsmethode zu ermitteln. Da sich die Produktionsbedingungen des Anwenders außerhalb unseres Einflussbereiches befinden, übernehmen wir keine Verantwortung für die Verarbeitungsergebnisse, die von den jeweils vorherrschenden Bedingungen beeinflusst werden. Es werden in jedem Falle Durchführungen von Versuchsreihen sowie regelmäßige Überprüfungen empfohlen.

#### **Contact Information**

Stockholm, Sweden +46 8 743 40 00  
High Point, USA +1 336 841 5111  
Singapore +65 6762 2088  
Medellin, Colombia +57 4 3618888  
[www.akzonobel.com/cascoadhesives](http://www.akzonobel.com/cascoadhesives)

**Version:** 4 (2015-06-15)

**Reason for changes:** update according to EN14080:2013



## Appendix C

Fire Design recommendations of timber elements and a worked example of determining a parametric time-temperature curve including the contribution of exposed CLT

## C.1) A Review of Fire Design Recommendations

In this section of the Appendix, the current design recommendations pertaining to the fire design of timber elements subjected to elevated temperatures, as well as recommendation regarding the fire exposure of CLT, is presented. A description of various types of fire curves is first discussed, followed by the Eurocode codification of timber charring, a design recommendation that seeks to characterise the contribution of combustible CLT to the overall fuel load, and finally a brief description of zone modelling.

### C.1.1) Fire Curves

A fire curve depicts the variation in gas temperature with respect to time. It is important in defining the behaviour of structures exposed to fire and it is subsequently used as a baseline against which to perform design calculations. Fire curves can be divided into two main categories, namely the standard fire curve (SFC) and parametric fire curves (PFC). All technical data presented in this section is sourced from Eurocode EN 1991-1-2 (2002) unless noted otherwise.

The SFC as proposed in 1918 represents a standardised curve of enclosure temperatures during a post-flashover fire. It is by no means indicative of real fire behaviour- it is merely a benchmark against which fire ratings are assessed internationally. The details of the Standard Fire Curve are presented in the International Organization for Standardization (ISO) 834 document as well as EN 1363-1 and EN 1991-1-2. The gas temperature in the firecell ( $\theta_g$  measured in °C) is defined as a variable of time ( $t$  measured in minutes) by Equation 1, and is graphically depicted in Figure 70:

$$\theta_g = 20 + 345 \log_{10}(8t + 1) \quad (1)$$

Caution should however be advised when employing this fire curve. The SFC is not representative of a real fire, as it does not account for the fire characteristics of a compartment (including geometry, openings, fuel loads etc.), nor does it contain a decay phase. The SFC is used to perform standardised fire testing of materials (according to EN 1363) and establish fire ratings relevant to post flash-over conditions. The SFC is also used to demonstrate sufficient structural capacity of members when exposed to fire. A fire rating (stated in minutes) is calculated as the time a member is able to satisfactorily resist exposure to the SFC.

Other simple fire curves have been developed to account for hydrocarbon fires (higher fuel load conditions such as in the petrochemical industry), as well as the external fire curve which accounts for flames that emerge from buildings and are at a lower intensity than the standard fire curve. The two additional curves are depicted against the standard curve, in Figure 70, for comparative purposes but are not discussed further (for more information refer to EN 1991-1-2)

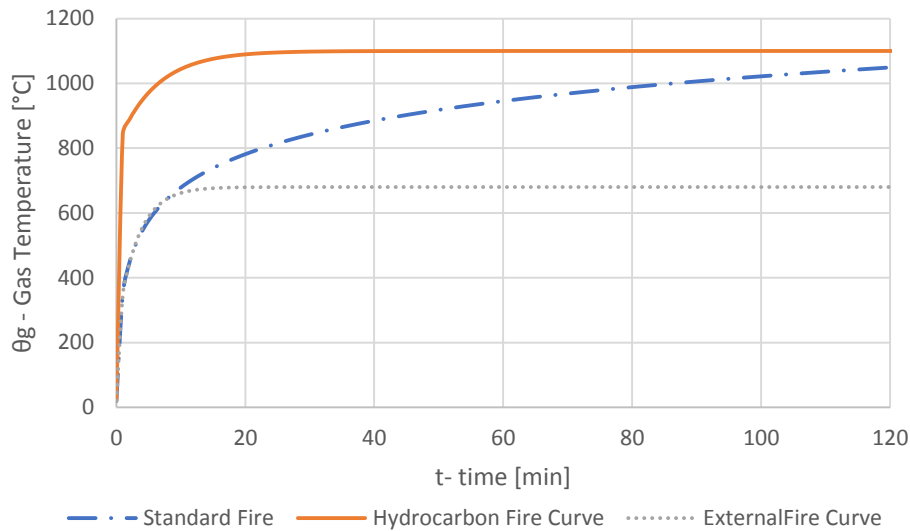


Figure 70: Fire Curves

As mentioned before, the SFC is merely used as a benchmark by which to (internationally) determine the fire rating of structural elements and does not represent a realistic fire since it does not contain a decay phase nor does it take any enclosure characteristics (such as thermal properties of the enclosure boundaries, ventilation openings, fuel type, fuel load etc.). Real compartment fires display a growth, flashover and a decay period under appropriate conditions. In order to account for these situations, parametric fire curves have been developed. These curves are more complicated in nature as they depict the growth and decay periods (EN 1991-1-2, 2002). It is important to note that parametric fire curves are used to carry out performance based design of structures in post-flashover conditions that are ventilation controlled (Brandon, 2018a).

The EN 1991-1-2 parametric fire curve is only valid for compartments of floor area up to 500 m<sup>2</sup>, containing no openings within the roof and restricts the height of the compartment to 4m. An additional assumption is that the entire fire load is completely combusted during the fire event.

The concept underpinning a parametric fire curve is that the fire temperature within an enclosure is predicted based on the enclosure parameters. Enclosure parameters include: openings; thermal inertia of the enclosure boundaries and the fuel load in the compartment. A parametric fire curve, however, does not include the formation of a second flashover due to heat induced delamination of CLT lamella. Delamination should therefore be avoided in order to employ a parametric fire curve to predict enclosure temperatures. As presented by Brandon and Dagenais (2018), this can be achieved by using non-delaminating adhesives, or by applying a sufficiently thick outer lamella (Crielaard, 2015).

The EN 1991-1-2 (Annex A) parametric fire curve is defined as follows:

$$\theta_g = 20 + 1325(1 - 0.324e^{-0.2t.\Gamma} - 0.204e^{-1.7t.\Gamma} - 0.472e^{-19t.\Gamma}) \quad (2)$$

where:

$\theta_g$  is the gas temperature in the compartment in °C

$\Gamma$  is factor that corresponds to the thermal inertia of the compartment (taken at ambient temperature) and the opening factor, and is referred to as the heating rate factor:

$$\Gamma = \left( \frac{O}{\sqrt{\rho c \lambda}} \right)^2 / \left( \frac{0.04}{1160} \right)^2 \quad (3)$$

note that the following limits are imposed:  $100 \leq \sqrt{\rho c \lambda} \leq 2200$  [J/m<sup>2</sup>s<sup>1/2</sup>K]

$t$  is time in hours

$\rho$  is the density of boundary of the enclosure [kg/m<sup>3</sup>]

$c$  is the specific heat of the boundary of the enclosure [J/kgK]

$\lambda$  is the thermal conductivity of boundary of the enclosure [W/mK]

$O$  is the opening factor:

$$O = \frac{A_v}{A_t} \sqrt{h_{eq}} \text{ with } 0.02 \leq O \leq 0.2 \text{ [m}^{0.5}\text{]} \quad (4)$$

$A_v$  is the total area of the vertical openings on all walls [m<sup>2</sup>]

$A_t$  is the total area of the enclosure (all walls, ceiling, floor including openings) [m<sup>2</sup>]

$h_{eq}$  is the weighted average of window heights on all (vertical) walls [m]:

$$h_{eq} = \sum \frac{A_i \cdot h_i}{A} \quad (5)$$

The maximum temperature in the compartment ( $\theta_{max}$  at  $t = t_{max}$ ) during the heating phase is determined as follows:

$$t_{max} = \max \left\{ \frac{0.2 \cdot 10^{-3} q_{t,d}}{O}, t_{lim} \right\} \quad (6)$$

where:

$q_{t,d}$  is the design value of the fire load density related to the total fuel load divided by the surface area  $A_t$  of the enclosure. The following limit is imposed:  $50 \leq q_{t,d} \leq 1000$  [MJ/m<sup>2</sup>]. This value may be obtained from Annex E of EN1991-1-2, and is related to the floor surface area ( $A_f$ ) by the following relationship:  $q_{t,d} = q_{f,d} \cdot \frac{A_f}{A_t}$  [MJ/m<sup>2</sup>].

$t_{lim}$  refers to the time to reach maximum compartment temperature in a fuel controlled fire. Depending on the fire growth rate  $t_{lim}$  is 0:15h, 0:20h or 0:25h for fast, medium and slow fire growth respectively.

After the peak compartment temperature is reached (at  $t_{max}$ ), the cooling phase commences and the compartment temperature linearly decreases to 20°C according to the following relationships:

$$\theta_g = \theta_{max} - 625(t \cdot \Gamma - t_{max} \cdot \Gamma \cdot x) \text{ if } t_{max} \cdot \Gamma \leq 0.5 \quad (7)$$

$$\theta_g = \theta_{max} - 250(3 - t_{max} \cdot \Gamma)(t \cdot \Gamma - t_{max} \cdot \Gamma \cdot x) \text{ if } 0.5 < t_{max} \cdot \Gamma < 2 \quad (8)$$

$$\theta_g = \theta_{max} - 250(t \cdot \Gamma - t_{max} \cdot \Gamma \cdot x) \text{ if } t_{max} \cdot \Gamma \geq 0.5 \quad (9)$$

and

$x$  is equal to 1.0 if  $t_{max} > t_{lim}$ , or equal to  $t_{lim} \cdot \frac{\Gamma}{t_{max}}$  if  $t_{max} = t_{lim}$

For comparative purposes, Figure 71 depicts the SFC against a few parametric fire curves for a set fuel load and compartment thermal inertia, but different opening factors. Note that the SFC is well approximated when  $\Gamma = 1$ .

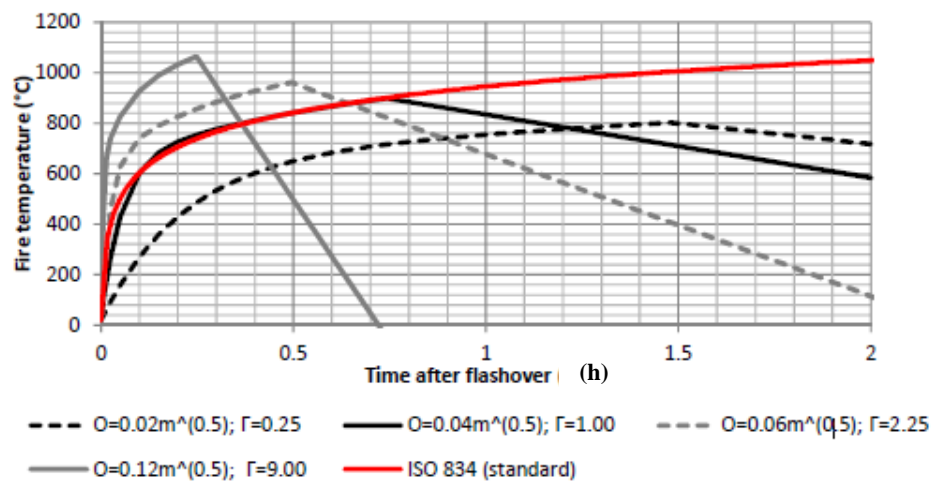


Figure 71: SFC vs various parametric fire curves, as reported by Brandon (2018b)

### C.1.2) Charring of Timber Design Equations according to EN 1995-1-2

As with the aforementioned fire curves, a distinction is once again made between the standard fire curve and a natural fire curve (for example a parametric fire curve). The charring of timber, as codified in EN1995-1-2, is described by a charring rate based on fire exposure to either the SFC or a PFC, and each of these will be discussed separately in this section.

The general idea behind the design method proposed in EC1995-1-2, namely the reduced cross-section method, is that both the SFC and the PFC result in charring rates of timber which in turn are used to determine char depths. These char depths are subtracted from the original timber cross section to obtain the effective cross section for structural use that remains during a fire.

#### *Charring according to the SFC*

When a timber section is exposed to a fire, and more specifically the standard fire according to the SFC, a char layer develops at a predictable rate depending on the type of timber product and its density. According to EN 1995-1-2, a distinction is made between a one dimensional ( $\beta_0$  in  $[\frac{\text{mm}}{\text{min}}]$ ) and a notional charring rate ( $\beta_n$  in  $[\frac{\text{mm}}{\text{min}}]$ ). The former is used when a timber element is exposed to a fire on one side only, whereas the latter is used when the element is exposed to a fire from more than one side (and therefore includes the effect of rounding at corners as well as fissures). According to EN1995-1-2, the one-dimensional and notional charring rate result in a one-dimensional charring depth ( $d_{char,0} = \beta_0 \cdot t$ ) and a notional charring depth ( $d_{char,n} = \beta_n \cdot t$ ), respectively. Figure 72 depicts the difference between the notional and one-dimensional charring depth.

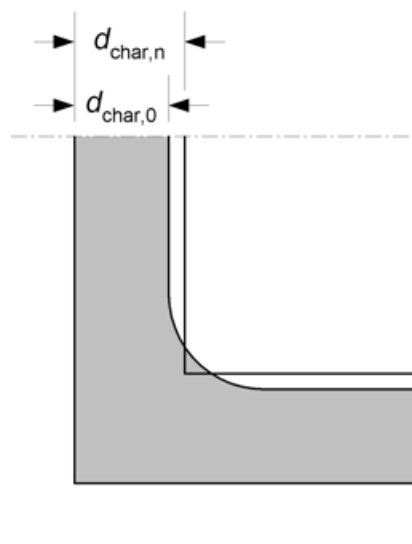


Figure 72: Difference between the notional and one dimensional charring depth according to EN 1995-1-2

As stated before, the charring rate depends on the type of timber product as well as its density. Table 43 (from EN1995-1-2, Table 3.1) displays the codified charring (both one-dimensional and notional)

rates. Note that CLT is not included in the charring rate table presented in EN1995-1-2. For comparative purposes, Brandon and Dagenais (2018) experimentally obtained a one-dimensional CLT charring rate of 0.67 mm/min which is similar to that of solid softwood timber. Frangi *et al.* (2009) also investigated charring of CLT and found that heat induced delamination significantly increases the observed charring rate. In his study, Frangi found that CLT panels manufactured using MUF adhesives displayed stable fire behaviour in the sense that delamination was not observed. An experimentally obtained charring rate of approximately 0.6 mm/min was found for MUF based CLT panels, which is even lower than that specified in EN 1995-1-2 for solid softwood timber. In contrast, CLT panels manufactured using a PU adhesive resulted in experimental charring rates varying between approximately 0.85 to 1.10 mm/min and depended heavily on the occurrence of delamination.

Table 43: One-dimensional and notional charring rate according to EC1995-1-2

	$\dot{\rho}_0$ mm/min	$\dot{\rho}_n$ mm/min
<b>a) Softwood and beech</b>		
Glued laminated timber with a characteristic density of $\geq 290 \text{ kg/m}^3$	0,65	0,7
Solid timber with a characteristic density of $\geq 290 \text{ kg/m}^3$	0,65	0,8
<b>b) Hardwood</b>		
Solid or glued laminated hardwood with a characteristic density of $\geq 290 \text{ kg/m}^3$	0,65	0,7
Solid or glued laminated hardwood with a characteristic density of $\geq 450 \text{ kg/m}^3$	0,50	0,55
<b>c) LVL</b>		
with a characteristic density of $\geq 480 \text{ kg/m}^3$	0,65	0,7
<b>d) Panels</b>		
Wood panelling	0,9 <sup>a</sup>	–
Plywood	1,0 <sup>a</sup>	–
Wood-based panels other than plywood	0,9 <sup>a</sup>	–
<sup>a</sup> The values apply to a characteristic density of $450 \text{ kg/m}^3$ and a panel thickness of 20 mm; see 3.4.2(9) for other thicknesses and densities.		

The charring rate and subsequent charring depth is used in the EC1995-1-2 reduced cross-section method to determine the effective timber cross section remaining during a fire. The method is described in section 4.2.2 of EN1995-1-2. The main principle is to reduce the timber cross-section at each exposed side by an effective charring depth ( $d_{ef}$ ). The effective charring depth is calculated as follows (for cross-sections exposed to a fire on more than one side):

$$d_{ef} = d_{char,n} + k_0 d_0 \quad (10)$$

Where:

$k_0 d_0$  is the zero strength layer adjacent to the char base (and therefore in the pyrolysis zone). This layer is assumed to be degraded to zero strength and stiffness when

performing resistance calculations, and therefore forms part of the effective char depth.

$k_0$  depends on if the timber is protected or unprotected. In the case of exposed timber (therefore unprotected),  $k_0$  is obtained from Table 4.1 in EN1995-1-2 (t in minutes):

Table 44:  $k_0$  factor to determine the zero strength layer depth, from EN1995-1-2 Table 4.1

	$k_0$
$t < 20$ minutes	$t/20$
$t \geq 20$ minutes	1,0

$d_0$  is the assumed (constant) heat affected depth adjacent to the char base. According EN1995-1-2  $d_0 = 7\text{mm}$

Figure 73 indicates the relevant dimensions used in the reduced cross-section method (note that the dimension labelled “c” in the figure corresponds to  $d_{ef}$  in EN1995-1-2), and  $b_f$  and  $d_f$  are the remaining cross sectional dimensions that are to be used in resistance calculations under fire exposure.

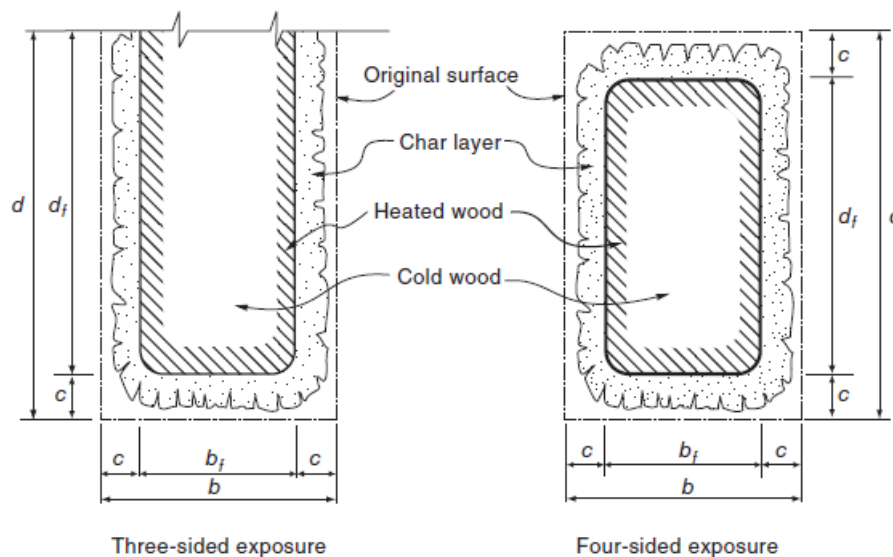


Figure 73: Design concepts pertaining to exposed mass timber, obtained from (Buchanan and Abu, 2017)

#### Charring according to a Parametric Fire Curve

EN1995-1-2 in Annex A also provides an equation to determine the parametric charring rate (units: [mm/min]), for unprotected softwood, during the heating phase of a PFC:



$$\beta_{par} = 1.5\beta \cdot \frac{0.2\sqrt{\Gamma} - 0.04}{0.16\sqrt{\Gamma} + 0.08} \quad (11)$$

Where:

$\beta$  is either the notional or one-dimensional charring rate depending on the section configuration such as exposed corners (Brandon, 2018a).

It is however, noteworthy that Brandon and Dagenais (2018) proposed the following parametric charring rate, which was shown to be more conservative and in better accordance with furnace test:

$$\beta_{par} = \beta \cdot \Gamma^{0.25} \quad (12)$$

The difference between the parametric rate as proposed in EN1995-1-2 and that of Brandon and Dagenais (2018), along with the results of recent furnace tests is depicted in Figure 74:

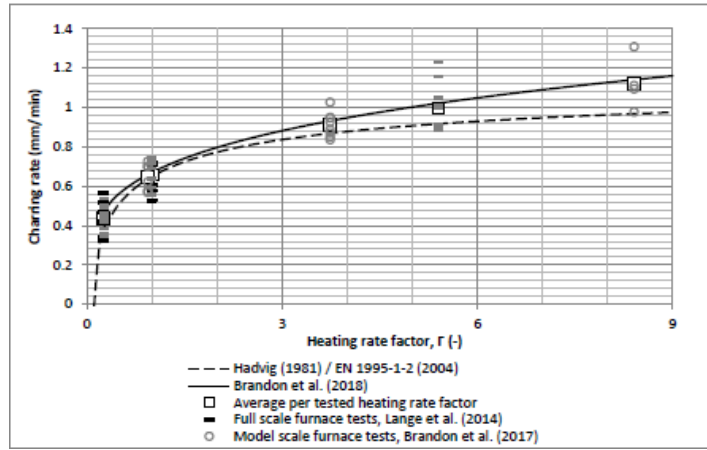


Figure 74: Comparison of different parametric charring rate proposals, from (Brandon, 2018a)

The parametric charring rate codified in EN1995-1-2 is based on the research by Hadvig (1981). The charring rate according to Hadvig depends on the notional charring rate and the opening factor. The formulation of the parametric charring rate in EN1991-1-2 includes the effect of the boundaries by basing the parametric charring rate on the heating rate factor ( $\Gamma$ ) instead of the opening factor. The charring rate formulas as proposed by EN1995-1-2 will be used in this study.

After the heating phase of the PFC, the charring rate reduces during the decay phase. This is illustrated in EN1995-1-2 as follows: during the heating phase (until time  $t=t_0$  corresponding to the constant char rate period) the charring rate is constant and equal to  $\beta_{par}$ . During the decay phase, the parametric char rate reduces linearly from  $\beta_{par}$  at time  $t=t_0$  to a zero-charring rate at time  $t=3t_0$ , and is shown graphically as:

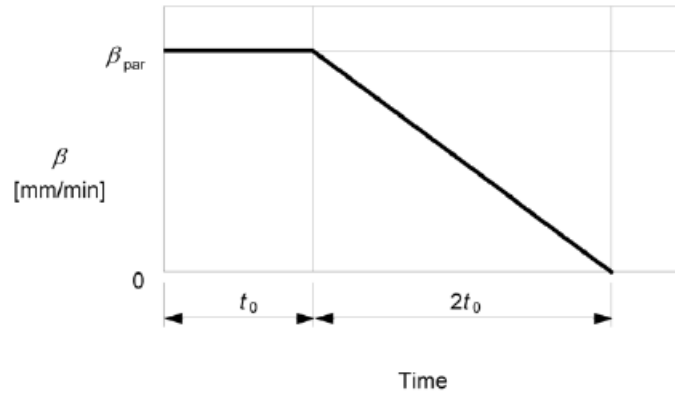


Figure 75: Reduction of the parametric charring rate during the decay phase from EN1995-1-2

The (parametric) charring depth is then calculated as follows:

$$d_{char} = \beta_{par} \cdot t \text{ for } t \leq t_0 \quad (13)$$

$$d_{char} = \beta_{par} \cdot \left(1.5t_0 - \frac{t^2}{4t_0} - \frac{t_0}{4}\right) \text{ for } t_0 \leq t \leq 3t_0 \quad (14)$$

$$d_{char} = 2 \cdot \beta_{par} \cdot t \text{ for } 3t_0 \leq t \leq 5t_0 \quad (15)$$

and,

$$t_0 = \frac{0.009q_{t,d}}{O} \quad (16)$$

### C.1.3) Recommendations proposed by Brandon (2018b)

The PFC, as codified in EN1995-1-2, does not account for the contribution to the fuel load by a combustible construction material. The fuel load in the compartment is described in the PFC by the fire load density ( $q_{t,d}$ ).

According to Brandon (2018b), the contribution of exposed CLT to the fuel load in an enclosure can be estimated based on the parametric charring rate. Two methods are proposed. The **first method** conservatively assumes that CLT combustion efficiency is 100%, and the heat release rate by CLT is given by the following equation:

$$q_{CLT} = \alpha_2 \cdot \beta_{par} \cdot A_{CLT} \cdot \rho_{dry} \cdot H_{wood} \quad (17)$$

where

$\alpha_2$  is the fraction of mass loss relative to the initial timber mass (approximately 0.7)

$A_{CLT}$  is the surface area of the exposed CLT [m<sup>2</sup>]

$\rho_{dry}$  is the dry density (therefore excluding the mass of moisture) of the wood

$H_{wood}$  is the heat of combustion of dry wood (approximately 18.75 MJ/kg)

The **second suggested method** includes an iterative calculation procedure according to the following equation:

$$q_{td}^{i+1} = q_{mfl} + \frac{A_{CLT} \cdot \alpha_1 \cdot (d_{char}^i - 0.7 \cdot \beta_{par} \cdot t_{max}^1)}{A_c} \quad (18)$$

where

$q_{mfl}$  is the fuel load corresponding to movable fuel divided by the total area of the compartment boundaries (including walls and ceilings) [MJ/m<sup>2</sup>]

$\alpha_1$  is the ratio between the heat release and char depth [5.39MJ/(m<sup>2</sup>.mm)]

$t_{max}^1$  is the start time if the decay phase in the first calculation iteration and remains constant throughout the iterative calculation [hours]

$A_c$  is the total surface area of the compartment boundaries [m<sup>2</sup>] including walls and ceilings

Note that the superscript “i” denotes the iterative nature of the method. The first step is to calculate the parameters corresponding to a non-combustible compartment. Subsequently, this first result will be adapted to include the contribution of CLT to the fuel load (per total compartment area), and iteratively recalculate the char depth until it converges. If no convergence is obtained, it is stated that the fire will be continuously fully developed.

A calculation example using this second method is presented in Appendix C.2 of this report.

In his study, Crielaard (2015) also proposed an assessment to characterise the self-extinguishment potential of CLT structures. When considering the contribution of CLT to the fire load, Crielaard suggests a similar iterative approach to that of Brandon. The main difference between these two approaches is the manner by which the charring depth is converted into a fuel load contribution. Crielaard proposes that the charring depth be calculated on the basis of the parametric charring rate

proposed by Hadvig (1981). The obtained charring depth is then multiplied with the effective heat of combustion (which relates the weight of a material to the amount of energy released during incomplete combustion).

In contrast, Brandon (2018b) proposes that: “approximately 70% of the contribution of the timber combusts outside for at least the duration of the fully developed phase of a similar compartment without combustible linings ( $t_{max}^1$ )”. This method appears to correlate well with the results of Su *et al.*, (2018), as illustrated in the example described in Appendix C of this report.

#### C.1.4) Zone Modelling of Enclosure Fires

The more traditional (hand) calculation methods, as presented in the preceding sections of this report, are suitable to determine general fire behaviour (such as compartment gas temperatures as well as timber charring). They are, however, ill-suited to perform detailed fire performance analyses that seek to characterise the complicated and interrelated relationships of physical and chemical processes that occur during a fire (Walton, Carpenter and Wood, 2016). In addition, the growing use of performance based fire design, as well as the trend to design ever more complicated structures, has necessitated the use of computer software to characterise fire behaviour (Karlsson and Quintiere, 1999).

To satisfy the need to accurately simulate complicated fire behaviour, software models have been created to solve intricate fire dynamics equations in a fraction of the time required to manually solve them. An example of a type of fire model is a zone model and will be discussed in this section.

Zone models are commonly used in fire safety engineering to model the development and decay of an enclosure fire. These models are attractive since they are relatively inexpensive and yield results in a short period of time. The fundamental principle underpinning any zone model is that a compartment is divided into zones, namely a *hot upper layer* and a *cool lower layer*. As mentioned in Section 3.1, pyrolysis gases are released when fuels are heated, are subsequently ignited under appropriate conditions and rise as combustion gases from the combusting fuel to the top of a compartment forming the aforementioned hot upper layer. The fire behaviour over various time periods, within a compartment, is computed in a zone model by means of enforcing conservation of mass and energy equations within each of these two zones (Hopkin, Anastasov and Brandon, 2017).

Pre-flashover, a two zone model (graphically displayed in Figure 76) calculates key parameters (such as zone temperature) within both the hot and cold layers. A key assumption is that each zone possesses a uniform temperature. Heat is released from a fire source in the lower zone and transported to the higher zone in a fire plume due to buoyancy and the resulting process of air entrainment (Karlsson and Quintiere, 1999). The process of air entrainment is as follows: hot air rises from the combusting fuel due to its buoyancy (hot air has a lower density than cold air), and cold air is mixed into the plume from its surroundings due to the pressure differences. The model then calculates the

growth of the top zone until conditions are suitable to cause flashover, resulting in the formation of a uniform hot zone throughout the whole compartment (Cadorin and Franssen, 2003). A two zone model is therefore suitable in pre-flashover conditions, whereas a one zone model is suited to a post-flashover fire.

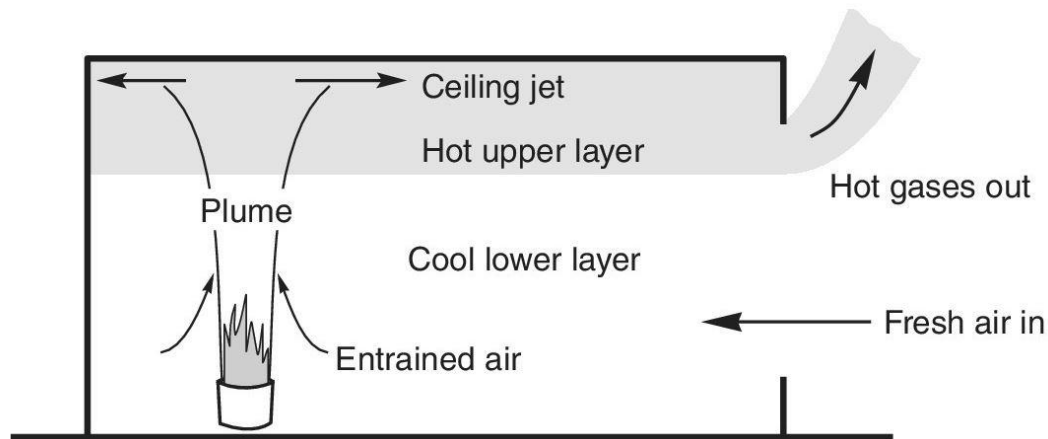


Figure 76: Visualisation of a two zone compartment model, from Buchanan (2017)

Hopkin, Anastasov and Brandon (2017) demonstrated in their study that a one zone model can be extended with a one-dimensional heat transfer model to include that the material properties of the compartment linings are temperature dependant. In addition, their zone model accounted for the contribution of CLT to the overall HRR in the compartment by means of converting the rate at which the char layer is formed to an amount of released energy (by assuming each millimetre of char formed contributes  $5.39\text{MJ/m}^2$  of energy). Their model did not account for heat induced delamination and included only a uniform charring rate throughout the compartment. In their results it was concluded that the post-flashover phase of the compartment fire (as measured during experimental studies) is satisfactorily modelled by a single zone model. The occurrence of heat induced delamination does however hinder the accuracy of the modelling exercise due to the inherent variability associated with delamination. Figure 77 demonstrates the difference between an experimentally obtained temperature-time curve (Medina Hevia, 2014 labelled “Experiment”) and one obtained from zone modelling (labelled “Simulation”). Note that the experimentally tested compartment contained two exposed CLT walls, and delamination was observed during the experiment.

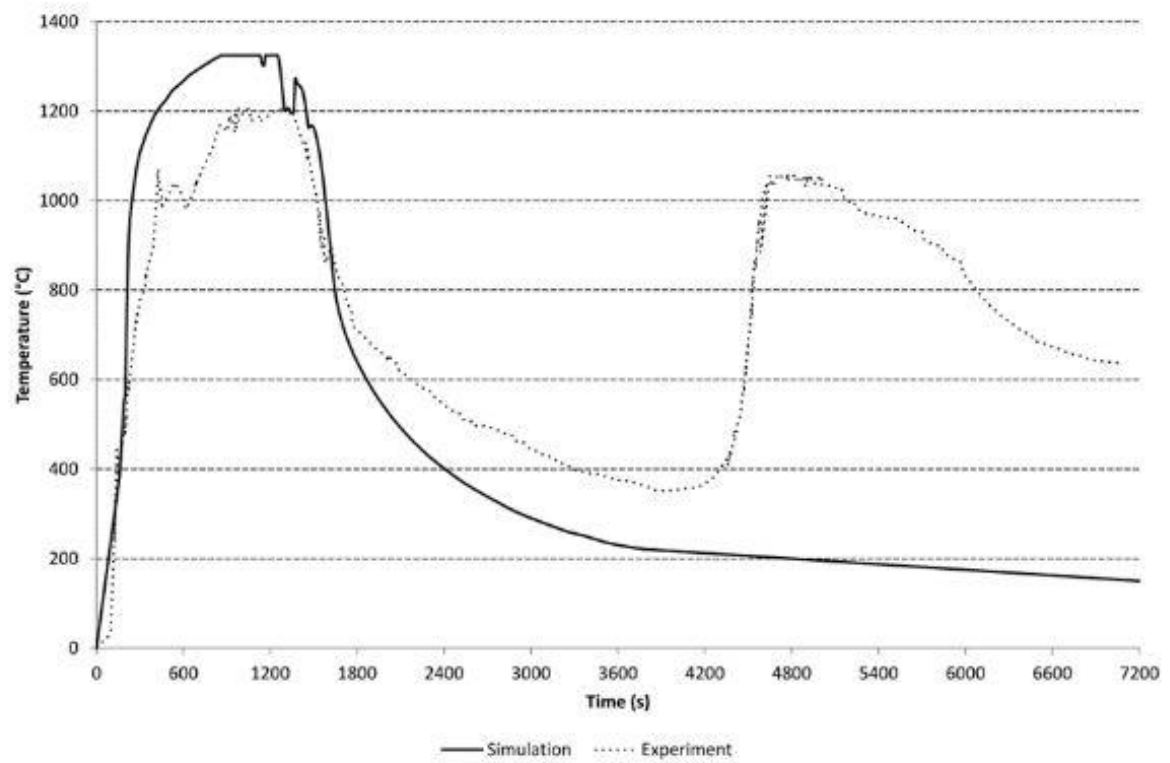


Figure 77: Zone modelling results as report by Hopkin, Anastasov and Brandon (2017)

## C.2) Worked example of determining a parametric time-temperature curve including the contribution of exposed CLT

Source:

Brandon, D. (2018b) Fire Safety Challenges of Tall Wood Buildings – Phase 2: Task 4 – Engineering Methods. Pages 32 to 35. Fire Protection Research Foundation and Research Institutes of Sweden. Borås, Sweden.

In this appendix an example of the process to determine a parametric curve according to the method described in sections 4.1 to 4.3, including the contribution of exposed CLT is presented. The example is based on FPRF Test 1-5, which is shortly described in section 2.1. It should be noted that delamination and fall-off of the base layer should be avoided in order for the method to be valid. Therefore, the application of non-delaminating adhesives in accordance with Annex B of the 2018 version of ANSI/APA PRG 320 is necessary. It should be noted that the adhesives used in Test 1-5 did not meet these requirements.

### Details:

- Compartment internal dimensions: 4.6 x 9.1 x 2.7 m (width x depth x height)
- Ventilation opening: 1 opening of 1.8 x 2.0 m (width x height).
- Fire growth rate: fast ->  $t_{lim} = 0:15\text{min}$  (see section 4.1)
- Fuel load density excluding CLT: 550MJ/m<sup>2</sup>. The fuel load comprises of typical residential furniture capable of causing a fully developed fire in a completely non-combustible compartment.
- Exposed CLT surface: 1 wall of 9.1 x 4.6 m is fully exposed.
- Gypsum board protection: all other surfaces are protected with gypsum board. Three layers of 15.9mm type X gypsum boards on the remaining wall and the ceiling.

### Calculation:

Table 8 provides the steps needed to calculate parameters corresponding to a compartment in which the CLT does not contribute. The contribution of CLT will be included using an iterative procedure. The calculations determined in Table 8 correspond to the 1<sup>st</sup> iteration.

Table 8: Steps to determine parameters for the calculations of parametric time-temperature curves.

Step	Parameter	Equation and notes	Eq.	Value
1	Opening factor	$O = \frac{A_v}{A_t} \sqrt{h_v}$	3	0.032 m <sup>1/2</sup>
2	Heating rate factor	$\Gamma = (O / \sqrt{pc\lambda})^2 / (0.04/116 \text{ s})^2$ note: $\sqrt{pc\lambda}$ is assumed to be 770W / m · K	2	1.48

Step	Parameter	Equation and notes	Eq.	Value
		during the whole fire, which is in line with Section 3.2		
3	Start time of decay (1 <sup>st</sup> iteration)	$t_{\max}^1 = \max \left[ (0.2 \cdot 10^{-3} q_{t,d} / O); t_{\lim} \right]$ <p>note that <math>q_{t,d}</math> is the fuel load divided by the total surface area of the compartment boundaries, which is not equal to the fuel load density.</p>	4	0.90 h
4	Initial charring rate	$\beta_{\text{par}} = 1.5\beta_o \frac{0.2\sqrt{\Gamma} - 0.04}{0.16\sqrt{\Gamma} + 0.08}$ <p>note: the one dimensional charring rate is chosen as <math>\beta_o = 0.65 \text{ mm/min}</math></p>	8	0.74 mm/min
5	Time at which char rate reduces	$t_o^1 = 0.009 \frac{q_{t,d}}{O}$	9	40.7 min
6	Final char depth (1 <sup>st</sup> iteration)	$d_{\text{char}}^1 = 2\beta_{\text{par}} t_o$	12	60.1 mm

Once the parameters of the 1<sup>st</sup> iteration are known the following iterations can be performed. Table 9 shows the steps needed in each following iteration in order to include the contribution of CLT. The calculation can be stopped once the resulting char depths of the iterations converge. If the fire does not converge, the fire would be continuously fully developed according to the calculations.

Table 9: Steps of every iteration to include the contribution of CLT.

Step	Parameter	Equation and notes	Eq.
1	Total fuel load divided by the surface area of comp. boundaries	$q_{td}^{i+1} = q_{mfl} + \frac{A_{CLT} \cdot \alpha_i \cdot (d_{\text{char}}^i - 0.7 \cdot \beta_{\text{par}} \cdot t_{\max}^1)}{A_c}$ <p>note: <math>t_{\max}^1</math> does not change in different iterations.</p>	14*
2	Start time of decay (1 <sup>st</sup> iteration)	$t_{\max}^{i+1} = \max \left[ (0.2 \cdot 10^{-3} q_{td}^{i+1} / O); t_{\lim} \right]$ <p>note that <math>q_{td}</math> is the fuel load divided by the total surface area of the compartment boundaries, which is not equal to the fuel load density.</p>	4*



Step	Parameter	Equation and notes	Eq.
3	Time at which char rate reduces	$t_o^{i+1} = 0.009 \frac{q_{i,d}^{i+1}}{O}$	9*
4	Final char depth (i-1 <sup>th</sup> iteration)	$d_{char}^{i+1} = 2\beta_{par} t_o^{i+1}$	12*

\*equations are adjusted to be applicable for the iterative procedure

Table 10 shows the results for 10 iterations. It can be seen that the results converged within 10 iterations. The temperatures in the fully developed phase can be calculated using:

$$\Theta = 20 + 1325(1 - 0.324e^{-0.2t\cdot\Gamma} - 0.204e^{-1.7t\cdot\Gamma} - 0.472e^{-19t\cdot\Gamma}) \quad (15)$$

The temperatures in the decay phase can be calculated using:

$$\Theta = \Theta_{max} - 625(t \cdot \Gamma - t_{max} \cdot \Gamma \cdot x) \quad \text{if} \quad t_{max} \cdot \Gamma \leq 0.5 \quad (16)$$

$$\Theta = \Theta_{max} - 250(3 - t_{max} \cdot \Gamma)(t \cdot \Gamma - t_{max} \cdot \Gamma \cdot x) \quad \text{if} \quad 0.5 < t_{max} \cdot \Gamma < 2 \quad (17)$$

$$\Theta = \Theta_{max} - 250(t \cdot \Gamma - t_{max} \cdot \Gamma \cdot x) \quad \text{if} \quad t_{max} \cdot \Gamma \geq 2 \quad (18)$$

$$x = 1.0 \text{ if } t_{max} > t_{lim} \text{ or } x = t_{lim}\Gamma/t_{max}\Gamma \text{ if } t_{max} = t_{lim}$$

Table 10: Results for 10 iterations

Iteration	$t_{max}$ (h)	$d_{char}$ (mm)
1	0.90	60.1
2	1.07	71.4
3	1.13	75.3
4	1.15	76.7
5	1.16	77.2
6	1.16	77.3
7	1.16	77.4
8	1.16	77.4
9	1.16	77.4
10	1.16	77.4

Figure 12 shows the resulting parametric design curve together with the plate thermometer temperature of Test 1-5. It should be noted that CLT of Test 1-5 is not

made in accordance with the 2018 version ANSI/APA PRG 320 and exhibited delamination of two layers of lamellae. It can be seen from the deviation after delamination that it is important to avoid delamination and fall-off, in order for the parametric design curves to be valid. Validation of the method is discussed in Section 4.4 and a method to predict parametric fires is discussed in Section 4.6.

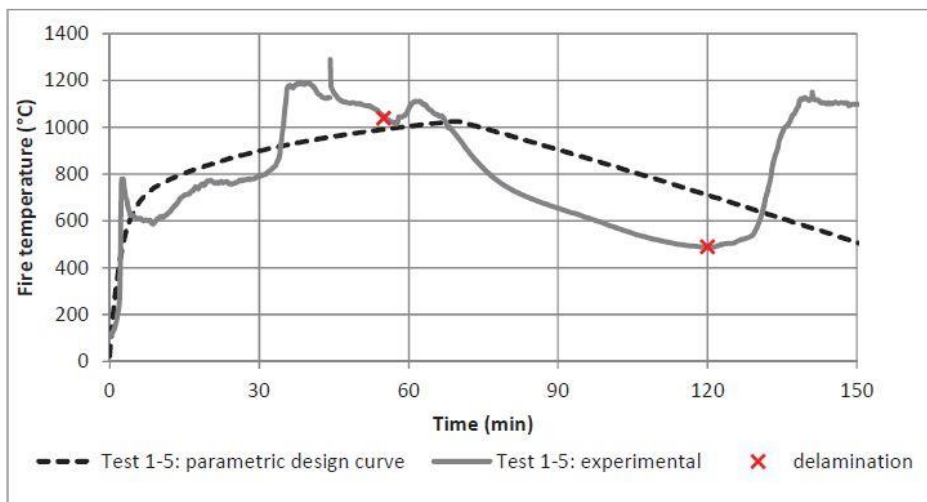


Figure 12: Parametric design curve versus plate thermometer temperature Test 1-5

## Appendix D

### CLT Emission Test

Emission test results following the prescriptions of the “Principles for the Health Assessment of Construction Products”, as published by the “German Institute for Structural Engineering” (Deutsches Institut für Bautechnik DIBt). Tests carried on Spruce Timber Glulam samples bonded with the Grip Pro Plus A011 adhesive.

Poppensieker & Derix GmbH & Co. KG  
Industriestraße 24  
49492 Westerkappeln

## Prüfbericht Nr. 51005-001

<b>Prüfziel:</b>	<b>Emissionsanalyse gemäß AgBB-Schema 2015</b>
<b>Probenbezeichnung laut Auftraggeber:</b>	<b>Brettschichtholz verklebt</b>
<b>Probenehmer:</b>	Dirk Leder, Fa. Casco
<b>Probenahmedatum:</b>	04.02.2016
<b>Probenahmeort:</b>	beim Auftraggeber
<b>Produktionsdatum:</b>	04.02.2016
<b>Probeneingang:</b>	15.02.2016
<b>Datum der Berichterstellung:</b>	13.04.2016
<b>Seitenanzahl des Prüfberichts:</b>	17
<b>Prüfendes Labor:</b>	eco-INSTITUT Germany GmbH, Köln
<b>Prüfziel erreicht:</b>	✓

## Inhalt

Übersicht der Proben.....	2
Gutachterliche Bewertung .....	3
Zusammenfassende Bewertung .....	3
Laborbericht.....	4
1 Emissionsanalysen.....	4
1.1 Flüchtige organische Verbindungen nach 3 Tagen .....	5
1.2 Flüchtige organische Verbindungen nach 28 Tagen .....	9
Anhang .....	12
I Probenahmebegleitblatt .....	12
II Begriffsdefinitionen.....	13
III Liste der analysierten flüchtigen organischen Verbindungen (VOC).....	15
IV Erläuterung zur Emissionsanalyse.....	16
V Erläuterung zur Spezifischen Emissionsrate SER.....	17

## Übersicht der Proben

eco-Proben-nummer	Probenbezeichnung	Zustand der Probe bei Anlieferung	Probenart
A001	Brettschichtholz verlebt	ohne Beanstandung	Fichte Lamellen



A001: Brettschichtholz verlebt

**Hinweis:** Die Untersuchungsergebnisse beziehen sich ausschließlich auf den vorgelegten Prüfgegenstand. Der Bericht verliert umgehend seine Gültigkeit bei Änderungen der Zusammensetzung oder des Produktionsverfahrens des Prüfgegenstandes. Eine vollständige oder auszugsweise Veröffentlichung des Prüfberichtes bedarf der Genehmigung.

## Gutachterliche Bewertung

Das Produkt **Brettschichtholz verlebt** wurde im Auftrag von **Akzo Nobel Hilden GmbH** einer Produktprüfung unterzogen.

Bewertungsgrundlage ist das „Vorgehensweise bei der gesundheitlichen Bewertung der Emissionen von flüchtigen organischen Verbindungen (VVO, VOC und SVOC) aus Bauprodukten“ des Ausschusses zur gesundheitlichen Bewertung von Bauprodukten (AgBB 2015).

Die im Prüfbericht dokumentierten Ergebnisse werden wie folgt bewertet.

Prüfparameter	Ergebnis	Anforderung	Anforderung erfüllt [ja/nein]
<b>Emissionsanalysen</b>			
<b>Messzeitpunkt: 3 Tage nach Prüfkammerbeladung</b>			
Summe VOC (C <sub>6</sub> -C <sub>16</sub> ) und SVOC mit NIK <sup>1)</sup>	0,089 mg/m³	≤ 10 mg/m³	ja
Summe Kanzerogene (EU-Kat. 1A und 1B)	< 0,001 mg/m³	≤ 0,01 mg/m³	ja
<b>Messzeitpunkt: 28 Tage nach Prüfkammerbeladung</b>			
Summe VOC (C <sub>6</sub> -C <sub>16</sub> ) und SVOC mit NIK <sup>1)</sup>	0,07 mg/m³	≤ 1 mg/m³	ja
Summe SVOC ohne NIK (C <sub>16</sub> -C <sub>22</sub> ) <sup>1)</sup>	< 0,005 mg/m³	≤ 0,1 mg/m³	ja
R-Wert (dimensionslos)	0,17	≤ 1	ja
Summe VOC ohne NIK	< 0,005 mg/m³	≤ 0,1 mg/m³	ja
Summe Kanzerogene (EU-Kat. 1A und 1B)	< 0,001 mg/m³	≤ 0,001 mg/m³	ja

1) bei der Summe VOC (C<sub>6</sub>-C<sub>16</sub>) und bei der Summe SVOC (C<sub>16</sub>-C<sub>22</sub>) werden nur Substanzen ≥ 5 µg/m³ berücksichtigt

## Zusammenfassende Bewertung

Das Produkt **Brettschichtholz verlebt** erfüllt die Anforderungen des AgBB-Schemas.

Köln, den 13.04.2016



Daniel Tigges, Dipl.-Holzwirt  
(Projektleiter)

**Hinweis:** Die Untersuchungsergebnisse beziehen sich ausschließlich auf den vorgelegten Prüfgegenstand. Der Bericht verliert umgehend seine Gültigkeit bei Änderungen der Zusammensetzung oder des Produktionsverfahrens des Prüfgegenstandes. Eine vollständige oder auszugsweise Veröffentlichung des Prüfberichtes bedarf der Genehmigung.



## Laborbericht

### 1 Emissionsanalysen

#### Prüfmethode

prEN 18516	Prüfung und Bewertung der Freisetzung von gefährlichen Stoffen; Bestimmung von Emissionen in die Innenraumluft
------------	--

#### Prüfstückherstellung

Datum:	04.03.2016
Vorbehandlung:	Stirnseiten abgedichtet
Abklebung der Kanten:	nein
Verhältnis offener Kanten zur Oberfläche:	entfällt
Beladung:	bezogen auf die Fläche
Abmessungen:	70 cm x 20 cm x 9 cm

#### Prüfkammerbedingungen nach DIN ISO 16000-9

Kammervolumen:	1,000 m <sup>3</sup>
Temperatur:	23 °C
Relative Luftfeuchte:	50 %
Luftdruck:	normal
Luft:	gereinigt
Luftwechselrate:	0,5 h <sup>-1</sup>
Anströmgeschwindigkeit:	0,3 m/s
Beladung:	0,4 m <sup>2</sup> /m <sup>3</sup>
Spez. Luftdurchflussrate:	1,25 m <sup>3</sup> /m <sup>2</sup> · h
Luftprobenahme:	3 und 28 Tage nach Prüfkammerbeladung

#### Analytik

Aldehyde und Ketone	DIN ISO 16000-3
Bestimmungsgrenze:	2 µg/m <sup>3</sup>
Flüchtige organische Verbindungen	DIN ISO 16000-6
Bestimmungsgrenze:	1 µg/m <sup>3</sup>

Hinweis: Die Untersuchungsergebnisse beziehen sich ausschließlich auf den vorgelegten Prüfgegenstand. Der Bericht verliert umgehend seine Gültigkeit bei Änderungen der Zusammensetzung oder des Produktionsverfahrens des Prüfgegenstandes. Eine vollständige oder auszugsweise Veröffentlichung des Prüfberichtes bedarf der Genehmigung.

## 1.1 Flüchtige organische Verbindungen nach 3 Tagen

### Prüfziel:

Flüchtige organische Verbindungen (VOC), Prüfkammer, Luftprobenahme 3 Tage nach Prüfkammerbeladung

### Prüfergebnis:

Probe: A001: Brettschichtholz verklebt

Nr.	Substanz	CAS Nr.	RT [min]	Konzentration+ (Prüfkammer- luft) Substanzen $\geq 1 \mu\text{g}/\text{m}^3$ nach 3 Tagen [ $\mu\text{g}/\text{m}^3$ ]	Toluol- äquivalent Substanzen $\geq 5 \mu\text{g}/\text{m}^3$ nach 3 Tagen [ $\mu\text{g}/\text{m}^3$ ]	KMR Einstu- fung++ ++	NIK AgBB 2015 [ $\mu\text{g}/\text{m}^3$ ]	R- Wert
3	Terpene							
3-1	3-Caren	498-15-7	13,67	4			1500	0,00
3-2	$\alpha$ -Pinen	80-56-8	12,00	17	20		2500	0,01
3-3	$\beta$ -Pinen	127-91-3	13,09	5	6		1400	0,00
3-4	Limonen	138-86-3	14,08	7	8		5000	0,00
3-5.6	Camphen	5794-03-6	12,46	1			1400	0,00
4	Aliphatische mono Al- kohole (n-, iso- und cyclo-) und Dialko- hole							
4-3	2-Propanol	67-63-0	4,01	5				
4-7	Pentanol (alle Isomere)	71-41-0	7,86	1			730	0,00
6	Glykole, Glykolether, Glykolester							
6-3	Ethylenglykol-mo- nobutylether (2- Butoxyethanol)	111-76-2	10,97	1			1100	0,00
6-5	Diethylenglykol-mo- nobutylether	112-34-5	17,12	1			670	0,00
7	Aldehyde							
7-2	Pentanal	110-62-3	6,55	2			800	0,00
7-3	Hexanal	66-25-1	8,63	7	7		900	0,01
7-17	Furfural	98-01-1	9,42	1		K2	20	0,05
7-20	Acetaldehyd	75-07-0		20		K2	1200	0,02
7-22	Formaldehyd	50-00-0		18		K1BM2	100	0,18

Hinweis: Die Untersuchungsergebnisse beziehen sich ausschließlich auf den vorgelegten Prüfgegenstand. Der Bericht verliert umgehend seine Gültigkeit bei Änderungen der Zusammensetzung oder des Produktionsverfahrens des Prüfgegenstandes. Eine vollständige oder auszugsweise Veröffentlichung des Prüfberichtes bedarf der Genehmigung.



Nr.	Substanz	CAS Nr.	RT [min]	Konzentration+ (Prüfkammer- luft) Substanzen $\geq 1 \mu\text{g}/\text{m}^3$ nach 3 Tagen [ $\mu\text{g}/\text{m}^3$ ]	Toluol- äquivalent Substanzen $\geq 5 \mu\text{g}/\text{m}^3$ nach 3 Tagen [ $\mu\text{g}/\text{m}^3$ ]	KMR Einstu- fung++	NIK AgBB 2015 [ $\mu\text{g}/\text{m}^3$ ]	R- Wert
8	Ketone							
8-10	Aceton	67-64-1		19			1200	0,02
9	Säuren							
9-1	Essigsäure	64-19-7	4,71	53	20		1250	0,04
9-9	n-Octansäure	124-07-2	12,13	2			600	0,00
10	Ester und Lactone							
10-2	Ethylacetat	79-20-9	4,25	1				
13	Weitere Substanzen in Ergänzung zur NIK- Liste							
	Dichlormethan	75-09-2	8,65	4		K2		
	alkyliertes Phenolderi- vat*		23,92	1				

+ identifizierte und kalibrierte Substanzen, substanz-spezifisch berechnet

++ Einstufung gem. Verordnung (EG) Nr. 1272/2008: Kategorien Carc. 1A und 1B, Muta. 1A und 1B, Repr. 1A und 1B, TRGS 905: K1 und K2, M1 und M2, R1 und R2, IARC: Group 1 und 2A, DFG MAK-Liste: Kategorie III1 und III2

\* nicht identifizierte Substanzen, berechnet als Toluoläquivalent

Krebserzeugende, Mutagene und erbgutverändernde Verbindungen	Konzentration nach 3 Tagen [ $\mu\text{g}/\text{m}^3$ ]	SE <sub>R</sub> [ $\mu\text{g}/\text{m}^3\text{h}$ ]
KMR 1: VOC (inkl. VVOC und TVOC) mit folgenden Einstufungen: Verordnung (EG) Nr. 1272/2008: Kategorien Carc. 1A u. 1B, Muta. 1A u. 1B, Repr. 1A u. 1B; TRGS 905: K1, K2, M1, M2, R1, R2; IARC: Group 1 u. 2A; DFG (MAK-Liste): Kategorie III1, III2 (Summe)	< 1	< 1,25
K 1: VOC (inkl. VVOC und TVOC) mit folgenden Einstufungen: Verordnung (EG) Nr. 1272/2008: Kategorien Carc. 1A u. 1B, TRGS 905: K1, K2; IARC: Group 1 u. 2A; DFG (MAK-Liste): Kategorie III1, III2 (Summe)	< 1	< 1,25

Hinweis: Die Untersuchungsergebnisse beziehen sich ausschließlich auf den vorgelegten Prüfgegenstand. Der Bericht verliert umgehend seine Gültigkeit bei Änderungen der Zusammensetzung oder des Produktionsverfahrens des Prüfgegenstandes. Eine vollständige oder auszugsweise Veröffentlichung des Prüfberichtes bedarf der Genehmigung.

TVOC, Summe flüchtige organische Verbindungen	Konzentration nach 3 Tagen [µg/m³]	SE <sub>h</sub> [µg/m³h]
Summe VOC gemäß prEN 16516	61	76
Summe VOC gemäß AgBB 2015 / DIBt	89	110
Summe VOC gemäß eco-INSTITUT-Label	110	130
Summe VOC gemäß ISO 16000-6	100	130

TSVOC, Summe schwerflüchtiger organischer Verbindungen	Konzentration nach 3 Tagen [µg/m³]	SE <sub>h</sub> [µg/m³h]
Summe SVOC gemäß prEN 16516	< 5	< 6,25
Summe SVOC ohne NIK gemäß AgBB 2015 / DIBt	< 5	< 6,25
Summe SVOC ohne NIK gemäß eco-INSTITUT-Label	< 1	< 1,25
Summe SVOC mit NIK gemäß AgBB 2015 / DIBt	< 5	< 6,25

TVVOC, Summe leichtflüchtiger organischer Verbindungen	Konzentration nach 3 Tagen [µg/m³]	SE <sub>h</sub> [µg/m³h]
Summe VVOC gemäß AgBB 2015 / DIBt und belgischer VO	62	78
Summe VVOC gemäß eco-INSTITUT-Label	63	79

Hinweis: Die Untersuchungsergebnisse beziehen sich ausschließlich auf den vorgelegten Prüfgegenstand. Der Bericht verliert umgehend seine Gültigkeit bei Änderungen der Zusammensetzung oder des Produktionsverfahrens des Prüfgegenstandes. Eine vollständige oder auszugsweise Veröffentlichung des Prüfberichtes bedarf der Genehmigung.

Weitere VOC-Summen	Konzentration 3 Tagen [µg/m³]	SE <sub>R</sub> [µg/m³h]
VOC ohne NIK gemäß AgBB 2015 / DIBt und belgischer VO (Summe)	< 5	< 6,25
VOC ohne NIK gemäß eco-INSTITUT-Label (Summe)	5	6,3
KMR 2: VOC (inkl. VVOC und TVOC) mit folgenden Einstufungen: Verordnung (EG) Nr. 1272/2008: Kategorien Carc. 2, Muta. 2, Repr. 2; TRGS 905: K3, M3, R3; IARC: Group 2B; DFG (MAK-Liste): Kategorie III3 (Summe)	25	31
Sensibilisierende Stoffe mit folgenden Einstufungen: DFG (MAK-Liste): Kategorie IV, BgVV-Liste: Kat A, TRGS 907 (Summe)	33	41
Summe Bicyclische Terpene (Summe)	27	34
C9 - C14: Alkane / Isoalkane als Dekan-Äquivalent (Summe)	< 1	< 1,25
C4-C11 Aldehyde, acyclisch, aliphatisch (Summe)	9	11
C9-C15 Alkylbenzole (Summe)	< 1	< 1,25
Kresole (Summe)	< 1	< 1,25

Rechenwert zur Bewertung der NIK-Stoffe	R-Wert
R-Wert gemäß eco-INSTITUT-Label	0,34
R-Wert gemäß AgBB 2015 / DIBt	0,27
R-Wert gemäß Belgischer VO	0,08
R-Wert gemäß AFSSET	2,18

Anmerkung: Aufgrund unterschiedlicher Vorgaben in den jeweiligen Richtlinien kommt es zu divergierenden Werten bei der Berechnung des TVOC, TVVOC, TSVOC und R-Wertes.

Hinweis: Die Untersuchungsergebnisse beziehen sich ausschließlich auf den vorgelegten Prüfgegenstand. Der Bericht verliert umgehend seine Gültigkeit bei Änderungen der Zusammensetzung oder des Produktionsverfahrens des Prüfgegenstandes. Eine vollständige oder auszugsweise Veröffentlichung des Prüfberichtes bedarf der Genehmigung.

## 1.2 Flüchtige organische Verbindungen nach 28 Tagen

### Prüfziel:

Flüchtige organische Verbindungen (VOC), Prüfkammer, Luftprobenahme 28 Tage nach Prüfkammerbeladung

### Prüfergebnis:

Probe: A001: Brettschichtholz verklebt

Nr.	Substanz	CAS Nr.	RT	Konzentration+ (Prüfkammer- luft)	Toluol- äquivalent	KMR	NIK	R- Wert
			[min]	Substanzen $\geq 1 \mu\text{g}/\text{m}^3$ nach 28 Tagen [ $\mu\text{g}/\text{m}^3$ ]	Substanzen $\geq 5 \mu\text{g}/\text{m}^3$ nach 28 Tagen [ $\mu\text{g}/\text{m}^3$ ]	Einstu- fung++ ++	AgBB 2015 [ $\mu\text{g}/\text{m}^3$ ]	
3	Terpene							
3-1	3-Caren	498-15-7	13,41	2			1500	0,00
3-2	$\alpha$ -Pinen	80-56-8	11,76	13	12		2500	0,01
3-3	$\beta$ -Pinen	127-91-3	12,83	4			1400	0,00
3-4	Limonen	138-86-3	13,82	5	5		5000	0,00
7	Aldehyde							
7-3	Hexanal	66-25-1	8,49	4			900	0,00
7-20	Acetaldehyd	75-07-0		9		K2	1200	0,01
7-22	Formaldehyd	50-00-0		11		K1BM2	100	0,11
8	Ketone							
8-10	Aceton	67-64-1		9			1200	0,01
9	Säuren							
9-1	Essigsäure	64-19-7	4,73	52	15		1250	0,04
9-7	n-Caprinsäure	142-62-1	11,92	1			490	0,00

+ identifizierte und kalibrierte Substanzen, substanz-spezifisch berechnet

++ Einstufung gem. Verordnung (EG) Nr. 1272/2008: Kategorien Carc. 1A und 1B, Muta. 1A und 1B, Repr. 1A und 1B, TRGS 905: K1 und K2, M1 und M2, R1 und R2, IARC: Group 1 und 2A, DFG MAK-Liste: Kategorie III1 und III2

\* nicht identifizierte Substanzen, berechnet als Toluoläquivalent

Hinweis: Die Untersuchungsergebnisse beziehen sich ausschließlich auf den vorgelegten Prüfgegenstand. Der Bericht verliert umgehend seine Gültigkeit bei Änderungen der Zusammensetzung oder des Produktionsverfahrens des Prüfgegenstandes. Eine vollständige oder auszugsweise Veröffentlichung des Prüfberichtes bedarf der Genehmigung.



Krebserzeugende, Mutagene und erbgutverändernde Verbindungen	Konzentration nach 28 Tagen [µg/m³]	SER <sub>1</sub> [µg/m³h]
KMR 1: VOC (inkl. VVOC und TVOC) mit folgenden Einstufungen: Verordnung (EG) Nr. 1272/2008: Kategorien Carc. 1A u. 1B, Muta. 1A u. 1B, Repr. 1A u. 1B; TRGS 905: K1, K2, M1, M2, R1, R2; IARC: Group 1 u. 2A; DFG (MAK-Liste): Kategorie III1, III2 (Summe)	< 1	< 1,25
K 1: VOC (inkl. VVOC und TVOC) mit folgenden Einstufungen: Verordnung (EG) Nr. 1272/2008: Kategorien Carc. 1A u. 1B, TRGS 905: K1, K2; IARC: Group 1 u. 2A; DFG (MAK-Liste): Kategorie III1, III2 (Summe)	< 1	< 1,25

TVOC, Summe flüchtige organische Verbindungen	Konzentration nach 28 Tagen [µg/m³]	SER <sub>1</sub> [µg/m³h]
Summe VOC gemäß prEN 16516	32	40
Summe VOC gemäß AgBB 2015 / DIBt	70	88
Summe VOC gemäß eco-INSTITUT-Label	81	100
Summe VOC gemäß ISO 16000-6	70	88

TSVOC, Summe schwerflüchtiger organischer Verbindungen	Konzentration nach 28 Tagen [µg/m³]	SER <sub>1</sub> [µg/m³h]
Summe SVOC gemäß prEN 16516	< 5	< 6,25
Summe SVOC ohne NIK gemäß AgBB 2015 / DIBt	< 5	< 6,25
Summe SVOC ohne NIK gemäß eco-INSTITUT-Label	< 1	< 1,25
Summe SVOC mit NIK gemäß AgBB 2015 / DIBt	< 5	< 6,25

TVVOC, Summe leichtflüchtiger organischer Verbindungen	Konzentration nach 28 Tagen [µg/m³]	SER <sub>1</sub> [µg/m³h]
Summe VVOC gemäß AgBB 2015 / DIBt und belgischer VO	29	36
Summe VVOC gemäß eco-INSTITUT-Label	29	36

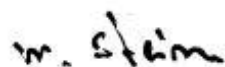
Hinweis: Die Untersuchungsergebnisse beziehen sich ausschließlich auf den vorgelegten Prüfgegenstand. Der Bericht verliert umgehend seine Gültigkeit bei Änderungen der Zusammensetzung oder des Produktionsverfahrens des Prüfgegenstandes. Eine vollständige oder auszugsweise Veröffentlichung des Prüfberichtes bedarf der Genehmigung.

Weitere VOC-Summen	Konzentration nach 28 Tagen [µg/m³]	SE <sub>R</sub> [µg/m³h]
VOC ohne NIK gemäß AgBB 2015 / DIBt und belgischer VO (Summe)	< 5	< 6,25
VOC ohne NIK gemäß eco-INSTITUT-Label (Summe)	< 1	< 1,25
KMR 2: VOC (inkl. VVOC und TVOC) mit folgenden Einstufungen: Verordnung (EG) Nr. 1272/2008: Kategorien Carc. 2, Muta. 2, Repr. 2; TRGS 905: K3, M3, R3; IARC: Group 2B; DFG (MAK-Liste): Kategorie III/3 (Summe)	9	11
Sensibilisierende Stoffe mit folgenden Einstufungen: DFG (MAK-Liste): Kategorie IV, BgVV-Liste: Kat A, TRGS 907 (Summe)	24	30
Summe Bicyclische Terpene (Summe)	19	24
C9 - C14: Alkane / Isoalkane als Dekan-Äquivalent (Summe)	< 1	< 1,25
C4-C11 Aldehyde, acyclisch, aliphatisch (Summe)	4	5
C9-C15 Alkylbenzole (Summe)	< 1	< 1,25
Kresole (Summe)	< 1	< 1,25

Rechenwert zur Bewertung der NIK-Stoffe	R-Wert
R-Wert gemäß eco-INSTITUT-Label	0,18
R-Wert gemäß AgBB 2015 / DIBt	0,17
R-Wert gemäß Belgischer VO	0,06
R-Wert gemäß AFSSET	1,39

Anmerkung: Aufgrund unterschiedlicher Vorgaben in den jeweiligen Richtlinien kommt es zu divergierenden Werten bei der Berechnung des TVOC, TVVOC, TSVOC und R-Wertes.

Köln, 13.04.2016



Michael Stein, Dipl.-Chem.  
(Stellvertretender technischer Leiter)

Hinweis: Die Untersuchungsergebnisse beziehen sich ausschließlich auf den vorgelegten Prüfgegenstand. Der Bericht verliert umgehend seine Gültigkeit bei Änderungen der Zusammensetzung oder des Produktionsverfahrens des Prüfgegenstandes. Eine vollständige oder auszugsweise Veröffentlichung des Prüfberichtes bedarf der Genehmigung.

## Anhang

### I Probenahmebegleitblatt

Produktprüfung Product testing  
Zertifizierung Certification  
Beratung consulting

EINGANG 15. FEB. 2016

**eco**  
INSTITUT

#### Probenahmebegleitblatt\*

<b>Prüflabor</b> eco-INSTITUT Germany GmbH Schanzenstr. 6-20, D-51063 Köln Tel. +49 (0)221 - 931245-0 Fax +49 (0)221 - 931245-33  <b>Name des Herstellers / Händlers am Probenahmeort</b> (Adresse / Stempel) <b>HOLZLEIMBAU POPPENSIEHER DERIX</b> <small>GmbH &amp; Co. Kommanditgesellschaft Industriestraße 24 - 49482 Wusterhausen *5419103-0 - Fax 05456/9265-33</small>	<b>Probenahmer</b> (Name, Firma, Telefon) H. Dirk Leder Fa. Carco  <b>ProduktHersteller</b> (falls abweichend vom Firmennamen am Probenahmeort)
<b>Produktname</b> Brettschichtholz  <b>Modell / Programm / Serie</b>  <b>Artikel-Nr.</b>	<b>Probeart</b> (z.B. Holzwerkstoff, Bodenbelag) Fichte  <b>Chargen-Nr.</b>  <b>Produktionsdatum der Charge</b> 04.02.2016
<b>Probe wird gezogen ...</b> aus der laufenden Produktion aus Lagerbeständen  <b>Wo wurde das Produkt vor Probenahme gelagert?</b> Fertigung Lager Sondergelagert Lagerort: beheizte Halle 6°C ± 20°C	<b>Datum der Probenahme</b> 04.02.2016 <b>Uhrzeit</b>  <b>Wie wurde das Produkt vor Probenahme gelagert?</b> offen verpackt Verpackungsmaterial: Alufolie + Kunststofffolie
<b>Besonderheiten</b> (mögliche negative Einflüsse durch Emissionen am Probenahmeort, Benzin-Abgase, Lösemittel-Emissionen aus der Fertigung, Unklimateilen, Fragen, etc.)	
<b>Bestätigung</b> Hiermit bestätigt der Unterzeichner die Richtigkeit der oben gemachten Angaben. Die Probe wurde eigenhändig gemäß Probenahmeanleitung ausgewertet. <b>Datum:</b> 11.02.2016 <b>Unterschrift:</b> (Stempel) <b>HOLZLEIMBAU POPPENSIEHER DERIX</b> <small>GmbH &amp; Co. Kommanditgesellschaft Industriestraße 24 - 49482 Wusterhausen *5419103-0 - Fax 05456/9265-33</small>	

\* Bitte pro Probe ein Probenahmebegleitblatt ausfüllen! Die Probenahmeanleitung ist unbedingt einzuhalten!

eco-INSTITUT Germany GmbH / Schanzenstr. 6-20 / Carlswerk Lagerzug 5,2 / D-51063 Köln / Germany  
Tel. +49 221 931245-0 / Fax +49 221 931245-33 / eco-institut.de / Geschäftsführer: Dr. Frank Kuebert  
HRB 17717 / USt-ID: DE 122453388 / Kaffeesieberei Friedrich Huth, 1849, DE69370623651701900010, BIC: GENODE33HAN

DAKKS  
Deutsche  
Akkreditierungsstelle  
D-49124 Lingen, DE

**Hinweis:** Die Untersuchungsergebnisse beziehen sich ausschließlich auf den vorgelegten Prüfgegenstand. Der Bericht verliert umgehend seine Gültigkeit bei Änderungen der Zusammensetzung oder des Produktionsverfahrens des Prüfgegenstandes. Eine vollständige oder auszugsweise Veröffentlichung des Prüfberichtes bedarf der Genehmigung.



## II Begriffsdefinitionen

VOC (flüchtige organische Verbindungen)	Alle Einzelstoffe mit Konzentrationen $\geq 1 \mu\text{g}/\text{m}^3$ im Retentionsbereich $\text{C}_5$ (n-Hexan) bis $\text{C}_{16}$ (n-Hexadecan)
TVOC	Summe flüchtige organische Verbindungen
TVOC gemäß prEN 16516	Summe aller VOC $\geq 5 \mu\text{g}/\text{m}^3$ im Retentionsbereich $\text{C}_5$ bis $\text{C}_{16}$ als Toluoläquivalent
TVOC gemäß AgBB/DIBt	Summe aller substanzspezifisch kalibrierten VOC und SVOC $\geq 5 \mu\text{g}/\text{m}^3$ mit NIK und nicht kalibrierten VOC $\geq 5 \mu\text{g}/\text{m}^3$ als Toluoläquivalent
TVOC gemäß eco-INSTITUT-Label	Summe aller substanzspezifisch kalibrierten VOC $\geq 1 \mu\text{g}/\text{m}^3$ , SVOC $\geq 1 \mu\text{g}/\text{m}^3$ mit NIK und nicht kalibrierten VOC $\geq 1 \mu\text{g}/\text{m}^3$ als Toluoläquivalent
TVOC gemäß ISO 16000-6	Gesamtfläche des Chromatogramms im Retentionsbereich $\text{C}_5$ - $\text{C}_{16}$ als Toluoläquivalent
TVOC ohne NIK gemäß AgBB/DIBt und belgischer Verordnung	Summe aller Stoffe $\geq 5 \mu\text{g}/\text{m}^3$ ohne NIK im Retentionsbereich $\text{C}_5$ bis $\text{C}_{16}$
TVOC ohne NIK gemäß eco-INSTITUT-Label	Summe aller Stoffe $\geq 1 \mu\text{g}/\text{m}^3$ ohne NIK im Retentionsbereich $\text{C}_5$ bis $\text{C}_{16}$
KMR (kanzerogene, mutagene, reproduktionstoxische VOC, VVOC und SVOC)	Alle Einzelstoffe mit folgenden Einstufungen: Verordnung (EG) Nr. 1272/2008: Kategorien Carc. 1A und 1B, Muta. 1A und 1B, Repr. 1A und 1B TRGS 905: K1 und K2, M1 und M2, R1 und R2 IARC: Group 1 und 2A DFG MAK-Liste: Kategorie III1 und III2
VVOC (leichtflüchtige organische Verbindungen)	Alle Einzelstoffe mit Konzentrationen $\geq 1 \mu\text{g}/\text{m}^3$ im Retentionsbereich $< \text{C}_5$
TVVOC	Summe leichtflüchtiger organischen Verbindungen
TVVOC gemäß AgBB/DIBt und belgischer Verordnung	Summe aller substanzspezifisch kalibrierten VVOC $\geq 5 \mu\text{g}/\text{m}^3$ mit NIK
TVVOC gemäß eco-INSTITUT-Label	Summe aller substanzspezifisch kalibrierten VVOC $\geq 1 \mu\text{g}/\text{m}^3$ mit NIK
SVOC (schwerflüchtige organische Verbindungen)	Alle Einzelstoffe $\geq 1 \mu\text{g}/\text{m}^3$ im Retentionsbereich $> \text{C}_{16}$ (n-Hexadecan) bis $\text{C}_{22}$ (Docosan)
TSVOC	Summe schwerflüchtige organische Verbindungen
TSVOC gemäß prEN 16516	Summe aller SVOC im Retentionsbereich $\text{C}_{16}$ bis $\text{C}_{22}$ als Toluoläquivalent
TSVOC ohne NIK gemäß AgBB/DIBt	Summe aller SVOC $\geq 5 \mu\text{g}/\text{m}^3$ ohne NIK
TSVOC ohne NIK gemäß eco-INSTITUT-Label	Summe aller SVOC $\geq 1 \mu\text{g}/\text{m}^3$ ohne NIK
TSVOC mit NIK gemäß AgBB/DIBt	Summe aller substanzspezifisch kalibrierten SVOC $\geq 5 \mu\text{g}/\text{m}^3$ mit NIK
SER	Spezifische Emissionsrate (siehe Anhang IV)
NIK	Niedrigste interessierende Konzentration; Rechenwert zur Bewertung von VOC, aufgestellt vom Ausschuss zur gesundheitlichen Bewertung von Bauprodukten (AgBB)

Hinweis: Die Untersuchungsergebnisse beziehen sich ausschließlich auf den vorgelegten Prüfgegenstand. Der Bericht verliert umgehend seine Gültigkeit bei Änderungen der Zusammensetzung oder des Produktionsverfahrens des Prüfgegenstandes. Eine vollständige oder auszugsweise Veröffentlichung des Prüfberichtes bedarf der Genehmigung.



R-Wert	Für jeden in der Prüfkammerluft nachgewiesenen Stoff wird der Quotient aus Konzentration und NIK-Wert gebildet. Die Summe der so erhaltenen Quotienten ergibt den R-Wert.
R-Wert gemäß eco-INSTITUT-Label	R-Wert für alle identifizierten Stoffe $\geq 1 \mu\text{g}/\text{m}^3$ mit NIK-Wert, berechnet nach der NIK-Liste des AgBB-Schemas 2015
R-Wert gemäß AgBB 2015/DIBt	R-Wert für alle identifizierten Stoffe $\geq 5 \mu\text{g}/\text{m}^3$ mit NIK-Wert, berechnet nach der NIK-Liste des AgBB-Schemas 2015
R-Wert gemäß belgischer Verordnung	R-Wert für alle identifizierten Stoffe $\geq 5 \mu\text{g}/\text{m}^3$ mit NIK-Wert, berechnet nach der NIK-Liste der Belgischen Verordnung
R-Wert gemäß AFSSET	R-Wert für alle identifizierten Stoffe $\geq 5 \mu\text{g}/\text{m}^3$ mit NIK-Wert, berechnet nach der NIK-Liste des ANSES (AFSSET) –Schemas (französische Behörde zuständig für Lebensmittelsicherheit, Umweltschutz und Arbeitsschutz)
RT (Retentionszeit)	Gesamtzeit, die ein Analyt für das Passieren der Säule benötigt (Zeit zwischen Injektion und Detektion des Analyten)
CAS Nr. (Chemical Abstracts Service)	Internationaler Bezeichnungsstandard für chemische Stoffe Für jeden registrierten chemischen Stoff existiert eine eindeutige Nummer.
Toluoläquivalent	Konzentration des in der Prüfkammerluft nachgewiesenen Stoffes, für den die Quantifizierung in Bezug auf Toluol erfolgte.

Hinweis: Die Untersuchungsergebnisse beziehen sich ausschließlich auf den vorgelegten Prüfgegenstand. Der Bericht verliert umgehend seine Gültigkeit bei Änderungen der Zusammensetzung oder des Produktionsverfahrens des Prüfgegenstandes. Eine vollständige oder auszugsweise Veröffentlichung des Prüfberichtes bedarf der Genehmigung.

### III Liste der analysierten flüchtigen organischen Verbindungen (VOC)

<b>Aromatische Kohlenwasserstoffe</b>	1-Nonanol	2-Hexenal	Chlorierte Kohlenwasserstoffe
Toluol	1-Decanol	2-Heptenal	Tetrachlorethen
Ethylbenzol	1,4-Cyclohexandimethanol	2-Undecenal	1,1,1-Trichlorethan
p-Xylol		Furfural	Trichlorethen
m-Xylol	<b>Aromatische Alkohole (Phenole)</b>	Glutaraldehyd	1,4-Dichlorbenzol
o-Xylol	Phenol	Benzaldehyd	
Isopropylbenzol	BHT (2,6-di-tert-butyl-4-methylphenol)	Acetaldehyd <sup>1,2</sup>	<b>Andere</b>
n-Propylbenzol	Benzylalkohol	Propenal <sup>1,2</sup>	1,4-Dioxan
1,3,5-Trimethylbenzol	Kresole	Propenal <sup>1,2</sup>	Caprolactam
1,2,4-Trimethylbenzol		Isobutanol <sup>1</sup>	N-Methyl-2-pyrrolidon
1,2,3-Trimethylbenzol		2-Octenal	Octamethylcyclotetrasiloxan
2-Ethyltoluol	<b>Glykole, Glykolether, Glykolester</b>	2-Nonenal	Hexamethylcyclotrisiloxan
1-Isopropyl-4-methylbenzol	Propylenglykol (1,2-Dihydroxypropan)	2-Decenal	Methenamin
1,2,4,5-Tetramethylbenzol	Ethylenglykol (Ethandiol)		2-Butanonoxim
n-Butylbenzol	Ethylenglykolmonobutylether	<b>Ketone</b>	Triethylphosphat
1,3-Diisopropylbenzol	Diethylenglykol	Ethylmethylketon <sup>1</sup>	5-Chlor-2-methyl-4-isothiazolin-3-on
1,4-Diisopropylbenzol	Diethylenglykolmonobutylether	3-Methyl-2-butanon	2-Methyl-4-isothiazolin-3-on (MIT)
Phenylacetat	2-Phenoxyethanol	Methylisobutylketon	Triethylamin
1-Phenyldecan <sup>1</sup>	Ethylencarbonat	Cyclopentanon	Decamethylcyclopentasiloxan
1-Phenylundecan <sup>1</sup>	1-Methoxy-2-propanol	Cyclohexanon	Dodecamethylcyclohexasiloxan
4-Phenylcyclohexen	Texanol	Aceton <sup>1,2</sup>	Tetrahydrofuran (THF)
Styrol	Glykolsäurebutylester	2-Methylcyclopentanon	1-Decen
Phenylacetylen	Butyldiglykolacetat	2-Methylcyclohexanon	1-Octen
2-Phenylpropen	Dipropylenglykolmono-methylether	Acetophenon	2-Pentylfuran
Vinyltoluol	2-Methoxyethanol	1-Hydroxyacetan	Isophoron
Naphthalin	2-Ethoxyethanol		Tetramethylsuccinonitril
Inden	2-Propoxyethanol	<b>Säuren</b>	Dimethylformamid (DMF)
Benzol	2-Methylethoxyethanol	Essigsäure	Triethylphosphat
1-Methylnaphthalin	2-Hexoxyethanol	Propionsäure	N-Ethyl-2-pyrrolidon
2-Methylnaphthalin	1,2-Dimethoxyethan	Isobuttersäure	Anilin
1,4-Dimethylnaphthalin	1,2-Diethoxyethan	Buttersäure	4-Vinylcyclohexen
	2-Methoxyethylacetat	Pivalinsäure	
<b>Gesättigte aliphatische Kohlenwasserstoffe</b>	2-Ethoxyethylacetat	n-Valeriansäure	1 VVOC
2-Methylpentan <sup>1</sup>	2-Ethoxyethylacetat	n-Capronsäure	2 SVOC
3-Methylpentan <sup>1</sup>	2-(2-Hexoxyethoxy)-ethanol	n-Heptansäure	3 Analyse gem. DIN ISO 16000-3
n-Hexan	1-Methoxy-2-(2-methoxy-ethoxy)-ethan	n-Octansäure	
Cyclohexan	Propylenglykol-di-acetat	2-Ethylhexansäure	
Methylcyclohexan	Dipropylenglykol		
n-Heptan	Dipropylenglykolmonomethyletheracetat	<b>Ester und Lactone</b>	
n-Octan	Dipropylenglykolmono-n-propylether	Methylacetat <sup>1</sup>	
n-Nonan	Dipropylenglykolmono-t-butylether	Ethylacetat <sup>1</sup>	
n-Decan	1,4-Butandiol	Vinylacetat <sup>1</sup>	
n-Undecan	Tripropylenglykolmonomethylether	Isopropylacetat	
n-Dodecan	Triethylenglykoldimethylether	Propylacetat	
n-Tridecan	1,2-Propylenglykoldimethylether	2-Methoxy-1-methylethylacetat	
n-Tetradecan	TXIB (Texanolisobutylrest)	n-Butylformiat	
n-Pentadecan	Ethylidiglykol	Methylmethacrylat	
1-Butanol	Dipropylenglykol-dimethylether	Isobutylacetat	
1-Pentanol	Propylencarbonat	1-Butylacetat	
1-Hexanol	Hexylenglykol	2-Ethylhexylacetat	
n-Hexadecan	3-Methoxy-1-butanol	Methylacrylat	
Methylcyclopentan	1,2-Propylenglykol-n-propylether	Ethylacrylat	
1,4-Dimethylcyclohexan	1,2-Propylenglykol-n-butylether	n-Butylacrylat	
	Diethylenglykol-phenylether	2-Ethylhexylacrylat	
<b>Terpene</b>	Neopentylglykol	Adipinsäuredimethylester	
δ-3-Caren	Diethylenglykolmethylether	Fumarsäuredimethylester	
α-Pinen	1-Ethoxy-2-propanol	Bernsteinsäuredimethylester	
β-Pinen	Tert.-Butoxy-2-propanol	Glutarsäuredimethylester	
Limonen		Hexandiolacrylat	
	<b>Aldehyde</b>	Maleinsäuredimethylester	
<b>Aliphatische Alkohole und Ether</b>	Butanol <sup>1,2</sup>	Butyrolacton	
1-Propanol <sup>1</sup>	Pentanol <sup>1</sup>	Glutarsäuredimethylester	
2-Propanol <sup>1</sup>	Hexanol <sup>1</sup>	Bernsteinsäuredimethylester	
tert-Butanol	Heptanol	Dimethylphthalat	
Cyclohexanol	2-Ethylhexanol	Diethylphthalat <sup>1</sup>	
2-Ethyl-1-hexanol	Octanol	Dipropylphthalat <sup>1</sup>	
2-Methyl-1-propanol	Nonanol	Diisobutylphthalat <sup>1</sup>	
1-Octanol	Decanol	Texanol	
4-Hydroxy-4-methyl-pentan-2-on	2-Butanol <sup>1</sup>	Dipropylenglykoldiacrylat	
1-Heptanol	2-Pentanol <sup>1</sup>		

**Hinweis:** Die Untersuchungsergebnisse beziehen sich ausschließlich auf den vorgelegten Prüfgegenstand. Der Bericht verliert umgehend seine Gültigkeit bei Änderungen der Zusammensetzung oder des Produktionsverfahrens des Prüfgegenstandes. Eine vollständige oder auszugsweise Veröffentlichung des Prüfberichtes bedarf der Genehmigung.



## IV Erläuterung zur Emissionsanalyse

### Prüfmethode

Die Messung der flüchtigen organischen Verbindungen erfolgt in der Prüfkammer in Anlehnung an praxisnahe Bedingungen. Je nach Art des Prüfstückes und erforderlicher Richtlinie werden standardisierte Prüfbedingungen für Beladung, Luftwechsel, Luftfeuchte, Temperatur und Anströmgeschwindigkeit der Prüfkammerluft festgelegt. Diese und die zugrunde liegenden Normen sind dem Kapitel Prüfmethode des Laborberichtes zu entnehmen.

Während der kontinuierlich laufenden Prüfung werden zu definierten Zeitpunkten Luftproben aus der Prüfkammer entnommen. Hierzu werden ca. 5 L Prüfkammerluft mit einem Volumenstrom von 100 mL/min auf Tenax und ca. 100 L mit einem Volumenstrom von 0,8 L/min auf DNPH (Dinitrophenylhydrazin) gezogen. Die an Tenax adsorbierten Stoffe werden nach thermischer Desorption mittels gaschromatographischer Trennung und massenspektrometrischer Bestimmung analysiert. Die gaschromatographische Trennung erfolgt unter Einsatz einer 60 m langen, schwach polaren Kapillarsäule.

Die mit DNPH derivatisierten Stoffe für die Bestimmung von Formaldehyd und anderen kurzkettigen Carbonylverbindungen (C1 - C6) werden über eine Hochleistungs-Flüssig-Chromatographie analysiert.

Mehr als 200 Verbindungen, darunter flüchtige organische Verbindungen (C6 - C16), schwerflüchtige organische Verbindungen (C16 - C22) und – soweit mit diesem Verfahren darstellbar – auch sehr flüchtige organische Verbindungen (kleiner C6) werden einzelstofflich bestimmt und quantifiziert.

Alle anderen Stoffe werden – soweit möglich – durch Vergleich mit einer Spektren-Bibliothek identifiziert. Die Quantifizierung dieser und nicht identifizierter Stoffe erfolgt durch Vergleich ihrer Signalintensität mit dem Signal von Toluol.

Die ermittelten Stoffkonzentrationen werden anhand der Wiederfindungsrate eines internen Standards (d8 Toluol) korrigiert. Die Identifizierung und Quantifizierung der Stoffe wird ab einer Konzentration (Bestimmungsgrenze) von 1 µg pro m<sup>3</sup> Prüfkammerluft bzw. 2 µg/m<sup>3</sup> für DNPH-derivatisierte Stoffe vorgenommen.

### Qualitätssicherung

Die eco-INSTITUT Germany GmbH ist mit flexiblem Geltungsbereich gemäß DIN EN ISO/IEC 17025 akkreditiert. Die Akkreditierung umfasst die analytische Bestimmung sämtlicher flüchtiger organischer Verbindungen einschließlich Prüfkammerv Verfahren.

Zur Überprüfung des Analysesystems wird bei jeder Auswertung ein Standard analysiert, dessen Zusammensetzungen auf den Vorgaben der Norm prEN 18516 basiert. Die Stabilität der analytischen Systeme wird mittels Kontrollkarten über einen Teststandard dokumentiert.

In Ringversuchen, die mindestens einmal jährlich durchgeführt werden, wird die Leistungsfähigkeit des Labors durch Vergleich von Ergebnissen identischer Proben mit anderen Laboren überprüft.

Vor dem Einbringen des Prüfstücks in die Prüfkammer erfolgt eine Blindwertkontrolle auf eventuell bereits vorhandene flüchtige organische Verbindungen.

Hinweis: Die Untersuchungsergebnisse beziehen sich ausschließlich auf den vorgelegten Prüfgegenstand. Der Bericht verliert umgehend seine Gültigkeit bei Änderungen der Zusammensetzung oder des Produktionsverfahrens des Prüfgegenstandes. Eine vollständige oder auszugsweise Veröffentlichung des Prüfberichtes bedarf der Genehmigung.

## V Erläuterung zur Spezifischen Emissionsrate SER

Emissionsmessungen werden in Prüfkammern unter definierten physikalischen Bedingungen (Temperatur, relative Luftfeuchte, Raumbeladung, Luftwechselrate etc.) durchgeführt.

Prüfkammer-Messergebnisse sind nur dann unmittelbar vergleichbar, wenn die Untersuchungen unter den gleichen Rahmenbedingungen durchgeführt wurden.

Wenn sich die Unterschiede der physikalischen Bedingungen nur auf die Luftwechselrate und/oder die Beladung beziehen, kann zur Vergleichbarkeit der Messergebnisse die „Spezifische Emissions-Rate“ (SER) herangezogen werden. Die SER gibt an, wie viele flüchtige organische Verbindungen (VOC) von der Probe je Materialeinheit und Stunde (h) abgegeben werden.

Die SER kann für jede nachgewiesene Einzelkomponente der VOC aus den Angaben im Prüfbericht nach unten stehender Formel errechnet werden.

Als Materialeinheit kommen in Frage:

$l$ = Längeneinheit (m)	bezieht die Emission auf die Länge
$a$ = Flächeneinheit ( $m^2$ )	bezieht die Emission auf die Fläche
$v$ = Volumeneinheit ( $m^3$ )	bezieht die Emission auf das Volumen
$u$ = Stückerinheit (unit = Stück)	bezieht die Emission auf die komplette Einheit

Daraus resultieren die verschiedenen Dimensionen für die SER:

längenspezifisch	$SER_l$ in $\mu g/m \cdot h$
flächenspezifisch	$SER_a$ in $\mu g/m^2 \cdot h$
volumenspezifisch	$SER_v$ in $\mu g/m^3 \cdot h$
stückspezifisch	$SER_u$ in $\mu g/u \cdot h$

Die SER stellt somit eine produktspezifische Rate dar, die die Masse der flüchtigen organischen Verbindung beschreibt, die von dem Produkt pro Zeiteinheit zu einem bestimmten Zeitpunkt nach Beginn der Prüfung emittiert wird.

$$SER = q \cdot c$$

$q$	spezifische Luftdurchflussrate (Quotient aus Luftwechselrate und Beladung)
$c$	Konzentration der gemessenen Substanz(en)

Das Ergebnis kann anstelle von Mikrogramm ( $\mu g$ ) auch in Milligramm (mg) angegeben werden, wobei  $1 \text{ mg} = 1000 \mu g$ .

Hinweis: Die Untersuchungsergebnisse beziehen sich ausschließlich auf den vorgelegten Prüfgegenstand. Der Bericht verliert umgehend seine Gültigkeit bei Änderungen der Zusammensetzung oder des Produktionsverfahrens des Prüfgegenstandes. Eine vollständige oder auszugsweise Veröffentlichung des Prüfberichtes bedarf der Genehmigung.

## Appendix E

Results of Configuration MUF-2SW, MUF-SW-1, MUF-C-1 and MUF-BW+C-1

As presented in the Results section of this report (Chapter 6), an important distinction is to be made between instances of char fall-off and delamination. During all compartment tests, it was recorded that small pieces of char broke and fell-off from the MUF bonded CLT panels. At no instance did an entire plank (or multiple planks) within a lamella delaminate and fall-off (which would expose a large surface area of virgin timber). A distinction will also be made between char fall-off that occurred during the heating phase (i.e. before the charring front propagated through the first lamella and reach the adhesive line at 20mm from the fire side) and char fall-off that occurred after turning off the burner bed (i.e. after the charring front had passed the 1<sup>st</sup> adhesive line at 20mm).

### E.1) Configuration MUF-2SW: Two CLT Side Walls

This test involved a compartment containing both side panels made from exposed CLT. All other panels were constructed from non-combustible boards.

#### **Visual Observations**

After igniting the burner bed, it took approximately 1 minute for the exposed CLT panels to enter flaming combustion and release pyrolysis gases. It took 32 minutes until the charring depth had penetrated through the first 20mm of CLT in both side panels, and as such the burner bed was turned off. Even after 2 minutes had passed since switching off the burner, significant cross-flaming occurred between the two side panels, as shown in Figure 78. In addition, during the decay phase, local char fall-off occurred on both panels, as shown in Figure 79. The CLT remained glowing for another 25 minutes after switching off the burner bed. The test was ended after self-extinguishment was observed 284 minutes after the start of the tests. The charring behaviour is depicted in Figure 80 and Figure 81 for the left and right CLT panels, respectively. The charring depth had penetrated through the first two layers of both the left panel and right. A significant amount of char had fallen off from both panels, as shown in Figure 79.

It was recorded visually that small char pieces fell-off during the heating phase of the fire (therefore not indicating breaking off of char segments at the adhesive line). In addition, after turning off the burner bed char segments fell off locally from both panels, with instances where larger segments of char (although not entire planks) broke off as compared to during the heating phase. This was observed on both panels.



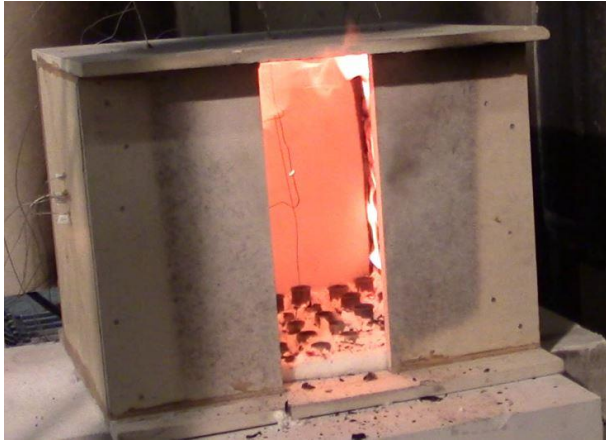


*Figure 78: (Cross) flaming combustion two minutes after switching off of the burner bed*



*Figure 79: Evidence of local char fall-off from the left side wall. Picture taken after a period where char segments broke-off gradually.*



*Figure 80: Charring depth after the experiment on the left wall*



*Figure 81: Charring depth after the experiment on the right wall*

## Heat Release Rates

Figure 82 Illustrates the HRR recorded during this experiment. The average HRR during the heating phase was measured as 73.4kW. After the burner bed was extinguished, it took 251:50 minutes to achieve self-extinguishment (i.e. all thermocouples recorded temperatures less than 200°C without the transformation of 3 or more lamellas to char).

On the figure, instances of char fall-off are indicated with black arrows. These events lead to spikes in the measured total HRR, and will be analysed during the discussion of temperature recordings.

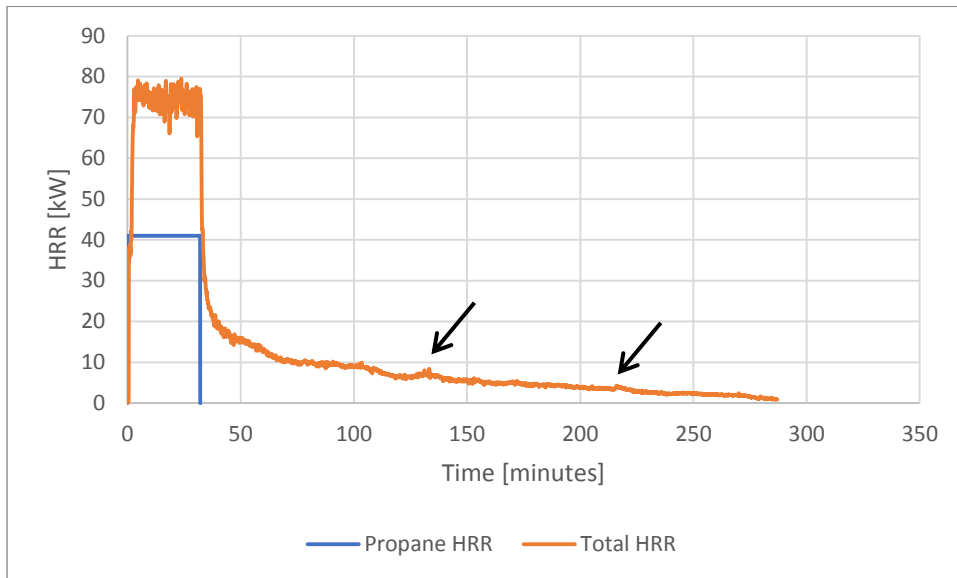


Figure 82: HRR recorded during Configuration MUF-2SW. Small spikes in the HRR are indicated with black arrows and correspond to instances of char fall-off

## Temperatures

Figure 83 illustrates the enclosure temperature development within the compartment, as recorded in the centre of the compartment at heights of 0.2m and 0.4m from the floor panel, referred to as top and bottom respectively. The average temperature during the heating phase was 937°C at the top of the compartment and 865.3°C at the bottom. The heating phase was consistently defined as the period of time post flashover (compartment temperatures >600°C) and the moment the propane burner was switched off. Temperatures reduced gradually after turning off the propane burner bed.

As recorded during the HRR measurements, small spikes in the compartment temperature at approximately 130 minutes and 220 minutes occurred. These spikes correlate with the instances where it was visually observed that larger segments of char broke-off from the CLT side walls.



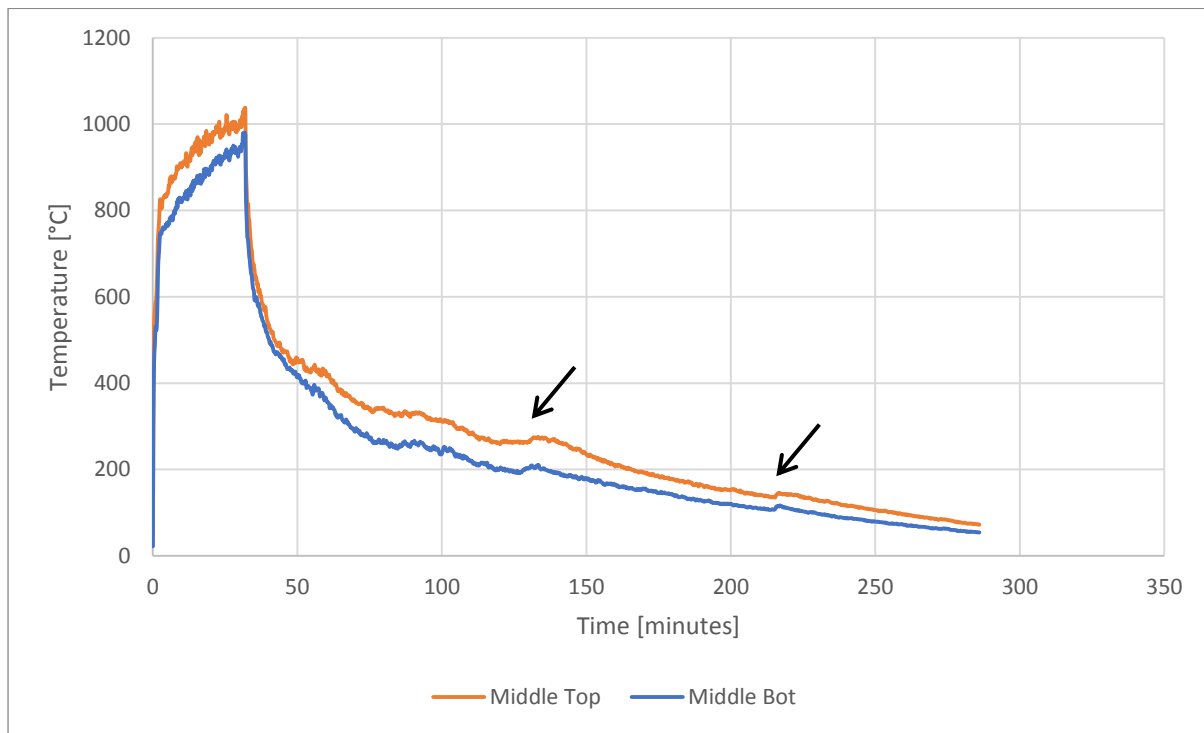


Figure 83: Compartment Temperatures recorded during Configuration MUF- 2SW

Figure 84 illustrates the enclosure temperature development within the compartment, as recorded in front of the right CLT wall panel of the compartment at heights of 0.2m and 0.4m from the floor panel. The average temperature during the heating phase was 967.7.0°C at the top of the compartment and 885.3°C at the bottom. At approximately 130 minutes, it was observed that a larger segment of char fell-off from the right panel, leading to a small peak in temperatures measured in front of the wall. This also occurred at approximately 220 minutes resulting in a spike in recorded temperatures.

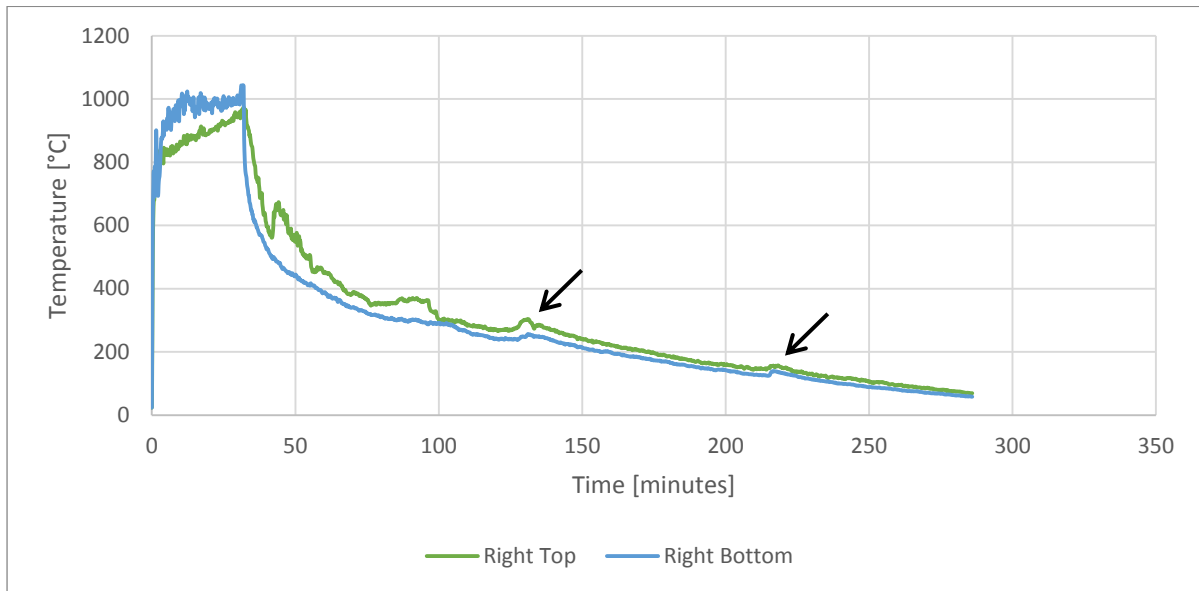


Figure 84: Enclosure temperatures recorded in Configuration MUF-2SW at the Right Panel

The same sets of measurements were recorded in front of the exposed CLT left wall panel and are depicted in Figure 85. The average temperature during the heating phase was 1011.2°C at the top of the compartment and 971.0°C at the bottom. The same temperature peaks (at comparable time instances, i.e. 130 minutes and 220 minutes) as recorded in front of the right wall also occurred at the left wall, as indicated by the arrows in the figure.

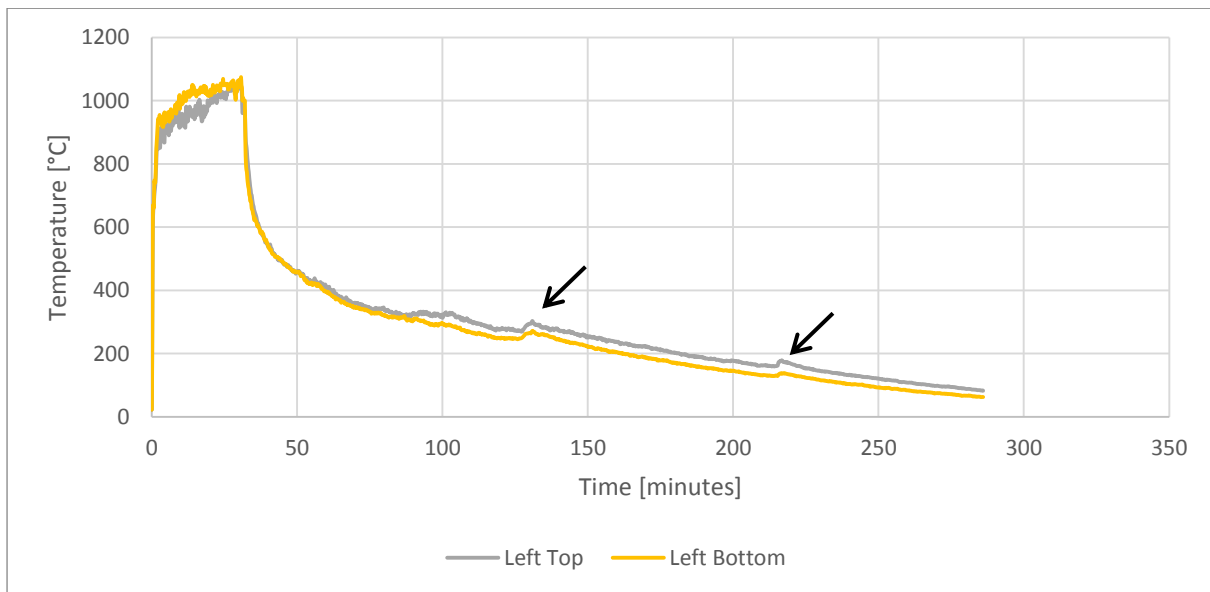


Figure 85: Enclosure temperatures recorded in Configuration MUF-2SW at the Left Panel

The recorded temperature development curves of the various thermocouples installed in the depth of the right and left CLT wall panels are depicted in Figure 86 and Figure 87, respectively.

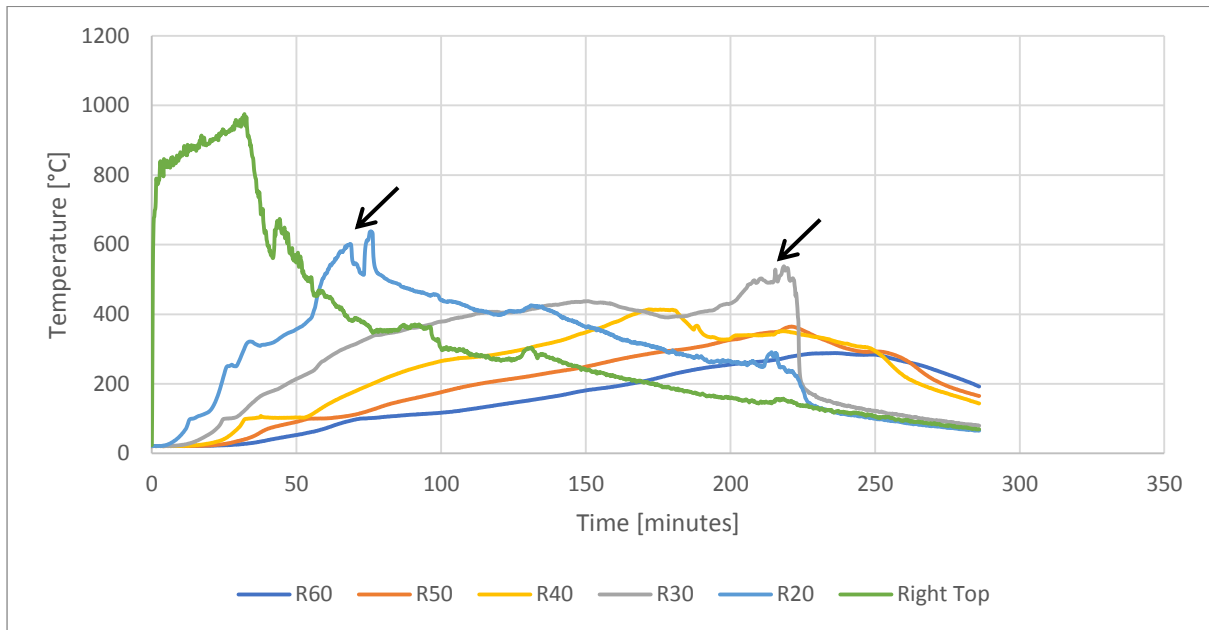


Figure 86: Right CLT panel in-depth temperatures

At approximately 65 minutes, compartment temperatures dropped dramatically at a depth of 20 mm from the fire side of the right CLT wall. This decrease is attributed to an instance of local char fall-off. After this event, compartment temperatures dropped and followed the measured temperatures in front of the right wall within the enclosure (as shown by the curve plotted in green). During a short period (approximately 20 minutes) of time prior to 220 minutes, a small char piece flared-up and flamed locally in front of the thermocouples. This resulted in the sharp increase in temperatures measured at a depth of 20 and 30 mm. After the small char piece ceased to flame and fell-off, the in-depth temperatures dropped again, eventually to below 200°C when it was deemed that self-extinguishment was achieved.

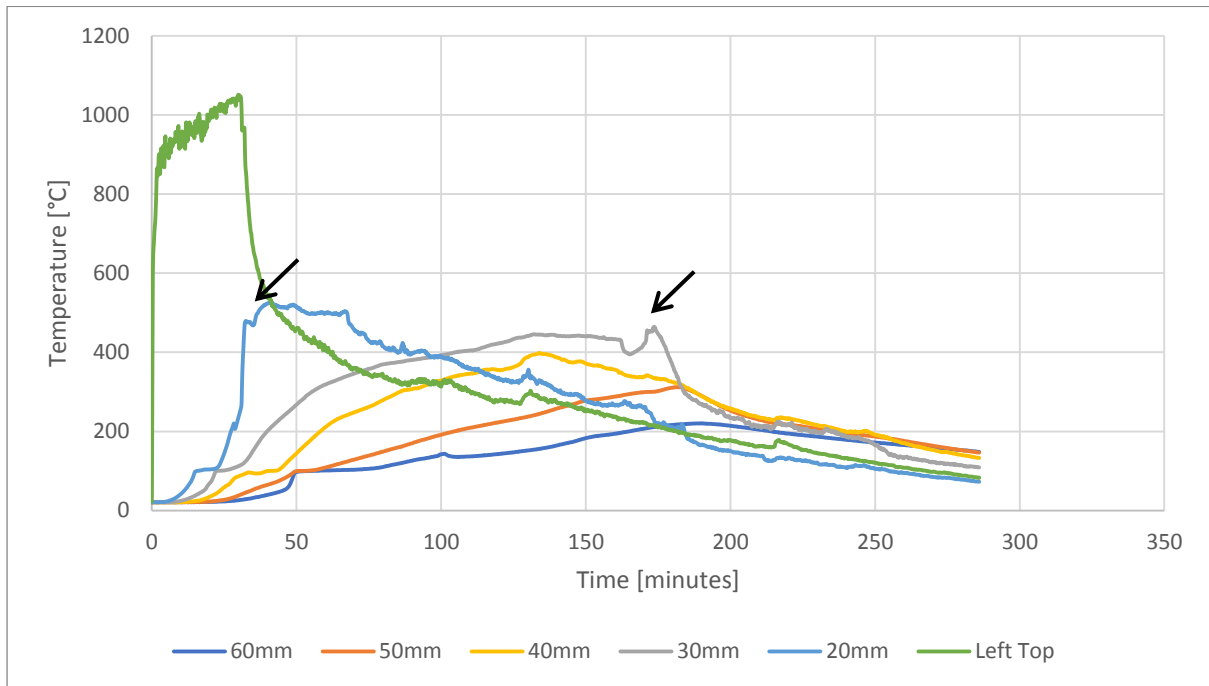


Figure 87: Left CLT panel in-depth temperatures

Similarly to the right CLT panel, local char fall-off was also recorded to have occurred at approximately 41 minutes. After this, the temperature recorded at a depth of 20mm from the fire side followed the temperature curve measured in front of the Left CLT panel within the compartment (as shown by the curve plotted in green). After this drop at 20mm, temperatures continue to rise at subsequent depths of the CLT panel indicating that the charring front had passed through the first lamella after char fall-off had occurred. At approximately 165 minutes, temperatures decreased gradually at all depths until self-extinguishment was deemed to have occurred.

## E.2) Configuration MUF-SW-1: One CLT Side Wall

This test involved a compartment with only its left wall constructed from exposed CLT. All other panels were made using non-combustible boards.

### Visual Observations

After igniting the burner bed, it took 1:30 minutes for the exposed CLT panels to enter flaming combustion and release pyrolysis gases. It took 33 minutes until the charring depth had penetrated through the first 20mm of the left CLT side panel, and as such the burner bed was turned off.

Subsequent to switching off the burners, flaming of the CLT significantly reduced 1 minute later. The CLT remained glowing for another 5 minutes after switching off the burner bed. Figure 88 indicates that only small pieces had broken off from the left panel. The test was ended after self-extinguishment was observed 70 minutes after the start of the test. The charring behaviour is depicted in Figure 89, with only the innermost lamella charred.

The instances of char fall-off occurred after the burner bed was switched off, and did not all occur simultaneously. Small pieces of char fell off (locally) from the CLT panel over a period of time and accumulated on the floor as shown in Figure 88.



Figure 88: Minor char fall-off observed, as indicated by the accumulation of char on the floor panel (arrow)



Figure 89: Left CLT panel char depth

## Heat Release Rates

Figure 90 indicates the HRR development as measured during the compartment tests. The total HRR was measured as 57.4 kW on average during the period which the burner bed was ignited. This correlated to a CLT only contribution of 16.4 kW to the HRR. After switching off the burner bed, the total HRR declined rapidly until self-extinguishment was recorded.

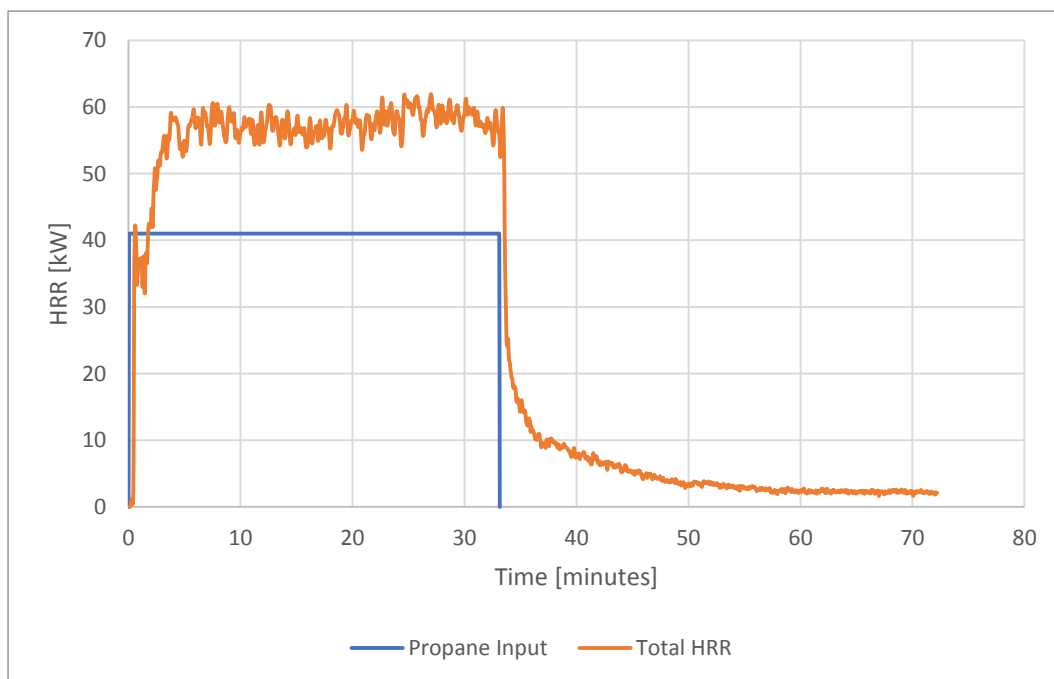


Figure 90: HRR measured during Configuration SW-1

## Temperatures

Figure 91 depicts the enclosure temperatures measured at the centre of the compartment at two heights (0.2m and 0.4m from the floor panel). During the heating phase, the average temperature was measured as 949.5°C and 765.8°C at 0.4m and 0.2m from the floor panel, respectively. Temperatures increased rapidly when the burner bed was ignited till approximately 800°C and then increased more gradually towards maximum temperatures at the moment the burner bed was switched off (1007.6°C and 853.1°C at 0.4m and 0.2m, respectively). After switching off the burner bed, temperatures decreased rapidly till approximately 400°C and then decreased at a slower rate during the remainder of the decay phase until self-extinguishment was recorded.

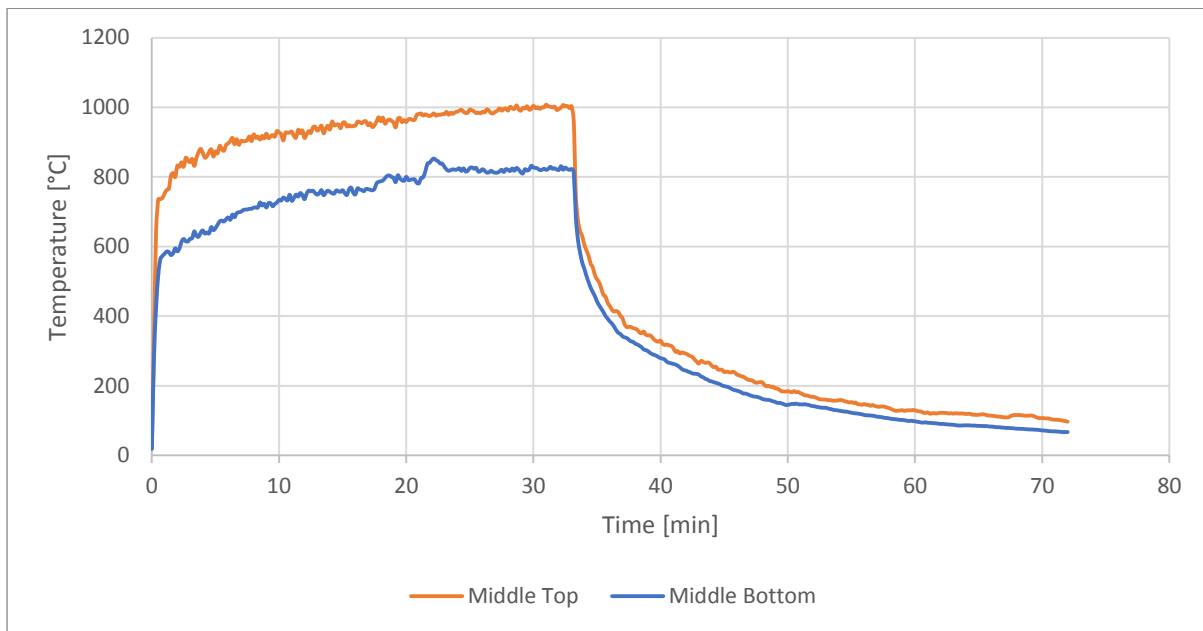


Figure 91: Compartment Temperatures measured at the centre of the compartment during Configuration SW-1

Figure 92 demonstrates the enclosure temperatures measured in front of the Right con-combustible panel at heights of 0.2m (bottom) and 0.4m (top) from the floor panel.

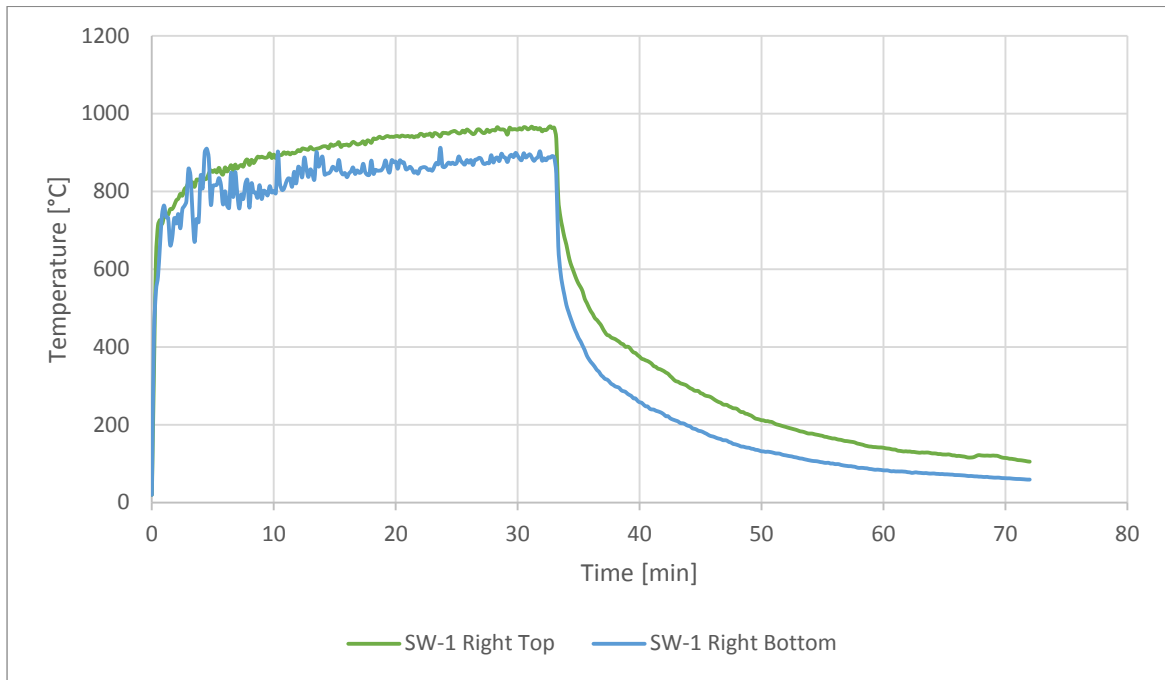


Figure 92: Compartment Temperatures measured at the face of the non-combustible right wall

Similarly to the right panel, enclosure temperatures were measured in front of the left exposed CLT wall, at the same heights as mentioned before.

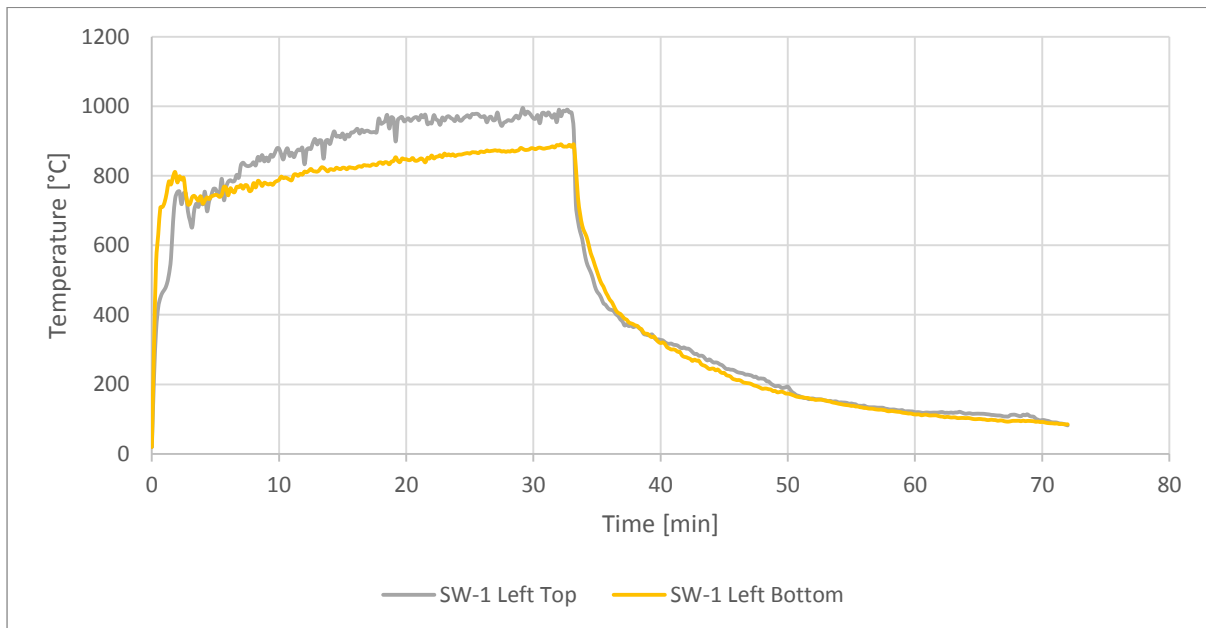


Figure 93: Compartment Temperatures measured at the face of the CLT left wall

From the figures above demonstrating enclosure temperatures, it is evident that temperatures did not vary greatly within the compartment since comparable temperature development curves were recorded at identical heights at the middle of the compartment as well as in front of the two side panels. During the decay phase, no distinct peaks were recorded in the temperature development in

front of the exposed CLT left wall (Figure 93), despite local char fall-off being recorded visually. This indicates that char fall-off in this compartment configuration, during the decay phase of the compartment fire, did not have an influence on enclosure temperatures.

Figure 94 shows the temperature development as recorded at various depths within the left exposed CLT panel. Temperatures rose rapidly to 300°C at 20mm until the burner bed was switched off. After this, the temperature recorded at 20mm decreased but remained at an elevated level until approximately 60 minutes. After 60 minutes it was observed that temperatures decreased at depths of 20mm and 30mm without the occurrence of local char fall-off in front of these thermocouples. Temperatures in the CLT pane decreased rapidly after this time instance, and self-extinguishment was recorded once all temperature readings were below 200°C.

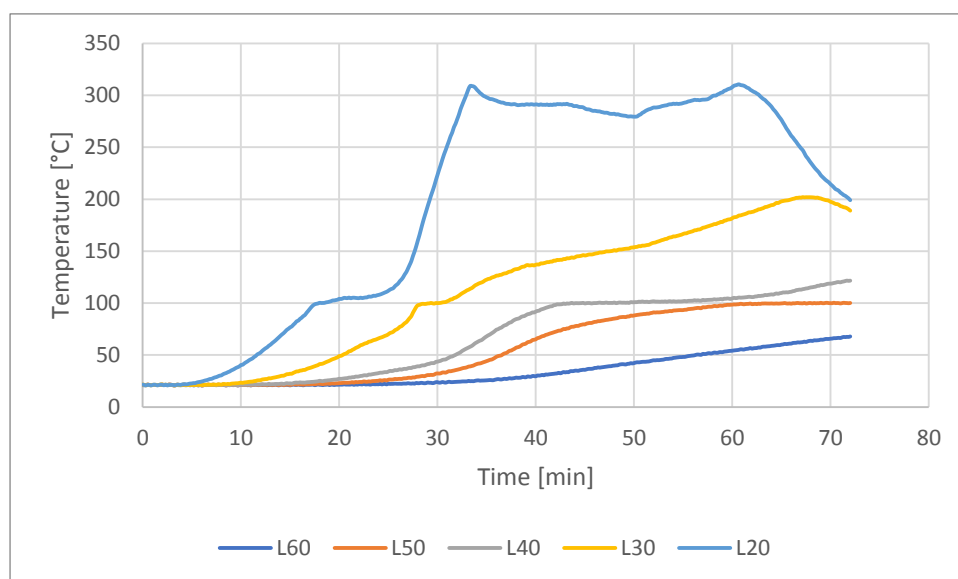


Figure 94: Temperatures measured within the CLT left wall

### E.3) Configuration MUF-C-1: CLT Ceiling

This test involved a compartment containing an exposed ceiling constructed from exposed CLT. All other panels were constructed from non-combustible boards.

#### Visual Observations

After igniting the burner bed, it took 1 minute for the exposed CLT panels to enter flaming combustion and release pyrolysis gases. It took 30:20 minutes until the charring depth had penetrated through the first 20mm of the CLT ceiling panel, and as such the burner bed was turned off. After switching off the burner bed, the flaming combustion of the ceiling panel had greatly reduced after 3 minutes. The CLT remained glowing for another 10 minutes after switching off the burner bed. Minor char fall-off occurred during the decay phase, as shown in Figure 95. These instances of char fall-off



occurred shortly after the burner bed was switched off, indicating failure at the adhesive line at local char pieces.

In contrast to the tests described up to thus far, a small CLT overhang was present at the junction of the roof CLT panel and the ventilation opening. This aforementioned overhang led to an additional area of charring, as shown in Figure 96 and Figure 97 at the overhang. Due to the limited area that charred in this 80mm overhang, it is postulate that the additional overhang would not significantly influence results. As such, it is expected that compartment and CLT temperatures would not be affected by the charring overhang, and that the influence on HRR would be insignificant.

The test was ended after self-extinguishment was observed 51:20 minutes after the start of the tests. The charring behaviour is depicted in Figure 98, where the charring depth progressed through the first lamella (edge charring at the ventilation edge is also visible).



*Figure 95: Minor pieces of char that fell off as indicated by the arrow*

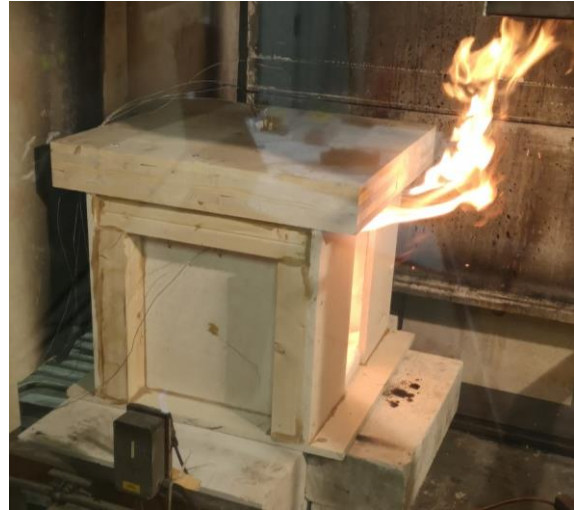


*Figure 96: Depiction of the additional CLT overhang at the ventilation opening*



*Figure 97: Additional charring at the ventilation opening post burner switch-off*



*Figure 98: Charring depth of the ceiling panel*

## Heat Release Rates

Figure 99 depicts the HRR development as measured during the compartment tests. The total HRR was measured as 59.1 kW on average during the period which the burner bed was ignited. This correlated to a CLT only contribution of 18.1 kW to the HRR. After switching off the burner bed, the total HRR declined rapidly until self-extinguishment was recorded.

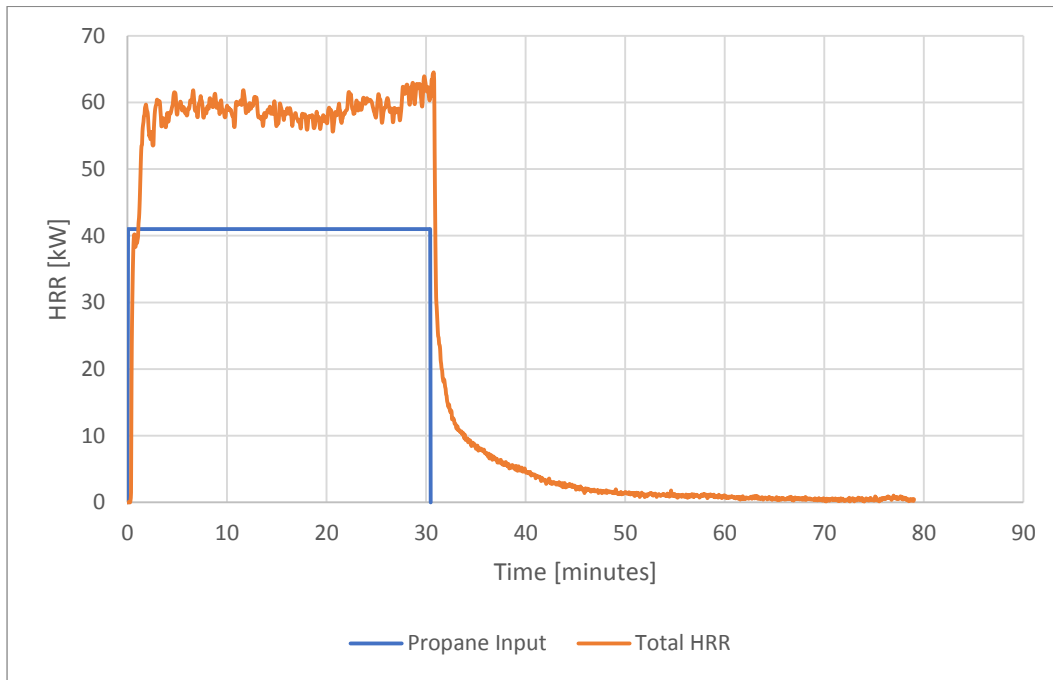


Figure 99: HRR measured during Configuration MUF-C-1

## Temperatures

Figure 100 depicts the enclosure temperatures measured at the centre of the compartment at two heights (0.2m and 0.4m from the floor panel). During the heating phase, the average temperature was measured as 977.3°C and 872.5°C at 0.4m and 0.2m from the floor panel, respectively. Temperatures increased rapidly when the burner bed was ignited till approximately 800°C and then increased more gradually towards maximum temperatures at the moment the burner bed was switched off. After switching off the burner bed, temperatures decreased rapidly till approximately 500°C and then decreased at a slower rate during the remainder of the decay phase until self-extinguishment was recorded. Instances of char fall-off shortly after turning off the burner bed are not visible in Figure 100 since the influence of the burner bed outage overshadowed compartment fire behaviour as compared to local char fall-off.

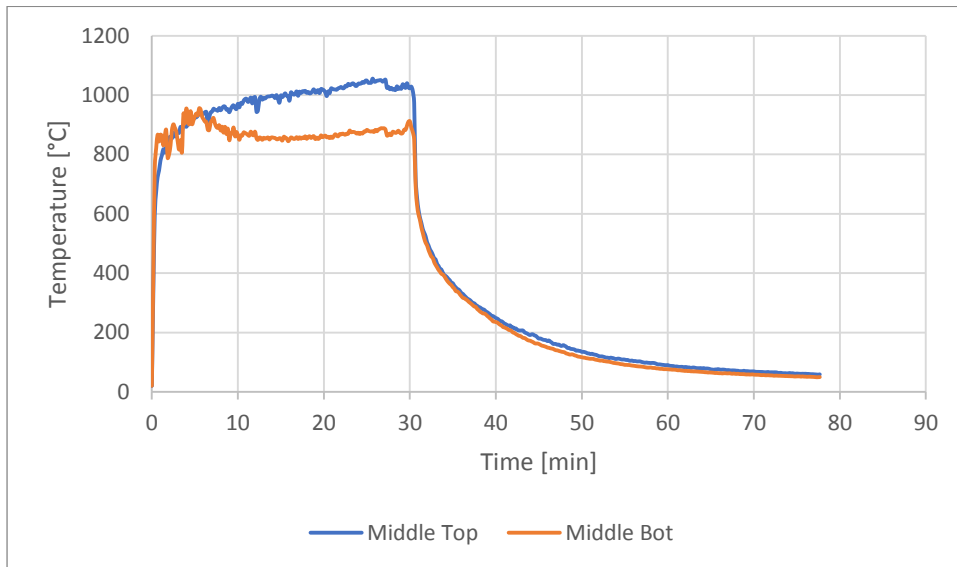


Figure 100: Enclosure Temperatures as recorded in the centre of Configuration MUF-C-1

The in-depth temperatures measured in the CLT panel are depicted in Figure 101. It can be seen that temperatures rose sharply at a depth of 20mm from the fire exposed side up till 100°C and then plateaued for a period correlating to the time to evaporate moisture from the CLT. After this, temperatures rose less rapidly initially at 20mm and then at an accelerated rate up until the moment which the burner bed was switched off. After the burner bed was turned off, temperatures decreased steadily at 20mm until self-extinguishment was recorded once temperatures dropped below 200°C. Due to the smooth nature of the Temperature curves, it is postulated that the occurrence of local char fall-off at the time of burner extinguishment did not influence the charring behaviour at the centre of the ceiling panel.

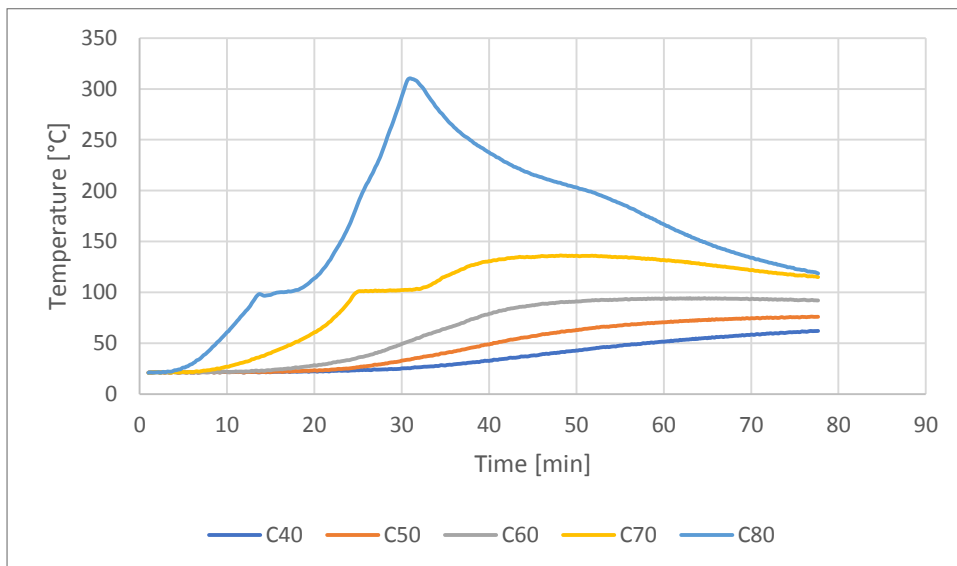


Figure 101: Temperatures as measured through the depth of the CLT Ceiling panel

#### E.4) Configuration MUF-BW+C-1: CLT Back Wall and Ceiling

This test involved a compartment containing a back and ceiling constructed from exposed CLT. All other panels were constructed from non-combustible boards.

##### **Visual Observations**

After igniting the burner bed, it took 1 minute for the exposed CLT panels to enter flaming combustion and release pyrolysis gases. It took 30 minutes until the charring depth had penetrated through the first 20mm of CLT in both panels, and as such the burner bed was turned off (the state of the compartment at this instance is shown in Figure 102). During the period which the burner bed was ignited, small pieces of char fall-off was recorded from the ceiling panel.

6 minutes after switching off the burner bed, flaming combustion of the CLT panels had significantly died out. The CLT remained glowing for another 25 minutes after switching off the burner bed. At 37 minutes and 40 minutes, large segments of char fall-off were recorded at the ceiling panel and back wall, respectively. Evidence of char fall-off is shown in Figure 103 with the depiction of char pieces on the floor of the compartment (also evident in Figure 102). The test was ended after self-extinguishment was observed 121 minutes after the start of the test.

During the decay phase, after large pieces of char fell-off at 37 and 40 minutes from the ceiling and back panel respectively, a period of local char fall-off was recorded. The local char fall-off process lead to the fall-off of a significant portion of the exposed CLT from the 1<sup>st</sup> and 2<sup>nd</sup> lamellas. The innermost lamella of the back wall had fallen off at the time the test was stopped, whereas the entire first lamella and a large extent of the second lamella of the ceiling fell off as well. The charring behaviour is depicted in Figure 104 and Figure 105. It is evident that the two innermost lamella of the ceiling had been charred through, and the first and a great extent of the second innermost lamellas had charred of the back panel.





*Figure 102: CLT panels at the instant the burner bed was switched off. Char Fall-Off during the heating phase indicated by the black arrow*

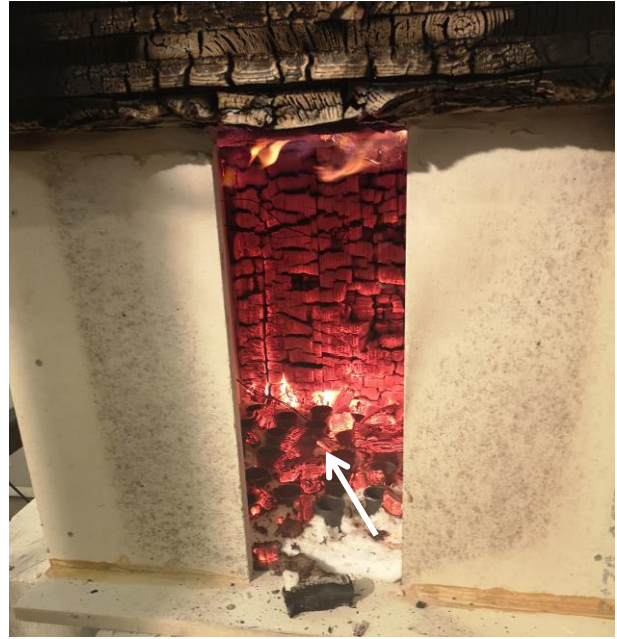


*Figure 103: Evidence of char fall off based on char pieces on the floor panel, indicated by the white arrow*



*Figure 104: Charring behaviour of the ceiling panel*



*Figure 105: Charring behaviour of the back panel*

## Heat Release Rates

Figure 106 depicts the HRR development as measured during the compartment tests. The total HRR was measured as 72.9 kW on average during the period which the burner bed was ignited. This correlated to a CLT only contribution of 31.9 kW to the HRR. After switching off the burner bed, the total HRR declined rapidly until self-extinguishment was recorded.

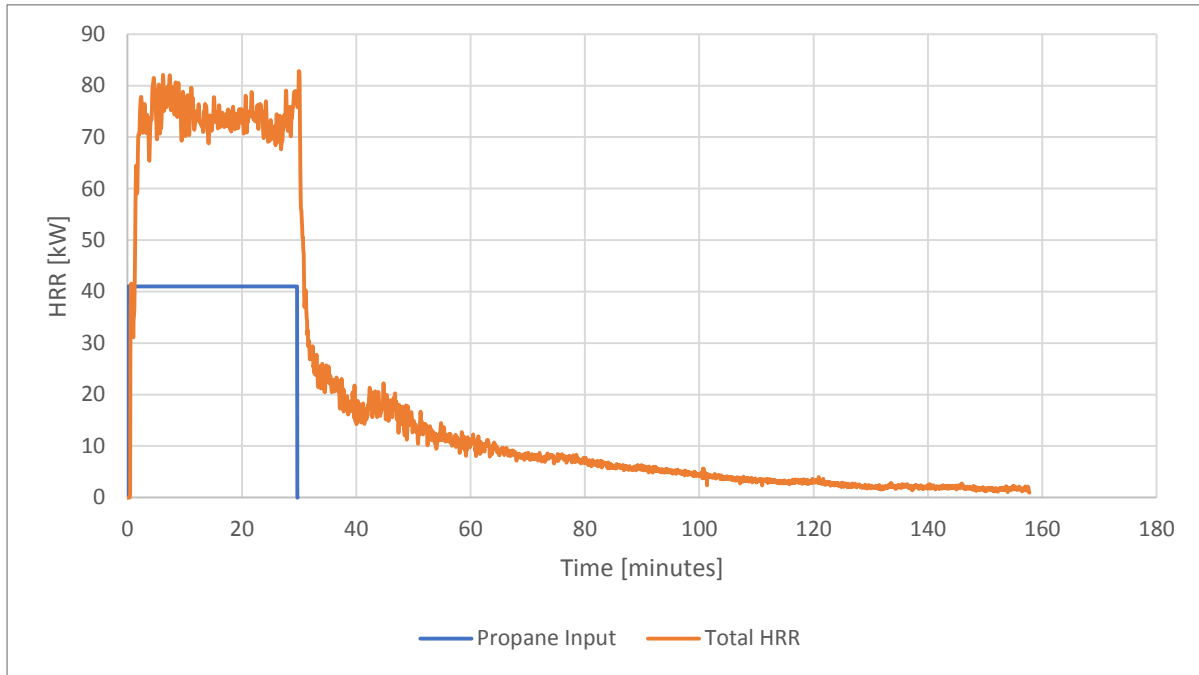


Figure 106: HRR as measured during Configuration MUF-BW+C-1

## Temperatures

Figure 107 depicts the compartment temperatures measured during the experiments. It can be seen that temperatures rose sharply after turning on the burner bed to approximately 800°C, and then more gradually until the burner bed was turned off. A small peak was recorded at 31 minutes at the bottom of the compartment, and was attributed to the visual observation of a small char piece falling and resting on top of the thermocouple. At the moment this small char piece dislodged from the bottom thermocouple, temperatures decreased rapidly. At 40 minutes a peak in the enclosure temperature came as a result of a large piece of char failing-off from the back wall panel. Despite the aforementioned discrepancies, temperatures decreased gradually during the decay phase until self-extinguishment was recorded.

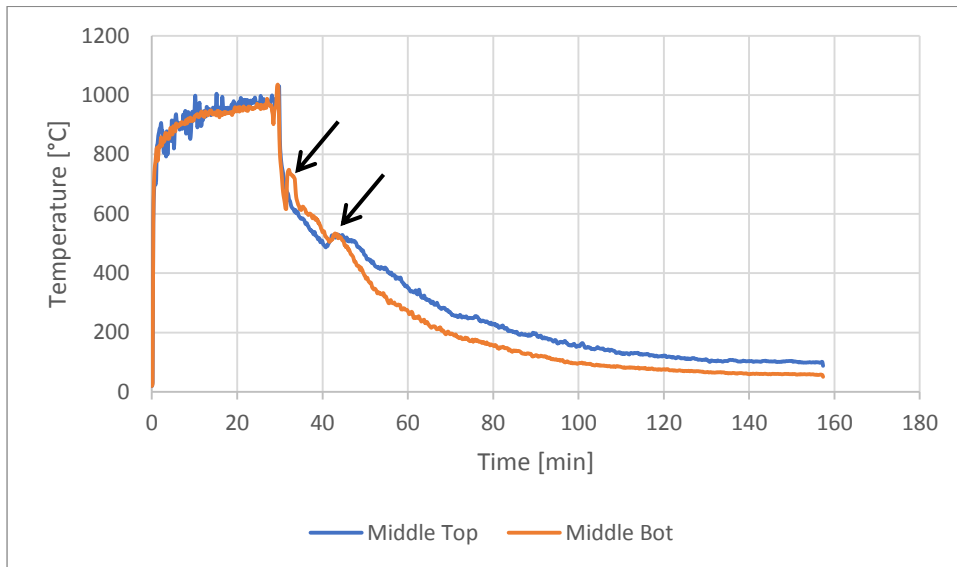


Figure 107: Enclosure Temperatures recorded at the centre of Configuration MUF-BW+C-1

The temperature development with the ceiling panel is demonstrated in Figure 108. Temperatures rose steadily at all depths until the burner bed was turned off at 30 minutes. After this, the temperatures increase rate declined at 20mm, until 37 minutes. As mentioned previously, a large segment of char broke off from the ceiling panel at this instance. It is speculated that the char piece did not break off at the adhesive interface, since temperatures measured at 20mm declined at this instance instead of being elevated to the compartment temperature at that instance (approximately 500°C). Char pieces were glowing shortly before the occurrence of fall-off, and after fall-off lead to the decrease in temperature measured at 20mm depth, since the heat released by the glowing char was instantaneously removed. Since compartment temperatures were still elevated during at this moment (see the green curve depicting the top compartment temperature), the virgin timber below the section (just in front of the 20mm thermocouple) where the large char segment had fallen off was heated rapidly and temperatures rose again at 20mm. This phenomena had a delayed effect (namely a peak in temperature) on temperatures measured 10mm deeper into the panel (i.e. at 30mm)



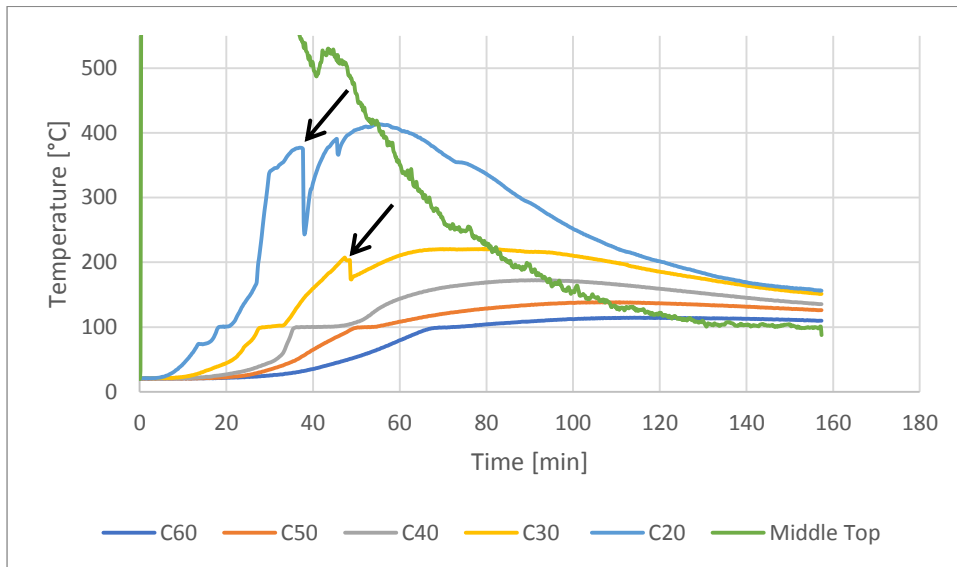


Figure 108: Temperatures recorded within the ceiling

Figure 109 illustrates the temperature development measured within the CLT back wall at the connection of the CLT Ceiling and CLT Back Wall. Temperatures rose gradually whilst the burner bed was ignited for 30 minutes, but did not breach the transformation to char threshold of 300°C. After burner outage, temperatures declined gradually until the end of the test.

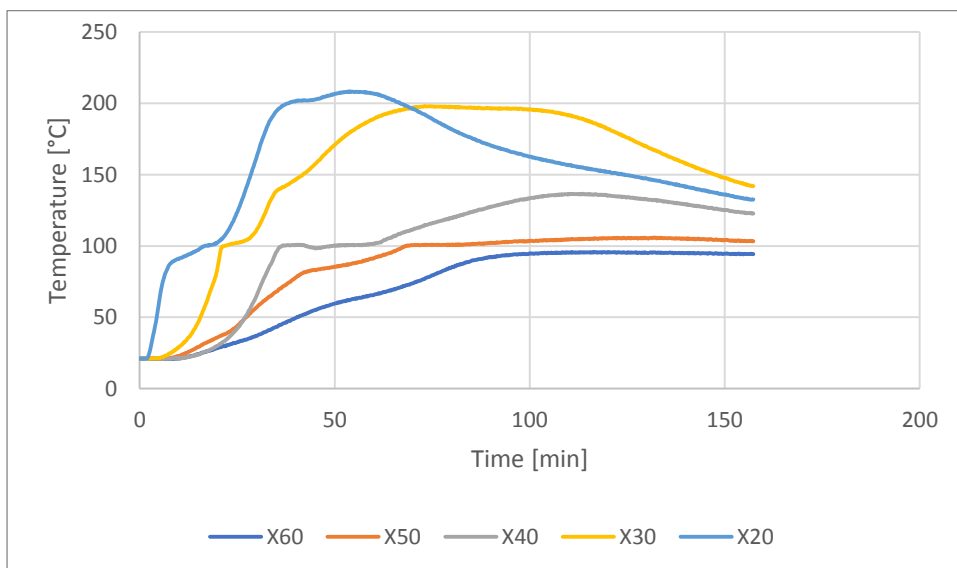


Figure 109: Temperatures recorded at the connection between the back wall and the ceiling

Similarly to the ceiling panel, Figure 110 demonstrates the temperature development in the exposed CLT back wall. Temperatures rose steadily during the heating phase of the fire (i.e. the first 30 minutes of the test). After burner extinguishment, temperatures decreased gradually until 40 minutes. As was the case with the ceiling panel at 37 minutes, a large section of char broke off from the back panel at 40 minutes. Unlike the observed temperature drop as recorded at 20mm in the ceiling panel, temperatures at 20mm in the back wall rose steadily after the char fall-off, indicating that the

insulative char layer shielding the 20mm thermocouple (i.e. at the adhesive line) had broken off and as such temperatures increased steadily after this event. This event was not deemed to be classified as delamination due to the limited area of char that broke off. A relatively small (local) segment of char broke off at the centre of the panel instead of an entire timber plank within a lamella as would occur during delamination.

After approximately 50 minutes temperatures decreased at 20mm until approximately 150 minutes. At this instance it was recorded that the virgin timber posts on the exterior of the compartment that were used to support the ceiling (not constructed of CLT) were entering glowing combustion. As this was not a phenomena related to the CLT, and all CLT temperatures measured temperatures below 200°C, the tests was stopped and self-extinguishment was deemed to have been achieved.

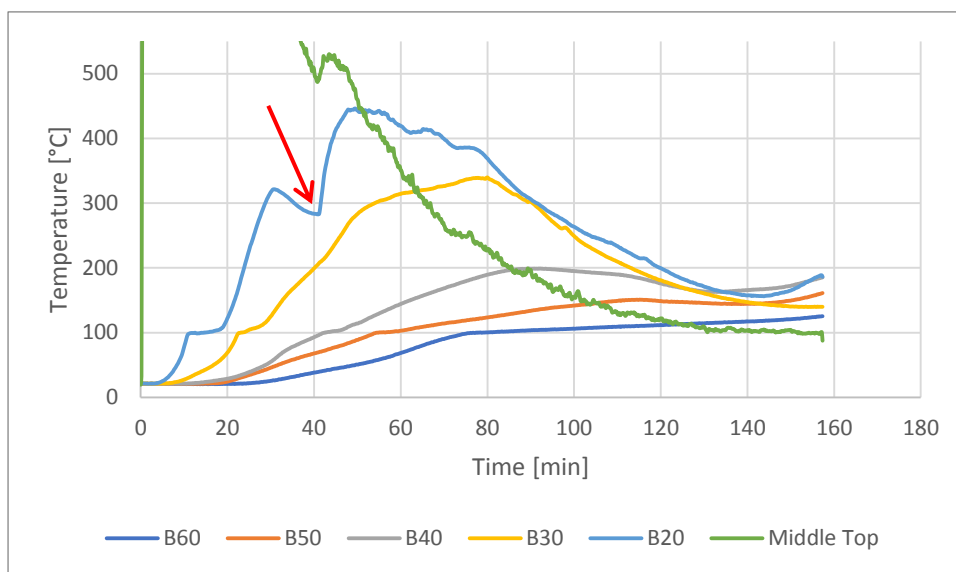


Figure 110: Temperatures measured within the Back Wall

## Appendix F

Results of the repetition experiments MUF-SW-2, MUF-C-2 and MUF-BW+C-2

### F.1) Configuration MUF-SW-2: One CLT Side Wall

This test involved a compartment with only its right wall constructed from exposed CLT. All other panels were made using non-combustible boards.

#### **Visual Observations**

After igniting the burner bed, it took 1:30 minutes for the exposed CLT panels to enter flaming combustion and release pyrolysis gases. It took 34:40 minutes until the charring depth had penetrated through the first 20mm of the right CLT side panel, and as such the burner bed was turned off. The state of the CLT panel at this instance is shown in Figure 111.

Subsequent to switching off the burners, flaming of the CLT significantly reduced 2 minute later, as seen in Figure 112. The CLT remained glowing for another 10 minutes after switching off the burner bed. Figure 113 indicates that a small amount of char had fallen off from the right panel. The majority of char fall-off occurred during the heating phase (i.e. before turning off the burner bed) indicating that char pieces broke off before the charring front had penetrated to the adhesive line at 20mm (therefore indicating that adhesive failure did not occur). During the decay phase, local pieces of char fell off from the CLT panel without influencing fire behaviour.

The test was ended after self-extinguishment was observed 102 minutes after the start of the test. The charring behaviour is depicted in Figure 114, with the charring depth consuming the innermost lamella (i.e. the layer exposed to the fire) only.

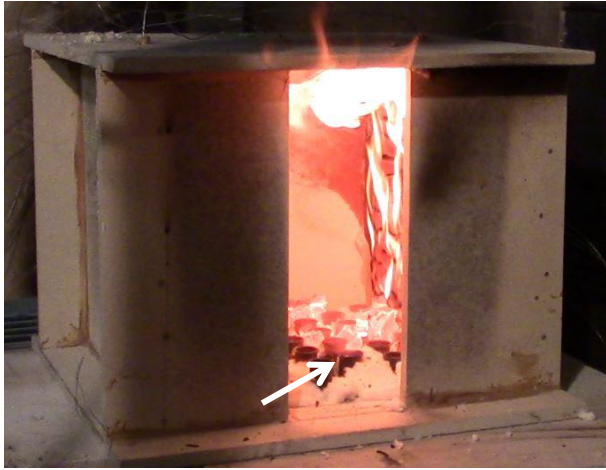


*Figure 111: CLT Panel at the moment of turning off the burner bed. White arrow indicates char that broke off during the heating phase*

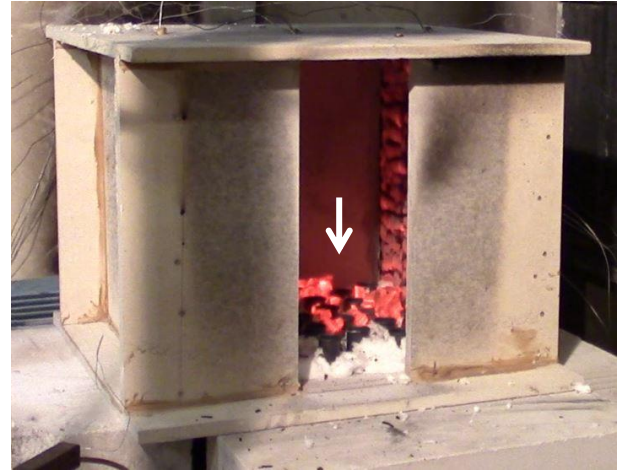


*Figure 112: CLT panel 2 minutes after turning off the burner bed with fallen pieces of char indicated by the white arrow*



*Figure 113: Small pieces of fallen off char as indicated by the white arrow*



*Figure 114: Right CLT panel char depth post testing*

## Heat Release Rates

Figure 115 depicts the HRR development as measured during the compartment tests. The total HRR was measured as 56.9 kW on average during the period which the burner bed was ignited. This correlated to a CLT only contribution of 15.9 kW to the HRR. After switching off the burner bed, the total HRR declined rapidly until self-extinguishment was recorded.

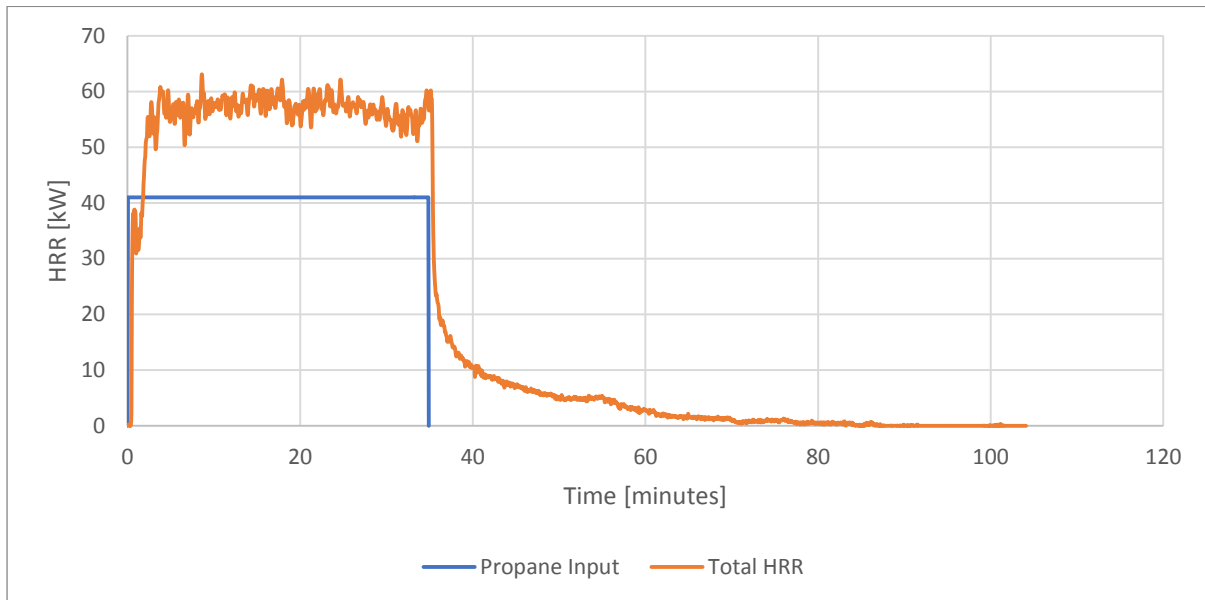


Figure 115: HRR measured during Configuration MUF-SW-2

## Temperatures

The development of enclosure temperatures as measured in the centre of the compartment is depicted in Figure 116. After burner ignition, temperatures rapidly to 800°C and 700°C at the top and bottom position, respectively. This was followed by a period of gradual temperature increase until the burner bed was turned off at approximately 35 minutes. During the decay phase, a few instances of small local char fall-off occurred but it did not significantly influence compartment temperatures.

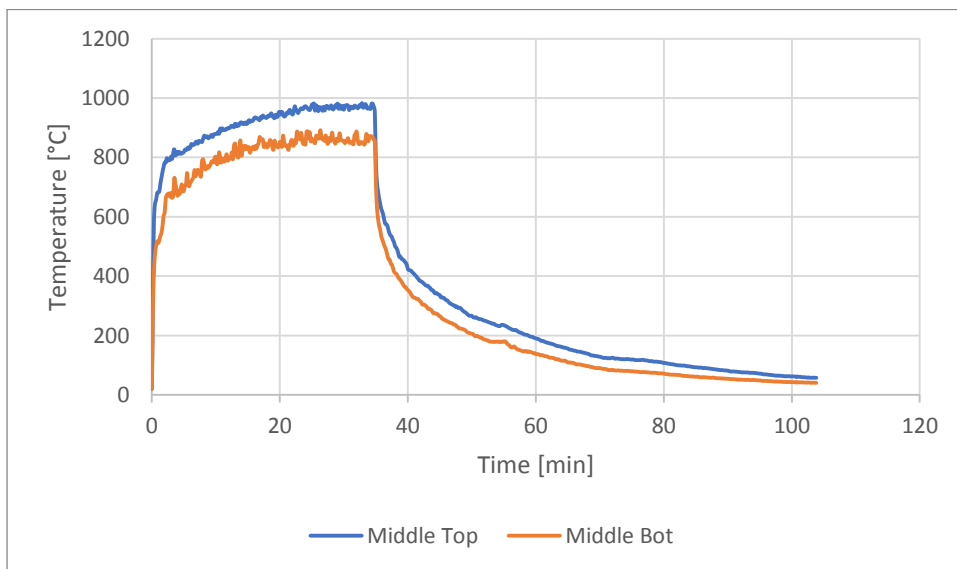


Figure 116: Enclosure Temperatures measured at the centre of Configuration MUF-SW-2

Figure 117, which depicts compartment temperatures at the face of the right exposed CLT panel, illustrates a similar trend as measured at the centre of the compartment. As was measured in Compartment 3-1, temperatures did not differ significantly within the compartment.

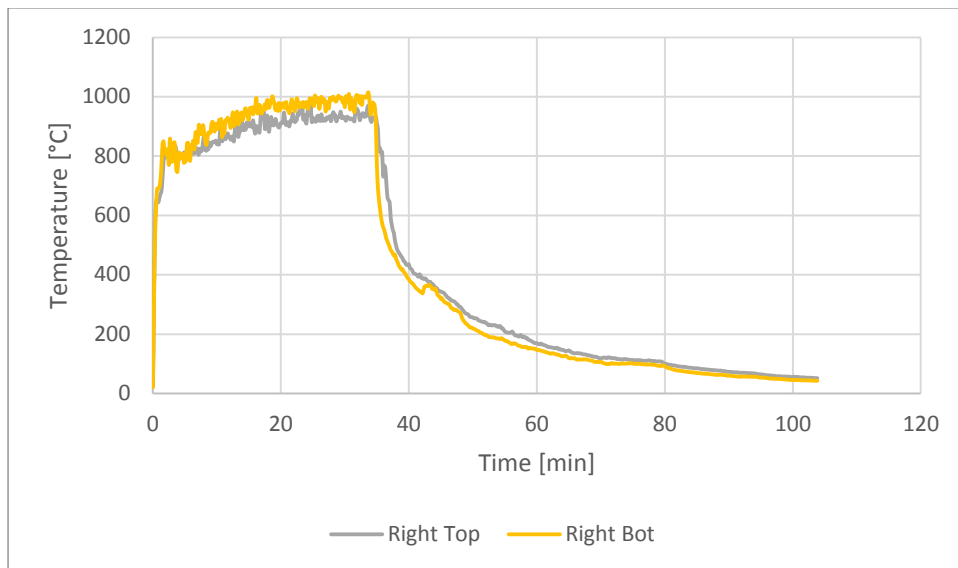


Figure 117: Enclosure Temperatures measured in front of the right CLT panel of Configuration MUF-SW-2

The temperatures measured in front of the left non-combustible wall are shown in Figure 118. These temperatures were similar to those measured in front of the right CLT panel.

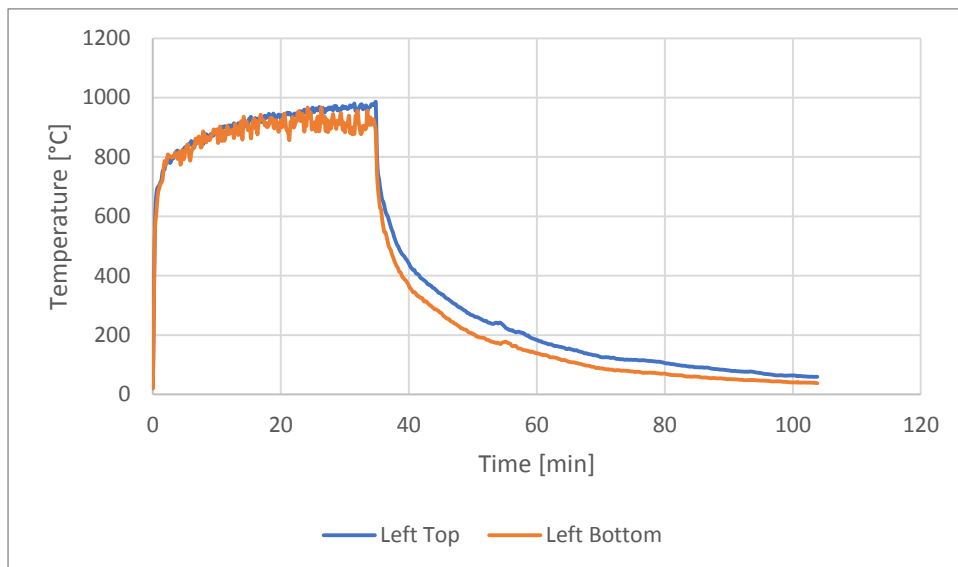


Figure 118: Enclosure Temperatures measured in front of the right non-combustible panel of Configuration MUF-SW-2

The temperatures measured within the right CLT panel are shown in Figure 119. Charring occurred rapidly during the period where burner bed was ignited and slowed down after the burner bed was ignited. Charring of the panel stagnated occurred at a significantly slower rate at 50 minutes and

onwards, until approximately 75 minutes where temperatures declined sharply until self-extinguishment was recorded.

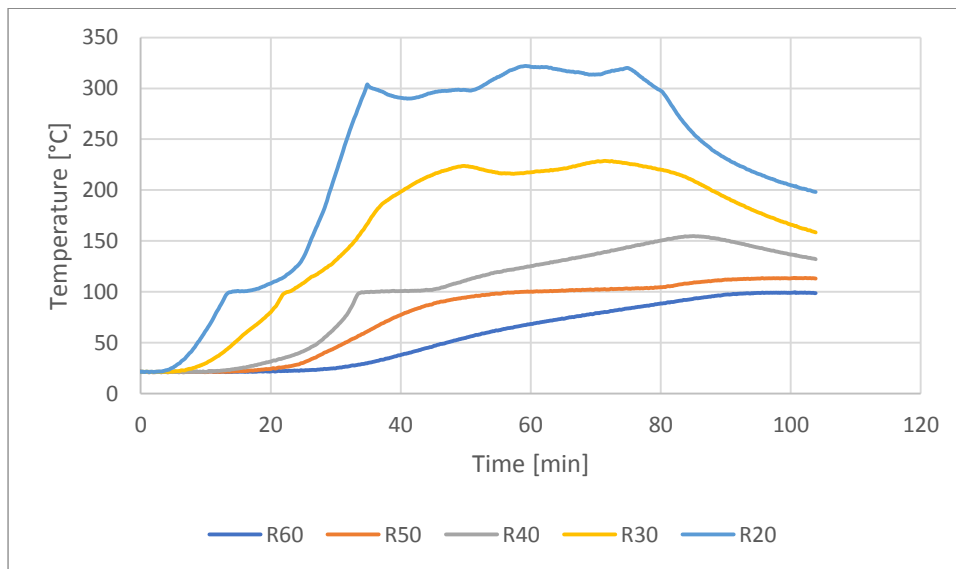


Figure 119: Temperatures measured within the right CLT panel

## F.2) Configuration MUF-C-2: CLT Ceiling

This test involved a compartment containing an exposed ceiling constructed from exposed CLT. All other panels were constructed from non-combustible boards.

### Visual Observations

After igniting the burner bed, it took 1 minute for the exposed CLT panels to enter flaming combustion and release pyrolysis gases. It took 28:20 minutes until the charring depth had penetrated through the first 20mm of the CLT ceiling panel, and as such the burner bed was turned off.

After switching off the burner bed, the flaming combustion of the ceiling panel had greatly reduced after 3 minutes. Minor char fall-off occurred during the period which the burner bed was ignited, indicating that char pieces broke off before the charring front had reached the adhesive layer. Figure 120 shows the char pieces that fell off (predominantly) during the heating phase. In addition, a single instance of char fall-off occurred at approximately 35 minutes (i.e. during the decay phase of the fire). The test was ended after self-extinguishment was observed 56:20 minutes after the start of the tests.

The charring behaviour is depicted in Figure 121, where the charring depth progressed through the first lamella (edge charring at the ventilation edge is also visible).





Figure 120: Minor char fall-off during MUF- C-2



Figure 121: Charring behaviour of the ceiling panel

## Heat Release Rates

Figure 122 depicts the HRR development as measured during the compartment tests. The total HRR was measured as 55.0 kW on average during the period which the burner bed was ignited. This correlated to a CLT only contribution of 14.0 kW to the HRR. After switching off the burner bed, the total HRR declined rapidly until self-extinguishment was recorded.

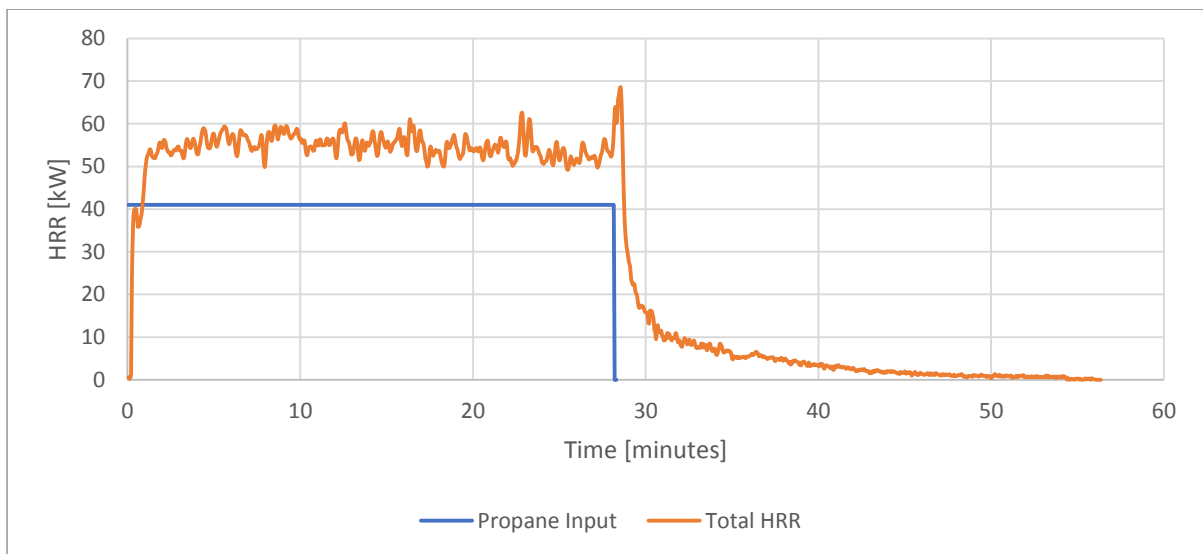


Figure 122: HRR measured during Configuration MUF-C-2

## Temperatures

The development of enclosure temperatures as measured in the centre of the compartment is depicted in Figure 123. After burner ignition, temperatures rapidly to 900°C and 800°C at the top and bottom position, respectively. This was followed by a period of gradual temperature increase until the burner bed was turned off at approximately 28 minutes. During the decay phase, a single instances of small local char fall-off occurred at 35 minutes but it did not significantly influence compartment temperatures.

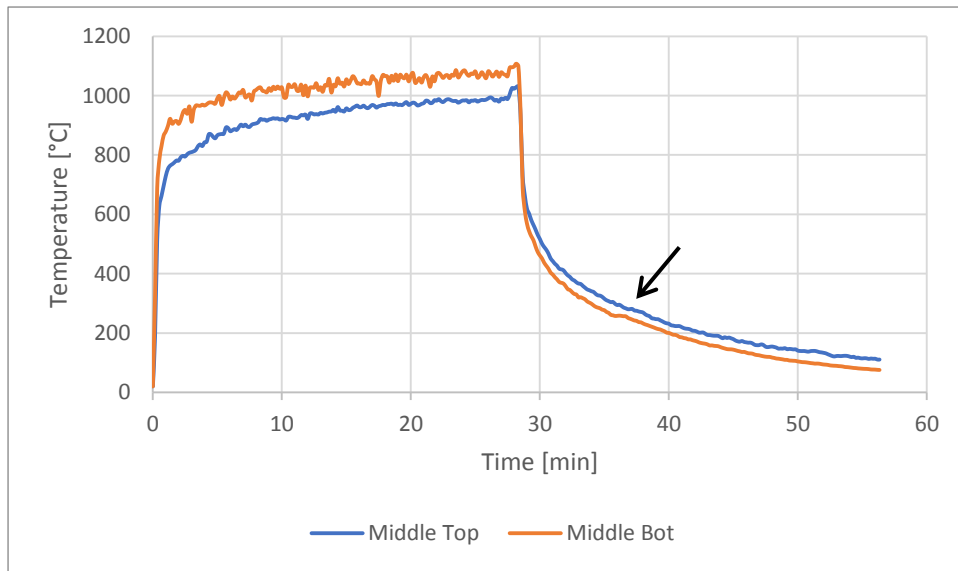


Figure 123: Enclosure temperatures measured at the centre of Configuration MUF-C-2

The development of temperatures within the CLT ceiling panel is depicted in Figure 124. It can be seen that the general trends observed in Configuration S1 were also observed in this experiment. Temperatures rose sharply at a depth of 20mm until 100°C was recorded, marking the instance where moisture evaporation within the CLT commenced. After the moisture had evaporated, temperatures increased further until it was recorded that the charring front had progressed to 20mm (i.e. at the adhesive line). Temperatures measured at 20mm decreased gradually after the burner bed was turned off at 28 minutes, up until all temperatures measured less than 200°C and as such self-extinguishment was deemed to have occurred.

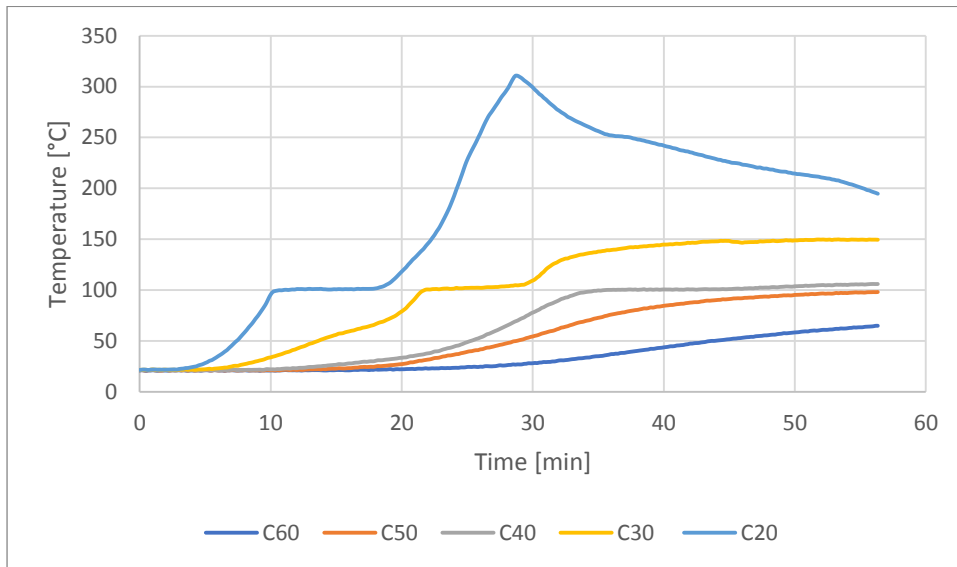


Figure 124: Temperatures measured within the CLT ceiling panel in Configuration MUF-C-2

### F.3) Configuration MUF-BW+C-2: CLT Back Wall and Ceiling

This test involved a compartment containing a back and ceiling constructed from exposed CLT. All other panels were constructed from non-combustible boards.

#### Visual Observations

After igniting the burner bed, it took 1 minute for the exposed CLT panels to enter flaming combustion and release pyrolysis gases. It took 33:10 minutes until the charring depth had penetrated through the first 20mm of CLT in both panels, and as such the burner bed was turned off. Figure 125 depicts the state of the compartment at the moment the burner bed was switched off. Significant char fall-off occurred in both the ceiling and back panel during the heating phase at 25 minutes. This indicates that char pieces broke off before the charring front had reached the adhesive line at 20mm from the fire exposed surface.

8 minutes after switching off the burner bed, flaming combustion of the CLT panels had significantly died out. During the decay phase, a process of local char fall-off (with small char pieces falling off at intervals) was recorded to have occurred in the back panel and ceiling. This process resulted in the fall off of the 1<sup>st</sup> lamella of the back wall and to a great extent the 2<sup>nd</sup> lamella of the ceiling panel. Evidence of this local char fall-off process is shown in Figure 126 with the depiction of accumulated char pieces on the floor of the compartment. The test was ended after self-extinguishment was observed 119:30 minutes after the start of the tests. The charring behaviour is depicted in Figure 127 and Figure 128. It is evident that the two innermost lamellas of the ceiling had been charred through, and the innermost lamella had been charred of the back panel.

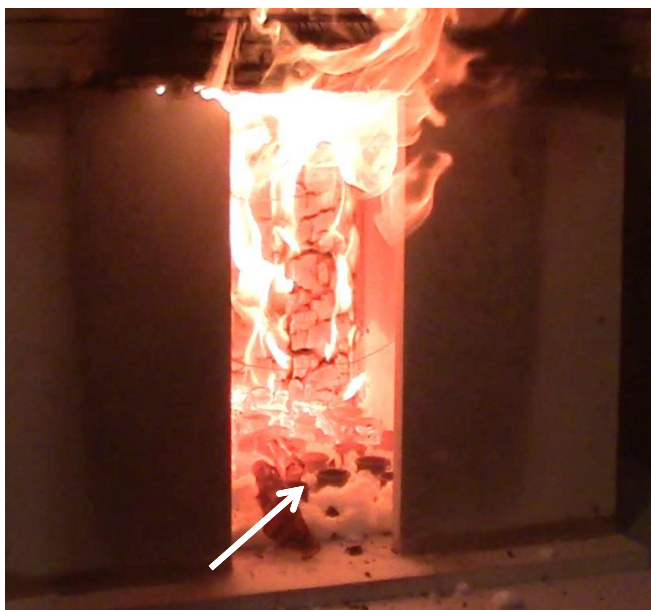


*Figure 125: Compartment at the moment the burner bed was turned off, with fallen off char indicated with a white arrow*



*Figure 126: Evidence of local char fall-off as indicated by accumulated char on the floor panel*



*Figure 127: Charring behaviour of the back panel*



*Figure 128: Charring behaviour of the Ceiling Panel*

## Heat Release Rates

Figure 129 depicts the HRR development as measured during the compartment tests. The total HRR was measured as 72.3 kW on average during the period which the burner bed was ignited. This correlated to a CLT only contribution of 31.3 kW to the HRR. After switching off the burner bed, the total HRR declined rapidly until self-extinguishment was recorded.



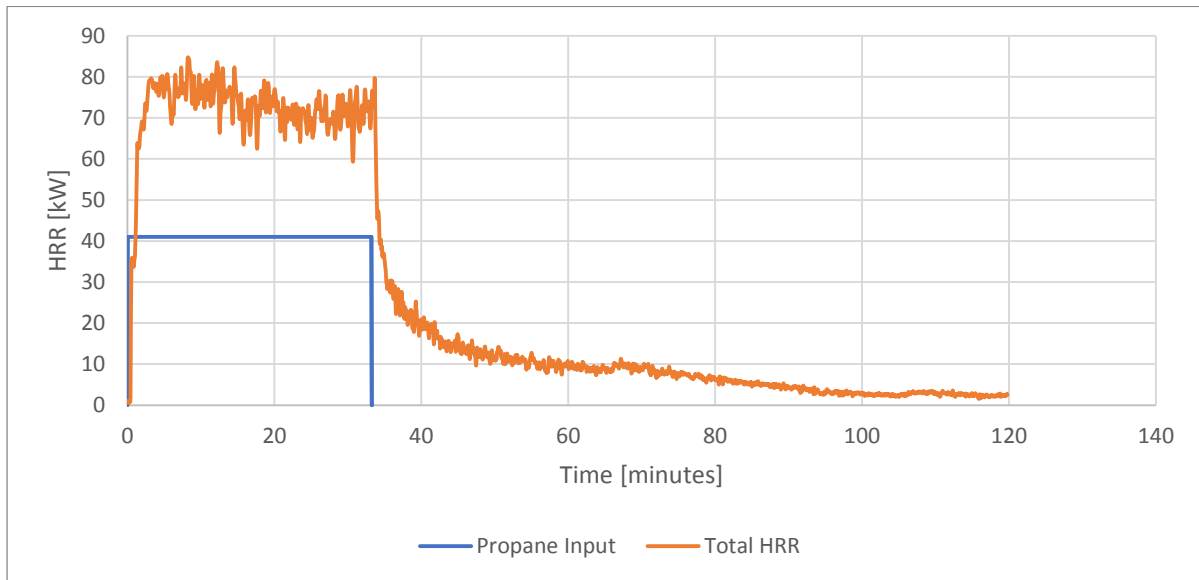


Figure 129: HRR measured in Configuration MUF-BW+C-2

## Temperatures

Figure 130 depicts the enclosure temperatures measured at the centre of the compartment at 0.2m and 0.4m from the floor panel, referred to as top and bottom respectively. Temperatures rose rapidly in the compartment as soon as the burner bed was ignited, and rose till approximately 900°C. After this initially rapid increase, temperatures steadily increased until 25 minutes. At this point a sharp decrease in temperature was recorded, and occurred at approximately the same time char fall-off occurred from the ceiling panel. Local char fall from the ceiling panel also led to a minor increase in compartment temperatures at approximately 65 minutes.

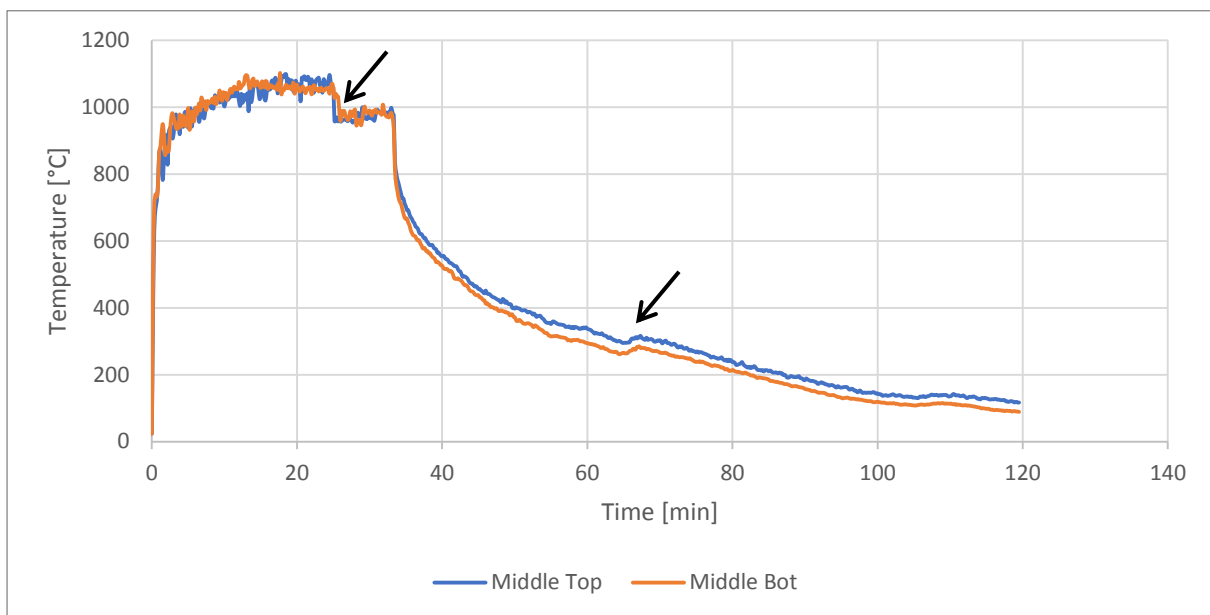


Figure 130: Enclosure temperatures as measured at the centre of Configuration MUF-BW+C-2

Figure 131 demonstrates the temperatures measured in the ceiling panel. As indicated by the black arrows, char fall-off occurred at 25 minutes, 35 minutes, 45 minutes and 65 minutes. These instances of char fall-off lead to a deviation from steady charring behaviour. The general trend of an increased 10mm temperature was recorded up until burner outage at 33 minutes, and a steady decline in CLT temperature in the decay phase until self-extinguishment was recorded.

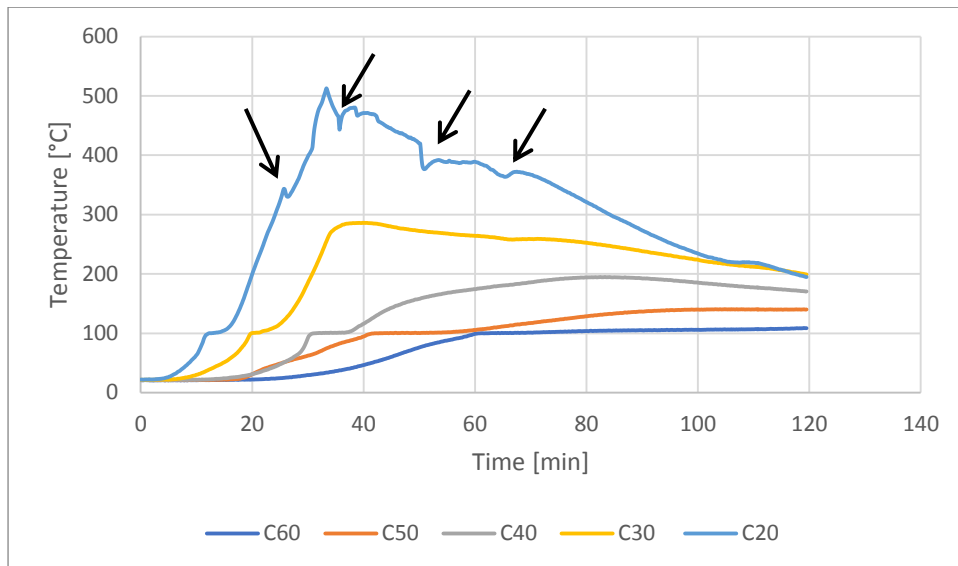


Figure 131: Temperatures measured within the ceiling panel

Figure 132 illustrates the temperature development measured within the CLT back wall at the connection of the CLT Ceiling and CLT Back Wall. Temperatures rose gradually whilst the burner bed was ignited for 33 minutes, but did not breach the transformation to char threshold of 300°C. A small deviation was recorded at 25 minutes, corresponding to an instance of char fall-off from in front of the 20mm thermocouple. After the burner outage, temperatures declined gradually until the end of the test.

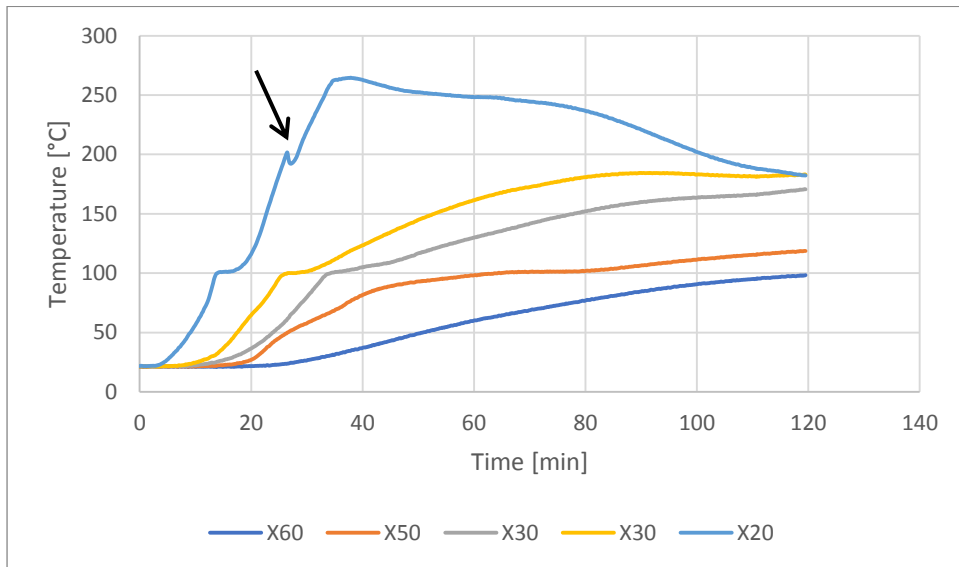


Figure 132: Temperatures as measured at the connection between the ceiling and the back wall

The temperatures recorded in the back panel are depicted in Figure 133. Temperatures rose gradually during the 33 minutes which the burner bed was ignited. After this, temperatures plateaued at a depth of 20mm until approximately 55 minutes. After this, temperatures soared at the thermocouple locations due to the occurrence of local flaming of char at the centre of the back panel. Once this local flaming ceased, temperatures decreased gradually until it was deemed that self-extinguishment was recorded.

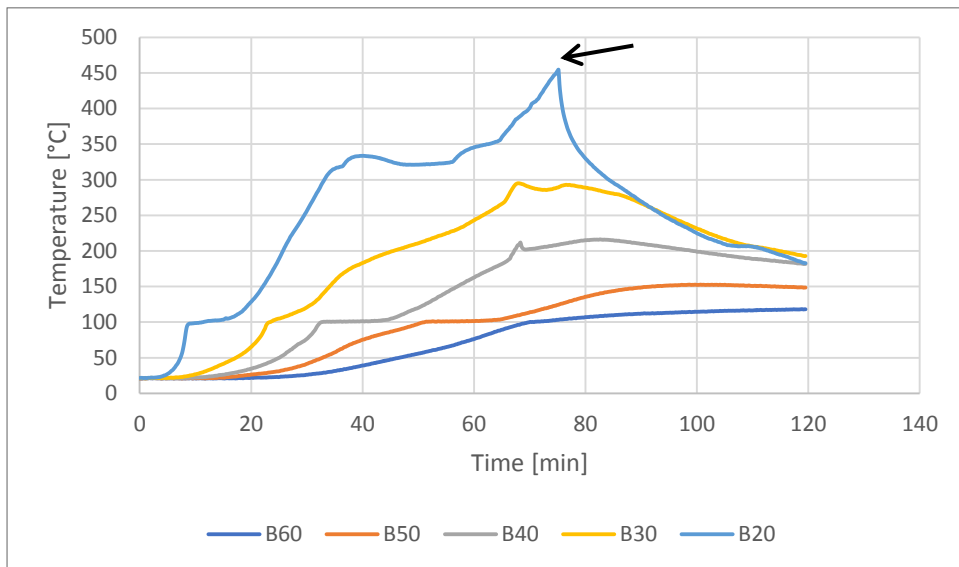


Figure 133: Temperatures measured in the back wall panel

## Appendix G

Configuration analysis based on results from the repetition experiments



In order to assess the validity of the conclusions drawn in Section 7.3 of this report, an analysis of the influence of CLT panel configuration, as derived from experimental results (bases on repeat experiments 2SW, C-2 and BW+C-2) is presented in this appendix. The same four sets of comparisons drawn in Section 7.3 are presented in this section of the report. The compartment configurations that will be compared to one another are visualised in Figure 134:

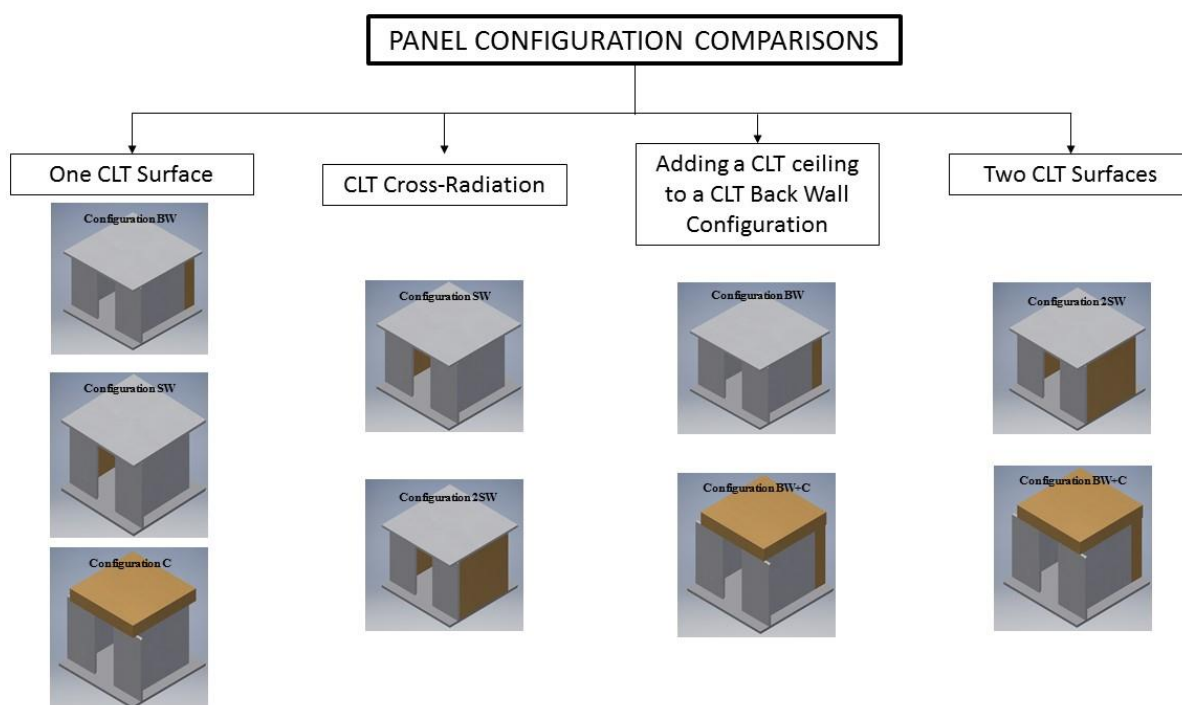


Figure 134: Visualising the 4 compartment configuration comparison sets

### G.1) Characterising the behaviour of compartments with one exposed CLT surface

A discussion of the influence of panel configuration in compartments containing a single exposed CLT wall is presented in this section. A discussion of the HRR and temperature development of compartments with a CLT back wall (BW), side wall (SW-2) or ceiling (C-2) is presented.

#### HRR

The Total HRR measured during each of the three experiments involving one exposed CLT surface is presented in Figure 135.

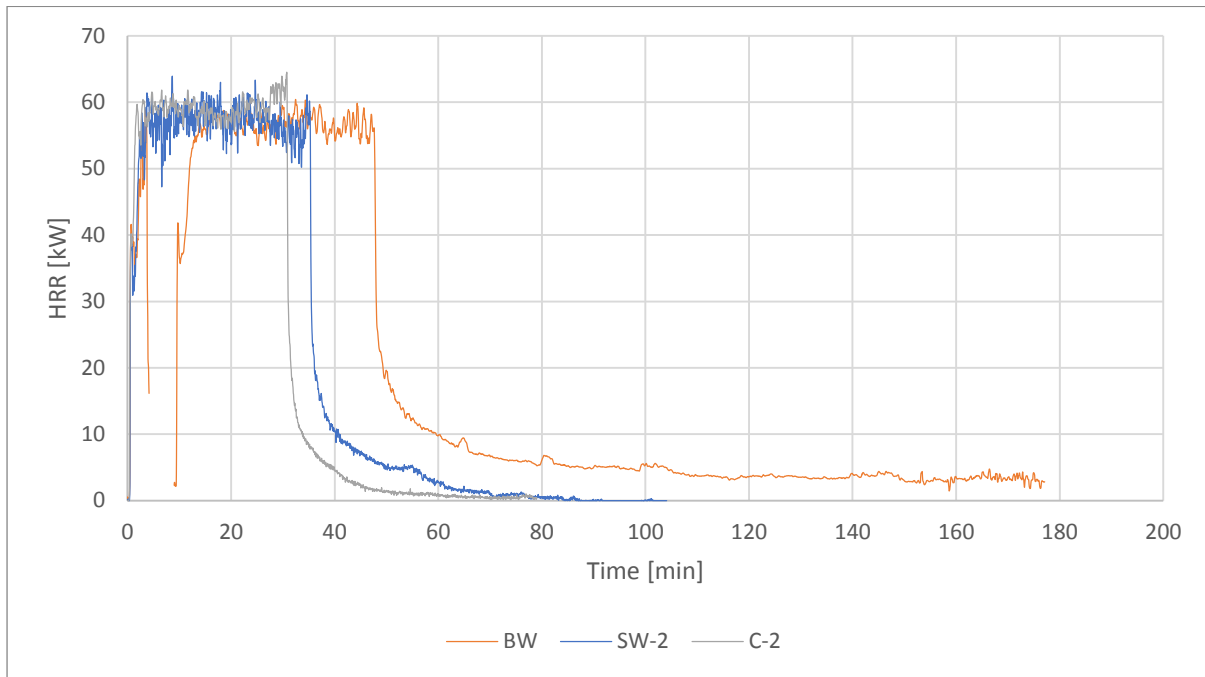


Figure 135: Comparing HRR amongst repeat compartment configurations with one exposed CLT surface

Just as recorded for the first set of experiments, averaged HRR during the heating phase were comparable between all experiments involving one exposed CLT wall, and was measured at 56.6kW, 56.9kW and 55.0kW in Configurations BW, SW-2 and C-2 respectively. The decay phase of the various experiments also followed the same rapid decrease in HRR to approximately 10kW, followed by a gradual decrease till self-extinguishment occurred.

## Temperatures

Figure 136 also illustrates similar trends as identified in Section 7.3. The shortest decay phase duration was documented in the Ceiling CLT configuration (26:50 minutes), followed by the Side CLT wall configuration (67:40minutes) and finally the Back Wall configuration (126:20 minutes).

The average compartment temperature at the top of the compartment did not vary greatly between the 3 configurations, namely 918°C, 919°C and 927°C (Back, Side and Ceiling, respectively). The highest average compartment (Top) temperature was recorded during the exposed CLT ceiling test.

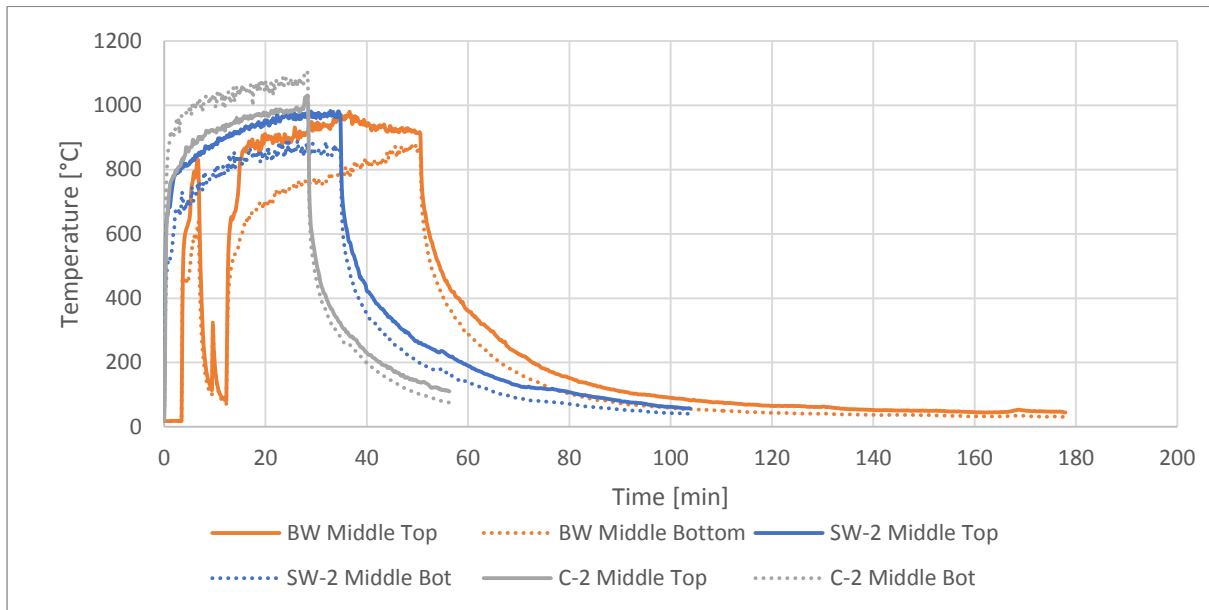


Figure 136: Comparing compartment temperatures amongst repeat configurations with one exposed CLT surface

The charring behaviour recorded during the three tests is depicted in Figure 137. It is clear that temperatures within a CLT panel remained elevated for a longer period of time in the Back Wall configuration as compared to the Side Wall and Ceiling tests. Temperature dropped faster within the ceiling panel as compared to the side panel and back wall, possibly due to the notion that the oxygen content at the ceiling is lower than in comparison to other surfaces due to the build-up of combustion gases. Since there is relatively less oxygen available at the ceiling level, once the heat source (i.e. the burner bed) is extinguished the components necessary to sustain combustion are not present, and subsequently combustion dies out.

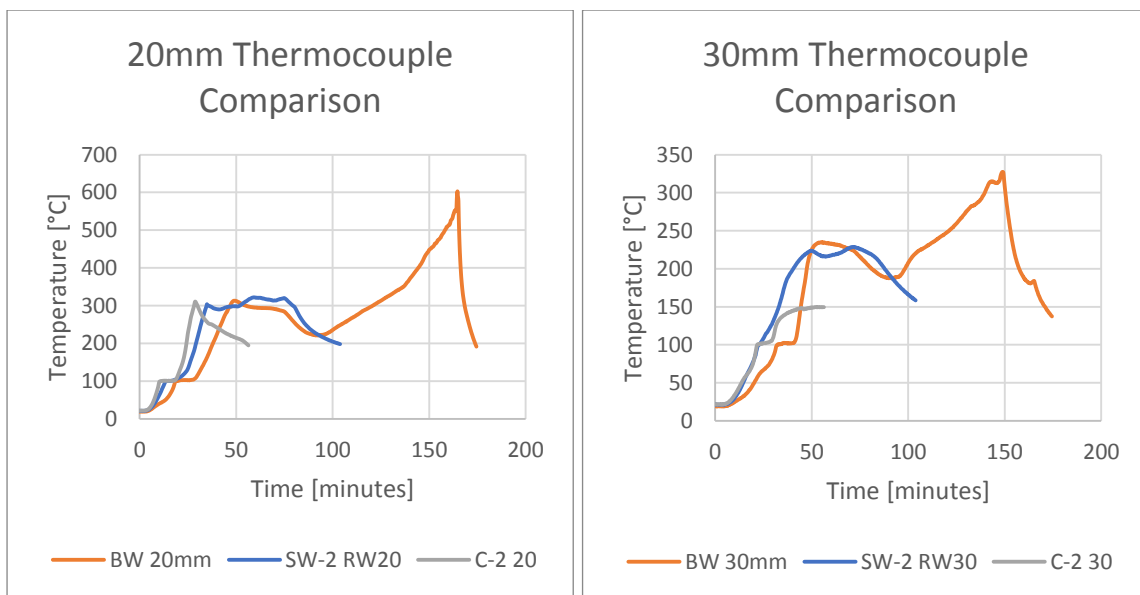


Figure 137: Comparing CLT panel temperature development amongst repeat configurations with one exposed CLT surface

Just as presented for the first set of experiments, the following general conclusions are confirmed by the repeat experiments:

- When comparing compartments with single exposed CLT surfaces, the total HRR and compartment Temperature was comparable across all experiments. The duration of the decay phase was shorter in the experiment involving an exposed CLT ceiling as compared to an exposed CLT Back Wall or Side Wall.

## G.2) Characterising the cross-radiation behaviour of facing CLT side walls

To investigate the influence of cross-radiation between two exposed CLT side walls, the results of a compartment test with both exposed walls (2SW) are compared to those of a repeat single side wall compartment test (S2). Based on these comparisons, trends are identified.

### HRR

Figure 138 illustrates the total HRR measured during the compartment experiment with two side CLT walls (2SW) and one CLT side wall (SW-2). On average, the total HRR during the heating phase was 73.4kW in the 2SW configuration, as compared to 56.9kW in the SW-2 configuration (representing an increase of 80% and 39% in addition to HRR delivered by the propane burner in both experiments). These trends are nearly identical to those identified by the first test series comparison.

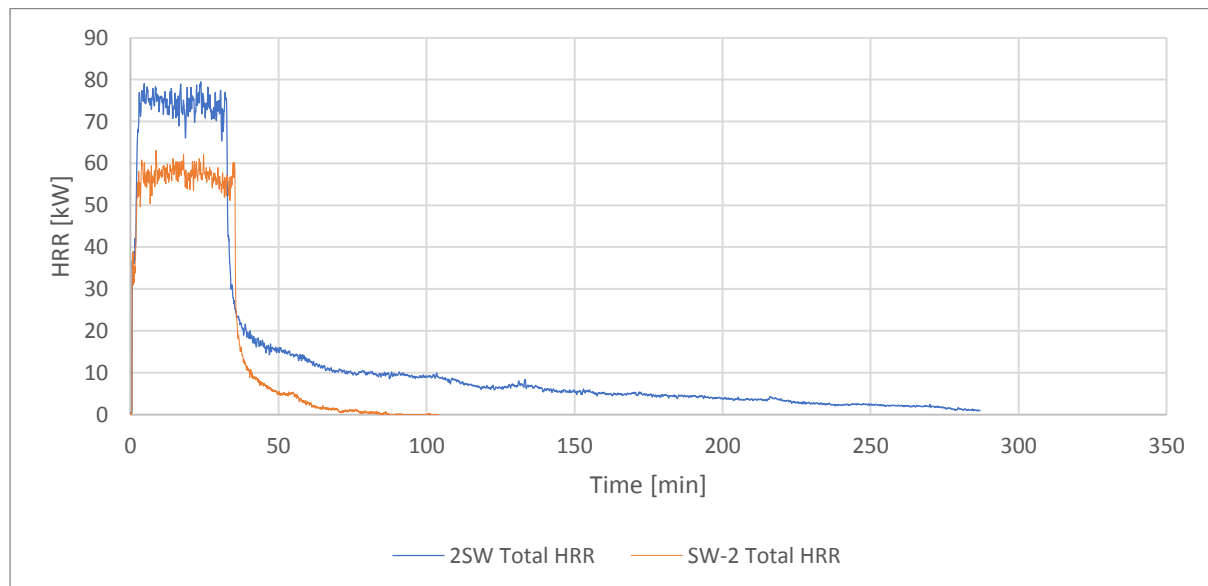


Figure 138 Comparing HRR amongst repeat compartments with one or two exposed Side Walls:

## Temperatures

Figure 139 shows the compartment temperatures measured at the face of the exposed CLT side wall in both compartments 2SW and SW-2. The temperature development during the heating phase is comparable between these two configurations, and the moment that the propane burner was switched off occurred at comparable instances (32 minutes in Compartment 2SW and 34 minutes in compartment SW-2). The temperature decay at the face of the CLT panel was however much more gradual in configuration 2SW as compared to configuration SW-2. Test SW-2 showed a sharp decline in compartment temperature and decay phase duration of 67:40 minutes, as compared to the approximately 3.7 times longer decay phase recorded in Configuration S. This decay phase duration factor is less than the 6.5 factor recorded in the first experiment. Nonetheless, it gives a strong indication of the effect of the addition of another side wall to configuration 2SW, namely that compartment temperatures remained elevated for an extended period of time due to mutual cross-radiation between two exposed (facing) side walls.

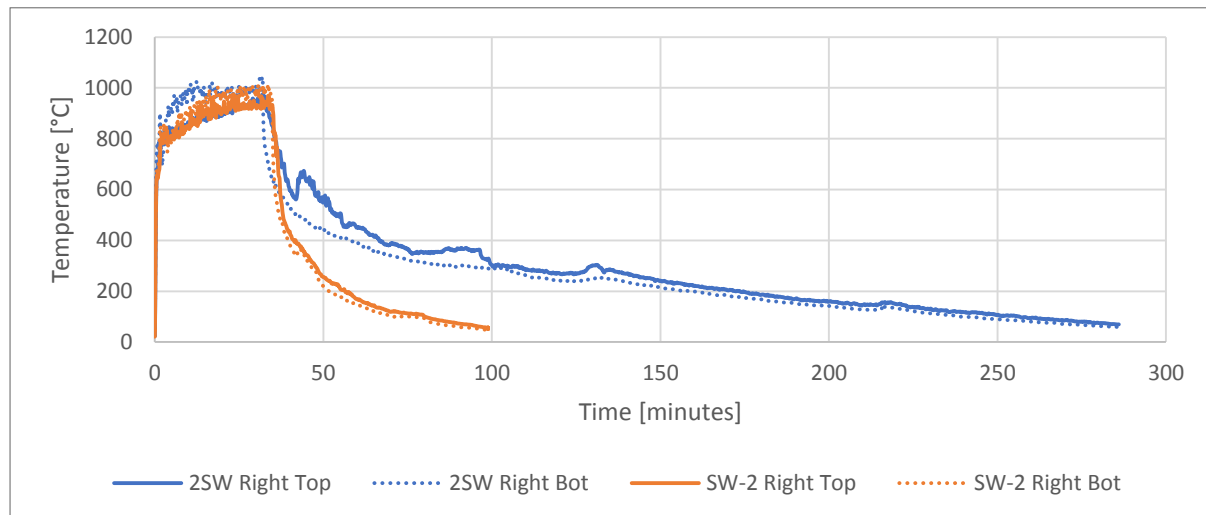


Figure 139: Comparing Compartment Temperatures at CLT surfaces in Configurations 2SW and SW-2

Figure 140 illustrates that elevated temperatures within the CLT left side wall in Compartment 2SW were sustained for longer as compared to Compartment SW-2. Since the rate of temperature decrease inside the compartment with two exposed CLT side walls is slower than in Compartment SW-2, the CLT temperature decline is also slower, which prolongs the decay phase. In short, compartments with two exposed CLT walls leads to a sustained period of elevated temperatures within the compartment during the decay phase, leading to a deeper depth of charring within the CLT panels as well as a longer period required to achieve self-extinguishment. The charring rate of the first lamella was not increased significantly by the addition of another side wall when comparing Compartments SW-2 and 2SW (0.58 and 0.62 mm/min, respectively), but the charring front did propagate deeper into the right

CLT Panel of configuration 2SW (to a depth of 50mm) as compared to the right panel of configuration SW-2 (namely 20 mm).

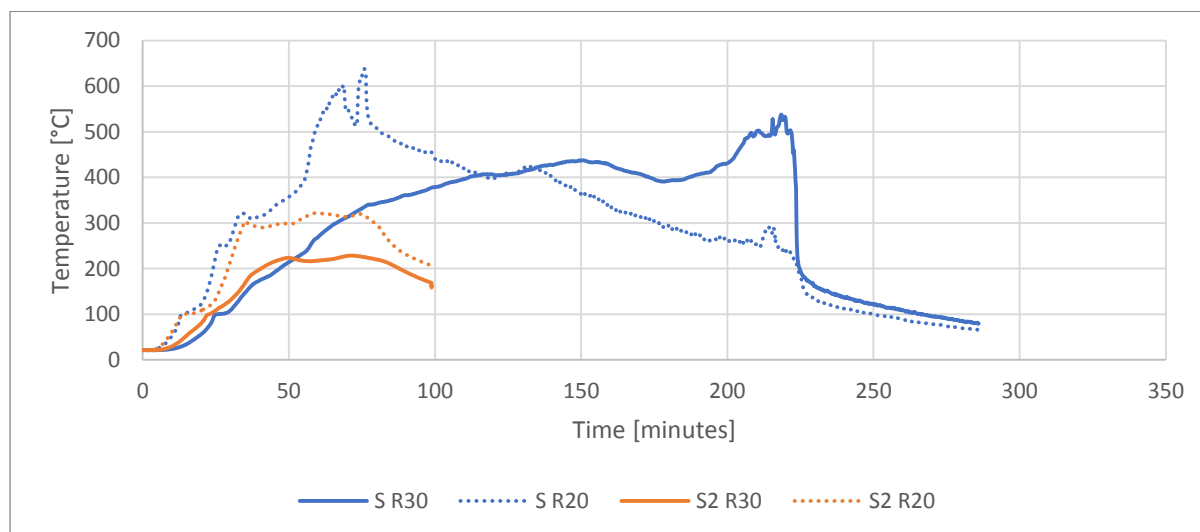


Figure 140: Charring behaviour of CLT panels in Compartments 2SW and SW-2

### G.3) Characterising the addition of an exposed Ceiling CLT to a compartment with a CLT back wall

Due to the error that the propane burner bed turned off for a period of 5:30minutes, only trends will be identified when comparing the BW Configuration to the BW+C-2 Configuration.

#### HRR

Figure 141 compares the total HRR measured during the compartment test containing an exposed CLT back Wall (BW) and exposed Back Wall and Ceiling (BW+C-2). It can be seen that in both tests that the exposed CLT contributed to the total HRR in addition to the input 41kW fire as supplied by the propane burner. The CLT contributed on average 15.6kW and 31.3kW to the HRR during the heating phase during the BW Compartment Test and BW+C-2 compartment test, respectively. The addition of a second exposed CLT surface to the BW configuration therefore approximately doubles the additional HRR released by the CLT only.

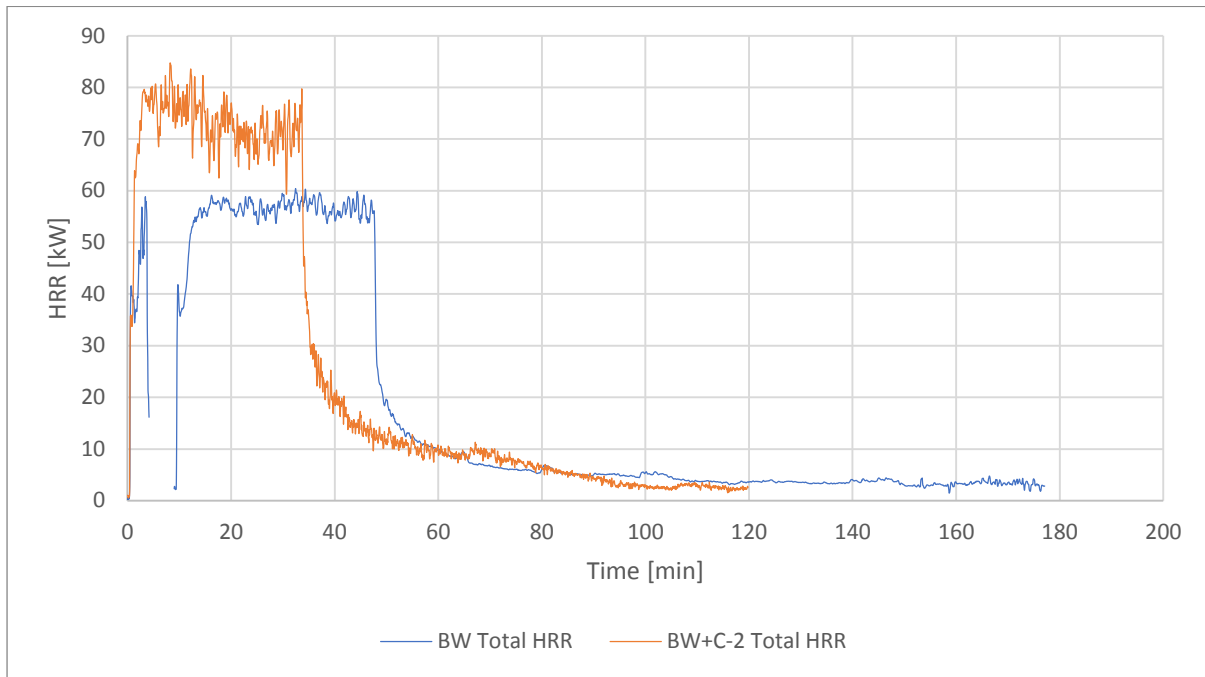


Figure 141: Comparing HRR between Configuration BW and BW+C-2

## Temperatures

Figure 142 plots the compartment temperatures measured during Compartment tests BW and BW+C-2. During the heating phase, the average temperature in the middle of the compartment, measured at a height of 0.4m from the floor panel, was comparable between the two experiments (917.6°C and 1003.6°C in Compartments BW and BW+C-2 respectively). These results indicate a similar trend as identified from the results of the 1<sup>st</sup> set of experiments which identified that temperatures are not influenced by the addition of a second exposed CLT surface in this under-ventilated fire scenario. The duration of the decay phase, as documented in Table 23, was measured as 126:20minutes and 87:20 minutes in Compartments BW and BW+C-2, respectively. As mentioned previously, these durations should not be compared directly due to the occurrence of the burner bed outage in Compartment Test BW.

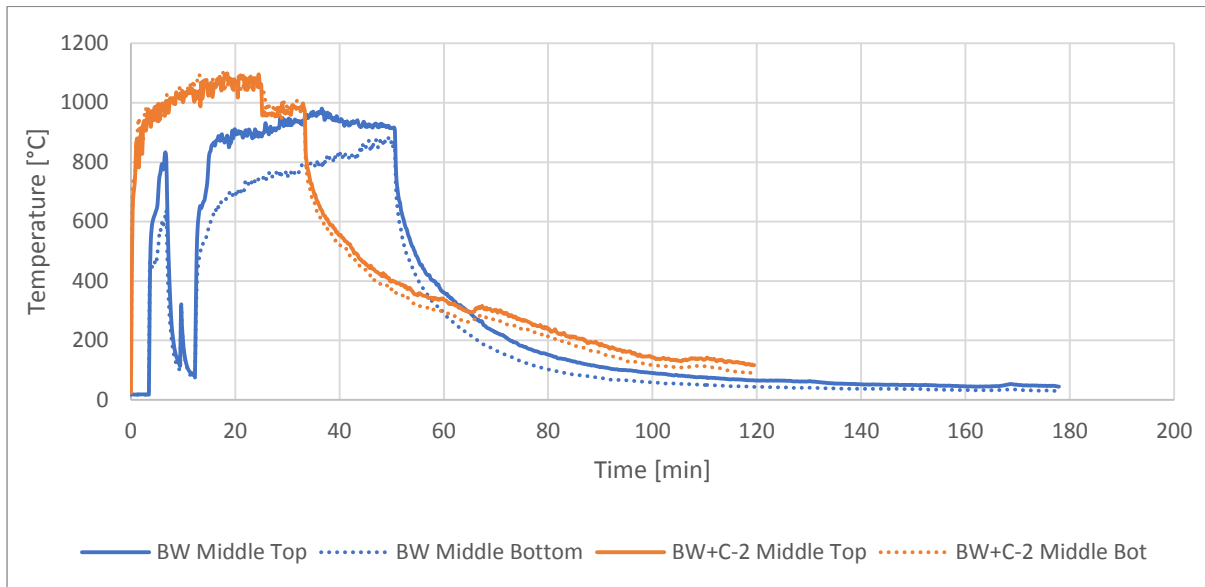


Figure 142: Comparing compartment temperatures between Configuration B and BC2

The charring behaviour of the BW and BW+C-2 configurations are illustrated in Figure 143.

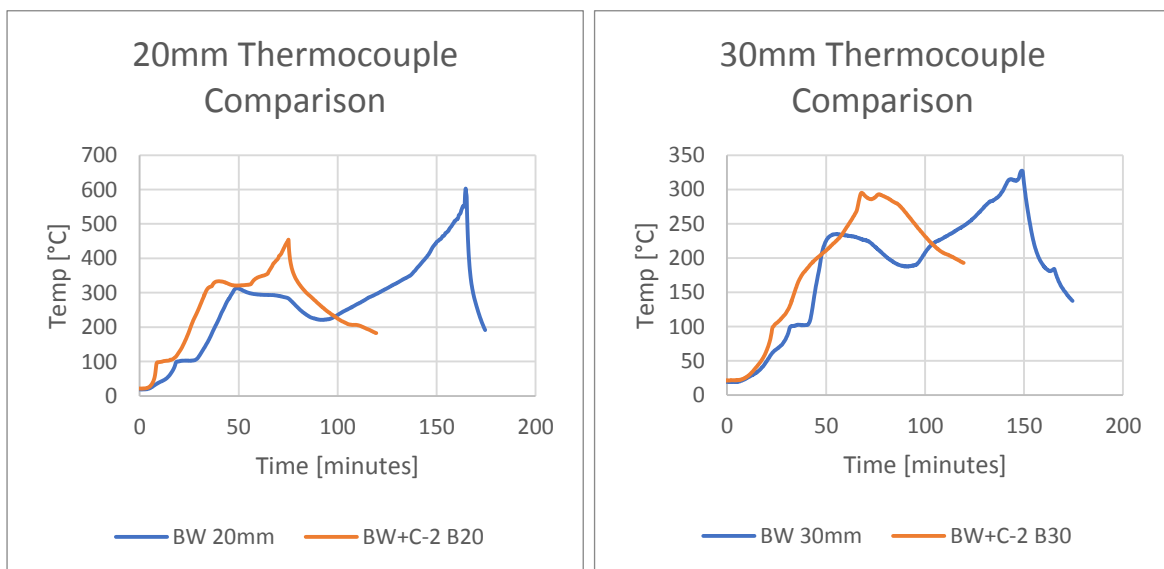


Figure 143: Charring behaviour of Compartments BW and BW+C-2

The charring rate of the back wall panel in Compartment BW+C-2 is 25% higher in the first lamella (20mm) as compared to Compartment BW (0.60mm/min compared to 0.48mm/min, respectively).

The BW Configuration also displayed longer decay duration. It is interesting to note that the CLT temperatures in compartment BW+C-2 were higher than those of compartment BW (when considering the back wall) for the first 100 minutes of the test. A sharp decline in CLT temperature was observed at 50 minutes at a depth of 20mm in the back panel of Compartment BW. Temperatures continued to decline till approximately 80 minutes. At this instance a local char flare-up at the location of the thermocouples led to an increase in temperature as measured by the 20mm and 30mm



thermocouples. If this instance of char flare-up did not occur it is speculate that compartment and CLT temperatures would have dropped to the point of self-extinguishment (as measured in Compartment BW+C-2). This indicates the highly variable nature of compartment fires.

#### G.4) Characterising the behaviour of compartments with two exposed CLT surfaces

This section of the Analysis is dedicated to comparing compartment configurations with two exposed CLT surfaces, namely Configuration 2SW and BW+C-2.

##### **HRR**

Figure 144 illustrates the measured HRR during compartment Tests 2SW and BW+C-2. During the phase of the fire when the propane burner bed was ignited, the averaged total HRR did not vary significantly between the two compartment configurations (73.4kW and 72.3kW in Compartments 2SW and BW+C-2, respectively). This indicates that the additional HRR by two CLT panels is independent of the orientation of the CLT panels, and measures between 32.4kW and 31.3kW in Compartments 2SW and BW+C-2 respectively (which corresponds to approximately 75% additional HRR as supplied by only the propane burner bed). The duration of the decay phase was significantly longer (i.e. by a factor of x2.9) in the 2SW configuration as compared to the BW+C-2 Configuration (251:50 minutes and 87:20 minutes, respectively).

Despite the similarities in HRRs during the heating phase and time required to char the first CLT lamellas, the TER in both compartment experiments differed significantly. The TER released by the combusting CLT alone was measured at 163MJ and 107MJ in Compartments 2SW (facing panels) and BW+C-2 (adjacent panels), respectively. In the facing CLT configuration as compared to the adjacent CLT configuration, the contribution to the TER increased by a factor of x1.5 due to this configuration's x2.9 times longer decay duration.

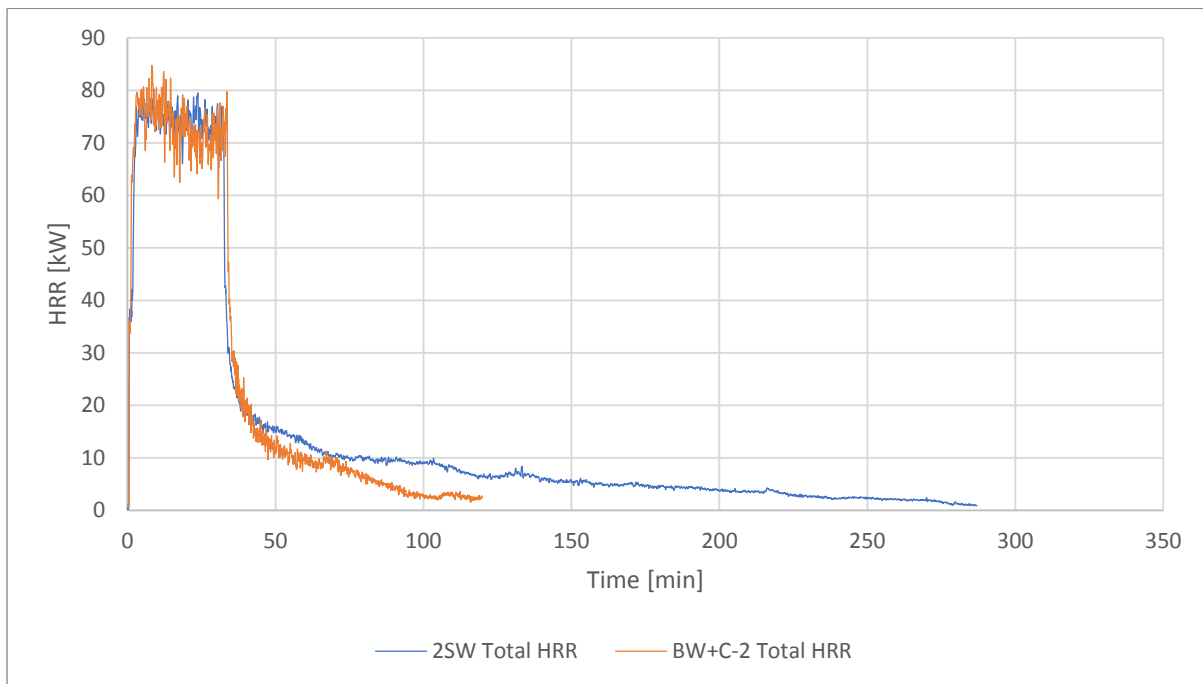


Figure 144: Comparing HRR between Configurations with two exposed CLT surfaces

## Temperature

Figure 145 shows that, during the heating phase of the fire, enclosure temperatures did not vary significantly at the top of compartments 2SW and BW+C-2 (averages of 937.0°C and 1003.6°C). The decay phase did, however, differ significantly between the two compartments. The configuration with two side walls measured elevated enclosure temperatures for a longer period of time as compared to the Back Wall and Ceiling configuration. It is postulated that this is as a result of the relative orientation between the exposed CLT panels. In a configuration where the exposed surfaces face another directly, heat is emitted directly between the two CLT panels. As heat is released from one Side Wall, it is radiated onto the other opposing CLT side wall. In the BW+C configuration, this cross-radiation is not as effective since the exposed CLT panels are positioned adjacent to one another (i.e. at right angles instead of parallel).

This observation of a prolonged period of elevated temperatures associated with facing CLT panels was also observed by Medina Hevia (2014) in his tests involving compartments with two facing side walls and a compartment with adjacent CLT panels (a single side panel and back wall).

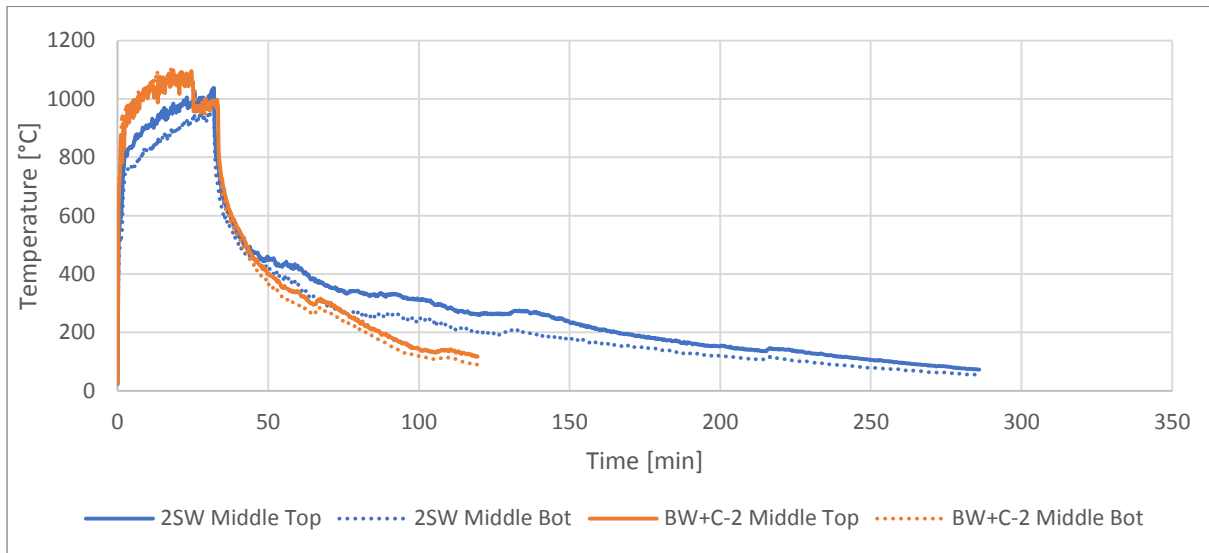


Figure 145: Comparing enclosure temperatures between compartments with two exposed CLT surfaces

The charring behaviour of the exposed CLT panels in both Compartments 2SW and BW+C-2 are depicted in Figure 146. CLT temperatures were elevated relatively longer in Compartment 2SW as compared to Compartment BW+C-2. This observation is also evident in the charring rates recorded in Table 30. The charring front penetrated to a depth of 50mm in Compartment 2SW and to 20mm in Compartment BW+C-2.

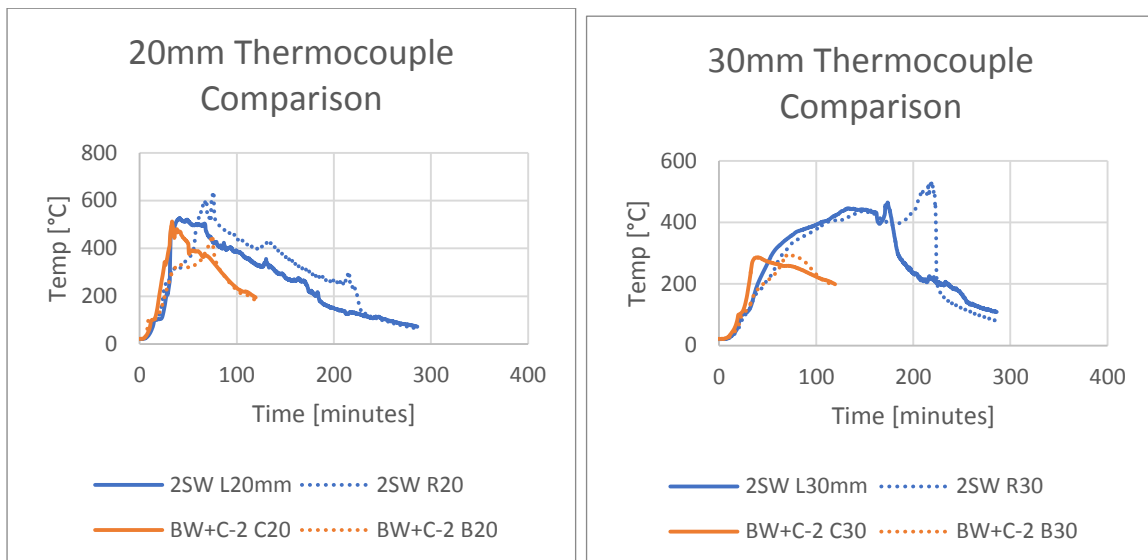


Figure 146: Comparing charring rates in compartments with two exposed CLT surfaces

Besides the ceiling panel of test BW+C-2 (0.83 mm/min), all CLT panels displayed similar charring rates within the first lamella (ranging from 0.60mm/min to 0.64mm/min).

## Appendix H

### Charring Rates of the Compartment Experiments

The charring rates obtained experimentally are also displayed graphically in section of the report. As done throughout this report, the results of the 1<sup>st</sup> set of experiments (MUF-BW; MUF-2SW; MUF-SW-1; MUF-C-1 and MUF-BW+C-1) will be discussed separately from the results of the repeat experiments (Compartments MUF-SW-2, MUF-C-2 and MUF-BW+C-2). The figures contained in this Appendix plot the charring front depth (as identified by the position of the 300°C isotherm) against the time required to reach this temperature at the specific depth. The charring rate can subsequently be visualised from the gradient of each curve.

The charring rates of the 1<sup>st</sup> set of experiments (MUF-BW; MUF-2SW; MUF-SW-1; MUF-C-1 and MUF-BW+C-1) are depicted in Figure 147. It can be seen that charring rates are comparable between all experiments, besides the CLT Back Wall configuration, when comparing charring rates up to the 1<sup>st</sup> adhesive line (i.e. 20mm). After this, only Compartments BW, 2SW and BW+C-1 showed a continuation of the charring front to deeper layers within the CLT panels. As previously mentioned, the compartment with an exposed back wall demonstrated sustained charring due to relatively larger distance of the exposed CLT back wall to the opening (thereby trapping heat within the compartment) as compared to other wall panels and a ceiling panel. Configurations with two exposed CLT surfaces experienced mutual cross-radiation (the extent of this depending on the relative orientation between these panels) which sustained the charring to reach layers beyond the 1<sup>st</sup> adhesive line. The charring rate of configuration BW was corrected by subtracting the burner outage time (5:30 minutes) from the time required for the 300°C isotherm to reach the 1<sup>st</sup> adhesive line.

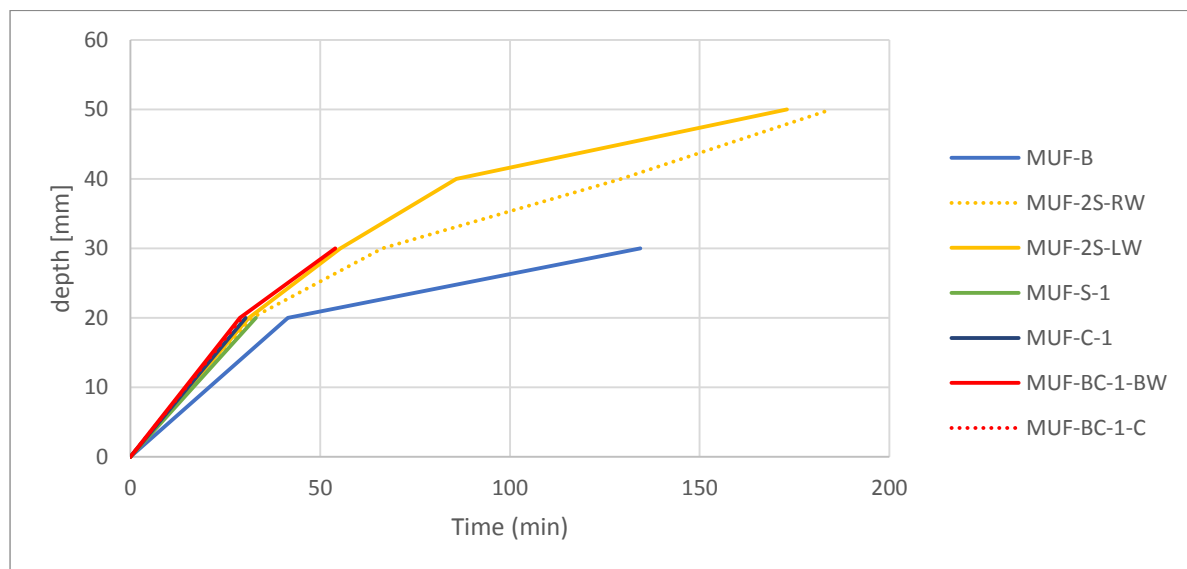


Figure 147: Progression of the charring front in the 1<sup>st</sup> set of compartment experiments. RW= Right Wall; LW=Left Wall; BW= Back Wall; C= Ceiling Panel

The progression of the charring front, as measured during the repeat experiments, is documented in Figure 148. The charring rates of the 1<sup>st</sup> lamella (i.e. 20mm) varied in a similar range (minimum of 0.58mm/min and maximum of 0.83mm/min, averaging 0.68 mm/min) as compared to the 1<sup>st</sup> set of

compartment tests (minimum of 0.48mm/min and maximum of 0.69mm/min, averaging 0.63 mm/min). This verifies the validity of the conclusions drawn from the 1<sup>st</sup> set of experiments pertaining to the influence of CLT panel configuration, as documented in Section 7.3

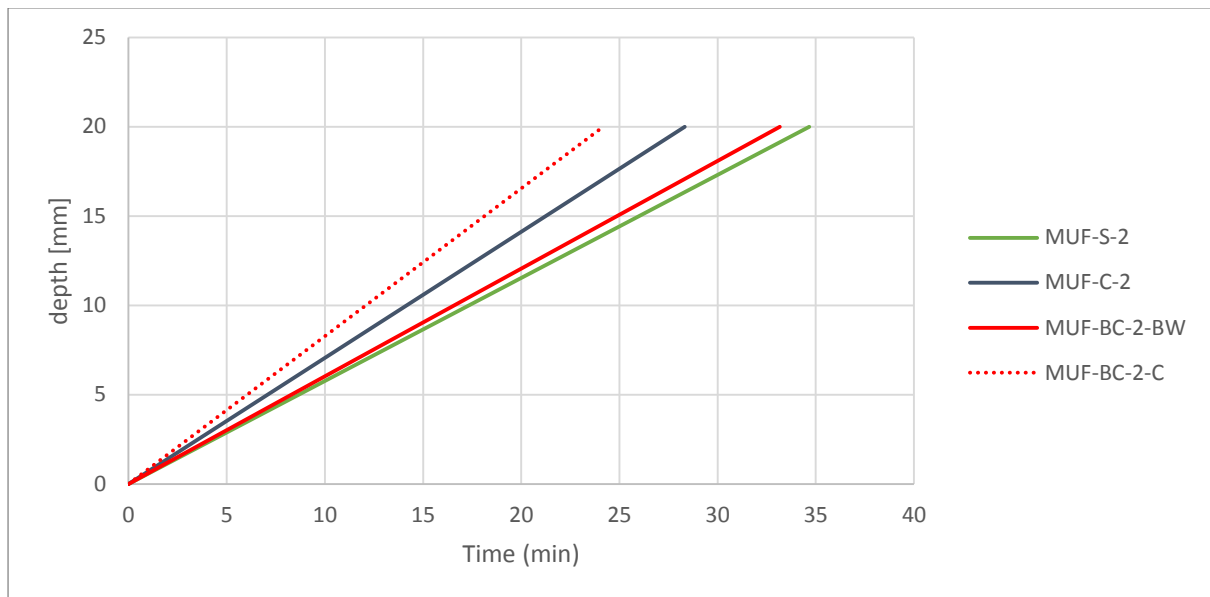


Figure 148: Progression of the charring front in the 2nd set of compartment experiments. RW= Right Wall; LW=Left Wall; BW= Back Wall; C= Ceiling Panel

# Appendix I

## Results of the 90 minute SFC Furnace Test on Ceiling CLT Panels

To facilitate the extrapolation of experimental charring rate results from the obtained compartment configuration experiments to a design recommendation, an additional experiment was conducted. The results of this additional experiment (conducted in a small horizontal furnace) are documented in this section of the report. By performing this test, charring rates observed from the compartment tests conducted in this investigation are also compared to charring rates obtained from exposure to the standard fire curve (SFC) for extended fire exposure durations.

The experimental methodology of the experiments documented in this report pertaining to compartment tests required the extinguishment of the initial fuel load once the first lamella (i.e. 20mm) had been charred. In Fire Safety design, design calculations are generally facilitated by means of a standardised resistance period (i.e. amount of time a material/element can retain its integrity when exposed to a standardised fire). As such the charring rates contained in this report are not directly applicable to design recommendations, since the initial fire load was extinguished in a range of 28 to 42 minutes in the various experiments.

A small furnace test was performed which exposed CLT panels (placed in a horizontal configuration) to the SFC (see Appendix C1.1 of this report). The panels were exposed to the SFC for duration of 90 minutes to obtain averaged charring rates between the 4 exposed panels. Furnace temperatures were recorded just below each of the 4 CLT panels. The average temperature recorded between these 4 readings during the tests was used to calibrate temperatures in the furnace to the SFC. The average furnace temperature (below the exposed CLT panels) is plotted against the SFC in Figure 149 to verify the fire exposure conditions implemented in this test:

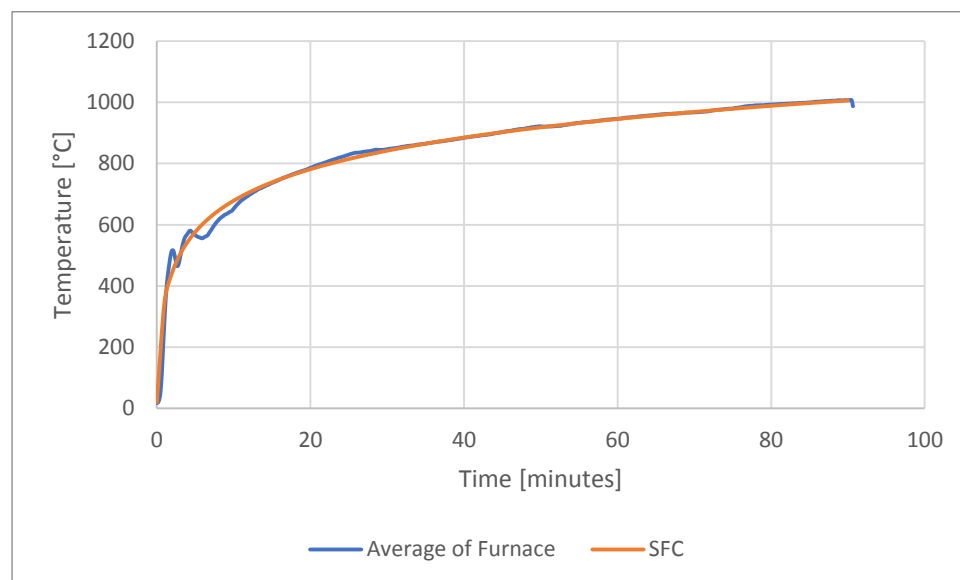


Figure 149: Verifying averaged furnace temperatures against the SFC

CLT panels from the same production batch as the panels used in the compartment tests were used in this furnace tests. The four CLT panels were also placed in a climate controlled room (regulated to



23°C and 50% relative humidity) for a comparable period (i.e. at least two weeks) as the CLT samples used in the compartment tests of this research project. Moisture content was not measured prior to testing, but based on the similarity of specimen preparation, it is postulated that moisture content was in the range of 12% to 14%. Furthermore, panels were weighed prior to testing to estimate densities based on panel dimensions. The average density prior to testing was calculated as 477.7kg/m<sup>3</sup>.

Each exposed panel was exposed to the fire within the furnace over a surface area of 0.3m x 0.3m. As in the case of the compartment experiments performed as part of this research, thermocouples were installed at various depths within each of the 4 exposed CLT panels. The thermocouples were installed in the centre of each of the 4 panels to depths of 10mm, 20mm, 30mm, 40mm, 60mm, 80mm, and 90mm (i.e. the side exposed directly to the fire within the furnace). Additionally, as implemented in the main investigation of this research project, thermocouples were installed perpendicular to the lamellas of each panel. This was done since CLT panels were delivered as final products to the laboratory where they were tested, and as such thermocouples could not be installed parallel to the lamellas (as was done by Frangi *et al.* (2009) and recommended by Fahrni *et al.* (2018)). The associated shortcomings of this limitation are acknowledged, namely an underestimation of temperature within CLT samples (due to a cooling affect by which heat is transferred away from the tip) and possible underestimation of the charring rate by 10%. Figure 150 depicts the thermocouple positions and depths from the fire side:

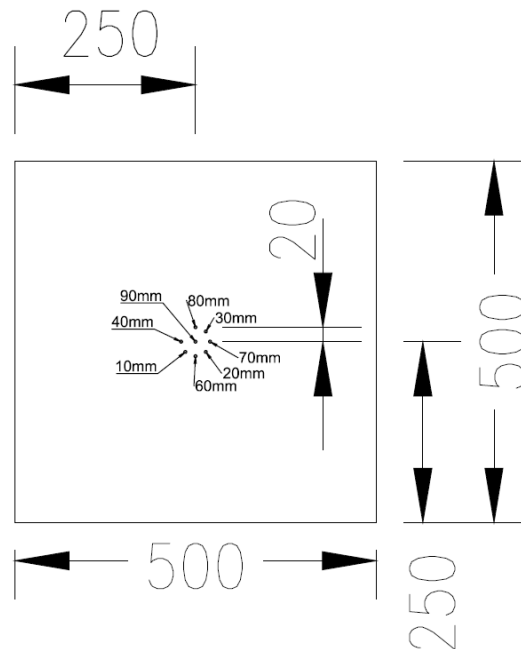


Figure 150: Thermocouple locations, with depths quoted as the distance from the tip of the thermocouple to the fire exposed side of the CLT panel

The test set-up was used to expose the CLT panels to a SFC, as well as the positions of the 4 exposed horizontal CLT panels on top of the furnace are indicated in Figure 151 and Figure 152, respectively:

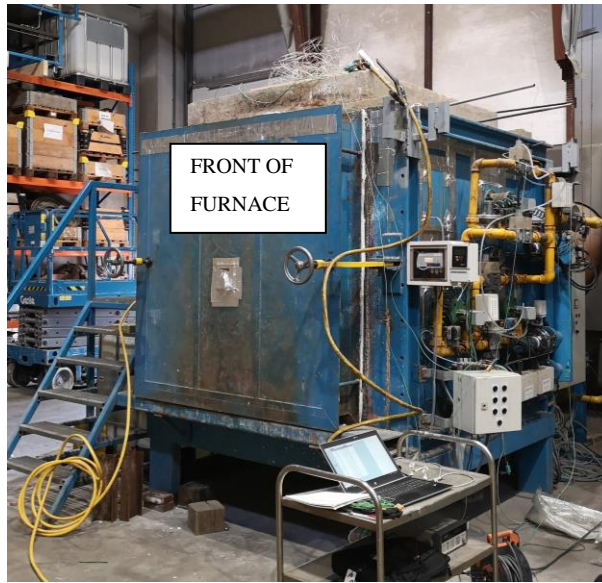


Figure 151: Furnace used to expose the 4 CLT panels to a SFC

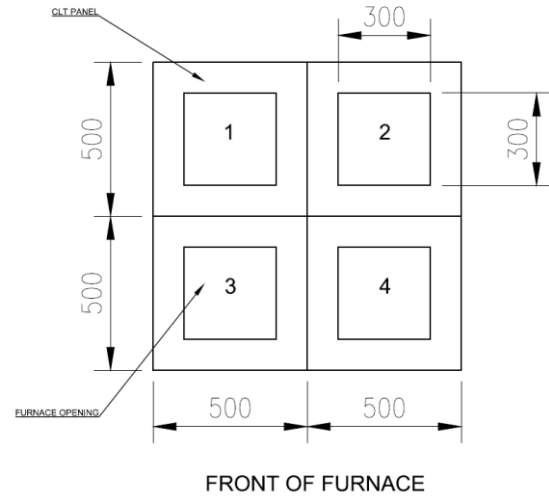


Figure 152: Positions of the CLT panels on top of the Furnace, with furnace openings below the CLT panels indicated

The objective of this furnace test was to char the CLT panels in one direction only (namely in the thickness direction). This was done by placing the four 0.5m x0.5m CLT panels on top of a fire-resistant concrete frame. The frame contained four open panels measuring 0.3m x 0.3m each. Ceramic fibre blanket was placed in between the CLT panels and the concrete frame.

In order to calculate charring rates, the methodology implemented by Frangi *et al.* (2009) was followed by which the charring rate ( $\beta$ ) was calculated per layer ( $\beta_{\text{layer}}$ ) as well as per panel ( $\beta_{\text{panel}}$ ). The following equations were used to calculate each of these charring rates:

$$\beta_{\text{layer}} = \frac{\Delta d_{\text{char,layer}}}{\Delta t_{\text{layer}}} \quad (19)$$

$$\beta_{\text{panel}} = \frac{d_{\text{char}}}{t_{300^{\circ}\text{C}}} \quad (20)$$

Where:

$\Delta d_{\text{char,layer}}$  is the distance between consecutive charring depths [mm]

$\Delta t_{\text{layer}}$  is the time required for the 300°C isotherm to propagate between subsequent depths [minutes]

$d_{char}$  is the depth of charring [mm]

$t_{300^{\circ}C}$  is the time required for the 300°C isotherm to propagate to a specific charring depth [minutes]\*

\*As implemented in the main investigation of this report, the 300°C was used as a threshold for the transition of timber to char. This value was obtained from the research of White (2016).

The following table documents the charring rates ( $\beta_{layer}$  and  $\beta_{panel}$ ) for each of the 4 panels tested in this experiment, as well as the  $t_{300^{\circ}C}$  per panel:

Table 45: Charring rates of all 4 panels subjected to a SFC exposure

Panel	$d_{char}$ [mm]	10	20	30	40
1	$t_{300^{\circ}C}$ [min]	29	44	55	74
	$\beta_{layer}$ [mm/min]	0.35	0.64	0.98	0.50
	$\beta_{panel}$ [mm/min]	0.35	0.45	0.55	0.54
2	$t_{300^{\circ}C}$ [min]	35	48	71	*
	$\beta_{layer}$ [mm/min]	0.29	0.75	0.43	*
	$\beta_{panel}$ [mm/min]	0.29	0.42	0.42	*
3	$t_{300^{\circ}C}$ [min]	30	42	54	71
	$\beta_{layer}$ [mm/min]	0.33	0.82	0.82	0.61
	$\beta_{panel}$ [mm/min]	0.33	0.47	0.55	0.56
4	$t_{300^{\circ}C}$ [min]	37	49	62	76
	$\beta_{layer}$ [mm/min]	0.27	0.86	0.78	0.71
	$\beta_{panel}$ [mm/min]	0.27	0.41	0.48	0.53

\* due to a technical error, no measurement was recorded at the thermocouple situated 40mm from the fire side in Panel 2.

The averaged results based on the charring rates of the individual panels are shown in Table 46:

Table 46: Average charring rates of CLT panels exposed to a SFC exposure

$d_{char}$ [mm]	10	20	30	40
$t_{300^{\circ}C}$ [min]	33	46	61	74
$\beta_{layer}$ [mm/min]	0.31	0.77	0.75	0.61
$\beta_{panel}$ [mm/min]	0.31	0.44	0.50	0.54

During the experiment, visual observations of the state of the CLT panel were observed through a small viewport in the furnace. The same observations regarding local char fall-off, as recorded regarding identical MUF bonded CLT panels in the compartment tests (see section 7.2 of this report), were also observed in this SFC furnace tests. Although these observations are only visual (and not based on measured quantities), the notion of char fall-off in the tested MUF bonded CLT panels as opposed to lamella delamination in the tested PU bonded CLT panels, is enforced.

It was measured that the thermocouples in all 4 panels placed at a depth of 60mm from the fire side did not reach 300°C after 90 minutes of exposure to the SFC: temperatures of 143.7°C, 160.3°C, 219.4°C and 108.1°C were recorded at depth of 60mm from the fire side in Panel 1, 2, 3 and 4, respectively. Furthermore, temperatures of 510.8°C, 653.7°C, 921.6°C and 502.8°C in Panel 1, 2, 3 and 4, respectively, were recorded after 90 minutes at a depth of 40mm mm from the fire side.

By a process of linear interpolation per panel, the position (between 40mm and 60mm) of the 300°C at 90 minutes was determined. The analysis resulted in charring depths of 51.5mm, 54.3mm, 57.7mm and 50.3mm after 90 minutes of SFC exposure (averaging 53.5mm).

In summary, the furnace SFC exposure tests yielded an experimental averaged panel charring rate 0.54mm/min up to a depth of 40mm after 73 minutes of exposure to the SFC. After 90 minutes, the average charring rate over 90 minutes was 0.59mm/min (based on an average charring depth of 53.5mm). Subsequently, the reported panel charring rates documented in this appendix prove a comparable CLT charring rate to that of solid timber (i.e. 0.65mm/min as specified for softwoods in EN1995-1-2, Table 3.1).

The data obtained from the SFC Furnace tests can be compared to the fire tests on small-scale compartments containing exposed CLT ceilings, based on the charring rate of the first CLT lamella (i.e. 20mm). As listed in Table 29 and Table 30 of this report, charring rates over the 1<sup>st</sup> lamella of a CLT ceiling panel was measured at 0.66mm/min, 0.71mm/min, 0.68mm/min and 0.83 mm/min in Compartments MUF-C-1, MUF-C-2, MUF-BW+C-1 and MUF-BW+C-2, respectively. The SFC

furnace test demonstrated an averaged charring rate of 0.44 mm/min as compared to the averaged charring of 0.72mm/min in compartments containing an exposed CLT ceiling. The discrepancy between the SFC charring rate (0.44mm/min) and the charring rates of CLT Ceilings in small compartments (0.72mm/min) is explained by considering the difference in fire exposure between the tests, as shown in Figure 153:

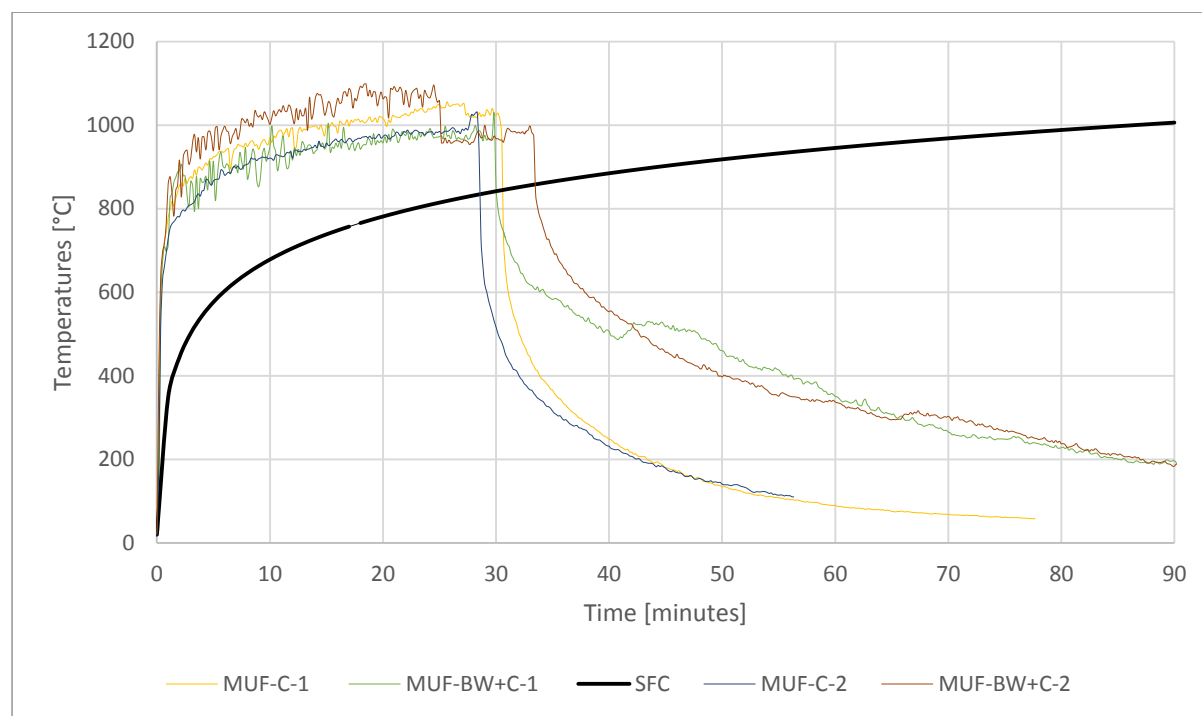


Figure 153: Comparing SFC exposure to compartment tests containing exposed CLT ceilings

Whilst ignited, the propane burner (supplying a HRR of 41kW) delivered a more severe fire as compared to the SFC, as seen in the figure above. Since the propane burner was ignited in the compartment tests only for the period of time required to char the first CLT lamella (i.e. 20mm), it can be concluded that the 1<sup>st</sup> lamella charring rates as recorded in Table 29 and Table 30 are more conservative as compared to charring rates obtained from a SFC exposure.

Furthermore, from the averaged SFC charring rates reported in Table 46, it is concluded that charring rates did not vary greatly across CLT lamellas. The averaged SFC charring rate over the 1<sup>st</sup> lamella was measured at 0.44mm/min, whereas the averaged charring rate over 90 minutes (with an associated charring depth of 53.5mm, i.e. 2.5 lamellas) was 0.59mm/min. As such it is concluded that the 1<sup>st</sup> lamella charring rates of small scale-compartments containing exposed CLT ceilings are also representative of fire situations with a longer heating phase (i.e. charring by the initial fuel load that is more than 20mm only).

As such, it is postulated that, based on the similarity in charring rates between the two experimental series as well as the similarities in visual observations pertaining to a process of local char fall-off,

that the conclusions drawn from the series of compartment tests are also representative of fires with a longer heating phase (i.e. charring by the initial fuel load more than 20mm).